



Cranfield University

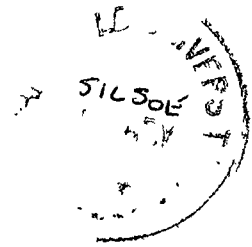
D. G. Weston

1999,

Molecular Engineering of the Biosensor Interface

Institute of Bioscience and Technology

PhD Thesis



Cranfield University

Institute of Bioscience and Technology

PhD Thesis

Academic Years 1999 - 2000

D. G. Weston

Molecular Engineering of the Biosensor Interface

Supervisor: Dr D.C. Cullen

October 1999

*This thesis is submitted in partial fulfilment of the requirements of the
degree of Doctor of Philosophy*

Dedication

This thesis is dedicated to the memory of my Grandfather, Richard Lyndon,
a man of great wisdom and grace, the last of his generation.

We shall never see the like of them again.

"If a man is called to be a streetsweeper, he should sweep streets even as Michelangelo painted, or Beethoven composed music, or Shakespeare composed poetry. He should sweep streets so well that all the hosts of heaven and earth will pause to say, 'Here lived a great streetsweeper who did his job well.'"

Martin Luther King, Jr.

Abstract

The research described in this thesis concerns the investigation of technologies for the molecular engineering of the biosensor interface. Two avenues of investigation have been explored: the use of polymer matrices to modify the properties and functions of optical biosensor interfaces and the conjugation of photochromic dyes to protein systems to achieve photomodulation of protein function for biosensor applications.

A comparison of the industry standard polymer, carboxymethyl dextran (CMD) was made against carboxymethyl cellulose and mixed systems, including a novel synthetic polymer, carboxylated polynoxylin. While CMD was found to provide the highest surface loading of protein, mixed polymers demonstrated the ability to allow prediction of surface loading, and showed features such as improved resistance to biological degradation.

A novel method of depositing interfaces was investigated, allied to a study of liquid handling methods. A system was developed that allowed a printed heterogeneous array to be produced which showed preferential binding of specific analytes to defined areas of the sensor, whilst the other printed arrays retaining a high degree of non-specific interaction.

The use of photochromic dyes to modulate protein function was applied to glucose oxidase and horseradish peroxidase. From the initial results, a hypothesis regarding the mechanism of photomodulation and its effect concerning the molecular weight of the conjugated protein was proposed. This was examined by the photomodulation of members of the peroxidase super family, antibodies and Fab fragments. From these results, the hypothesis was proved to be correct but incomplete, and was modified to include the disruption of the hydration shell around the protein caused by photochromic switching.

Further research directly related to these experiments, and in novel fields of investigation have been proposed.

Acknowledgements

This project has been partially funded by the EU Climate and Environment Program via the ENVIROSENSE project (ENV4-CT96-0333).

I would like to express my gratitude to my supervisor, Dr Dave Cullen, who let me do it my way, and who will master clear English, eventually. My thanks are also extended to the members of the EC biosensor community, especially Dr Karl Kramer of TU Munich. Thanks are owed to Richard Day, who wrote the SPR software used in Chapter 4.

The staff of IBST have been invaluable, in their assistance throughout practical work, but especially for the effort they put in proof reading posters, papers and draft chapters: Alison Amatsah, Ned Ashby, Lesley Branston, John Bolbot, Liz Day, Dawn Fowler, Naresh Magan, Jeff Newman, Jane Rixon, Jude Taylor and Steve White.

My many friends at IBST were a constant source of humour, and it would have been difficult without them. In particular, thanks are owed to, Gordon and Katherine Baxter, John Hayes, Kal Karim, Silke Kroger, Andrew Moody, Lawry Ritchie and the mighty Damian Baskeyfield.

Finally, a great debt of thanks is owed to my family: my father, my friend and colleague, who has taught me so much of scientific method and the value of humility. My mother who has fought for me and with me, and my brother and sister, who have had to tolerate my temper and my butterfly mind.

<u>Contents</u>	<u>Page number</u>
Title page	i
Dedication	iii
Abstract	iv
Acknowledgements	v
Contents	vi
List of figures	x
List of tables	xiv
Abbreviations	xv
Chapter 1: Introduction and literature review	1
1.1 The application of molecular engineering	1
1.2 Current biosensor technology	4
1.2.1 Optical biosensors and detection of molecular interaction	4
1.2.2 Biomolecule immobilisation for biosensor fabrication	5
1.2.3 Adherence of the biorecognition molecule to the transducer	7
1.2.4 Transducer modifying agents and their deposition	8
1.2.5 Surface chemistry for transducer modification	10
1.2.6 Polymers as transducer modifying agents	12
1.2.7 Surface modification as an area to investigate	14
1.3 Molecular engineering of active biomolecules	15
1.3.1 Antibody technology	15
1.3.2 Synthetic receptors	17
1.3.3 Modulation of biological activity and applications for sensor regeneration	18
1.3.4 Photochromic dyes and their role in bio-modulation	19
1.4 Conclusions drawn from current literature	22
1.4.1 Objectives	22
1.4.1.1 Polymer interfaces for biosensor transduction	23
1.4.1.2 Protein engineering for the modification of function	23
Chapter 2 General materials and methods	24
2.1 Introduction	24
2.2. Materials	24

2.3 Preparation of surfaces	24
2.3.1 Acid washing	24
2.3.2 Solvent washing	24
2.4 Silanisation of surfaces	25
2.5 Surface examination by contact angle measurement	26
2.6 Atomic force microscopy	28
2.6.1 General theory	28
2.6.2 AFM equipment and settings	28
2.7 Surface plasmon resonance	30
2.7.1 General theory	30
2.7.2 SPR equipment	31
2.7.3 Metal deposition to solid surfaces	33
2.7.4 Angular-based scans	33
2.7.5 Time-based studies utilising SPR	34
2.7.6 Scanning in air	35
2.7.7 Scanning in liquids	35
2.7.8 Data analysis of SPR results	37
2.8 Chemistries for modification of the transducer interface	37
2.8.1 Covalent coupling of carboxylated polymers to aminated surfaces via EDC reactions.	37
2.8.2 Covalent coupling of proteins to carboxylated molecules via EDC reactions	37
Chapter 3: The use of polymers to modify transducers	39
3.1 Introduction	39
3.1.1 Modification of the transducer surface	39
3.1.2 The application of carboxylated glucose polymers to modify transducers	40
3.1.3 Aims	42
3.2 Materials and methods	43
3.2.1 Materials	43
3.2.2 Covalent attachment of carboxylated polymers to APTS modified surfaces	43
3.2.3 Covalent attachment of carboxylated polymers to pre-aminated microtitre plates	43
3.2.4 Covalent attachment of proteins to carboxylated polymers	44
3.2.5 Synthesis of carboxylated polyoxynin	44
3.2.6 Microbiological screen for resistance to biological degradation	46

3.3 Results	48
3.3.1 Deposition of polymers to APTS modified glass	48
3.3.2 Deposition of carboxylated polymers and proteins to APTS modified metal	50
3.3.3 Protein loading to modified microtitre plates	52
3.3.4 Mixed polymer systems	53
3.3.4.1 Synthesis and introduction of CPN to carboxylated glucose polymers	54
3.3.4.2 Deposition of mixed polymers to APTS modified glass	55
3.3.4.3 Deposition of mixed polymers and proteins to APTS modified metal	56
3.3.4.4 Protein loading to mixed polymer modified microtitre plates	57
3.3.5 Microbiological screen for resistance to biological degradation	60
3.4 Discussion and conclusion	63
3.4.1 Surface modification of glass and metals	63
3.4.2 Polymer modification of interfaces	63
3.4.3 Mixed polymer systems	65
3.4.4 Biodegradation of polymeric systems	66
3.4.5 Conclusions	67
Chapter 4: Novel transducer fabrication techniques	68
4.1 Introduction and aims	68
4.1.1 Multi-analyte biosensors and alternative approaches to transducer fabrication	68
4.1.2 Fabrication methods for biosensor production	69
4.1.3 Reverse deposition – a fabrication method suitable for high throughput manufacturing	70
4.1.4 Aims	72
4.2 Methods	73
4.2.1 Conjugation of biological molecules with carboxylated polymers in bulk solution	73
4.2.2 Linear and reverse deposition to aminated microtitre wells	73
4.2.3 Comparison of RD and LD interfaces by SPR assay	74
4.2.4 High density array printing via touch-off printing	74
4.2.5 Biojet deposition and interrogation of functional arrays	75
4.2.6 Analysis of heterogeneous arrays with multi-channel SPR	76
4.3 Results	78
4.3.1 Synthesis of the CMD-HRP conjugate	78
4.3.2 Comparison of Linear and Reverse Deposition of CMD and HRP to aminated microtitre wells	79
4.3.3 Comparison of Linear and reverse deposition of CMD and HRP to APTS modified silver	79
4.3.4 Synthesis of the CMD-atrazine conjugate	80

4.3.5 Comparison of linear and reverse deposition of CMD and atrazine to aminated microtitre wells	81
4.3.6 Comparison of linear and reverse deposition of CMD and atrazine to APTS modified silver	82
4.3.7 High density array printing via the biojet	84
4.3.8 Synthesis of CMD-FITC	86
4.3.9 Automated deposition of functional arrays	87
4.3.10 Analysis of heterogeneous arrays	89
4.4 Discussion and conclusions	92
4.4.1 Reverse deposition of CMD conjugates	92
4.4.2 Array printing via the Cavo	95
4.4.3 Heterogeneous array printing and analysis	95
4.4.4 Conclusions	97
Chapter 5: Photomodulation of enzymes	99
5.1 Introduction	99
5.1.1 Modulation of biological activity and applications for sensor regeneration	99
5.1.2 Spiropyran dyes	100
5.1.3 The role of spiropyran dyes in bio-modulation	101
5.1.4 Aims	102
5.2 Methods	103
5.2.1 Synthesis of the spiropyran precursor, 1-carboxymethyl-2,3,3-trimethylindolenium iodide	103
5.2.2 Synthesis of carboxylated spiropyran	104
5.2.3 Photochromic activity of SP-COOH in ethanol	105
5.2.4 Spiropyran - protein conjugation	106
5.2.5 Protein assay of dye protein conjugates	106
5.2.5 Determination of retention of biological activity by SP-protein conjugates	107
5.2.5.1 SP-GOx conjugate	107
5.2.5.2 SP-HRP conjugate	108
5.3 Results	109
5.3.1 Synthesis of 1-carboxymethyl-2,3,3-trimethylindolenium	109
5.3.2 Synthesis of carboxylated spiropyran	110
5.3.3 Photochromic activity of SP-COOH in ethanol	111
5.3.4 Synthesis SP-Gox	113
5.3.5 The activity of SP-Gox compared to native Gox under visible and UV illumination	114
5.3.6 Synthesis of SP-HRP	117
5.3.7 The activity of SP-HRP compared to native HRP under visible and UV illumination	118
5.4 The effect of variation in conjugation time on photochromic activity	120

5.4.1 Variation of SP content to glucose oxidase activity	120
5.4.2 Variation of SP content to HRP activity	121
5.5 Discussion and conclusions	124
5.5.1 synthesis of SP-COOH	124
5.5.2 synthesis of photomodulation of SP-protein conjugates	124
5.5.3 The mechanism of photomodulation	126
5.5.4 Conclusion relating to the proposed hypothesis	127
5.5.4 Conclusions	128
 Chapter 6: The effect of molecular weight on photochromic activity	 129
6.1 Introduction	129
6.1.1 Molecular weight as the restricting factor to photomodulation	129
6.1.2 Aims	130
6.2 Methods	131
6.2.1 Conjugation of enzymes to SP-COOH	131
6.2.2 Assay of enzyme activity	131
6.3 Results	132
6.3.1 Synthesis of spiropyran-protein conjugates	132
6.3.2 Photomodulation of HRP	135
6.3.3 Photomodulation of lactoperoxidase	137
6.3.4 Photomodulation of myeloperoxidase	139
6.3.5 Photomodulation of microperoxidase	140
6.4 Discussion and Conclusions	142
6.4.1 The photomodulation of various peroxidases	142
6.4.3 Conclusions	144
 Chapter 7: Photomodulation of Antibodies	 145
7.1 Introduction	145
7.1.1 The application of antibody technology to diagnostics	145
7.1.2 Antibody structure and function	146
7.1.3 Aims	147
7.2 Methods	149
7.2.1 Immobilisation of protein to microtitre plates	149
7.2.2 Conjugation of spiropyran dyes to immobilised proteins	149
7.2.3 Creation of Fab fragments	150
7.2.4 Assay for photochromic modulation of antibody and Fab affinity	150
7.3 Results	151

7.3.1 The photomodulation of immobilised native and SP modified HRP	151
7.3.2 The photomodulation of native and SP modified anti FITC IgG	152
7.3.3 The creation of Fab fragments from anti FITC IgG	154
7.3.4 The comparative photomodulation of IgG and Fab	155
7.4 Discussion and conclusions	157
7.4.1 The photomodulation of immobilised native and SP modified HRP	157
7.4.2 The photomodulation of native and SP-modified anti-FITC IgG and Fab	157
7.4.3 Conclusions	158
8. Final conclusions and future work	159
8.1 Final conclusions	159
8.1.1 The use of polymers to modify transducers	159
8.1.2 Advanced and novel transducer fabrication techniques	161
8.1.3 Deposition and analysis of printed arrays	162
8.1.4 The photochromic modulation of protein activity	163
8.1.5 The application of generic technologies	165
8.2 Future work	166
8.2.1 Characterisation of active surface	166
8.2.2 Advanced sensor fabrication	167
8.2.3 Photomodulation of affinity systems	168
8.2.4 Optical control of bioreactors	169
8.3 Final conclusions	170
References	172
Appendix	185
A1 Published papers	185
A2 Conference proceedings	192
A3 Conference Posters	194

List of Figures

Page Number

Figure 1.1 An Idealised representation of IgG antibodies immobilised by physical adsorption	7
Figure 1.2 Physical adsorption of a recognition molecule (Y) to a transducer Surface	9
Figure 1.3 Covalent attachment of a recognition molecule (Y) to a modified transducer surface	10
Figure 1.4 Covalent attachment of a recognition molecule (Y) to an extended matrix attached to a transducer surface	10
Figure. 1.5 Representation of a mixed polymer system which utilises complex orientations	13
Figure 1.7 Schematic of the photo-isomerisation of the spiropyran dye (1'-(2-carboxethyl)3',3'-dimethyl-6-nitrospiro [2 <i>H</i> – benzopyran-2'2indoline)	19
Figure 2.1 A representation of a droplet as a sector of a circle	26
Figure 2.2 A schematic of the apparatus used for SPR experiments	31
Figure 2.3: the result of an SPR angle scan showing the angle chosen for subsequent time scans	34
Figure 2.4: a representation of static (A) and flow liquid cells (B) for SPR analysis	36
Figure 3.1 Molecular Structures of Cellulose and Dextran	41
Figure 3.2 AFM image of CMD immobilised on vapour silanised glass	48
Figure 3.3 AFM image of CMC immobilised on vapour silanised glass	49
Figure 3.4: Example SPR responses obtained from a APTS-modified silver surface	51
Figure 3.5 The differential enzyme activity of HRP immobilised to CMD and CMC interfaces	53
Figure 3.6: The structure of polynoxylin	54
Figure 3.7: Noxylin dicarboxylic acid	55
Figure 3.8 AFM image of CMC/CMD on vapour silanised glass	56

Figure 3.9 the effect of increasing CMC concentrations on a CMD interface	58
Figure 3.10: the effect of increasing CPN concentrations on a CMD interface	59
Figure 3.11: The availability of polymeric carbon sources to a mixed bacterial culture (n = 4).	60
Figure 3.12: The effect of polynoxylin on the utilisation of polymeric carbon sources by a mixed bacterial culture (n = 4).	61
Figure. 4.1 A representation of linear sensor fabrication	71
Figure. 4.2 A representation of reverse deposition for sensor fabrication	71
Figure 4.3 The front end of the MC-SPR software	76
Figure 4.4: The elution profile of CMD-HRP from a 65 ml G100 column	78
Figure 4.5: the elution profile of CMD-atrazine from a 65 ml G100 column	81
Figure 4.6 Graphical representation of the printing pattern used to determine droplet volume : separation characteristics of different surfaces	84
Figure 4.7 Elution profile of CMD-fluorescein from a PD10 column	86
Figure 4.8 The printing pattern for the creation of the heterogeneous array	88
Figure 4.9 A printed array of CMD on silanised silver	88
Figure 4.10 Interaction of anti-FITC IgG with a CMD-fluorescein / CMD-BSA / CMD heterogeneous printed array	89
Figure 4.11. The effect of multiple regeneration cycles to the Δ SPR of printed CMD-fluorescein interacting	91
Figure 4.12: a representation of sequential immobilisation of protein	93
Figure 4.13: a representation of reverse deposition of a complete interface	94
Figure 5.1. Schematic of the photo-isomerisation of the spiropyran dye (1'-(2-carboxyethyl)-3',3'-dimethyl-6-nitrospiro[2H-benzopyran-2,2'-indoline])	100
Figure. 5.2 The reaction sequence to synthesis a spiropyran dye	104
Figure. 5.3 A representation of an 'open door' UV/visible Spectrophotometer Time Scan Print Out	108
Figure. 5.4 Representation of TLC plate of 1-carboxymethyl-2,3,3-	

trimethylindolenium and its precursor	109
Figure 5.5 Representation of a TLC plate of SP-COOH and its precursor	110
Figure 5.6 Fade back of the merrocyanine form of SP-COOH to the spiropyran form	111
Figure 5.7 The absorption of SP-COOH in ethanol under visible and UV illumination	112
Figure 5.8 Elution profile of SP-GOx from a PD10 column	113
Figure. 5.9 The reaction mechanism of the glucose oxidase assay	114
Figure. 5.10 The effect of UV and visible illumination on native glucose oxidase	115
Figure. 5.11 The effect of UV and visible illumination on SP-glucose oxidase	116
Figure 5.12 Elution profile of SP-HRP from a PD10 column	117
Figure 5.13 The effect of UV and visible illumination on native HRP	118
Figure 5.14 The effect of UV and visible illumination on SP-HRP	119
Figure 5.15 Effect of conjugation reaction time on the photo-modulation of enzyme activity of glucose oxidase - spiropyran dye (SP-GOx) conjugates	120
Figure 5.16 Effect of conjugation reaction time on the photo-modulation of enzyme activity of spiropyran dye - horseradish peroxidase (SP-HRP) conjugates	122
Figure 6.1: Elution profile of SP-HRP from a PD10 column	132
Figure 6.2: Elution profile of SP-Lpod from a PD10 column	133
Figure 6.3: Elution profile of SP-myeloperoxidase from a PD10 column	133
Figure 6.4: Elution profile of SP-microperoxidase from a PD10 column	134
Figure 6.5: The effect of UV and visible light on native HRP	135
Figure 6.6: The effect of UV and visible light on native SP-HRP	136
Figure 6.7 The effect of visible and UV light on native Lpod	137
Figure 6.8 The effect of visible and UV light on SP-Lpod	138
Figure 6.9 The effect of visible and UV light on native Micropod	140

Figure 6.10 The effect of visible and UV light on SP- Micropod	141
Figure 7.1: A representation of the IgG molecules and the reduction in size of the relevant fragments	146
Figure 7.2 The activity of immobilised native and SP- HRP under visible Illumination	151
Figure 7.3: The effect of photomodulation on native and SP modified IgG under UV and visible illumination	153
Figure 7.4: The effect of Photomodulation on Native and SP modified IgG and the corresponding Fab fragment under UV and visible illumination	155

List of Tables	Page number
Table 1.1: The published results of the photomodulation of protein systems to date	20
Table 2.1 AFM Scanning Parameters	29
Table 2.2 Parts list of the SPR system	32
Table 3.1: The constituents of FAM2 Medium	46
Table 3.2: a comparison of attachment and immobilisation of proteins to CMD and CMC	51
Table 3.3: interaction of HRP with mixed polymer interfaces	56
Table 4.1: A comparison of the RD and LD of CMD and HRP to an aminated microtitre plate	79
Table 4.2: A comparison of LD and RD of CMD and HRP to APTS-modified Ag	80
Table 4.3: The results of LD and RD of CMD and atrazine to aminated microtitre wells	82
Table 4.4: A comparison of LD and RD of CMD and atrazine to APTS-modified Ag	83
Table 4.5 Dispense Characteristics of Small Volumes on Various Surfaces via a Biodot™ Cavro Printer	85
Table 4.6: Printing parameters used with the Biodot Biojet printer for deposition of printed arrays	87
Table 4.7 Differential response of a heterogeneous printed array with CMD-fluorescence active channels and CMD / CMD-BSA control channels to antiFITC IgG	90
Table 5.1: the increase in protein dye loading as a function of incubation time	123
Table 7.1: Variation in activities between visible and UV illumination of IgG, Fab and the spiropyran modified proteins expressed as ratios and percentage change	185

List of Abbreviations

ABTS	2,2' azino-bis-ethylbenzthiazoline-6-sulfonic acid
AFM	Atomic Force Microscope
BSA	Bovine Serum Albumin
CMC	Carboxymethyl Cellulose
CMD	Carboxymethyl Dextran
EDC	1-ethyl-3(3-dimethyl amino propyl) carbodiimide
Fab	Fragment - antibody
FC	Fragment – cell binding
Gluc	Glucose
GOx	Glucose Oxidase
HRP	Horse Radish Peroxidase
IgG	Immunoglobulin G
Lpod	Lactoperoxidase
MES	2-[N-Morpholino]ethanesulfonic acid
Mpod	myeloperoxidase
Micropod	microperoxidase
NHS	N-Hydroxy Succinimide
OPD	o-phenyl diamine
PA	Physically Adsorbed
RO	Reverse osmosis
RTP	Room temperature and pressure
SP	Spiropyran
SP-COOH	Spiropyran carboxylate
SPR	Surface Plasmon Resonance
TLC	Thin Layer Chromatography

Chapter 1. Introduction and Literature Review

1.1 The Application of Molecular Engineering

The concept of engineering structure and function is not novel. Terms such as chemical engineering and genetic engineering are commonplace to the non-scientist. Both of these concepts, and other such scientific disciplines, rely on the ability to engineer products from “the ground up”. In the case of genetic engineering this involves the creation of a sequence of base pairs and its effective expression from a suitable cell. In one sense, chemical engineering involves the creation of complex molecules using many individual specific processes, which utilise precise catalysed reactions to create a defined product of high purity.

Molecular engineering has been defined as a tool to construct and organise molecular aggregates that interlock and interact (Kuhn, 1988). From this definition it is evident that molecular engineering has a different role, and performs its task in a fundamentally different way to both chemical engineering and genetic engineering. Where as other forms of molecular science revolve around the creation of compounds from simple precursors, molecular engineering is interested in the modification of existing complex compounds to alter their characteristics and allow them to be used in novel areas. Examples of molecular engineering are evident in many fields:

Medical implants - The use of medical implants has become widespread in the last decade. The range of replacement parts and instruments that are currently in use is vast, and includes replacement heart valves, joints, blood vessels and heart pacemakers. All of these items have one thing in common: they must not react with the system to which they are being implanted. Piveteau *et al* (1999) have used a matrix of calcium phosphate and titanium dioxide to create a linker layer which is compatible to both bone and the titanium of the implant. Kursawe *et al* (1998) developed a system of biodegradable silica fibres for reinforcement of medical implants that were prepared by sol-gel processing.

In the case of smaller more delicate devices, such as heart valves and pacemakers, biofouling with plasma components, particularly albumins can be a problem. To avoid this, surfaces of these devices have been engineered to be resistant to fouling. DiTizio

et al (1998) have developed a liposomal hydrogel system that significantly reduces bacterial adhesion to silicone catheter material. The system consists of a poly (ethylene glycol)-gelatin hydrogel in which liposomes containing the antibiotic ciprofloxacin are sequestered.

Selective membranes - Selective membranes have been in use for dialysis machines for the last twenty years. The need for more specialised membranes has been highlighted by the introduction of implantable sensors. Implantable biosensors must have membranes that allow the selective diffusion of the analyte of interest, but are biocompatible (Quinn *et al*, 1997).

Photoactive compounds - The use of engineered molecules has also been applied to electronics, in the form of polymers for the fabrication of light emitting diodes (LED's). Traditionally, LED's have been available in a limited range of colours, red, green yellow and orange, but not blue. The need for blue LED's has been driven by the need for outside broadcast colour displays, which need red green and blue light sources to generate a total colour spectrum. Indium gallium nitride (InGaN) single-quantum-well-structure blue LEDs were grown on epitaxially laterally overgrown GaN (ELOG) and sapphire substrates (Nakamura, 1999) to generate light emitting diodes.

The polymeric aspects of LED's have also been considered. The synthesis of a new poly(methacrylate) copolymer bearing an efficient blue light emitting chromophore, a charge transporting aromatic oxadiazole and a UV-sensitive crosslinkable unit has been reported by Li *et al* (1997).

Catalytic reactors - In the areas of industrial science, effluent treatment has become an area of increasing interest, as regulations on chemical disposal have become more stringent. Catalytic reactors have been proposed as a system for efficient waste processing. Systems based on porous ceramic membranes are broadly chemically inert and catalytically active, and represent a technique that is applicable for use in harsh environments, such as effluent streams and solvents (Coronas and Santamaria, 1999; Cote *et al*, 1999).

This thesis examines the application of molecular engineering in relation to the manufacture and function of biosensors. The areas of molecular engineering which are of direct interest to the research presented are:

- The modification of molecules to alter their charge ratio and/or solubility (Treloar, Christie and Vadgama, 1995)
- The conjugation of molecules, such as antibodies and fluorescent reporter groups, to modify their function for analytical purposes (Chang, *et al.*, 1995)
- The alteration of surface groups to allow direct immobilisation of molecules to otherwise unavailable surfaces (Jonsson, *et al.*, 1985; Sasaki, *et al.*, 1998)

An area of increasing interest is the application of advanced analytical methods for use in real time monitoring for both medical and environmental applications. A biosensor can be divided into a number of parts, namely a data logger, the transducer and the biologically active component, either enzyme, antibody or biomimetic molecule. Within this project, biosensor systems will be examined as targets for molecular engineering in two different ways:

- **The modification of biosensor interfaces at the molecular level**
- **The conjugation of proteins with photochromic dyes to photomodulate function**

To demonstrate the generic nature of molecular engineering, many of the techniques employed will be applied to a range of systems, varying polymers and surfaces for transducer modification and a range of protein systems for photomodulation.

The remainder of this chapter will review the literature as it relates to molecular engineering of surfaces and molecules, concentrating on two specific areas: the modification of biosensor transducers by covalent attachment of polymer systems and the modulation of molecular function by the interaction of covalently attached photochromic dyes.

1.2 Current biosensor technology

A biosensor has been defined as “a compact analytical device incorporating a biological or biologically-derived sensing element either integrated within or intimately associated with a physicochemical transducer”,(Turner *et al*, 1987). The usual aim of a biosensor is to produce either discrete or continuous electronic signals that are proportional to a single analyte or a related group of analytes. This is an ideal concept, which falls short of what many current biosensors are able to deliver.

To date, the most common form of biosensor have been electrochemical sensors which have relied on redox reactions to produce a voltage or current change, which can be detected as a variance between a sample electrode and a reference value. These methods have given rise to both advanced and medically useful devices, such as the “glucose pen” for diabetic self-monitoring (Wilson and Turner, 1992). Electrochemical biosensors have not been more widely adopted as there are few single analyte system, such as blood glucose, which are targets for commercial development of biosensors, and the creation of multianalyte sensors has proved problematic. The main difficulties in the creation of multianalyte sensors have been the lack of a generic immobilisation technique, requiring all proteins to have individual immobilisation methods.

Of the biosensors that are commercially available, most have used an electrical transducer. Electrochemical methods can have a lower limit of detection comparable to existing techniques, such as microtitre assays (Goodrow and Hammock, 1998), they are susceptible to interference from electroactive compounds with in the sample matrix, and a degree of electrode fouling. Both of these effects can result in a high and variable base line.

1.2.1 Optical biosensors and detection of molecular interaction

Recently there has been increased interest in utilising optical detection methods for use as biosensors. Optical biosensors can be used for the detection of receptor-analyte interactions that are not naturally electroactive, such as antibody-antigen interactions. Currently, optical biosensors of major interest are based on evanescent wave technology, such as Surface Plasmon Resonance (SPR) (Davies, 1994) and

Evanescent Wave Interferometry (EWI) (Hutchinson, 1995; Robinson, 1995; Hall and Winzor, 1997).

Both systems utilise evanescent waves created by interaction of light with an interface between two mediums, at an angle greater than that required for total internal reflection. The mode of operation of the two systems is considerably different. Primarily, SPR measures variance in the angle of reflectance of incident light at which surface excitation of atoms occurs, (Liedberg and Lundstrom, 1993) which creates a surface plasmon (Davies, 1994). In contrast EWI utilises an optical comparator, where variation of surface characteristics at the surface of a waveguide induces a phase shift in the evanescent wave, which is detected by direct comparison to a reference beam (Heideman *et al* 1993, Stamm and Lukosz 1996). Both systems are reliant on changes in refractive index when used as a biosensor and this effect can be due to the binding of ligands to surface immobilised biological recognition systems. **Therefore, the common features to both systems are the use of a biological recognition molecule and the detection of variation of an interfacial refractive index.**

1.2.2 Biomolecule immobilisation for biosensor fabrication

The most common feature of biosensors is that they use a biological layer, which must be effectively immobilised to a transducer. The chemistry used to create the immobilised biological layer and the function it performs is determined both by the surface to which the layer is being adhered, the size of the biological recognition molecule and the environment in which it has to function.

Effective immobilisation of the biological component to the transducer is central to the successful operation of a biosensor, and is considered a critical step in the development of a biosensor (Scouten *et al*, 1995). There are several problems that must be overcome to ensure the biological component interacts with the transducer and remains functional:

1. The biological component should be immobilised to the sensor in a non-reversible and stable way. Direct adsorption to the sensor surface has proved

to be both imprecise and easily disrupted, therefore a method of chemical immobilisation is required (Williams and Blanch, 1994).

2. Non-specific interaction of molecules should be kept to a minimum. In many of the monolayer methods of surface modification, non-specific binding can contribute a significant component of all interaction that is detected, thus raising the lower limit of detection (LLOD) to an unacceptably high level (Karube *et al*, 1995).

3. Reduction of receptor function by the random orientation and denaturation of the molecule must be kept to a minimum. To ensure the immobilised recognition molecule remains active, the orientation of the molecule must ensure that active sites remain available for ligand binding. Also, the local environment must be such that the recognition molecule can function normally in non-ideal environments, such as complex solutions of chemicals and biochemicals that are encountered in industrial or medical analysis (Williams and Blanch, 1994).

4. The methods used to fabricate the biosensors must ensure that the final device is reproducible and stable, thereby allowing commercial development of the system (Galanvidal *et al*, 1995).

Therefore, an ideal method of immobilisation must be stable, easy to characterise, must help to avoid non-specific binding and be central to the correct orientation of the active biological element. To add to the challenges of effective surface immobilisation, the range of surfaces that have been used for biosensors is very diverse, including metals, oxides, glass, silicon and plastics. A long-term goal would be to find a system of immobilisation that would be equally efficient for all surfaces.

Broadly, there are two methods for the complex immobilisation of biological elements to transducers: physical entrapment, which involves encapsulating the biological element into a porous matrix which is attached to the transducer (Hall, *et al*, 1999), and molecular attachment of the biological element either directly to the transducer or

to a modifying layer (Williams and Blanch, 1994; Jones, 1997). A third system exists, which is widely used both as a base line measurement of activity and for the production of immobilised surfaces: direct physical adsorption (Andrade *et al*, 1992a). While many substances, proteins among them, will readily adsorb onto a solid substrate, the created surface is disordered, leading to loss of activity by blocking of active sites, and can result in extensive denaturation of proteins and is poor stability (Andrade, *et al*, 1992b).

1.2.3 Adherence of the biorecognition molecule to the transducer

Historically, coupling chemistries have relied on the random coupling of proteins through the amino acid side chains such as the amino groups of lysine residues present within the structure of a protein (Lin *et al*, 1991). This often results in a decrease in protein activity due to improper orientation of the receptor, such as an antibody, to the surface (figure 1.1).

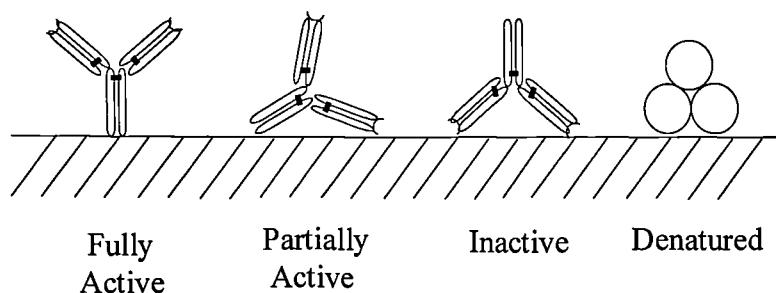


Figure 1.1 An Idealised representation of IgG antibodies immobilised by physical adsorption (Lu, *et al*, 1996)

To achieve oriented or semi-orientated binding, coupling systems that rely on the formation of defined linkages need to be used. If naturally produced proteins are to be used, either groups which are naturally present on the proteins, or groups which can be chemically attached to the protein, must be used to couple the protein to the support. These systems utilise a variety of coupling methods:

carbohydrate groups - can be oxidised to aldehydes under exposure to sodium periodate, and are then linked to hydrazide-activated supports (Hoffman and

O'Shannessy, 1988). Certain molecules have regions which have a high percentage of carbohydrate compared to the rest of the molecule, such as the Fc region of IgG.

sulfhydryl groups – reduction of disulfides results in the creation of sulfhydryl groups which can be directly attached to iodoacetyl activated surfaces. In antibody technology, Fab fragments are produced by the reduction of the inter-heavy-chain disulfide bond of F(ab')₂ fragments. This process results in a fragment that contains a single sulfhydryl group opposite the antigen-binding site. This can be used to create an orientated linkage, with the active site of the antibody fragment opposite the point of immobilisation (Lu *et al*, 1995).

gluteraldehyde - one of the most used methods for coupling proteins to collagen, aminopropyl glass and amine containing supports. Its mode of action is to form linking imines between the supporting matrix and the protein amine. The method can be complex, resulting in poor reproducibility of surfaces. (Hermanson, *et al*, 1994)

carbodiimide - carbodiimides can be used to catalyse the formation of amide bonds between a carboxylate and an amine. The water-soluble carbodiimide, 1-ethyl-3-(3-dimethyl amino propyl) carbodiimide (EDC) is widely used for conjugation reactions and peptide synthesis. *N*-substituted carbodiimides can react with carboxyl groups of Glu, Asp or the C-terminal to form the short lived reactive species *O*-acylisourea. This can then react with a primary amine to form a peptide bond, with a sulfhydryl to generate a thiol-ester linkage, or with water to regenerate a carboxyl group. (Timkovich, 1977)

succinimide ester and maleinimide (Lu, *et al*, 1995) have also been utilised. However, the loss of biological activity upon immobilisation is notable in many cases where these coupling methods have been used.

1.2.4 Transducer modifying agents and their deposition

The transducer surface is the primary interface between the biological component and the transducer. The layer, or interface, containing the biological component has an inherent need to be uniform in both thickness and composition, to ensure that a well-defined and reproducible interaction occurs between the biological element and its ligand. The possible methods currently used for surface modification are:

Adsorption of monolayers – There are two principal methods of adsorption to surfaces:

Physical adsorption - the protein of interest is allowed to adhere directly to the sensor surface by simple adsorption from bulk solution. These systems can result in disorientated layers, and a subsequent loss in activity of the immobilised molecule, as the active site has a high probability of being partially or completely blocked by the surface or other molecules, and the protein can be easily denatured, as shown in figure 1.2.



Figure 1.2 Physical adsorption of a recognition molecule (Y) to a transducer surface - the recognition molecule can assume a number of orientations, and may be denatured (O) by the adsorption process.

Chemisorption – occurs when a chemical, but non-covalent, interaction occurs between the surface and the molecule that is in contact with it, resulting in creation of a surface compound (Moore, 1978). This system can be used to achieve oriented linking via active groups, such as poly-thiol tails, which adhere naturally to gold surfaces resulting in stable linkages (Lu *et al*, 1995).

Covalent attachment to modified surfaces – are created by the interaction of molecules to either activated surfaces or by the interaction of two molecules with a chemical reagent, a cross linker, such as EDC or glutaraldehyde. This can result in a semi-mobile covalently attached monolayer (figure 1.3).

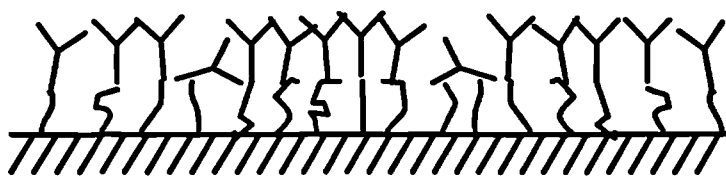


Figure 1.3 Covalent attachment of a recognition molecule (Y) to a modified transducer surface - The linker molecule has been shown larger than actual size to emphasise its role in the modification procedure.

By selecting appropriate surface modifying chemistries, a degree of organisation can be introduced to the surface.. For example, a propyl linker (C3) allows some freedom of movement away from the surface (figure 1.3) which may be more conducive to the recognition element retaining an active format. In the case of IgG, which has a lysine rich area away from the recognition site, the covalent attachment that is achieved favours the correct orientation of the antigen binding site.

Covalent attachment of polymer layers - By adhering a polymer to a sensor surface, the open mesh is allowed to extend into the liquid phase, and in so doing, increases the surface area that may interact with potential analytes, as shown in figure 1.4.

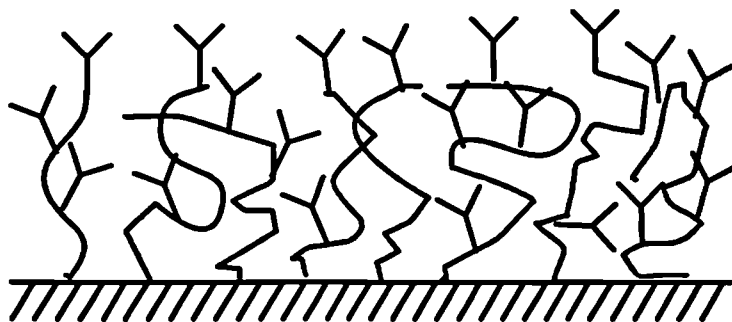


Figure 1.4 Covalent attachment of a recognition molecule (Y) to an extended matrix attached to a transducer surface

Certain polymers, such as those with hydrophilic properties, have the advantage that they help to prevent non-specific binding. By utilising an extended coupling matrix, such as a modified polysaccharide, the surface area of the transducer can be expanded away from the surface. This results in a surface that potentially has a higher loading than a two dimensional substrate, which can result in greater sensitivity of the sensor.

1.2.5 Surface chemistry for transducer modification

The surfaces of SPR and EWI sensors can be considerably different. SPR sensors use a metal, usually gold or silver, deposited on to a glass prism, whereas EWI can have a metal oxide, glass, silicon or quartz surface. The disadvantage of both types of surface is that they are chemically inactive towards biological molecules, and as such need to be modified to allow ease of attachment of the biological element. The common methods used for the above surfaces both rely on the inherent properties of interaction of reactive species to broadly unreactive surfaces. These are described below:

Silane activation - silane groups interact with glass/quartz surfaces by the substitution of a hydrogen atom bound to a hetero atom of the inorganic substrate with a silyl group, forming a silicon-hetero atom bond without further altering the substrate (Baldini and Bracci, 1993; Lesho and Sheppard, 1996). Therefore, by using molecules which contain a silane group at one end and appropriate active group at the other, for example, NH_2 , the organofunctional silane molecule can be used as a linker to attach other molecules to a glass surface (Frantz and Granick, 1992). The greater the distance between the silane and secondary active group, the more ordered the silanised layer would become. If alkane silanes are used, the optimal length is C_6 to C_{12} (Frantz and Granick, 1992).

Thiol activation - To create a covalent linkage between a gold surface and a protein or polymer, a linker is required. Due to a natural adherence between gold and thiol ($-\text{SH}$) groups, alkane thiols with either carboxyl or amine end groups are the molecules of choice (Laibinis *et al*, 1989; Pale-Grosedemange *et al*, 1991). The use of thiol activation for the attachment of molecules to surfaces, especially for the use of SPR analysis, has been well documented in literature (Plant, *et al*, 1995; Debono, *et al*, 1996; Pierrat *et al*, 1997). After a surface has been activated, attachment to the surface can then be achieved by condensation reaction with amine, carboxyl groups or the aromatic rings of tyrosine and histidine (Williams and Blanch, 1994). These groups are either present on side chains of an activated polymer or on the protein of interest itself.

1.2.6 Polymers as transducer modifying agents

As stated in section 1.2.4, polymers can and are used extensively as transducer modifying agents. The use of polymers in this role is well documented. Polymers that have been used include:

carboxylated dextran (Lofas and Johnsson, 1990; Johnsson *et al* 1995; Lofas, 1995)

polyethene oxide - $\text{-OH}(\text{-CH}_2\text{-CH}_2\text{-O})_n\text{-H}$ (Huan *et al*, 1996)

carboxylated latex (Bastos-Gonzalez *et al*, 1995)

polyvinylalcohol-polyacrylic acid (Disley *et al*, 1997)

Synthetic polymers have been shown to be very durable, commercially available and relatively easy to conjugate to biological molecules (Scouten *et al*, 1995). Cross linking can be used to stabilise a polymer layer, but it may reduce the surface area available for interaction with the substrate, due to the reduction in sites available for receptor binding, and the reduced open volume within the polymer matrix. Both the polymer and the protein need to be attached with a given orientation in relation to the transducer surface, so as to retain the maximum functionality. This can be achieved by linking functional groups to the polymer or the receptors that are to be bonded to other molecules, and is discussed below.

There has been research into using two or more polymers on a surface. For example, Semonva and Savilova (1998) have shown that the interaction between the components a mixture of polymers (dextran and globulins) when deposited on a surface could be varied by modifying the concentration of components in bulk solution. They have also shown that modifying the molecular weight of polymers can change the space occupied by the polymer and thus alter the mesh size of the deposited matrix. To increase the usefulness of mixed polymer systems, polymers

with alternative functionalities have been used by Lui *et al* (1994). This method may have benefits for increasing the chemical and physical durability of a transducer by using a mixed polymer system in the place of a single polymer system, and introducing a broad range of functions to the interface. This may have the effect of increasing resistance of the transducer surface to damage when placed in a hostile environment (Weston *et al*, 1999). Alternatively, it may be possible to link one polymer to another, and in so doing, create an extended linked polymer chain (Pavey and Ollif, 1999), such as a multiple poly(ethylene oxide) or polyvinyl alcohol (PVA) molecules linked to a dextran backbone, as shown in figure 1.5.

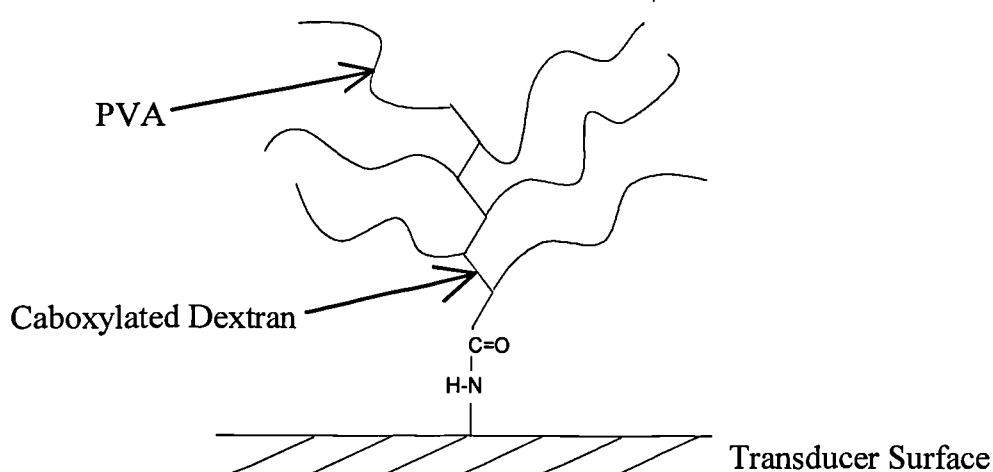


Figure 1.5 Representation of a mixed polymer system which utilises complex orientations – systems such as this have advantages over single polymer systems, as it is possible to use the characteristics of one polymer to link to the transducer, and the characteristics of the second to bind to the recognition molecule (modified from Pavey and Ollif, 1999).

The possibility of using mixed polymer systems with a combination of organic and inorganic polymers has been explored by Corriu *et al* (1992) who have used a combination of silica and organically substituted alkoxides to create complex porous ceramic interfaces, which could have uses in thick film biosensors. The possibility exists to create complex organic : inorganic polymer interfaces for use with optical

biosensors which could contain more functionality's than a simple mono-polymer interface.

1.2.7 Surface modification as an area to investigate

Within this thesis, biological surface science is of particular interest, as an understanding of the importance of polymer characteristics and ways to modify the created interface are central to the retention of biological activity of the immobilised recognition molecules. As the demand for micro sensors and total analysis systems (TAS) increases (Cowen, 1999), the need to integrate separation systems and active molecules to glass and silicon surfaces will increase.

Chemistries that are suitable for the creation of stable and reproducible interfaces and for can be used with high throughput manufacturing systems are of importance for the potential transfer of experimental production methods to high throughput manufacturing. For example systems such as Langmuir Blodgett (LB) films are in common use for laboratory based production of biosensor interfaces. The dip-coating method employed to create LB films is time consuming and space and labour intensive. The created films can be easily damaged and are therefore difficult to handle and package. These features restrict the use of LB films for commercial production of biosensors.

To further the research into the fabrication of biosensors, a variety of polymer systems and deposition methods will be examined to determine the characteristics which particular features impart to a sensor interface. Allied to this, liquid handling techniques will be examined in relation to deposition of interface components to examine systems suitable for effective high-throughput fabrication of biosensors.

1.3 Molecular Engineering of Active Biomolecules

Biologically systems can create molecules that are either difficult or impossible to artificially synthesis. However, these biological systems often have stringent requirements for effective operation, which may restrict their widespread technological use. By modifying molecules, both by replacing certain areas within the molecular structure, or by introducing additional side groups to the molecule, the protein function can be modified, making them more appropriate for non-natural uses, such as analytical systems (Hellings and Marvin, 1998).

Specific and sensitive receptors are need to detect small amounts of compounds in complex solutions. Antibodies have been widely used in this role, as they are both highly specific and sensitive to low concentrations of analytes (Kuby, 1991). The disadvantage of antibodies is that they are large molecules (150 kDa) and are easily disrupted or denatured, resulting in a loss of affinity. This is especially likely where antibodies are in contact with environmental or medical solutions that may contain proteases. The need for molecules which are smaller and more robust than whole antibodies has lead to the creation of synthetic molecules which have a complimentary structure to proteins and therefore can posses biological recognition (Lam *et al*, 1991; Takeuchi and Matsui, 1996). The use of antibodies and biomimetic receptors is discussed below.

1.3.1 Antibody technology

There are few molecules that surpass antibodies for their specificity and affinity for a target molecule. This specificity has been the principal reason that antibodies have been used extensively for biological detection systems, particularly in the form of RIA and ELISA. Initially polyclonal antibodies raised from a host animal were used (Kuby, 1991). Increasingly, monoclonal antibodies (Mab's) and antibody fragments (Fab's) derived from single cell expression systems have been used to increase specificity and improve assay performance. (Verma *et al*, 1998; Kramer, 1998)

As the need for affinity molecules with precisely defined characteristics has increased, antibody technology has developed by finding new expression systems for antibodies, such as plants, but also by engineering antibodies (George and Epenetos, 1996; Hayden *et al*, 1997). Antibody engineering has taken two principle forms. Firstly, antibodies are modified by an altered post-translational modification system to either remove parts of the protein or to introduce novel cofactors, such as defined carbohydrate groups (Hoffman and O'shannessy, 1988; Lu *et al*, 1996). Secondly, antibodies can be engineered at the genetic level, introducing a modified genetic sequence into an expression system, allowing pre-defined molecules to be produced.

The molecular biology of recombinant proteins is well defined within the literature. (Watson *et al*, 1992). The advantage of creating molecular engineered proteins over selecting Mab's, is twofold. Firstly, it is possible to alter proteins at the genetic level to change their function and attach or incorporate predefined groups within the primary structure of the protein, which will be engineered into the protein at the point of transcription.

A commonly seen group on engineered molecules is a polyhistadine tail (Carlsson *et al* 1996; Guergovakuras *et al*, 1999). This is subsequently used to purify the protein by affinity chromatography, but it can also be used to connect the protein of interest to the molecular support in an orientated manor (Mateson and Little, 1988) and has been demonstrated for sensor applications (Catimel, 1997).

Secondly, for large-scale production, bacterial expression has the potential to be considerably cheaper than the classical large mammalian derived systems (Verma *et al*, 1998).

This method has given rise to a variety of antibody variations, including single chain Fv fragments (scFv). The scFv has benefits over IgG derived Fabs as the protein does not rely on the interchain interactions to stabilise the protein structure and retain the conformation of the antigen binding site, and are therefore potentially more stable (Dogan *et al*, 1998).

An alternative to antibodies derived from mouse or rabbit has been the introduction of antibodies derived from camelids (lamas and camels). The advantage of camelid antibodies is that the antigen binding site is constructed from two heavy chains, not one light and one heavy as seen in other mammals (Vu *et al*, 1997). The variable heavy heavy (VHH) antigen binding site differs from the heavy chain – light chain in having an extended CDR3 loop to compensate for the lack of a variable light chain (Decanniere *et al*, 1999). The VHH binding domain is well suited to being expressed in a bacterial system, as the VHH structure is inherently stable and therefore can be expressed as a small fragment (Mulydermans and Lauwereys, 1999). This stability is also an important feature in the fabrication and use of immuno diagnostic systems.

1.3.2 Synthetic receptors

While monoclonal antibodies are an essential component of many bioanalytical systems, the cost of initially production and screening can often be prohibitive. Recently, alternatives to traditional affinity molecules have become available in the form of biomimetic receptors.

There is an increasing interest in the use of artificial receptors which mimic biological function (Kriz *et al*, 1995), due to the cost effectiveness of producing a well defined, artificial receptor, and the reduction in size which can be achieved. Perhaps the most significant feature of biomimetic receptors is that, due to the stability of the molecular framework, they can be used in harsh environments that would destroy biological derived systems.

Much of the current work on biomimetic receptors has centred on the use of crown ethers (Quici, 1999; Rimmel and Bauerle, 1999) and artificial peptide sequences (Lam *et al*, 1991), containing both L and D amino acids, to recreate the functionality that are found within the active sites of immunoglobulins and enzymes. The reduction in size when compared to IgG can be considerable. Some proposed artificial receptors have used as few as 8 amino acids (G. Bestettie, personal communication). While these systems show promise in theory, they overlook the role of the extended tertiary

structure of proteins, which is central to ensuring the correct spatial orientation of required active groups on individual amino acids. It is primarily for this reason that very small molecular weight receptors may be impossible to create for low molecular weight analytes.

Molecular imprinted polymers (MIP's) represent an area of increased interest. MIP's are created by using a suitable polymer that is mixed with a template molecule. The polymer is then cross linked and the template molecule is entrapped within the matrix. The template is then washed clear of the matrix, leaving a shape and chemical recognition pocket which can then be used as a receptor molecule (Takeuchi and Matsui, 1996). These receptors have been used for purposes as diverse as screening for lead compounds (Wright and Linck, 1996), solid phase extraction (Stevenson, 1999) and liquid chromatography (Tan and Remcho, 1998). While the use of molecular imprinted polymers has not been clearly demonstrated for optical sensors, there is a distinct potential for this technology to come to the fore in the near future.

1.3.3 Modulation of biological activity and applications for sensor regeneration

The biosensors that have reached large-scale production have generally utilised cheap disposable sensors external to the electronics needed to process the signal (Cass *et al*, 1984). One reason for this is that immunological systems are rarely able to release the bound analyte due to the high affinity between the antigen binding site and the epitope, therefore most biosensors that utilise immunorecognition molecules are used once and discarded. In cases where sensors can be regenerated, there is often a loss of sensitivity, due to both incomplete reversal of binding and damage to the biological layer caused by the aggressive chemicals used in the regeneration process. Commonly, either chaotropic agents, for example, 8 M urea (Guilbault and Luong, 1989), acid-glycine buffers (Bier *et al* 1994) or strong solvents, such as 85% ethanol in water, have been employed to disrupt the association between the recognition molecule and its substrate.

The use of protease for regeneration have reportedly been used to regenerate surfaces effectively over 600 times, but other systems have reported as much as a 10% drop in

sensitivity with every regeneration of the sensor surface (Wijesuriya, 1994). To date, the methods used for the renewal of recognition molecules have been both imprecise and overtly aggressive towards the sensor. An alternative method is required which will allow surfaces or bioactive molecules to be regenerated without the use of chemicals that have the potential to degrade sensor sensitivity.

1.3.4 Photochromic dyes and their role in bio-modulation

The use of photochromic molecules associated with proteins to modulate protein function, or photomodulation, is an area to which considerable research has been devoted, resulting in theories of photostimulation for biosensor applications (Rubin and Willner, 1994). Many of these systems are based around the use of photochromic dyes, which under exposure to certain wavelengths of light change not only colour, but also chemical structure. More significant even than this is the fact that under exposure to visible light, the reverse effect takes place. An example of this reaction is shown in figure 1.7.

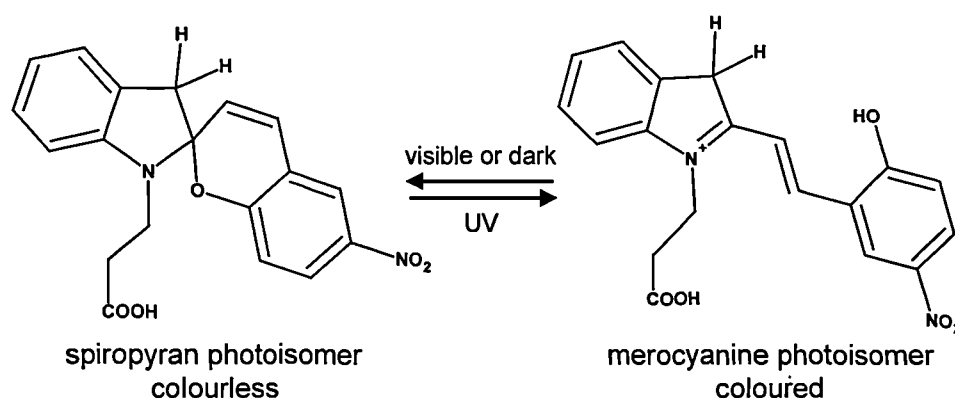


Figure 1.7 Schematic of the photo-isomerisation of the spiropyran dye (1'-(2-carboxethyl)3',3'-dimethyl-6-nitrospiro [2*H* – benzopyran-2'2indoline). Visible illumination converts the red spiropyran form into the yellow merocyanine form and the schematic represents the merocyanine form after a cis-trans isomerisation of the central double bond and protonation of the oxygen group. UV illumination reverses the conversion. In addition a slow dark conversion of the merocyanine to spiropyran form can occur.

There has been broad application of photochromic dyes to photomodulate the activity of proteins (Rubin and Willner, 1994; Zahavy *et al*, 1994) by direct attachment of a

photochromic dye to the protein. An overview of the methods and degrees of modulation obtained is shown in Table 1.1.

Table 1.1: The published results of the photomodulation of protein systems to date – the protein and its molecular weight are shown for comparison. The dye, coupling chemistry and modulation are shown to indicate the variability that has been achieved within and between experiments. For the modulation (%) column, positive figures imply an increase in activity, where as negative figures imply a decrease in activity. Where N is used, the feature of that system was not defined.

Protein	MW (kDa)	Dye	Coupling Chemistry	Modulation (%)	Reference
amylase	96	nitrospyrans benzopyran	DCC	-36	Aizawa (1977)
amylase	96	nitrospyrans benzopyran	DCC	-22	Namaba (1975)
Chymotrypsin	25	4-methoxyazobenzene	PPDS / DMAPN	N	Willner (1993)
Chymotrypsin	25	nitrospyrans benzopyran	PPDS / DMAPN	N	Willner (1993)
Chymotrypsin	25	4-carboxy azobenzene	PPDS / DMAPN	N	Willner (1993)
Chymotrypsin	25	azobenzene boronic acid	boronate	200 - 300	Westmark (1993)
Concanavalin A	37	N-propionic acid spiropyran	NHS Ester	300	Zahavy (1994)
Concanavalin A	37	4-carboxy azobenzene	DCC - NHS	~ 400	Rubin (1994)
Concanavalin A	38	N-propionic acid spiropyran	substitution	-60	Willner (1993)
Glutathione reductase	118	eosin isothiocyanate	Direct	~ 500	Willner (1994)
Papain	39	4-carboxy azobenzene	DCC - NHS	300	Willner (1991)
Papain	39	Azobenzene aldehyde	Thiohemiacetal linkage	630	Westmark (1993)
Ribonuclease	N	phenylazophenylalanine	HATU-DIPEA	-25	Lui (1997)
Urease	26	SP-propane anhydride	Direct	-30	Karube (1976)

The results of the published work (table 1.1) demonstrate that the effect of photomodulation are very different when the same enzyme is conjugated to either, spiropyran or azobenzene photochromic dyes. In the case of concanavalin A, conjugated to an azobenzene, there has been a reported increase in activity of 400 % when compared to the native enzyme (Rubin, *et al*, 1993), but show a reduction in activity of 60% when conjugated to a spiropyran. All of the enzymes which demonstrate a reduction in activity when photostimulated have been conjugated to nitrospyrans benzopyran, and generally show reductions of 20 – 40 % (Aizawa, *et al*, 1977; Namaba, *et al*, 1975; Lui, *et al*, 1997). This implies that the mechanism is fundamentally different between the spiropyrans and the azobenzenes, due to the differences in the chemistries of the compounds. Although widely investigated, none of these systems was generally accepted as the methods often involved a complex method using an unstable form of photochromic dye or resulted in a poor yield of the protein - spiropyran conjugate

In theory, if a simple and relatively non-aggressive method could be used for attaching photochromic dyes to both proteins and supporting matrices (Arai *et al*, 1996), this system could find broad application for the modulation of biological molecules and for the modulation of proteins and polymers. A suggested standard method involves the binding of a class of photochromic dyes, spiropyrans (Gugliemetti, 1990), to the biologically active component, via a carboxyl side chain (figure 1.7). The purpose of this is that once covalent attachment has occurred, the spiropyran dye is exposed to UV light to induce a change in chemical conformation.

It has been stated (Lareginie *et al*, 1996) that this change in conformation results in two alterations to the molecule. Firstly, there is the creation of a polarised charge at the nitrogen in the centre of the molecule, and secondly there is a change in the orientation of the two benzene rings from a non-planar to a planar arrangement as shown in figure 1.7. Either of these changes is significant in itself. A change in polarisation may result in the disruption of hydrogen, Van der Waals and electrostatic bonds in close proximity, therefore allowing a change in the tertiary structure of the protein. Conversely, a rotation in the orientation of the side groups of the spiropyran may result in steric hindrance of either the active site or a complimentary region that may limit the induced fit of the active site. Theoretically, either effect has the potential to induce a change within the binding site of the protein, and in so doing force the dissociation or prevent the association of the substrate with the binding site.

The reversal of the photochromic effect is achieved by illuminating the protein-dye complex with light of a suitable wavelength and intensity. This reverse illumination returns the spiropyran dye to its original state, and will allow the protein to revert to its native conformation, thus allowing the active site to regain its native conformation, leaving it available to function as before. The effect of photochromic-induced structural disruption on the active site of the protein has the potential to be so large as to in a reduction of protein activity equivalent to several orders of magnitude. This can be of benefit to both enzyme systems, where the activity of the protein can be reduced significantly if the system is saturated, and to antibody systems, where the potential exists to reverse antigen binding.

1.4 Conclusions drawn from current literature

The development of protocols for improved surface binding of proteins is central for the production of biosensors. Many systems to date fail commercially because they cannot easily be mass-produced (Alvarez-Icaza and Bilitewski, 1993). By developing systems that involve a series of simple steps or are preferably completely self-assembly from solution, sensor production will become both simple and economically viable. Consideration of techniques that are compatible with automated liquid handling systems should become a central issue in the initial design of biosensors, to aid the transfer of research scale production to commercialisation of a system.

While not the only option for modulation of protein activity, photochromic dyes may present the best, and most easily obtainable method of achieving reversible protein recognition, which in turn will lead to systems which can be used for continuous monitoring in a wide variety of situations. The application of photochromic modulation only becomes apparent when you consider the number of systems that would benefit from being reversible or able to be modulated.

The modulation of enzyme systems forms a convenient and accessible system for investigating the mode of action of photochromic modulation, but ultimately enzymes are a minor system that would benefit from modulation. Far more important are the molecular recognition systems of immunoglobulins and the strepavidin-biotin interaction. The ability to reverse these stable and specific interactions would lead to simple regeneration of bioassays of all kinds, resulting in considerable savings in both time and expense for clinicians.

1.4.1 Objectives

The aim of this project is to develop methods of molecular engineering for the adaptation and manipulation of protein and polymer systems primarily for biosensor applications. As a model system the technologies for biosensor fabrication will be

used, focusing on novel approaches to sensor fabrication in relation to ease of manufacture, reproducibility and durability of the sensor in use.

1.4.1.1 Polymer interfaces for biosensor transduction

The use of polymers for transducer modification is established for the production of optical biosensors. Within this thesis, the commonly used transducer modifying agent, carboxymethyl dextran, is compared to alternative systems to determine the optimum loading which can be obtained. To further this, mixed polymer systems will also be examined to examine if the functionalities of polymer interfaces can be controlled.

As a demonstration of the molecular engineering of polymer interfaces, an examination of the method of interface deposition for an effective method of optical transducer fabrication will be proposed, with emphasis being placed on methods that are applicable for mass manufacturing. The deposition and analysis of spatially defined heterogeneous arrays will be investigated to demonstrate the application of molecular engineering to the production of complex transducers.

1.4.1.2 Protein engineering for the modification of function

Photomodulation of proteins will be examined by the application of conjugation chemistries to modify protein systems with spiropyran dyes. Two systems will be examined in detail: enzymes and antibodies.

By choice of model enzymes, it is intended that photomodulation will be shown by comparison of native protein function and a spiropyran conjugated protein, it is intended to determine the degree of photomodulation which can be achieved by photomodulation. By comparing two or more protein models, the project aims to develop a theory of structure-based dye-protein interaction, which conforms to observed results.

To examine the relationship of molecular weight to degree of modulation, the corresponding IgG and Fab fragments will be modified by spiropyran conjugation and tested for affinity and reversibility for the same substrate. By use of an ELISA based assay, it is intended to effectively determine the activity and affinity of the systems examined.

2. General Materials and Methods

2.1 Introduction

Due to the nature of this project, the methods that are in common use throughout the following chapters are presented within this chapter. These are predominantly physical analysis methods, but also include the commonly used chemical methods. Materials and methods specific to individual chapters are presented at the beginning of the relevant chapter.

2.2 Materials

All chemicals and biochemicals were of analytical grade and were obtained from Sigma, Poole, Dorset, UK, unless otherwise stated.

2.3 Cleaning of surfaces

The surfaces used for subsequent modification, either for AFM imaging or as SPR surfaces should be free from particulate and chemical contamination. To achieve this, an acid wash and solvent wash were used.

2.3.1 Acid washing

To clean glass surfaces, the surfaces of interest were immersed in 0.5 M HCl (BDH code: 101254 H) and heated to 80 °C for 20 minutes. The acid solution was replaced with reverse osmosis water and sonicated for 10 minutes. The water wash procedure was repeated and the surfaces were then dried under a nitrogen atmosphere at 100 °C in a drying oven for 60 minutes.

2.3.2 Solvent washing

For glass surfaces, acid washing may induce etching of the surface, and to avoid this, a solvent wash, using acetone, was used as an alternative. The surfaces of interest were immersed in acetone (BDH code: 10003 ED, 99.5%) and sonicated for 10 minutes. The acetone was replaced with reverse osmosis water and sonicated for 10 minutes. The washing step was repeated once and the surfaces were then dried under a nitrogen atmosphere at 100 °C in a drying oven for 60 minutes.

2.4 Silanisation of surfaces

To covalently immobilise polymers and proteins to surfaces such as glass and metals, it is necessary that the surface be modified to introduce functionalities that are compatible with existing covalent immobilisation chemistries. Glass, silicon and metals (Sasaki *et al*, 1998; Weiping *et al*, 1999) can be silanised to allow the introduction of active groups to the surface of a substrate, for example, primary amines (Jonsson *et al*, 1985).

While the immersion method for silanising glass has been well documented (Ariga and Okahata, 1989; Weiping *et al*, 1999), it has several disadvantages. Firstly, variability in the water content and purity of solvents may result in poor deposition or an irregular layer of silane, and secondly, the process creates a considerable amount of toxic waste, in the form of waste organic solvent. To avoid these problems, a vapour phase method was adopted from Jonsson, *et al* (1985) which takes advantage of the volatility of (3-aminopropyl) trimethoxysilane (APTS).

A previously unused glass desiccator was taken and 100 ml of self-indicating silica desiccant (Merck code: 30062) placed in the bottom. A small glass petri dish is placed on the silica desiccant, into which 2 ml of APTS (Sigma code: A3648) is pipetted. Acid washed slides were supported on a steel mesh above the APTS. This allowed nearly all of the surface area of the glass to be exposed. The desiccator was sealed and gently heated at 35 °C on a ceramic hotplate for 30 minutes, to aid vaporisation of the APTS. The slides were left to incubate for 6 hours, at which time the desiccator was flushed with nitrogen gas for 30 minutes to remove any excess silane vapour. The modified slides are stored in a desiccator until used.

2.5 Surface examination by contact angle measurement

Contact angle measurement is often used as a method to determine the hydrophobic/hydrophilic characteristics in surface free energy of a surface of a material (Dubois, Zegeraski and Nuzzo, 1990), and from this determine the chemical and physical nature of the surface of interest. This can be used to monitor the effect that modification processes have on a surface of interest.

Throughout this work the sessile drop method was used (Jonsson *et al*, 1985). In brief, a known volume of liquid, usually water, was placed on the surface of interest, and the height and width of the droplet measured. From these measurements, the contact angle can be calculated as shown in figure 2.1.

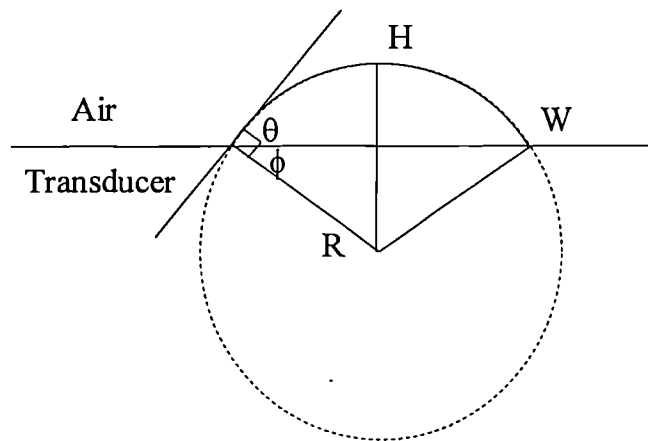


Figure. 2.1 A representation of a droplet as a sector of a circle - the profile of the droplet was taken to represent a sector of a circle, radius R , where H is the height and W the width of the droplet.

By using the equation:

$$\phi = \tan^{-1} \left(\frac{\frac{W^2}{4H} - H}{W} \right)$$

the contact angle, θ , can be calculated by:

$$\theta = 90 - \phi$$

Two practical approaches were used to determine the contact angle:

A) Travelling microscope measurements: a 100 μl droplet of water was applied to the surface of interest. A travelling microscope was used to measure and record the angle between the tangent to the droplet at its intersection with the surface, the height and width of the drop. This process was repeated three times, and the average of the measurements calculated. Eight to twelve droplets were measured for each surface of interest, to allow a representative mean and standard deviation to be calculated.

B) CCD camera measurements: a CCD camera (model MCD400S, Spectra Source Instruments, California, USA) was used with a 25 mm C mount lens (Computar, Japan) and two 8 mm extension rings, resulting in a maximum magnification of 5 times. Deposited droplets were viewed side on to determine the contact angle tangential to the surface.

The resolving power of the image was determined by the pixel resolution of the camera. The image obtained from the CCD camera was stored as a TIF image file, and analysed via a common image handling software package (Paint Shop Pro, version 3.11, JASC Software, Eden Prairie, MN 55344 U.S.A.). Values for height and width of the droplet were determined by counting the number of pixels each measurement covered and the contact angle calculated from these.

The travelling microscope was initially used, but was replaced by the CCD-based system when it became available. The use of a CCD camera allowed measurements to be collected more rapidly than the travelling microscope, therefore allowing a greater number of samples to be tested. The disadvantage of the CCD-based method of measurement and calculation is that any inherent error in measurement, due to pixel resolution, is magnified by the contact angle calculation.

While the travelling microscope has a smaller measurement error than images recorded with the CCD camera, the CCD camera was used as it allowed a higher throughput of measurements, enabling a more representative data set to be recorded.

2.6 Atomic Force Microscopy

Atomic force microscopy is a method for examining the physical characteristics of surfaces at high spatial resolution. For this project it has been used to examine deposited polymer layers and determine the variations which occur with differing deposition conditions.

2.6.1 General Theory

Atomic force microscopy (AFM) is a method of surface analysis that has been broadly used in recent years (Cullen and Lowe, 1994; Hayes and Cullen, 1997; Kossek *et al*, 1998; Ramachandran, *et al*, 1998; Steele *et al*, 1998). While the resolution of AFM can be as fine as electron microscopy, there is little need for extensive sample preparation, and as such less chance of systematic artefacts being found.

For solid surfaces, AFM can scan the surface with little or no damage to the surface of interest. With softer samples, such as those which are reported here, the possibility of sample dragging, tip fouling and inappropriate surface etching are possible (Weisenhorn, *et al*, 1993). These artefacts are only easily recognised by experience, and as such, interpretation of AFM images requires careful consideration based on results of known samples and the published literature. To determine that a representative sample was recorded, surfaces were sampled in four different locations to determine if observed features were commonly occurring. Up to 6 sample surfaces per condition were prepared and imaged to remove observed sample to sample variation.

2.6.2 AFM equipment and settings

The AFM used in the current work was a ResolverTM atomic force microscope, manufactured by Quesant Instrument Corporation (CA, USA) and purchased from Nanovision Ltd. (Slough, UK). A scanner of 40 μm maximum X-Y scanning range was used for all measurements. The AFM was connected to a 60 MHz Pentium PC, running Quesant standard scanning and analysis software (Ver 2.459) under Microsoft Windows 95TM. Silicon nitride cantilevers with standard pyramid tips were supplied

by Nanovision Ltd. and mounted in house. The tips used had nominal spring constant of 0.032 Nm^{-1}

The scanning parameters used for all images, unless stated otherwise, are given in Table 2.1.

Table 2.1 AFM Scanning Parameters – a definition of terms are given in the Quesant Resolver AFM manual (Quesant Instrument Corporation, Agoura Hills, California USA).

Parameter	Value
Scan Area	10 x 10 μm
Scan Rate	2 Hz
Setpoint Offset	0
Scan Direction	90°
Scan Resolution	400
Z-Dynamic Range	4 μm
Image Mode	Z height
Integral Gain	100
Proportional Gain	100
Derivative Gain	20
Laser Mode	constant
Z Input Gain	X 1
X/Y Disable	no
Scan Profile	hills and valleys

All image data was collected in contact imaging mode. All AFM images had nominal image processing applied to them (1st order polynomial levelling) to remove effects of tilt on the sample surface. No smoothing was applied to the images. Results are presented as Z height topographic images throughout.

2.7 Surface Plasmon Resonance

The techniques described previously provide information on the surface energy and spatial organisation of surfaces. To complement this, surface plasmon resonance has been employed to interrogate surfaces as they are modified to determine the average mass of material, as a function of refractive index change, that is attached to the surface.

2.7.1 General Theory

SPR is a phenomenon that can be caused by the interaction of light with thin metal films, predominantly gold or silver, coated on a transparent substrate. The reflected intensity of light of a certain wavelength from the transparent substrate surface decreases with the angle of incidence until a critical angle, θ_C , is reached, when the light is total reflected from the substrate. If a thin metal film is present on the surface of the substrate, weak attenuation of the incident light occurs, due to absorbance. This effect, total internal reflection, occurs for all angles greater than θ_C . When the surface of the substrate is coated typically with a 50 nm layer of metal, there is a second angle greater than θ_C , where the light is absorbed strongly by the metal film due to the excitation of surface plasmons. This effect only occurs for light of transverse magnetic (TM) polarisation.

Surface plasmons are oscillations of the electrons at the boundary of the metal film that propagate along the boundary metal layer and constitute surface plasmon waves (Davies, 1994). When the properties of the incident light matches the optical properties of the surface plasmons in the metallic film, the electrons resonate, creating surface plasmon resonance. The angle at which this occurs is θ_{SPR} , and is accompanied by a decrease in the reflected light, and it is this characteristic angle which is recorded in typical SPR experiments.

As interactions occur at the surface of the metal film, such as antibody-antigen binding, the θ_{SPR} changes, and it is this $\Delta\theta_{SPR}$ which allows the change in refractive index that occurs between a native surface and a modified surface to be determined

(Green *et al*, 1997). If the refractive index of the interface component is known, it is possible to determine the thickness of the layer attached to the surface (Davies, 1994).

2.7.2 SPR equipment

The SPR equipment used throughout the current work was built in-house using optical components mainly obtained from Melles Griot (Cambridge, UK). The system was designed around an optical prism, (10mm 60° prism SF15, Optical Technologies, Ongar Essex, UK), in the Kretschmann configuration (Kretschmann, 1971). A schematic diagram of the equipment is shown in figure 2.2.

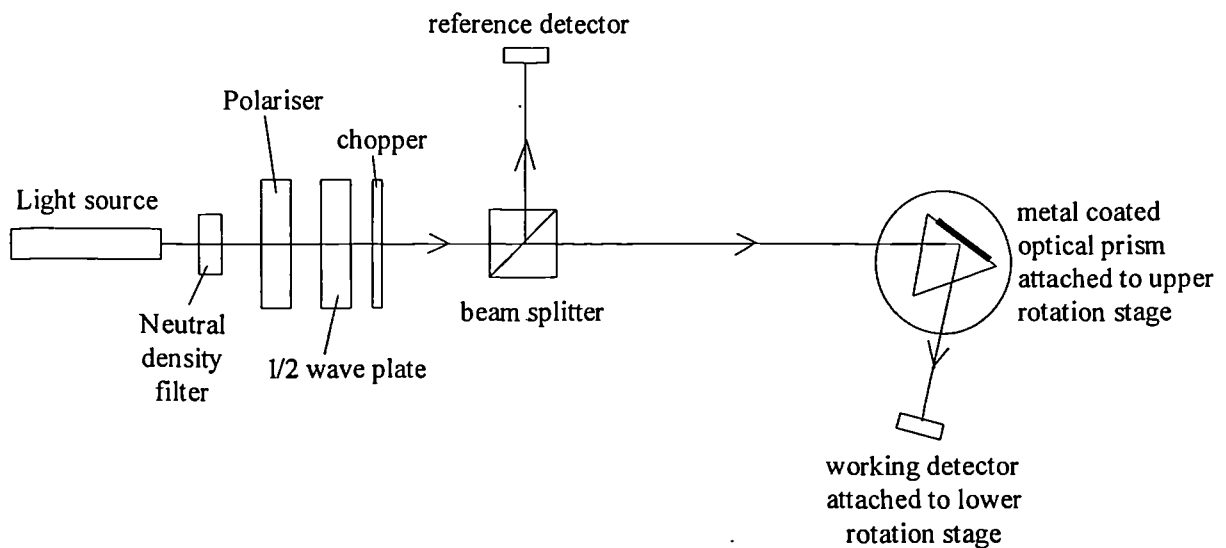


Figure 2.2 A schematic of the apparatus used for SPR experiments

The parts used for the SPR system were mounted on a 600 x 300 mm optical table, with M8 mounting points at a separation of 25 mm centre to centre. A parts list is shown in table 2.2

Table 2.2 Parts list of the SPR system – all parts obtained from Melles Griot (Cambridge, UK).

Part	Code
optical rail (50 x 500 mm)	007ORN003
optical rail carrier	07CN501
post holder (80 mm)	07PHS006
mounting post	07RMS003
laser holder	07HLC003
gimbal Mirror mount	07RES004
mirror (pyrex) W/011 25 mm dia	02MFG015
lens holder	07 LHF007
polariser holder	07HPR001
iris diaphragm holder	07HID001
pin actuated diaphragms	04IDC005
kinimatic prism table 25 mm ID	07MHT045
translation stage	07TSC504
X-Y-Z translation stage	07TMC521

In brief, the light source used was a laser diode emitting light at a wavelength of 670 nm. The light was passed through a neutral density filter to reduce the light intensity to prevent saturation of the detectors. A polariser is used to produce a plane polarised beam. A half wave plate is used to rotate the plane polarised beam to either transverse magnetic, where SPR occurs, or transverse electric, which is used as a reference. A beam chopper is used to produce a modulated light source at a frequency of 220 Hz. This allows the detectors to be phase sensitive, by using an analogue to digital interface and Labview software to identify the frequency dependent component at 220 Hz, thereby allowing rejection of ambient light sources.

The light path passes through a beam splitter, where half the light is reflected to a reference detector. The output of the reference detector was used to correct for fluctuations in the intensity of the light source. The remaining light interacts with a metal-coated prism positioned on a rotation stage. A detector is attached to a second rotation stage. The prism rotates through the angle at which SPR occurs, with the detector stage rotating twice as far to match the change in angle that occurs as light is reflected from the metal film.

The system described is an evolution of the SPR system described in Cullen, *et al* (1988) and Cullen and Lowe (1990).

2.7.3 Metal deposition to solid surfaces

For surface plasmon resonance studies, either silver (99.99% pure, Aldrich code: 26,743-0) or gold (99.99% pure, Aldrich code: 26,579-9) films were coated onto optical glass prisms (10mm 60° prism SF15, Optical Technologies, Ongar Essex, UK). An Edwards 306A vacuum evaporator, equipped with a high vacuum diffusion pump and resistively heated evaporation boats, was used in all cases. The cleaned prisms were supported on a cradle above the evaporation boats in which silver or gold was placed. The evaporator was sealed and evacuated to a pressure of $1 - 2 \times 10^{-6}$ atmospheres. A 0.4 nm adhesion layer of chromium (chrome plated tungsten rods, code NR1. Megatech, Cannock, Staffs, UK) was deposited onto the surface at a deposition rate of 0.05 nm/s. On to this, the metal of interest was deposited at a deposition rate 0.1 – 0.15 nm/s until the desired thickness was reached. The thickness required for optimum SPR excitation is approximately 50 nm. When the metal films had been deposited, the prisms were allowed to cool under vacuum for 30 minutes. The deposited surfaces were removed from the evaporator and then stored under vacuum until used.

2.7.4 Angular-based scans

The simplest method of scanning with the SPR arrangement is to determine the angular position at which the SPR minima occurs. This is achieved by aligning the prism to 0° and then rotating it to a starting angle, 44° in air and 10° in liquids. These starting points are higher than both the SPR minima and the angle of total internal reflection. The detector is aligned to the point of highest reflectance, determined by the detector output in volts.

A scan is initiated which progresses the prism and detector by x and x_2 degrees respectively over a determined range, usually 8 – 10° external angle. Over this range of angles, the SPR response occurs as a dip in reflected intensity. As subsequent modifications and depositions are made to the metal surface, further angle scans are

performed. The change in the angle at which the minima occurs is determined, and this allows the amount of material deposited on the surface to be determined.

2.7.5 Time-based studies utilising SPR

While the effect of change at the metal interface of an SPR prism is to change the angle of the reflected minima, it is possible to study an effect over time by measuring the shift in reflectance from the linear portion of the SPR dip towards reflectance at higher external angles. As the reaction at the surface of the interface progresses, the SPR dip will move towards a lower internal angle, and as such the reflectance at a given angle will change. This change is measured as a function of time and thus shows the rate of reaction at the surface.

An angle scan is performed with the surface in contact with an appropriate buffer. From this scan, the angle at which the linear portion of the falling arm of the SPR dip finishes is determined. This is the angle at which the time scan will be conducted. Figure 2.3 shows a representation of an SPR response, the angle to select for a time scan and the direction of the SPR shift.

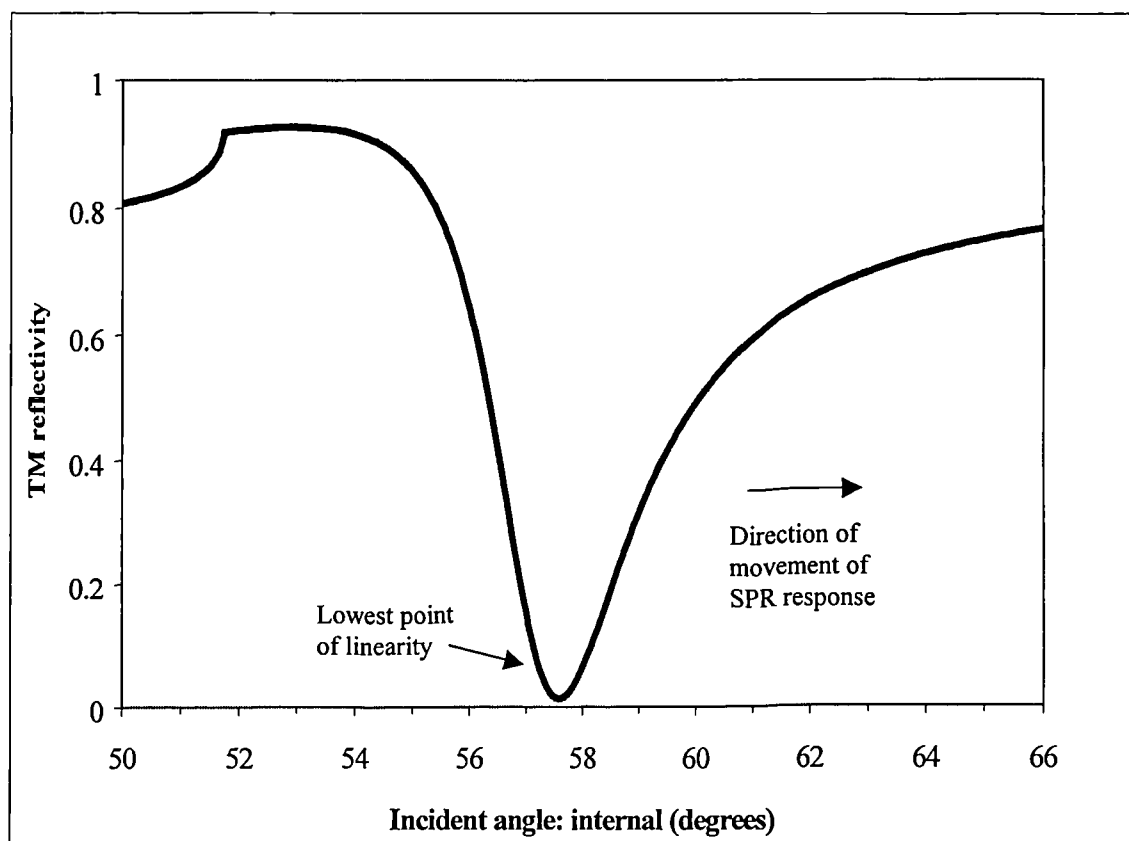


Figure 2.3: The result of an SPR angle scan showing the angle chosen for subsequent time scans.

A time scan is instigated and allowed to progress for 2 – 5 minutes to provide a stable base line for the experiment. After the base line has been established, the solution of interest is introduced to the liquid cell. As the time scan progresses and adsorption or covalent interaction occurs at the metal surface the signal from the reflected light will vary. The rate at which interaction occurs can be determined from the change in reflected intensity over time. When the time scan is complete, an angle scan is carried out to confirm the absolute shift in reflectance minima over the course of the experiment.

2.7.6 Scanning in air

To determine the presence of SPR response from a prepared surface, an initial scan in air is performed prior to more complex experiments. A prepared prism was placed in the SPR prism holder and the laser aligned with the prism and the detector. The prism is scanned (0.1° resolution) with transverse magnetic (TM) polarised light, between 44° and 36° external angle to determine the angular position of the intensity minima.

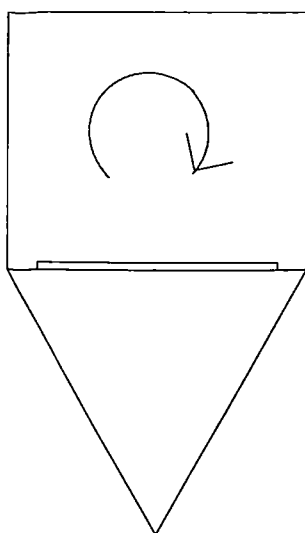
This scan was repeated with transverse electric (TE) polarised light. The TM and TE scans were then ratioed together to give a normalised result of the SPR response.

2.7.7 Scanning in liquids

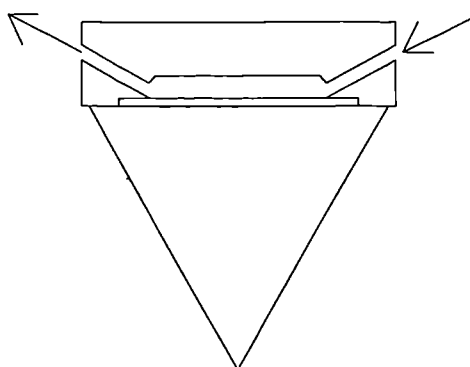
The majority of surface experiments are performed in a liquid medium, either water or buffer. Scanning in liquids is performed as for in air, with the reflectance minima scanned for between 10° and 0° external angle.

There are two common ways which SPR is used when measuring deposition from solution. Firstly, a static cell, (figure 2.4a) where a known solution is kept in contact with the surface of an SPR prism for an extended period, and solutions are removed and added to the top of the open cell. Secondly, a flow cell (figure 2.4b) is attached to the back of the SPR prism, which allows rapid exchange of active solutions and buffers.

These two methods of solution based SPR are used for different purposes as the solutions interact with the surfaces in different ways.



A)



B)

Figure 2.4: a representation of static (A) and flow liquid cells (B) for SPR analysis - while simple to use, static cells rely on convection to replace reagents at the active surface. Flow cells represent a dynamic system with active replacement of reagents, but the possibility of carry over of reagents and interference from trapped air can result in high base line signals.

While simple to use in operation, the static cell has several limitations. To add reagents during a time scan, concentrated solutions must be added to the buffer solutions within the static cell. The addition of small volumes of concentrated solutions can introduce variation in solution conditions, by resulting in incomplete mixing, which may not be present, if a flow cell is used.

Flow cells are more complex to set-up, but when in operation, work in a similar way to any flow based analysis system. A buffer solution is passed through the flow cell and allows a base line of response to be obtained. Active solutions are then either injected into the buffer flow or used to replace the buffer for a given volume. For a fixed flow rate, this equates to the active solution being in contact with the SPR surface for a specific time. After the active solution has passed through, it is followed by buffer to allow any unreacted or unadsorbed reagent to be removed from the surface.

2.7.8 Data analysis of SPR results

By creating a ratio of the reference and working detector output, a normalised signal independent of the light intensity is generated, The external incident angles are converted to internal angles using Snells law. This allows results to be presented in a manner consistent with published data.

2.8 Chemistries for Modification of the Transducer Interface

For the convenient covalent attachment of carboxylated compound to aminated surfaces, a water soluble heterobifunctional cross-linking agent is needed. 1-ethyl-3(3-dimethyl amino propyl) carbodiimide (EDC) is used as a zero length cross linker, as it catalyses the formation of amide bonds from free amine and carboxyl groups (Timkovich, 1977) while not introducing any extra molecules to the linkage. When EDC is used as a catalyst for immobilisation assays, N-hydroxy succinamide (NHS) is often used to increase the rate of reaction (Hermanson *et al*, 1992).

2.8.1 Covalent coupling of carboxylated polymers to aminated surfaces via EDC reactions

To modify carboxylated surfaces via EDC-NHS reactions, the surfaces are prepared to be clean and dry and to possess amine groups on the surface of the solid substrate. The polymer of interest is made as a solution, 0.1% (w/v) in 0.1 M MES buffer, pH 6.8. Up to 30 mg/ml EDC (Sigma code: E-7750) and 15 mg/ml NHS (Sigma code: H-7377) were added to the solution. An aliquote of this solution is brought into contact with the aminated surface of interest and allowed to incubate at room temperature for up to 2 hours. The surface is then washed three times with RO water and dried under nitrogen at room temperature.

2.8.2 Covalent coupling of proteins to carboxylated molecules via EDC reactions

A protein solution was made by dissolving 5 mg of the protein of interest in 10 ml of 0.1 M MES (pH 6.7). up to 50% ethanol could be used if the protein proved insoluble in 0.1 M MES. A 0.1% solution of the carboxylated species of interest was dissolved in 10 ml of 0.1 M MES (pH 6.7). The protein solution and carboxylated species are mixed and allowed to equilibrate. Up to 30 mg/ml EDC (Sigma code: E-7750) and 15 mg/ml NHS (Sigma code: H-7377) were added to the solution, which was then allowed to react for upto 4 hours, with gentle mixing at room temperature. (Hermanson *et al*, 1992)

To purify the conjugate, size exclusion chromatography was used. A Sephadex G25 PD 10 column (Pharmacia, Uppsala, Sweden) is equilibrated with ten 2.5 ml aliquots of buffer of the same component parts as that used in conjugation reaction, section . The PD 10 column has optimum performance with aqueous based buffers, but up to 75% methanol or 85% ethanol may also be used. When the column had equilibrated, a 2.5 ml aliquot of the protein conjugated was applied to the column. The high weight of the conjugated protein prevented the synthesised species from passing into the beads and will therefore pass through the column in the void volume and be present in the 4th or 5th fraction that is eluted from the column. The amount of protein in the purified fractions is determined by absorption at 280 nm using an M350 UV/visual spectrophotometer (Camspec, Cambridge, UK.).

Chapter 3: The use of polymers to modify transducers

3.1 Introduction

Molecular engineering has a range of potential applications in biosensor technology. One of the principal features of biosensors is the need to attach the biological or biomimetic recognition molecule to a transducer. The transducer surfaces currently used vary widely, and include screen-printed electrodes and metal coated glass surfaces (Galan-Vidal *et al*, 1995; Nascimento and Angnes, 1998). Increasingly, new and novel surfaces are being used as transducer surfaces. Surfaces currently being investigated include optical silicon transducers and silicon semiconductors in the form of field effect transistors (Jaffrezic-Renault and Martelet, 1997). As the range of materials used for biosensors and other microanalytical systems increases (Barrow *et al*, 1999), the ability to modify surfaces with common materials and methods will be brought to the fore.

3.1.1 Modification of the Transducer Surface

An effective modification of the transducer surface for affinity sensors has two criteria that it should address. Does the interface reduce non-specific binding, and as such reduce the lower limit of detection (LLOD) of the system, and is the surface loading of active receptor molecules increased compared to physically adsorbed surface, thus increasing the detection potential of the system (Piehler *et al*, 1996).

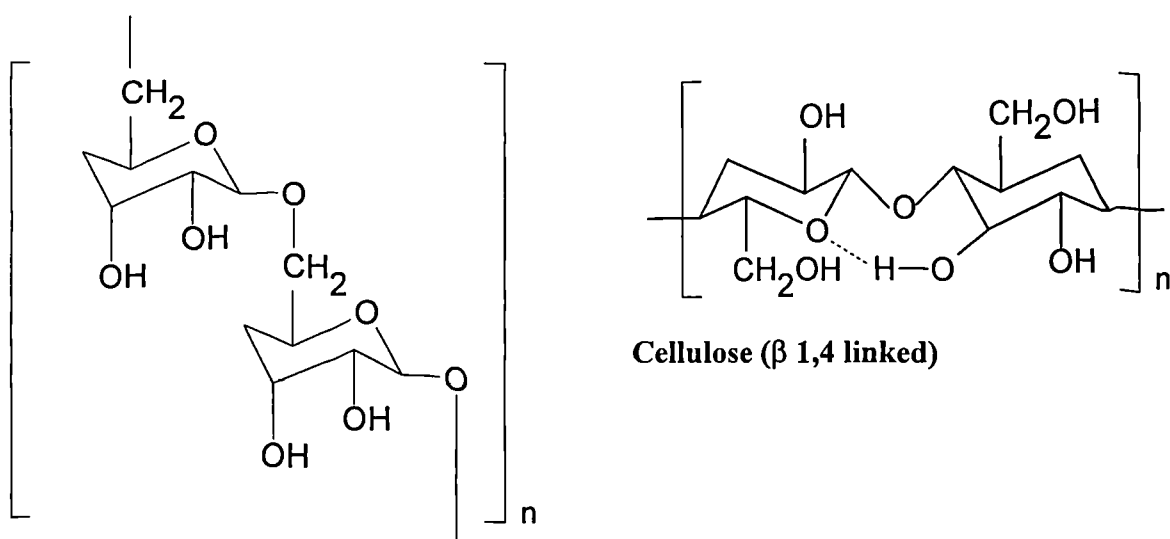
For biosensors, one of the central issues is the amount of biological molecule that is present within the active region of the biosensor interface. In the case of optical evanescent wave based sensor systems, this region can typically extend up to 300 nm from the transducer surface, for use with light of wavelength 670 nm (O'Shannessy, *et al*, 1993). The concentration of available biological component per unit surface area, or surface loading, is central to the sensitivity and LLOD of the sensor. In theory, the smaller the molecular weight of the biological molecule, the greater the possible molar loading for a given area. Alternatively, by increasing the surface area, by way of extended interfaces such as porous polymer layers (Johnsson, *et al*, 1995; Lofas, 1995), the three dimensional surface area is increased considerably over the flat surface area, as introduced in Chapter 1.

3.1.2 The application of carboxylated glucose polymers to modify transducers

Carboxylated polymers are currently the system of choice for the modification of optical transducers (Buckle *et al*, 1993; O'Shannessy *et al*, 1993; Catimel *et al*, 1998; Howell *et al*, 1998). By adhering a polymer with hydrophilic properties to the surface of a sensor levels of non-specific binding can be reduced. Polymer interfaces can also increase the number of possible biological receptor molecules that can be bound in close proximity to the surface. The most commonly used polymer is carboxylated dextran, this being the modifying agent used in many of the commercially available optical biosensor systems (Lofas *et al*, 1993; Karlsson *et al*, 1991).

Dextran is a hydrophilic linear polymer based on 1,6-linked glucose units. Synthesis of carboxylated dextran is relatively simple. By treatment with bromoacetic acid, carboxyl groups can be introduced to the dextran backbone (Lofas and Johnsson, 1990), which can then allow linkage of the dextran to amine groups commonly present on proteins using established covalent coupling chemistries, such as water soluble carbodiimides (section 2.7.1).

The differences between various polymers of glucose are due to the mode of polymerisation. The cross sectional, rigidity and persistence length area of the polymers varies due to the linkage that is present between the glucose residues. For cellulose, this results in an 'edge on' stacking of the glucose subunits, whereas dextran has an "overlapping", or "stepped", relationship between glucose subunits. This is shown in fig. 3.1.



Dextran (α 1,6 linked)

Figure 3.1 Molecular Structures of Cellulose and Dextran - cellulose is stabilised by the presence of hydrogen bonds (----) between the hydroxyl and oxygen of adjacent monomers. This bond ensures that cellulose is a more rigid molecule than dextran. It is this feature which accounts for the mechanical strength of cellulose.

This difference in cross sectional area may not be significant if a single polymer is used to modify a transducer, as the polymer chains will, ideally, form a packed hexagonal structure (Chidsey and Loiancono, 1990). Where the two polymers are used as a mixed system, the interface will involve two or more distinct phases of different cohesive energy and will be more interfacially dynamic. This can result in greater heterogeneity than exist for single polymers (Andrade, 1994), which may lead to a structure which is more open, and thus allow a greater degree of diffusion of analyte across the transducer surface.

The use of a single polymer to modify transducers is in common practice, but may limit the characteristics of the biosensor surface. The use of a mixed polymer system may increase the range of features that an interface possesses. For example, while some systems allow a high surface loading to the interface, they may suffer from chemical or biological instability when introduced to an aggressive environment. The use of two or more polymers as a mixed interface may result in system that has enhanced characteristics when compared to single polymer system.

3.1.3 Aims

Carboxymethyl dextran (CMD) is currently the most widely used and therefore, well characterised, of the carboxylated biologically derived polymers. In the following experiments, CMD has been compared to carboxymethyl cellulose (CMC) and mixed polymer systems to determine whether it is the transducer modifying agent with optimum loading capacity and stability for use with optical biosensors, and if so, why it is the optimum system.

To determine whether the characteristics of the transducer interface could be modified by the introduction of polymer other than a glucose polymer, a carboxylated straight chain aliphatic polymer, carboxylated polynoxylin, was synthesised and used as a component in mixed polymer systems.

In addition, the biological degradation characteristics of single and mixed polymer systems were examined to determine if there were benefits to a mixed system other than the surface loading of the biosensor interface.

3.2 Materials and Methods

3.2.1 Materials

Carboxymethyl dextran (carboxyl : glucose ratio: 1:3) was obtained from Fluka (code: 27560). Carboxymethyl cellulose (Avg. Mol. Wgt: 480,000, carboxyl : glucose ratio: ~1:4) was obtained from Sigma (Sigma code: C5678). Polynoxylin was obtained from Borden Chemicals, Southampton, UK. (Product code: UP10) The molecular weight and other details were not available for this reagent. All other reagents were as specified in Section 2.2.

3.2.2 Covalent attachment of carboxylated polymers to APTS modified surfaces

Both glass and silver surfaces have been used for analysis of polymer immobilisation. These surfaces were functionalised by silanisation with APTS (Section 2.4) resulting in primary amines being present on the surface.

The polymer of interest is made as a 0.1% (w/v) solution in RO water. This solution is activated by the addition of 2 mg/ml 1-ethyl-3(3-dimethyl amino propyl) carbodiimide (EDC) (Sigma code: E1769) and 1 mg/ml N-hydroxy succinamide (NHS) (Sigma code: H7377). A 50 µl aliquot of this solution is pipetted onto the APTS - modified surface and allowed to incubate for 30 minutes in a saturated water vapour environment to control evaporation from the surface of interest. The remaining solution is then washed clear with 3 ml of RO water and the surface is dried under nitrogen.

3.2.3 Covalent attachment of carboxylated polymers to pre-aminated microtitre plates

The use of microtitre based assays allows multiple repeats of conditions and rapid screening of various experimental parameters which are difficult to obtain with AFM and SPR based methods. To provide a microtitre well surface that is similar to the surfaces used for optical biosensors, a method has been devised to modify commercially available plates with carboxylated polymers.

The polymer of interest is made as a 0.1% (w/v) solution in RO water. This solution is activated by the addition of 2 mg/ml EDC (Sigma code: E1769) and 1 mg/ml NHS (Sigma

code: H7377). An aminated microtitre strip plate (Corning Costar, code: 2338) is taken. Aliquots of 100 µl of the activated polymer solution are pipetted into each well of the microtitre plate and allowed to incubate at 20 °C for 40 minutes. At the end of incubation, the plates are washed three times in RO water.

3.2.4 Covalent attachment of proteins to carboxylated polymers

The method for covalent attachment of biological molecules to carboxylated polymers is similar to the covalent attachment of carboxylated polymers to amine-modified glass, metals and microtitre plates.

The protein of interest is made as a 100 µg/ml solution in 0.1M MES buffer solution, pH 6.8. 1.5 mg/ml EDC is added to the protein solution of interest. For modified glass and metals, the surface is flooded with 100 µl of the EDC/protein solution and allowed to incubate at 20 °C for 40 minutes. For microtitre plates, aliquots of 100 µl of the EDC/protein solution are pipetted into each well of the microtitre plate and allowed to incubate at 20 °C for 40 minutes. At the end of incubation, surfaces are washed once in RO water, once in a solution of 0.1% Tween 20 in RO water and three times in RO water.

A 100 mM solution of glycine (Sigma code: G-6761) is made in phosphate buffered saline (PBS), pH 7.4. Aliquots of 100 µl of the solution are pipetted onto the surface of interest and allowed to incubate at 20 °C for 40 minutes. At the end of incubation, the surfaces are washed once in RO water, once in 0.1% Tween 20 and three times in RO water. The glycine acts a blocking agent for EDC activated carboxyl groups, and allows the polymer interface to retain a negative charge, due to the free carboxyl group on the immobilised glycine.

3.2.5 Synthesis of carboxylated polynoxylin

2 g of polynoxylin (Borden Chemicals, Southampton, UK) was dissolved in 250 ml of 0.2 M H₂SO₄ (Sigma code: S-1526) at 60 °C. 0.5 M KMnO₄ (Sigma code: P-9810) was added dropwise to the solution. As the polynoxylin is oxidised, the KMnO₄ was decolourised and an insoluble precipitate of manganese dioxide was formed. At the first indication of retention of colour, no further KMnO₄ was added and the solution was left to incubate for 30 minutes,

after which time, KMnO_4 was added until colour persists. This process was repeated until the colour did not degrade with time. When the solution had cooled, it was centrifuge at 1500 G for 5 minutes to remove any insoluble manganese dioxide.

The resultant polynoxylin carboxylic acid solution was decanted and 0.1 M NaOH was added until the polynoxylin carboxylic acid formed polynoxylin carboxylate and precipitated out of solution. The polynoxylin carboxylate was centrifuge at 1500 G for 5 minutes to form a pellet of product. The supernatant was decanted and discarded. The polynoxylin carboxylate was resuspended in 0.1 M NaOH and centrifuge again. This washing step was repeated twice. The polynoxylin carboxylate was resuspended in RO water and 0.1 M HCl was added until the carboxylic acid was formed and subsequently dissolved. The purified polynoxylin carboxylic acid was freeze dried for long term storage.

3.2.6 Microbiological screen for resistance to biological degradation of polymer components for biosensor fabrication

Biological degradation of the polymers was examined by incorporation of the polymers of interest into a mineral salts medium solidified with 2% w/v agar (Lab M No2). The mineral salts medium, designated FAM2 (Table 3.1), was developed for the enrichment of bacterial strains capable of growth on recalcitrant carbon sources (F. Taylor, personal communication).

Table 3.1: The constituents of FAM2 Medium - 2.5ml of trace elements solution are added per litre of salts solution, and autoclaved. The medium was made up 10 x concentrated and stored at 4°C.

Trace elements: solution components

Salt	g/L.
ZnSO ₄ .7H ₂ O	0.232
MnSO ₄ .4H ₂ O	0.178
H ₃ BO ₃	0.056
CuSO ₄ .5H ₂ O	0.100
Na ₂ MoO ₄ .2H ₂ O	0.039
CoCl ₂ .6H ₂ O	0.042
KI	0.066
EDTA	0.100
FeSO ₄ .7H ₂ O	0.040
NiCl ₂ .6H ₂ O	0.0004
0.1 M H ₂ SO ₄	8 µL.

Salts: solution components

Salt	g/L.
NaNO ₃	0.85
KH ₂ PO ₄	0.56
Na ₂ PO ₄ (.2H ₂ O) (.12H ₂ O)	0.86 (1.08) (2.17)
K ₂ SO ₄	0.17
MgSO ₄ .7H ₂ O	0.037
CaCl ₂ .2H ₂ O	0.007
Fe III EDTA	0.004

Polymers were presented at a concentration of 2%w/v in FAM2 agar. A positive control to demonstrate optimal bacterial growth was 2%w/v glucose in FAM2 agar. A negative control to demonstrate no bacterial growth was FAM2 agar with no supplementary carbon source. An un-inoculated blank was incubated for each set of conditions to determine the significance of airborne contamination.

The inoculum used to initiate biodegradation was 100 μL primary settled activated sludge (Cranfield sewage plant, Beds, UK) diluted 100 fold in sterile saline (0.9% w/v NaCl in RO water). Plates were prepared in triplicate and incubated at 37°C. The plates were examined daily for development of colonies. Colony numbers were recorded and the daily increase and variance between conditions was determined. The standard deviation across the conditions was calculated to show the reproducibility of the results.

3.3 Results

3.3.1 Deposition of polymers to APTS modified glass

Homogenous, reproducible transducer interfaces can be created by the immobilisation of polymer to the surface of transducers. Both CMD and CMC have been deposited onto modified glass surfaces and then examined via AFM for homogeneity, reproducibility and depth of deposited layer, as described in section 2.6. Samples of the images obtained are shown below.

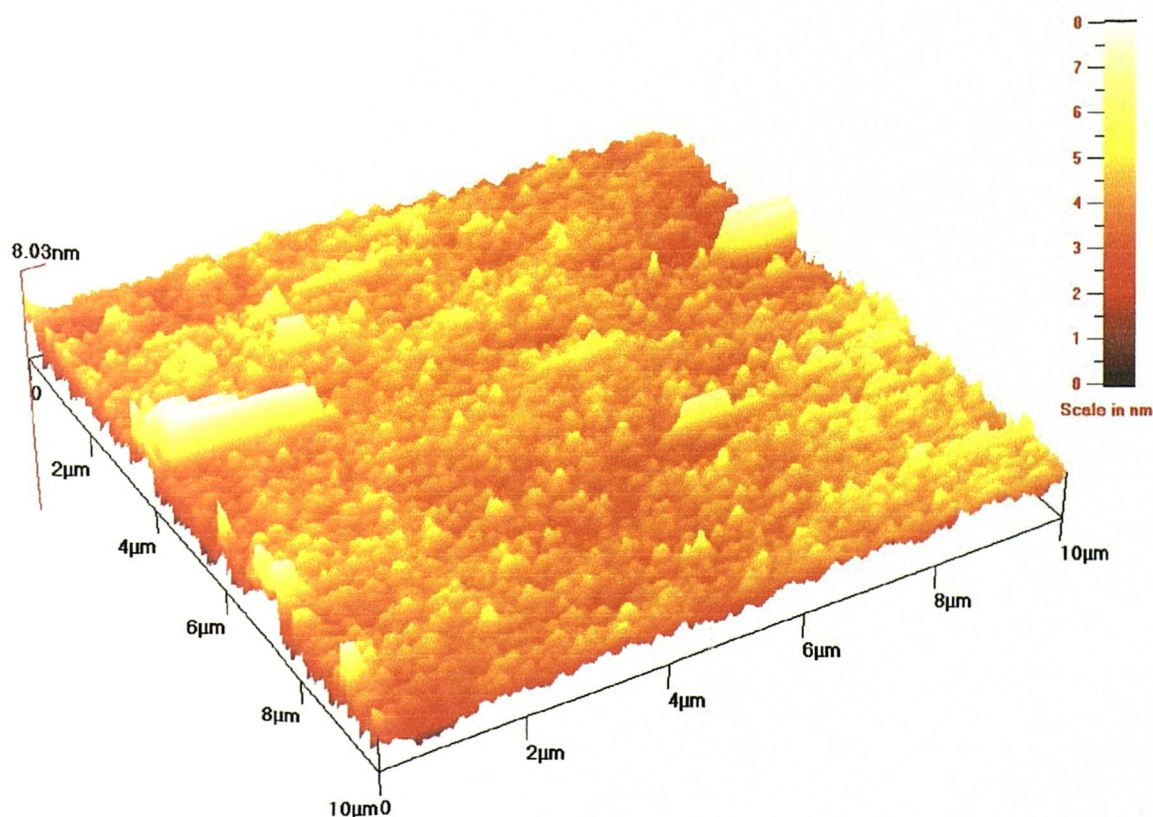


Figure 3.2 AFM image of CMD immobilised on vapour silanised glass - imaged in contact mode for variance in Z height, at a scan rate of 2 Hz. The image has been levelled for sample tilt in X and Y planes.

Figure 3.2 shows that the deposited CMD results in a homogenous surface with few faults and with regular repeating crenulation. Surface faults have been analysed and the thickness of the deposited layer has been determined as ~ 45 nm in ambient air by measuring the step height across a surface fault. The regularity of the CMD surface implies that it is homogenous and

therefore well suited for use as a transducer-modifying agent under the limited conditions that have been studied.

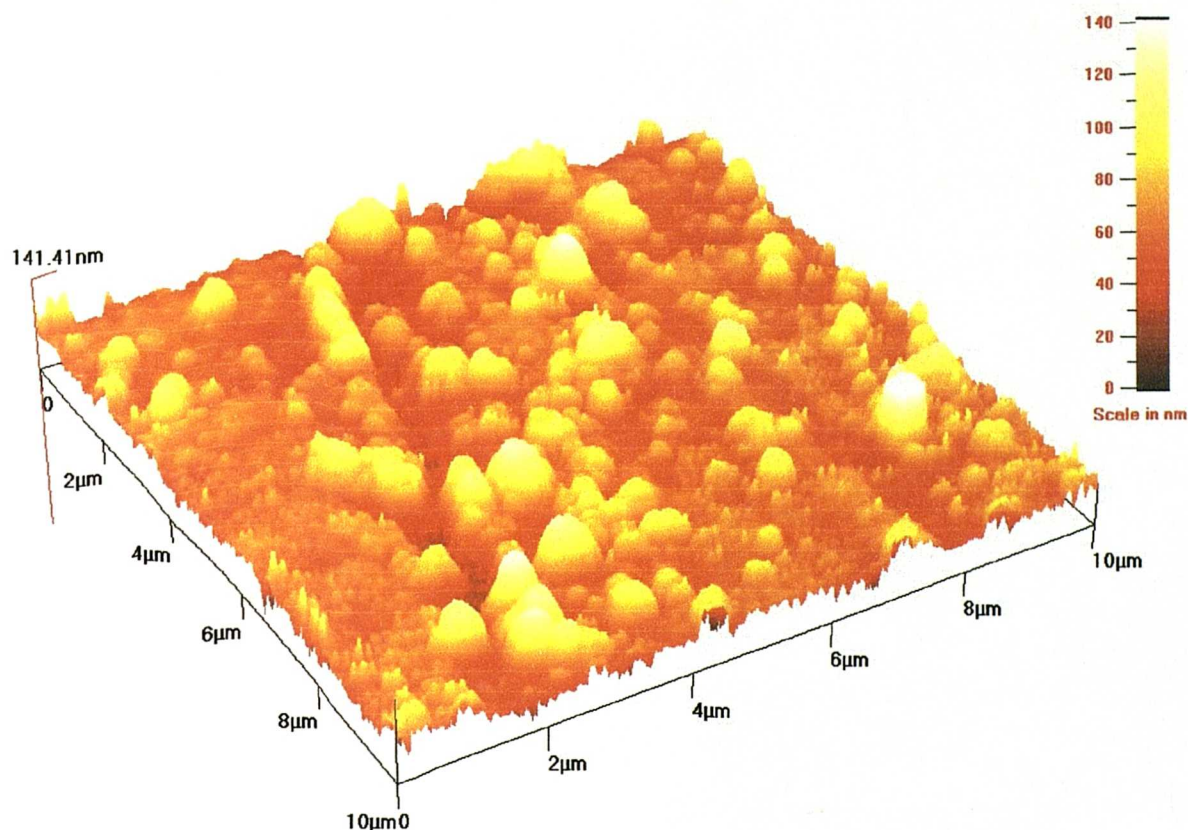


Figure 3.3 AFM image of CMC immobilised on vapour silanised glass – imaged in contact mode for variance in Z height, at a scan rate of 2 Hz. The image has been levelled for sample tilt in X and Y planes

Figure 3.3 shows that the deposited CMC results in an inhomogeneous surface with regular faults, and repeating crenulation which is greater than that seen for CMD. Surface faults have been analysed and the thickness of the deposited layer has been determined as ~ 40 nm in ambient air, by measuring the step height across a surface fault. The inhomogeneity of the CMC surface suggests that it would result in poorly reproducible sensors and is therefore not ideal for use as a transducer-modifying agent.

Alterations in incubation time between 10 and 45 minutes reveal an increase in polymer thickness up to 30 minutes (~ 45 nm maximum) for both polymers, after which no further increase in thickness was observed. This is most likely due to available amines on the

substrate surface being coupled to the carboxyls present on the polymers, thus there are no remaining amines to be bonded to. The depth of the polymer layers implies that the attached polymers are collapsed on the surface. If the polymer chains are fully extended and uncoiled, they would have a maximum length of $\sim 2 \mu\text{m}$, when coiled this is reduced to $\sim 900 \text{ nm}$ for CMC and $\sim 500 \text{ nm}$ for CMD.

The difference in surface features suggests that polymers associate with the surface in different formats, which effects the polymer packing on the surface. The repeating features, or crenalations, which are seen across the surface of these images, were a common feature to all surfaces that were examined. The CMD surfaces deposited onto vapour silanised glass show a greater homogeneity than those of CMC on silanised glass. This may be because the packing of CMD is more complete, as CMD has a higher degree of flexibility and is therefore less constrained than CMC.

3.3.2 Deposition of carboxylated polymers and proteins to APTS modified metal

CMD and CMC were attached to amino functionalised metals by the methods used in section 3.2.1. Following the attachment of a polymer matrix to an aminated surface, proteins were covalently attached to the polymer interface. This was intended to investigate the potential surface binding difference that can be achieved by the use of different polymer interfaces. The protein that was attached to the polymer interface was horseradish peroxidase, as it is inexpensive, of a mid-range molecular weight (42 kDa), and it is easily detected by colourimetric assay with a suitable substrate, such as o-phenyl diamine.

The deposited layers were analysed via SPR to determine the Δ_{SPR} , and from this compare the amount of material that has been covalently attached to the surface. Figure 3.4 shows an example of the profile of an SPR response that is obtained from a transducer surface.

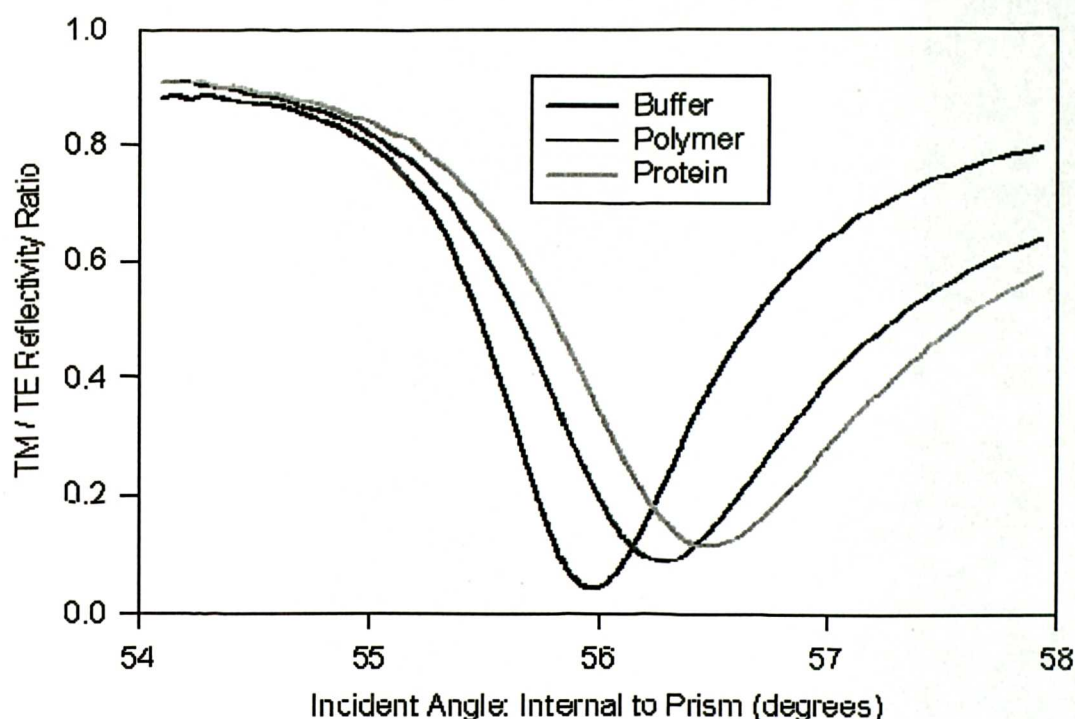


Figure 3.4: Example SPR responses obtained from a APTS-modified silver surface in 0.1M MES buffer, pH6.8 (Buffer) and after immobilisation of a polymer film (Polymer) and the subsequent covalent immobilisation of a protein to the polymer film (Protein). This result is representative of all the SPR obtained within these experiments.

CMD and CMC were both deposited as 0.1% w/v solutions, and incubated in contact with the SPR surface for 40 minutes. HRP was deposited from a 100 $\mu\text{g/ml}$ solutions in 0.1 M MES, pH 6.7. The resulting ΔSPR are shown in table 3.2

Table 3.2: A comparison of immobilisation of polymers and proteins to CMD and CMC - results are given as change in internal angle \pm SD where $n \geq 3$

Condition	CMD	CMC
Buffer	0.00	0.00
Polymer	0.22 ± 0.06	0.24 ± 0.07
Polymer & Protein	0.39 ± 0.04	0.32 ± 0.04
Total Change	0.61 ± 0.09	0.56 ± 0.11

These results show that similar amounts of the polymers are attached to the transducer surfaces, but the subsequent protein attachment is $\sim 18\%$ higher for CMD than for CMC. The standard deviation for the two interface systems is low for polymer and protein attachment individually, but when the systems are compared in their entirety, the CMD-protein interface has a standard deviation three times higher than the CMC-protein interface.

3.3.3 Protein loading to modified microtitre plates

To extend the experiments in the use of polymers to modify model transducer surfaces, pre-aminated microtitre wells were utilised as an alternative system for the analysis of polymer-protein immobilisation. This was performed as microtitre based assays to allow for proteins that are attached to deposited surfaces to be assayed for retention of biological activity by colourimetric enzyme assay. It is not possible to determine enzyme activity easily by SPR. CMD and CMC were compared directly on the same microtitre plate.

Both CMD and CMC were immobilised to microtitre plates, followed by the covalent attachment of HRP. The activity of the immobilised enzyme was assayed by the indicator o-phenyl diamine (OPD) (Sigma code: P-1526) as a substrate. While this does not give a direct measurement of the protein attached to the interface, it provides an indication of the activity retained by the protein. OPD was assayed for by absorption at a wavelength of 495 nm with a Dynex CX microtitre plate reader (Jencons Lab Supplies, Bucks, UK). The results are shown in figure 3.5.

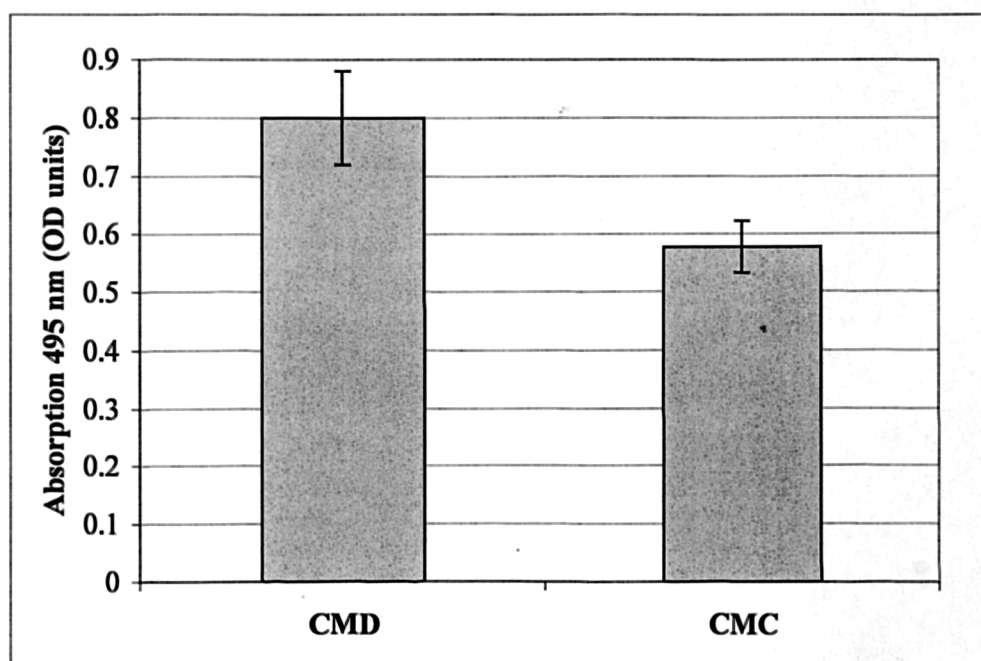


Figure 3.5 The differential enzyme activity of HRP immobilised to CMD and CMC interfaces - the determination was made by the interaction of OPD by HRP, regarding the activity of HRP as a function of protein loading to the interface.

From these results (figure 3.5) it can be determined that CMD results in a higher degree of protein activity (Abs 0.800) than CMC (Abs 0.577). This indicates that the CMD either has a higher capacity for protein immobilisation than CMC, or that the immobilised protein retains a higher degree of activity. Therefore, CMD may be the more sensitive biosensor transducer interface. As with the SPR study, the CMC has a lower variance, indicated by the standard deviation, and as such is the more reproducible interface. This suggests that the variation seen between the two interfaces is significant.

3.3.4 Mixed polymer systems

To examine the effect of using mixed interfaces, CMD and CMC were combined, and a novel polymer, carboxylated polynoxylin, was also synthesised and used. While the two carboxylated glucose polymers perform in similar ways in terms of attachment to APTS modified surfaces and the subsequent attachment of proteins to these polymers (see sections 3.3.1 – 3.3.3), the result of using a combination of glucose polymers has not been previously investigated.

Although CMC and CMD have near identical formulas, the different linkage between the glucose residues results in subtle differences between the two polymers. The supermolecular architecture is more extended for CMC and more tightly coiled in CMD, due to the inter-subunit hydrogen bonds present in CMC, as shown in figure 3.1. The effect of this may be to either increase or decrease the mesh size of the interface, thereby effecting the diffusion of molecules into the interface. By introducing a third component, CPN, in to the matrix, the characteristics of the interface may be further altered.

CMD has been shown to be effective as molecules for modifying transducer interfaces (Piehler *et al*, 1996; Catimel *et al*, 1998). The use of mixed polymers can introduce variable characteristics to the transducer interface (Csempesz *et al*, 1995; Semanova *et al*, 1998). To examine this, a synthetic aliphatic polymer, carboxylated polynoxylin, has been introduced as a component of mixed polymer systems.

3.3.4.1 Synthesis of CPN and its use as a component of mixed polymer interfaces

Polynoxylin is the condensation product of urea and formaldehyde (Blenkharn, 1985). It forms a long chain polymer with a $[\text{N}-\text{C}-\text{N}-\text{CH}_2]_n$ backbone, with CH_2OH moieties from each of the N atoms of the back bone, as shown in figure 3.6.

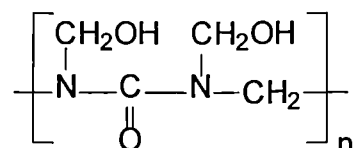


Figure 3.6: The structure of polynoxylin

The primary alcohols are oxidised to carboxylic acids via 0.5 M KMnO_4 in a 60 °C acidic (0.2 M H_2SO_4) environment, as described in Section 3.2.5. As the alcohol moieties are not directly associated to the polymer backbone, their direct oxidation is unlikely to disrupt the polymeric structure. The synthesised carboxylic acid is shown in figure 3.7.

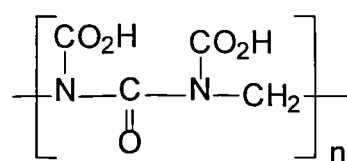


Figure 3.7: Noxylin DiCarboxylic Acid

The yield obtained from this synthesis was 15.2 %, with the majority of the loss occurring at the washing steps. The degree of carboxylation was determined by titration to be 1 carboxyl group to 7 noxylin subunits.

The synthesised polynoxylin was assayed by FTIR spectroscopy and elemental analysis (CHN). The FTIR trace showed a characteristic profile associated with carboxylated side groups. The elemental analysis resulted in CHN percentages of 32.6 : 5.4 : 33.6 for polynoxylin and 33.6 : 5.9 : 30.9 for the synthesised CPN.

The results showed that the synthesised polynoxylin was carboxylated, with an average of 1 COOH moiety per 7 noxylin subunits. From this, it was determined that the CPN could be used as component of the mixed polymer system and would associate with the aminated surfaces of interest.

3.3.4.2 Deposition of mixed polymers to APTS modified glass

To compare the differences between mixed interfaces and single polymer systems, a mixed polymer system of CMC/CMD was covalently attached to silanised glass and assayed with AFM. By comparison with the images of single polymer systems (section 3.3.2), the effect of mixing polymers on interface morphology can be examined.

A mix of 1:1 CMC : CMD, resulting in a combined 0.1% (w/v) solution of carboxylated polymer, was deposited on vapour silanised glass in the presence of 2 mg/ml EDC and 1 mg/ml NHS. Figure 3.6 shows a representative image of a surface incubated for 30 minutes.

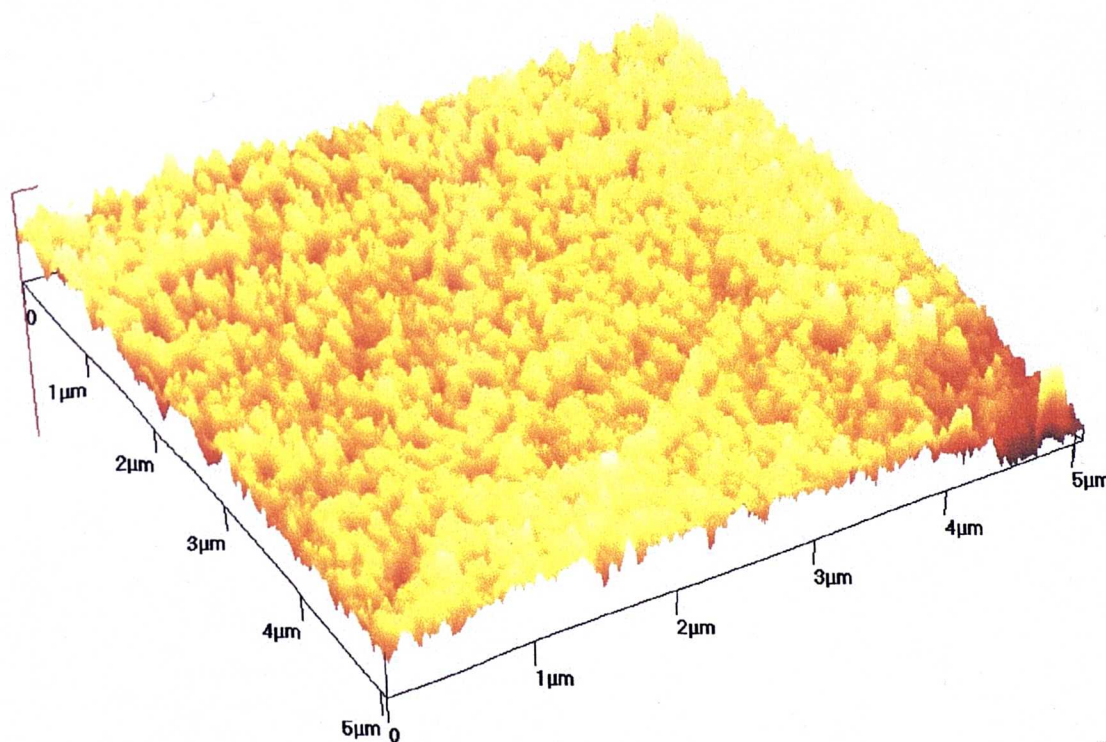


Figure 3.8 AFM image of CMC/CMD on vapour silanised glass - imaged in contact mode for variance in Z height, at a scan rate of 2 Hz. The image has been levelled for X and Y planes

Figure 3.8 has been imaged at 5 x 5 μm , as opposed to 10 x 10 μm used for the previous images. This is because the features that were imaged for the single polymer layers of CMC or CMD are less evident with mixed CMD/CMC. Surface faults of deposited mixed polymer surfaces, such as blistering, have shown that the deposited layer has a thickness of $\sim 40\text{ nm}$. The less evident surface features of mixed polymers may indicate that CMD/CMC is more effectively packed on the surface, which, while resulting in a more homogenous system, may reduce the porosity of the polymer interface by having a reduced void volume.

3.3.4.3 Deposition of mixed polymers and proteins to APTS modified metal

To extend the investigation of mixed polymer systems, two systems, CMD/CMC and CMD/CMC/CPN were deposited onto APTS modified silver prisms, to observe the difference in Δ_{SPR} between the mixed and single polymer systems. To these interfaces, HRP was covalently attached as for section 3.3.4. The resulting Δ_{SPR} are shown in table 3.3

Table 3.3: interaction of HRP with mixed polymer interfaces – the results are shown as changes in internal angle as a function of the relevant modification step.

Condition	CMD/CMC	CMD/CMC/CPN
Buffer	0.00	0.00
Polymer	0.39 ± 0.10	0.24 ± 0.10
Polymer & Protein	0.14 ± 0.09	0.16 ± 0.09
Total Change	0.53 ± 0.19	0.40 ± 0.19

Table 3.3 indicates that a larger amount of CMD/CMC is deposited than CMD/CMC/CPN. This may be an artefact of the CPN monomer having a lower molecular weight per monomer than the glucose polymers (~ 90 and 180 MW respectively) and as such reducing the mass of material immobilised to the surface, and therefore producing a lower Δ_{SPR} compared to CMD/CMC. The subsequent immobilisation of HRP to the polymer interfaces shows that a greater amount of HRP is attached to the CMD/CMC/CPN interface than to CMD/CMC.

The difference in polymer loading may be due to competition for binding sites between the CPN and the glucose polymers. The subsequent differential attachment of protein to the polymer interfaces may be a function of the amount of available binding sites that are present either due to the number of carboxyl moieties present in the respective interfaces or due to

steric hindrance resulting from interactions between the polymer species. The significance of this finding is that a polymer interface could be engineered to have a certain molecular loading by using defined percentages of polymers in the deposition solution. This introduces a greater capacity for controlling biosensor interface characteristics than has previously been possible

3.3.4.4 Protein loading to mixed polymer modified microtitre plates

While the effect of a protein loading to a CMC/CMD matrix was observed with SPR for a 1:1 ratio polymer mix, it is a complex and time consuming method for which to examine the degree of protein loading that is obtained with a changing ratio of CMD to CMC, therefore, a microtitre assay has been used to allow a high sample throughput and a representative sample to be examined.

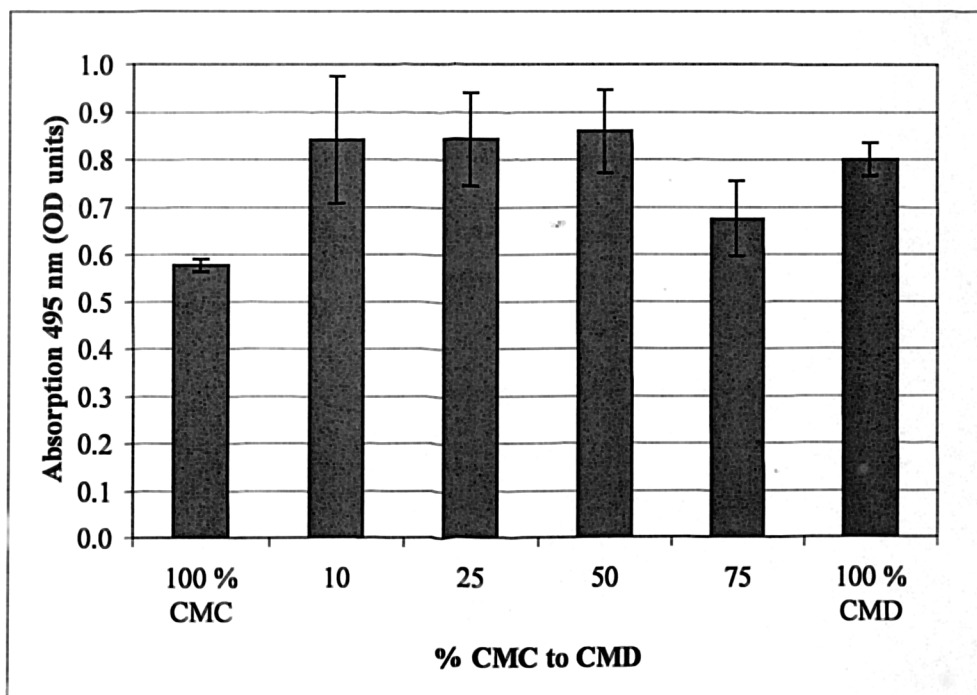


Figure 3.9 the effect of increasing CMC concentrations on a CMD interface – the determination was made by the interaction of OPD by HRP, regarding the activity of HRP as a function of protein loading to the interface.

The effect of increasing CMC concentrations on a CMD interface is shown in Figure 3.9. Total CMD and CMC have the same relationship which has been implied by the SPR analysis, where the CMD has a greater capacity for binding protein than the CMC. This may be an indication of the close packing of CMC compared to CMD, and as such its resistance to diffusion of large molecules into the polymer interface. In both cases, the standard deviation is low, indicating the high reproducibility of both systems. For the mixed polymer systems, a low percentage of CMC to CMD (< 50%) increased the potential loading of the interface compared to 100% CMD. This may be due to the differential surface packing between CMD and CMC resulting in an interface that has a more open structure than either single polymer system. As the percentage of CMC increases (75%), the characteristics of the interface become more like 100% CMC.

To examine the effect of variable protein loading by the introduction of a synthetic polymer to a glucose polymer interface, an assay to compare total CMD, total CPN and an increasing percentage of CPN, from 2.5 to 10 %, was conducted. The results are shown in figure 3.10

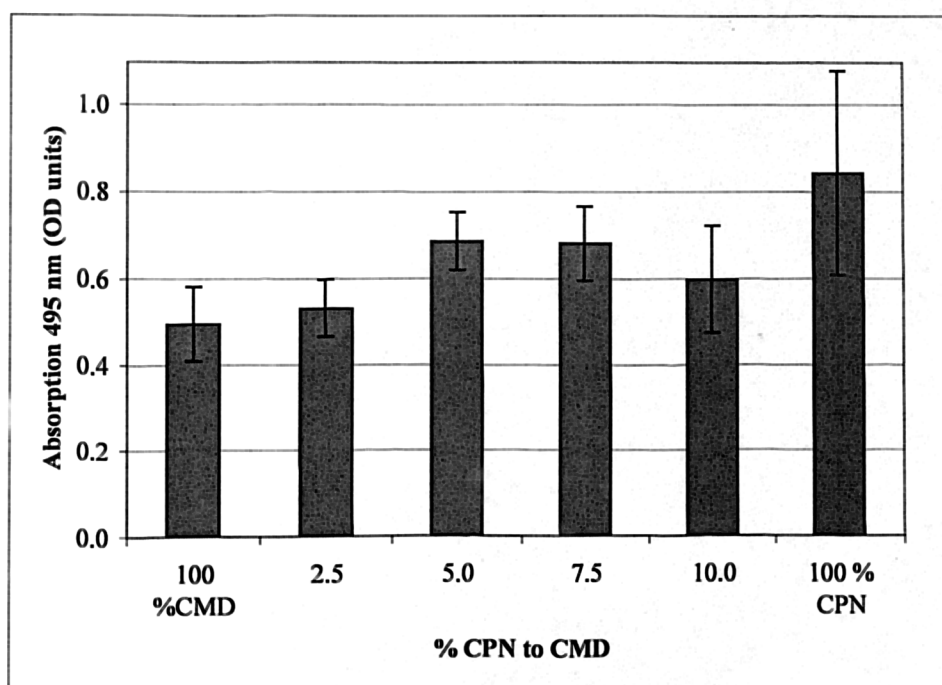


Figure 3.10: the effect of increasing CPN concentrations on a CMD interface – the determination was made by the interaction of OPD by HRP, regarding the activity of HRP as a function of protein loading to the interface.

That total CPN has a higher loading than CMD may be an indication of the number of carboxyl moieties available per unit area that are available for protein interaction. Conversely, the standard deviation of the enzyme response is twice as large for total CPN as it is for total CMD, indicating poor reproducibility of protein loading.

For the mixed polymer system, as percentage of CPN increases, the surface loading of HRP increases, until CPN equals 7.5% of the solution concentration, at which point, the protein response begins to be reduced. This may indicate that the higher percentage of CPN results in a surface packing that reduces the diffusion across into the interface, and thus reduces the protein binding capacity of the interface. It is interesting to note that as the percentage of CPN increases, so does the standard deviation, indicating that the variability of total CPN is being conferred to the mixed polymer system.

3.3.5 Microbiological screen for resistance to biological degradation of polymer components for biosensor fabrication

The use of polymer interfaces for biosensors is not restricted to medical analytical devices. Increasingly there is an interest in the use of biosensors for environmental monitoring, particularly for remote and long-term sensing. For these purposes, the common CMD interface may be unstable, as CMD is derived from a bacterial storage product and may be easily digested by organisms naturally present in the environment. To examine biological stability of various biosensor interface components, a petri dish based microbiological screen for resistance to biological degradation of interface components was developed. A minimal salt agar was used, with the interface polymers being introduced as the primary carbon source, as described in section 3.2.6. This creates a media that is selective for organisms that can utilise polymeric carbon sources.

A mixed bacterial culture derived primarily settled effluent was used as the primary inoculum. The initial assay was performed over 4 days. The number of colony forming units (CFU's) to develop on each plate was counted, and this data was used to indicate bacterial development on the different polymer based media.

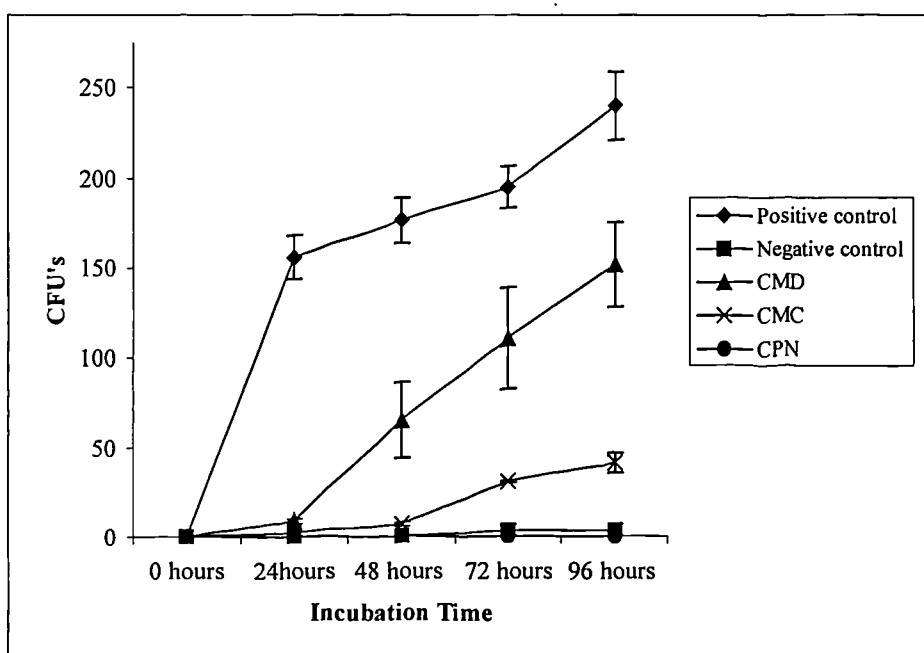


Figure 3.11: The availability of polymeric carbon sources to a mixed bacterial culture (n = 4).

This data (figure 3.11) clearly shows rapid growth for the positive control plates, indicating ready availability of the glucose carbon source. Of the carboxylated polymer sources, CMD shows a slow initial growth over 24 hours, followed by rapid expansion. A similar trend is seen for CMC, but with an increased lag phase. This indicates a greater degree of acclimation required before glucose monomers are liberated for use from the CMD polymeric chain than from CMC. No growth at all was seen on CPN. Indeed residual growth on the negative control plates was greater than the CPN test plates. Growth on the negative control plates was due to carry-over carbon source in the form of soluble BOD (Biochemical Oxygen Demand) derived from the primary settled effluent. This data clearly indicates strong inhibition of microbial growth by CPN.

To test this hypothesis a second assay was performed over a longer period (6d), using all of the conditions above, but including 2% CMD with 0.2% CPN and 2% CMC with 0.2% CPN. Results are shown in Figure 3.12.

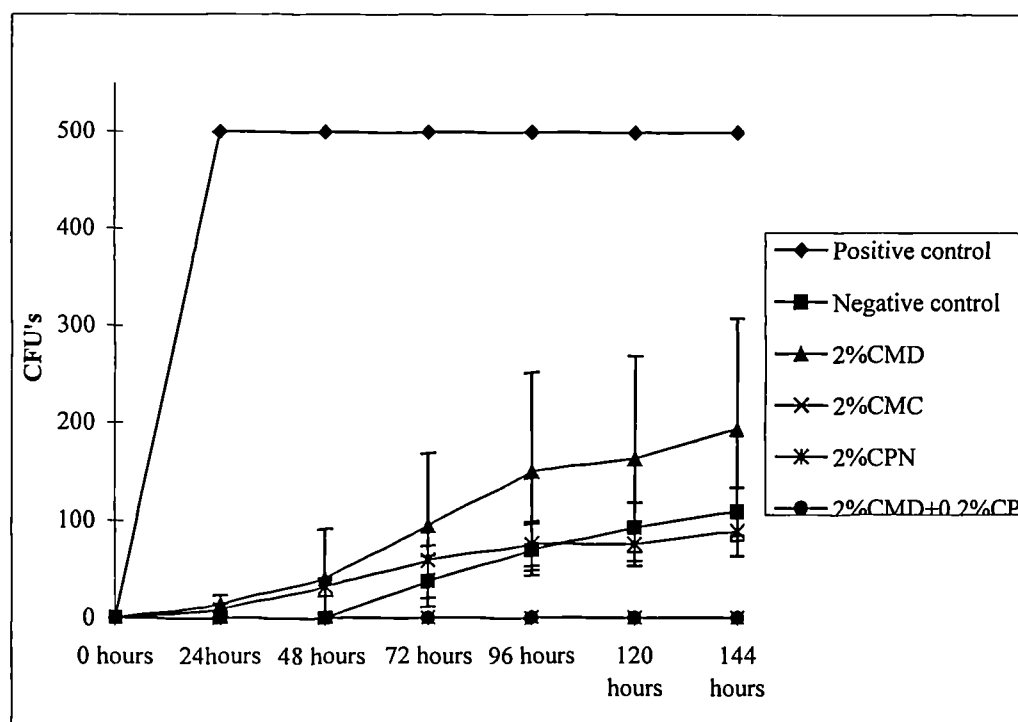


Figure 3.12: The effect of polynoxylin on the utilisation of polymeric carbon sources by a mixed bacterial culture (n = 4).

The data from figure 3.12 indicates that the presence of a low percentage of CPN not only resists bacterial growth but appears to have a potent antimicrobial effect. This is probably due to the release of formaldehyde into the media as terminal subunits of the polymer are degraded, resulting in a localised antibiotic effect (Blenkharn, 1985). While CPN may not be suitable as a primary component for transducer modification, due to the high variability seen with the microtitre assays in Section 3.3.4.4, these results imply that it may introduce a degree of resistance to degradation to glucose polymers.

3.4 Discussion and Conclusion

3.4.1 Surface modification of glass and metals

Silanisation was chosen as a technique to modify surfaces as it can be widely applied to a variety of materials with oxidised coatings, such as glass, silicon and metals (Sasaki *et al*, 1998; Weiping, *et al*, 1999). Vapour silanisation of surfaces was used, as while deposition from dry toluene is common, it can result in a multilayer that is up to 6 nm deep (Ariga and Okahata, 1989; Weiping *et al*, 1999). Vapour silanisation results in an orientated monolayer (Jonsson *et al*, 1985) that projects functional groups away from the transducer surface. The other benefit of vapour phase silanisation is that delicate surfaces can be functionalised (Jonsson *et al*, 1985) without the potential damage which could occur from a liquid based system, and also that there is less waste solvent to be disposed of. From a mass manufacturing viewpoint, these features makes vapour silanisation the preferred option.

3.4.2 Polymer modification of interfaces

The use of a range of carboxylated polymers has shown that homogenous transducer interfaces can be created by the deposition of carboxylated polymers to chemically activated supports.

EDC reactions were very simple to carry out, and the removal of any by-products could be easily achieved by a combination of centrifugation and gel filtration, as described in section 2.3.7. There were specific problems with using EDC-NHS in certain situations. The literature did describe a disadvantage with the use of EDC-NHS (Hermanson *et al*, 1992), in as much as extensive cross linking could be achieved which resulted in the product precipitating out of solution. This was observed in some cases, and resulted in the use of EDC independently of NHS, which is a less vigorous reaction than the co-catalysed EDC-NHS reaction.

CMD has produced very similar results to those reported by Lofas and Jonsson (1990a) and Lofas (1995) and as such as provided a good base line to which to compare the results of alternative and mixed polymer systems. The results indicate that the protein attachment to CMD is higher than for CMC. This may be an indication of the close packing of CMC compared to CMD, which results in resistance to diffusion of large molecules into the

polymer interface. The variance for protein interaction with CMC interfaces is higher than that for CMD interfaces, which indicates CMD interfaces are more reproducible than CMC interfaces.

The AFM results of CMD and CMC show distinct differences between the polymer surfaces, with CMD showing homogenous surfaces with defined regular features and CMC surfaces being inhomogenous with enlarged and irregular surface features. Occasional blister type defects have allowed the surface depth of polymer interfaces in ambient humidity to be determined as ~ 45 nm for CMD and ~ 40 nm for CMC. Studies of polyethylene show more defined features than glucose polymer (Magonov and Reneker, 1997), but this is due to the rigid nature of the polyethylene. The flexible structure of glucose polymers may result in tip interaction and the subsequent dragging and/or deformation of the interface.

The differences between the polymer surfaces may result from a more compact surface packing of the CMD onto the surface than CMC, but mathematical model may be needed to demonstrate this (Lidin *et al*, 1995). This difference in interface morphology maybe due to structural variance between the polymers which effect the packing of the polymer within the interface (Kurihari, 1997). Lofas and Johnsson, (1990b) have stated that the use of high weight polymers ($\sim 480,000$ MW) effects the layer thickness which is deposited, as the greater the molecular weight of a polymer, the further it can expand away from the surface which it is attached to. This issue is central to evanescent wave based sensors, where a transducer modifying agent should have a thickness matched to the depth of the evanescent wave to fully utilise the intensity of the wave.

Single polymer systems have been well defined in relation to biosensor interfaces. Witz, (1999) has constructed models which treat the polymer as an ideal system which has all of the polymers grafted at one extremity and the polymers extended perpendicularly to the surface. This model defines the void volume of the polymer interface in terms of the mesh size, ξ , which is proportional to the surface concentration of polymer, c . Therefore as the polymer concentration increases, the mesh size decreases. This model predicts that at high concentrations, the polymer interface restricts diffusion of reagents and recognition molecules into the polymer interface. Comparison of the results of CMD, CMC and mixed polymer systems suggests that the linkage between monomers effects mesh size, but also that mixed

polymer systems have a mesh size which is determined by the polymer components and their concentrations in solution.

The density of the polymer interface can effect the hydrodynamic flow of the buffer, with only 10 – 15% of the polymer interface being accessible to the buffer flow. The attachment of recognition molecules to the interface may be affected by the mesh size, resulting in the majority of the recognition molecules being attached near the surface of the interface, in the region where the evanescent wave has already lost ~ 40% of the intensity present at the interface surface. This in turn reduces the detection sensitivity of the system (Witz, 1999).

3.4.3 Mixed polymer systems

When examined with AFM, polymer interfaces comprising of mixed glucose polymers (CMD/CMC), appeared uniform and homogenous with a regular crenulation visible. This result implies that using two polymers with very similar characteristics allows them to interact with an activated surface to produce a more homogenous interface than a single polymer would do. Alternatively, one polymer may be preferentially to the interface and the second excluded, resulting in a single polymer layer, but the AFM results presented in Section 3.3.4.2 do not support this.

When the synthetic polymer CPN is introduced as an additive, the surface morphology becomes markedly different. The homogeneity is less pronounced and the surface features show increased dimensions over glucose polymers (Weston and Cullen, 1998). This result may be indicative of the difference between the structures of CMC and CMD, with CMC being a semi-rigid polymer, with dextran being more flexible and readily forming coils (Semanova and Savilova, 1998). Whether the difference between CMD and CMC result in a competitive attachment to the biosensor surface has not been examined. Csempesz *et al* (1995b) have investigated adsorption from complex multiple component solutions, and have found that a preferential adsorption process could occur.

It has been shown by Pavey and Olliff (1999) that the use of mixed polymer systems can have considerable benefit when compared to single polymer systems. This is most notable in relation to reduction in non-specific adsorption, and is believed to be due to the increased steric hindrance that is created by the use of mixed polymer interfaces. When CPN is added to

a CMD matrix, the potential loading of the interface increases, but the variation in characteristic also increases. This indicates that the introduction of a secondary polymer may make the interface more accessible to globular proteins, a feature that has been reported in the literature (Semanova and Savilova, 1998). To further this area of study, the use of polymer with flexible side chains may further increase the mesh size and potential loading of interfaces (Kim and Zin, 1997).

3.4.4 Biodegradation of polymeric systems

The degradation of CMD and CMC produced the trends that were expected, with CMD being easily degraded by the bacterial culture and CMC showing an increased lag phase, but again being easily degraded. The CMD was expected to be readily utilised as dextran is naturally a bacterial storage product and therefore the pathways exist for bacterial degradation. Also with CMC, cellulose is the most commonly available carbon source, and as such the ability of the bacteria to adapt to using CMC was expected, with the increased lag phase being indicative of an adaptation to a non-ideal substrate.

While CPN has not previously been reported as a component for interface modification, polynoxylin has been used as an antibacterial agent for medical purposes, particularly for oral applications (Gorman *et al*, 1988; Lynch *et al*, 1991). The mechanism of inhibition for noxylin has been attributed to the release of formaldehyde in solution (Blenkharn, 1985), but this has not been proven. The mechanism of inhibition by CPN has not yet been demonstrated. However, it is possible that the polymer is broken down to urea or ureates originating from the polynoxylin backbone itself or to formaldehyde and methanol resulting from partially oxidised side chains. It is relevant to note that the carboxylation of polynoxylin does not appear to restrict the antimicrobial effect of the polymer, but this may be due to incomplete carboxylation of the polymer.

The aspect of this study that is not shown from these results is the colony morphology of the test organisms. It was evident from all conditions that the bacteria had considerable difficulty in adapting to any polymeric substrate. Colonies formed on the positive control plates showed vigorous and rapid growth. Conversely, the polymeric substrates yielded a very slow progression in colony size.

The benefits of using a low percentage of CPN in conjunction with the principal glucose-based polymer to reduce biological degradation have been shown, and this represents a possible optical transducer interfaces system for continuous environmental monitoring. The same effect could be usefully applied to gel filtration media, where the possibility of microbial degradation can result in reduced performance and a shortened working life.

3.4.5 Conclusions

The experiments presented in this chapter are an investigation of current technologies and methods, but also introduce novel materials. The comparison of potential interface components for maximum loading of recognition molecule and resistance to degradation has revealed some interesting trends. While it has been demonstrated that CMD is the single polymer system that has the highest interface loading, it is also the most easily degraded. CMC is also relatively easily degraded, but shows a lower interface loading capacity.

CPN, while never being envisaged as a primary component, has been an interesting minor additive. The use of CPN as a variable percentage of interface components has resulted in a higher surface loading than was achieved with a single polymer system. The degree of analysis performed was not able to determine the reason for this. The use of CPN has proved to be beneficial in relation to resistance to biological degradation, where it has been shown to have a distinct antimicrobial effect. This feature is not of any great significance for sensors which are intended to have a limited operation life, but for situations such as continuous process or environmental monitoring, the ability of the biosensor interface to resist degradation may be a central feature.

To continue this area of investigation, it would be relevant to investigate both other individual polymers, possibly carboxylated lignin, and also the incorporation of other polymers and at varying concentrations into CMD interfaces. These experiments would allow the further development of a hypothesis concerning polymer interactions in interfaces and the mesh size they create, leading towards defined interface characteristics.

The experiments have provided a foundation for extended studies within the area of interface modification. Chapter 4 will extend this area of investigation to include technologies that are compatible with existing high throughput fabrication systems, but also to consider the chemical and biochemical systems involved for a fabrication method to be viable.

Chapter 4: The application of novel methods for sensor fabrication

4.1 Introduction and aims

In Chapter 3 a range of biosensor modifying agents were examined to determine if the currently widely used system, CMD, is the optimal polymer in a single component system. From these experiments, it was determined that CMD was the optimal single component system in relation to surface loading of proteins, but that the use of mixed interfaces introduced new properties, particularly a resistance to bacterial degradation.

The selection and design of individual components used to create a biosensor is only part of the issue involved in effective manufacturing of a commercially successful device. The ability to fabricate sensors cost effectively on a large scale is central to its commercial success. The methods currently used to fabricate biosensor transducers suffer from a variety of problems that interfere in the transfer of methods from laboratory-based systems to a manufacturing environment (Turner *et al*, 1995). Predominant amongst these problems are the inability to modify chemistries for use with existing high-throughput fabrication equipment and the reproducibility of produced transducers (Newman *et al*, 1992).

4.1.1 Multi-analyte biosensors and alternative approaches to transducer fabrication

A single channel biosensor can be a very useful device for monitoring a single analyte, such as blood glucose (Wilson and Turner, 1992). Many systems involve mixtures of analytes and interfering molecules, for example complex protein solutions such as blood and fermentation broth. To effectively analyse components within these situations, multi-analyte biosensors are needed to monitor a range of compounds. In these cases, the need to produce physically and chemically defined, multi-analyte sensor surfaces are central in developing a sensor system. To achieve this, a number of systems have been used to produce sensor surfaces, in particular screen-printing, photolithography, inkjet and touch-off printing (Tison, 1998). The type of process that is used depends on both the chemical composition of the interface components and the physical properties of the transducer substrate.

4.1.2 Fabrication methods for biosensor production

For a biosensor to be commercially viable, it should be able to be produced utilising existing manufacturing processes, hence reducing development costs. Many laboratory based, low volume fabrication techniques such as multiple depositions or unusual environments and curing processes are either too complex or too expensive to be applied to mass manufacturing (Alvarez-Icaza and Bilitewski, 1993). For example, the use of Langmuir Blodgett films is widely used to produce monolayer surfaces, yet it is not a system that can realistically be used for mass manufacturing, as it requires a complex series of actions involving the interaction of the transducer with the components to be immobilised (Kurthen and Nitsch, 1991; Ottova, et al, 1997).

The need for rapid and reproducible deposition of transducer-modifying components on to the transducer surface is central to efficient production of biosensors. A range of liquid handling techniques are available that can be used to print multi-analyte arrays onto both porous and non-porous substrates:

Inkjet - The two principal methods of inkjet printing are continuous or drop on demand. Continuous inkjet can operate with either polar or non-polar solutions, and is simply a pressurised stream of reagent broken into droplets by a solenoid. Drop on demand requires a polar solution, as the solution is passed between two high voltage plates that deflect the droplets as a function of the voltage and allow a pattern to be deposited. While more complex than continuous inkjet, drop on demand can deliver very small volumes and print complex patterns. The electrical control of the printing means that solution not used for pattern deposition is returned to the reagent reservoir, therefore the system can be economical when expensive reagents are being used (Chen and Wise, 1997; Fischer, 1999).

Touch-off printing uses a syringe pump to generate a positive pressure and a droplet at the tip of a needle (Millan and Mikkelsen, 1997), which is then brought into contact with the substrate. While this system is effective for printing large volumes ($> 10 \mu\text{l}$) onto porous substrates, it is liable to cause damage to solid substrates, due to the direct contact required.

Touch-off printing using ‘pins’ has been adapted to the production of DNA micro-arrays, as it allows a system of sampling from defined microreservoirs (Macas *et al*, 1998; Boncheva, et al, 1999), and this appears to be an area of increasing interest.

Biojet™ printing (Biodot Ltd, Huntingdon, Cambs, UK) also utilises a syringe pump to generate a positive pressure, but uses a solenoid driven nozzle to release droplets down to a minimum volume of 4.2 nl. As the droplets are driven from the nozzle, direct contact is not required, and printing can be more rapid than touch-off printing accordingly (Tisone, 1998). While the deposition method is similar to inkjet printing, it can not currently be able to print as small a volume as inkjet, as the minimum volume of the biojet is determined as the lowest volume able to be pumped. With the system used within this project this was equivalent to 1 step of the syringe stepper motor, equalling 8.3 nl.

4.1.3 Reverse deposition – a fabrication method suitable for high throughput manufacturing

The method of transducer fabrication used in Chapter 3, where transducer modifying components were attached to the surface in a series of processes (figure 4.1) has been shown to produce sensors which are reproducible and sensitive within a given batch. Within the context of this thesis, this will be termed “linear deposition”. The disadvantage of this system is that it is time consuming and requires extensive transducer handling, which may result in batch to batch variation and damage to the transducer surface.

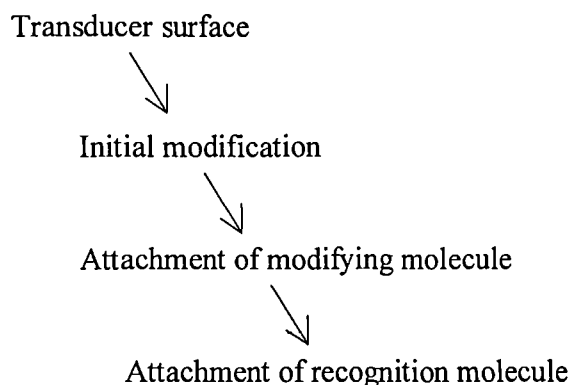


Figure. 4.1 A representation of linear sensor fabrication – each process is carried out as an independent event, needing the transducer to be incubated, washed and dried at each stage.

To address the issue of transducer modification suitable to high through put fabrication, an alternative concept of modification utilising bulk solution chemistries is proposed within this chapter. In this process the traditional, linear approach to transducer manufacturing is superseded by a simplified system, referred to as “reverse deposition” within this work. The term reverse deposition refers to the interaction of component parts in bulk solution prior to deposition (figure 4.2) which allows the fabrication process involving the transducer to be reduced to one step in many situations.

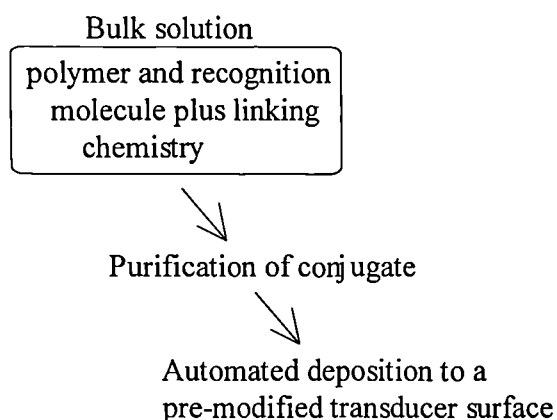


Figure. 4.2 A representation of reverse deposition for sensor fabrication – by conjugating the transducer modifying components in bulk solution and depositing the entire system in one operation, the handling of the transducer, and the variation and manufacturing costs are reduced potentially.

This system has the potential advantage over traditional fabrication of allowing very rapid fabrication of large numbers of complete sensors, as the number of processes involved in manufacturing is reduced. Also, the ability to perform the majority of the chemistry involved in the interface conjugation separate from the transducer surfaces allows the potential use of chemistries that are not compatible with the transducer material.

4.1.4 Aims

The aims of this chapter are two fold. Firstly, automated liquid handling methods will be applied to high density array printing, with two syringe driver methods, touch of printing and Biojet™ printing, being evaluated for printing arrays on model and actual sensor surfaces. The intention of these experiments is to confirm that high-density interfaces can be printed efficiently with existing technology, and to determine whether these surfaces can be interrogated by optical methods, such as SPR.

The second aim is to explore the *concept of reverse deposition (RD)* by the conjugation of a polymer and a recognition molecule, and the subsequent demonstration of biological activity that is achieved with RD interfaces by comparison to linear deposited (LD) interfaces. Two methods, SPR and microtitre plate assays will be used to evaluate the amount of material which is immobilised by the two deposition methods and the activity of the created interfaces respectively. As a comparison, a high molecular weight molecule (horseradish peroxidase) and low molecular weight molecules (aminated atrazine with an experimental anti-atrazine antibody, K4E7) will be examined as recognition elements. By using a combination of techniques, it will be possible to elucidate the differences between LD and RD interfaces, and therefore determine the structures which are created by the different methods.

The reverse deposition process will then be applied to the deposition of printed arrays and the arrays were then assayed utilising a modified 1 dimensional SPR imaging system that was constructed for this project. A system utilising FITC and anti FITC IgG was used for this assay as the antibody was more readily available than K4E7

4.2 Methods

4.2.1 Conjugation of aminated molecules with carboxylated polymers in bulk solution

The following method was adopted to attach proteins and low molecular weight species containing primary amine groups to CMD for subsequent use in reverse deposited immobilisation.

20 mg of CMD is dissolved in 10 ml of 0.1 M MES (pH 6.8). 10 mg of the molecule of interest is dissolved in 10 ml 0.1 M MES (pH 6.8). The two solutions are combined and 2 mg/ml of EDC is added to the solution and stirred until dissolved. The solution is allowed to incubate for 2 hrs at 20 °C.

The resulting conjugate is purified by centrifugation at 1500g for five minutes to remove insoluble by products, and high molecular weight species separated through a Sephadex G100 size exclusion column. The fractions that are eluted are collected as 2-ml aliquots and assayed for absorbing species utilising UV / visible spectroscopy at a suitable wavelength.

4.2.2 Linear and reverse deposition to aminated microtitre wells

To determine if there is an increase of the immobilised species within the deposited interface, a comparison of sequential and reverse deposition was made. Pre-aminated microtitre plates (Product code: 2366. Corning Costar, High Wycombe, Bucks, UK) were used as a surface to which a polymer interface could be easily attached. A 96 well plate was taken and washed in 0.1 M MES buffer (pH 6.8). A solution of 0.1% CMD was made and activated by the addition of 10 mg/ml EDC and 5 mg/ml NHS. This solution was pipetted into columns 1,3,5,8 and 10 of the microtitre plate and allowed to incubate for 60 minutes. At the end of incubation, the CMD solution was removed and the wells washed 3 times in RO water.

A 100 µg/ml solution of HRP was made in a 0.1 M MES buffer (pH 5.8). This solution is activated by the addition of 2 mg/ml EDC, as described in Section 2.9. 200

μl of this solution is immediately pipetted into columns 1,3,5,8 and 10 of the microtitre plate. The CMD-HRP conjugate that has been synthesised is activated by the addition of 2 mg/ml EDC. 200 μl of this solution is pipetted into columns 2,4,7,9 and 11 of the microtitre plate. Columns 6 and 12 are used as blanks. The plate is allowed to incubate for 60 minutes. At the end of incubation, all solution where removed and the wells washed 3 times in RO water.

The activity of the deposited interfaces is assayed for by the addition of 200 μl of 0.16 mg/ml o-phenyl diamine (OPD) and 0.01% (v/v) hydrogen peroxide citrate buffer, pH 5.5, to form a coloured end product in the presence of HRP. The activity of HRP is thus determined by absorption of the oxidised dye at 495 nm. The reaction is allowed to progress for 5 minutes before being stopped by the addition of 100 μl of 1.34 M HCl to each well. The absorbance of the plate is then read at 495 nm in a Dynex CX microtitre plate reader (Jencons Laboratory Supplies, Bucks, UK).

4.2.3 Comparison of RD and LD interfaces by SPR assay

SPR was used to examine some of the differences between RD and LD interfaces. The SPR system used has been described in Section 2.8. The modified silver surfaces where used in conjunction with a static liquid cell, volume 400 μl , in the Kretschmann configuration for SPR analysis as described in chapter 2.8. The reflectance minima of the APTS modified surface was determined in 0.1 M MES (pH 6.8), after which the deposition of CMD and HRP and the CMD-HRP conjugate was performed as for the microtitre assay above. The loading at the surface of the APTS modified silver was determined by change in the angle at which the reflectance minima occurs.

4.2.4 High density array printing via touch-off printing

The surface used for these experiments were glass microscope slides (BDH code: 406/0183/04), modified by either acetone washing or vapour silanisation (see Section 2.4). A microscope slide was wiped using a soft tissue and 50% ethanol in water

prior to being printed onto. The slide was placed in a predefined position on the XY table of Biodot XY3000 printing platform (Biodot Ltd, Cambridge, UK). A pre-programmed printing sequence was initiated via the Biodot controller unit. When the printing sequence was completed, the microscope slide was placed in a controlled humidity chamber to prevent evaporation of the deposited solutions.

The deposited pattern was imaged via a CCD camera, as described in Chapter 2.6, and the area and perimeter of the deposited droplet calculated. By comparison of these measurements for different surfaces and printing resolutions, the reproducibility of the process was determined. Failure to deposit a drop or for a drop to stay independent of its neighbour was counted as dispense failure.

4.2.5 Biojet deposition and interrogation of functional arrays

For the production of heterogeneous arrays for biosensor applications, effective deposition to spatially defined areas of the sensor surface is essential. To examine the deposition of high-density arrays that are compatible with optical analysis methods, Biojet™ printing was used to deposit solutions containing different components as spatially defined arrays onto silanised SPR prisms.

The conjugate solution was activated by the addition of 2.5 mg/ml of EDC and 1 mg/ml of NHS and rapidly mixed to aid dissolution. The Biojet™ was primed with the activated polymer solution. The pre-prepared surface was placed in a predefined position on the XY table of the printer. A pre-programmed printing sequence is initiated via the controller unit. When the printing sequence has been completed, the microscope slide was placed in a controlled humidity chamber to prevent evaporation of the deposited solutions. After an incubation of the required time, the incubated surface is washed three times with RO water and dried under nitrogen.

4.2.6 Analysis of heterogeneous arrays with multi-channel SPR

Heterogeneous arrays were deposited to demonstrate that the multichannel SPR (MC-SPR) system can determine if the spatially resolved surface would retain a differential binding capacity across the heterogeneous array, and thereby demonstrate that pattern deposition can be used to create a complex optical biosensor interface.

The modified SPR arrangement used a line-generating lens attached to the 670-nm laser to produce a vertical line. A 256-diode array (256 CMOS array, code number: S5462-256Q. Hamamatsu UK Ltd, Enfield Middlesex, UK.) was used as the detector. This produced a bargraph out put with the reflectance of the prism displayed as a voltage output from the array. The diode array is then rotated with the prism as was described in Chapter 2. The multichannel SPR software, written with Labview (R. Day, 1999) allows the parameters of the printed array to be selected, by choosing the pixel which corresponds to the centre point of a printed area, and stating the pixel width of that printed area (default = 6). In operation the software displays the current SPR trace and the change in position of the minima as interactions occur at the SPR interface (figure 4.10)

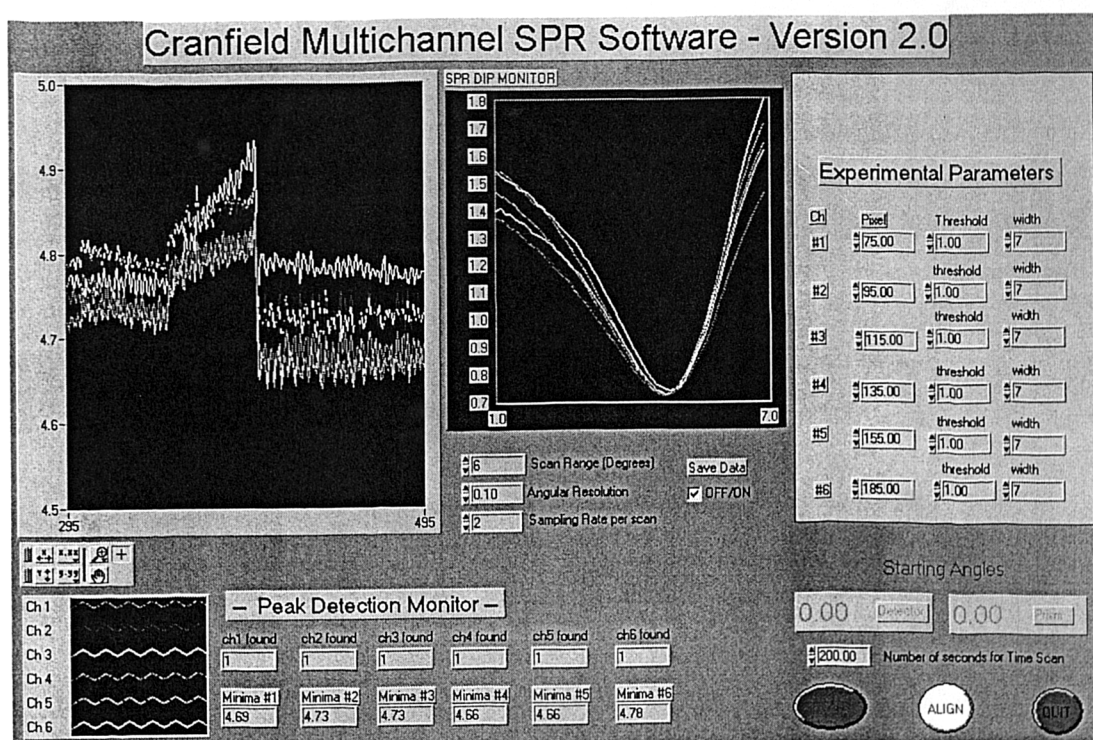


Figure 4.3 The front end of the MC-SPR software – the software allows the parameters of the printed array to be selected (right), and displays the current SPR trace (centre) and the change in position of the minima (left)

A heterogeneous CMD / CMD-BSA/ CMD-FITC array was deposited and interrogated by the interaction of anti-FITC IgG (monoclonal FL-D6, raised in mouse Sigma code: F5636). Briefly, the prism was aligned in the SPR equipment and attached to a 400 μ l static liquid cell, as described in Section 2.8.3. The liquid cell was filled with 400 μ l of PBS, pH 7.4. A 20 minute time scan was initiated. At 2 minutes the buffer was replaced with 100 μ g/ml anti-FITC IgG in PBS, pH 7.4. At 12 minutes, the solution was replaced by PBS, pH 7.4. At 15 minutes the PBS was replaced with a regeneration buffer of 0.5% SDS in RO water. At 18 minutes, the regeneration buffer is replaced with PBS.

The prisms with the printed arrays were placed in the MC-SPR apparatus. A 400 μ l static liquid cell was attached to the active face of the prism and the system aligned to scan in liquid. A 20 minute time scan is initiated. At 2 minutes, the PBS buffer, pH 7.4, is replaced with a 100 μ g/ml solution of anti-FITC. At 12 minutes, this solution was replaced with the PBS buffer, pH 7.4. This allows desorption from the surface to be monitored. At 15 minutes, the buffer is replaced with a regeneration buffer of 0.1% SDS in water. At 18 minutes the regeneration buffer is replaced with PBS buffer, pH 7.4. Therefore, this time scan shows antibody attachment, desorption of non-bound IgG, and the regeneration of the sensor interface.

4.3 Results

4.3.1 Synthesis of the CMD-HRP conjugate

HRP was chosen as the model protein to use for reverse deposition, as it has a mid-range molecular weight (~42 kDa) making the conjugate deposition simple to detect by SPR, and could be easily assayed for with colourmetric reagents. An CMD-HRP conjugate was produced using the method described in Section 4.2.1.

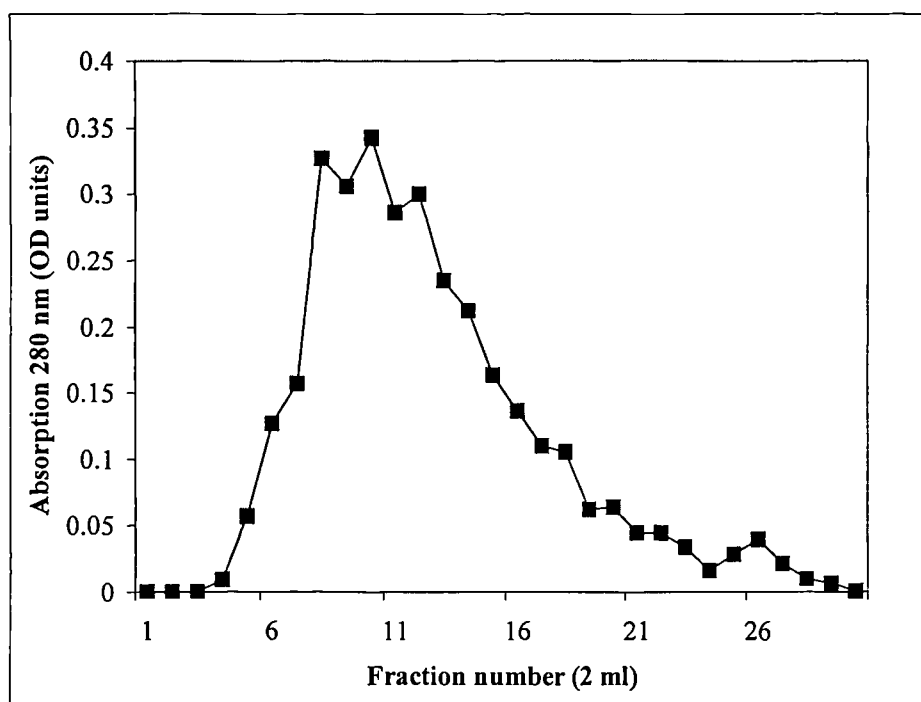


Figure 4.4: The elution profile of CMD-HRP from a 65 ml G100 column – 2 ml fractions were taken and assayed for protein concentration by adsorption at 280 nm.

The elution profile of CMD-HRP from the G100 column (figure 4.4) shows an absorption peak (fractions 8 – 12) just after the void volume (15 ml), which indicates that HRP has been conjugated to CMD. The ratio of HRP to CMD is ~ 1 HRP : 66 Glucose subunits. The fact that a second absorption peak is not evident implies that the majority of the protein has been attached to the polymer, or that the CMD-HRP and unconjugated HRP have not been clearly separated. This is unlikely, as the HRP has a molecular weight of 42 kDa, and the conjugate will be ~ 500 kDa, therefore separation should be evident.

4.3.2 Comparison of Linear and Reverse Deposition of CMD and HRP to aminated microtitre wells

To determine the difference in interface activity between linear and reverse deposited surfaces in a simple system, both approaches were used to immobilise system to aminated microtitre wells and the resultant immobilised enzyme activity assayed via the OPD method. The absorbance at 495 nm was measured and the mean and standard deviations determined for the two created interfaces.

Table 4.1: A comparison of the RD and LD of CMD and HRP to aminated microtitre plate – units are shown as absorption at 495 nm. For both conditions, n = 8

Mean Linear Deposition	1.757 +/- 0.198
Mean Reverse Deposition	2.473 +/- 0.225

Table 4.1 indicates that the reverse deposited interface has ~ 40% more activity than the linearly deposited interface. This indicates that covalent attachment of the protein to the linear deposited interface may be diffusion limited. As the reverse deposited interface is conjugated in bulk solution and deposited in one step, diffusion limitation is not an issue which influences interface loading.

4.3.3 Comparison of Linear and Reverse Deposition of CMD and HRP to APTS modified silver

The use of aminated microtitre plates has allowed the determination of the activity of enzymes immobilised by the reverse and linear methods. To determine the relative mass of material that is immobilised by the alternative methods, the polymer systems used above were attached to amino functionalised metals utilising the EDC reaction. The polymers of interest were analysed via SPR, as for Section 3.3, to determine the observed Δ_{SPR} and from this compare the amount of material that is deposited by the two methods.

The response of the modified surfaces was determined at each stage of the modification process. The values are expressed as internal angles, the change and SD of the repeats has been calculated and is show in Table 4.2:

Table 4.2: A comparison of LD and RD of CMD and HRP to APTS-modified Ag – the table shows the position of the SPR minima at each stage of the modification and the total change in angular response (Δ SPR) after all the processes have been performed. Results are shown in internal angles, with the error being standard deviation of the mean of three repeats.

	silanised Ag	CMD	CMD-HRP	Δ SPR
LD of CMD and HRP	56.47 +/- 0.37	56.98 +/- 0.33	57.48 +/- 0.29	1.01 +/- 0.25
RD of CMD-HRP	56.63 +/- 0.16	-	57.16 +/- 0.30	0.53 +/- 0.20

Table 4.2 indicates that a higher mass loading is achieved for the linearly deposited interfaces than for reverse deposited interfaces. This contradicts the microtitre assay results, (Table 4.1) which show a higher enzyme activity for the RD interfaces than the LD interfaces. This may indicate that the reverse deposition of HRP to CMD results in a conjugate that is less able to occupy the available binding sites than the linear deposited system, and thus results in a lower surface immobilisation of polymer. As the reverse deposition is not diffusion limited, the total interface loading of HRP may be higher than linear deposition, were the occupation of immobilisation points near the surface of the interface may restrict diffusion of HRP to immobilisation points closer to the transducer surface.

4.3.4 Synthesis of the CMD-Atrazine conjugate

Atrazine is a relevant analyte to use for demonstrating of reverse deposition, as it is an example of a low MW molecule and of environmental interest, being a commonly used pesticide. A monoclonal antibody, (code: K4E7, K. Kramer) which is specific for atrazine, was available allowing immobilised atrazine to be detected in both SPR and microtitre assays. As the degree of amination of the synthesised aminated atrazine (G. Besttati, personal communication) was not known, it was present in excess to the available CMD during the conjugation process, to ensure a high degree of loading of atrazine to the CMD. The method used was as for Section 4.2.1, with the use of aminated atrazine in place of a protein.

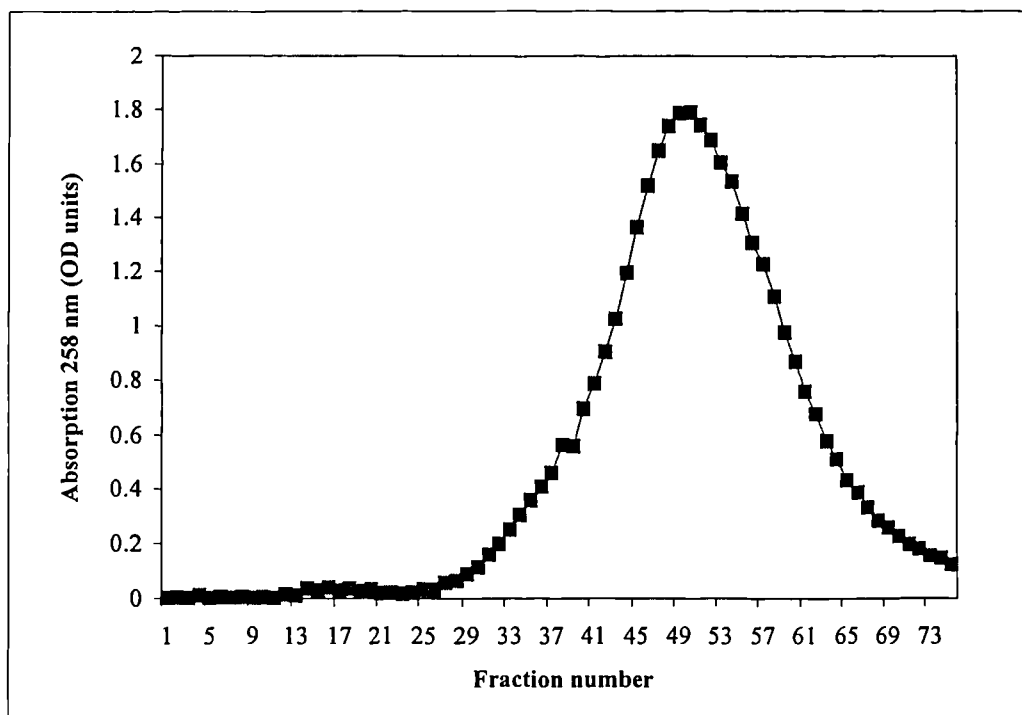


Figure 4.5: the elution profile of CMD-atrazine from a 65 ml G100 column – 2 ml fractions.

The elution profile (figure 4.5) shows a small peak of the conjugate being eluted immediately after the void volume of the column (22 ml). The conjugate is eluted in 4 to 5 fractions, followed by an increase in absorption, showing a long retention of atrazine to the column matrix. This result implies that the degree of amination of the synthesised aminated atrazine is low, and that a low percentage of atrazine has conjugated to the CMD. The estimated atrazine : glucose subunit ratio was 1:14, derived from the absorption of atrazine at 258 nm.

4.3.5 Comparison of Linear and reverse deposition of CMD and atrazine to aminated microtitre wells

As a comparison to the immobilisation of CMD and HRP, a small molecular weight system was used to determine the differences between the interactions of large and small MW molecules and the structure of the resulting interface.

To determine the difference in interface activity between linear and reverse deposited CMD and atrazine interfaces, both systems were immobilised to aminated microtitre

wells. The system was then reacted with an atrazine specific antibody. This antibody association was then detected by the use of an enzyme linked secondary antibody, rabbit anti mouse IgG conjugated to HRP. The enzyme activity was assayed via the OPD method. The absorbance at 495 nm was measured and the mean and standard deviations determined for the two created interfaces.

Table 4.3: The results of LD and RD of CMD and atrazine to aminated microtitre wells - units are shown as absorption at 495 nm. For both conditions, n = 8

Mean Linear Deposition	2.402 +/- 0.069
Mean Reverse Deposition	2.286 +/- 0.070

These results (Table 4.3) imply that the LD interface has higher binding capacity than the RD interface. The low standard deviation supports this interpretation, as it implies that the results are accurate and not an artefact of extreme results biasing the means. The reason for this may be the inverse of the result of Section 4.3.2, that is that the small molecular weight molecules are represented in a homogenous manner in the RD interface, but with a higher concentration of molecules near the interface surface in the LD system. The subsequent interaction of IgG is diffusion limited to interacting with the near surface region of the interface, resulting in a higher degree of binding of the LD interface compared to the RD interface.

4.3.6 Comparison of Linear and reverse deposition of CMD and atrazine to APTS modified silver

The use of aminated microtitre plates has allowed the determination of the availability of the atrazine immobilised by the reverse and linear methods. To determine the relative mass of material that is immobilised by the alternative methods, the polymer systems used for 4.3.5 were attached to amino functionalised metals utilising the EDC reaction. The polymers of interest were analysed via SPR, as for Section 3.3, to determine the observed Δ_{SPR} and from this compare the amount of material that is deposited by the two methods.

The response of the modified surfaces was determined at each stage of the modification process. The values are expressed as internal angles, the change and SD of the repeats has been calculated and is show in Table 4.4:

Table 4.4: A comparison of LD and SD of CMD and atrazine to APTS-modified Ag – the table shows the position of the SPR minima at each stage of the modification and the total change in angular response (Δ SPR) after all the processes have been performed. Results are shown in internal angles, with the error being standard deviation of the mean of three repeats.

	silanised Ag	CMD	CMD-Atr	10 ug/ml K4E7	Δ SPR
LD of CMD and Atr	57.52 +/- 0.16	58.17 +/- 0.66	58.44 +/- 0.47	59.39 +/- 0.64	1.87 +/- 0.17
RD of CMD-Atr	57.78 +/- 0.13	-	58.83 +/- 0.34	59.19 +/- 0.34	1.41 +/- 0.44

These results (table 4.4) indicate that the loading of the RD interface has an increased surface loading of 13 % in comparison to the linearly deposited interface. Conversely, the subsequent interaction of K4E7 is 62 % lower with the RD interface than it is with the linearly deposited interface (0.95° Δ SPR for LD compared to 0.36° Δ SPR for RD). This implies that the RD interface has reduced interaction with the antibody, as the antibody migration into the extended matrix is diffusion limited. As for the HRP CMD SPR assay (Section 4.3.3) this is probably due to a greater number of atrazine molecules being immobilised near the surface of the matrix in the LD system, but a more homogenous interface with the RD system. This in term results in the inverse of the situation with large MW species. The antibodies are restricted by diffusion in both situations, but more potential binding sites are available in the LD system. This is in conformation of the results obtained from the microtitre plate assay.

4.3.7 Initial array printing utilising cavro printing

Available techniques for automated liquid handling are capable of depositing volumes between μl and nl in reproducible and defined patterns. The resolution of the printed pattern may be a function of the solution and/or of the surface on to which the printing is being conducted. To examine the relationship between the surface and the printing solution, an experiment was conducted to determine the minimum separation that could be achieved with touch-off printing.

To examine the resolution of the printed pattern as a function of the solution and/or of the surface an array of droplets (4×4), was printed onto surfaces of interest, using the method described in section 4.2.4. To determine the droplet size and minimum spacing resolution ratio that could be achieved the pattern was printed at varying droplet volumes and centre to centre XY separations, as shown in figure 4.6.

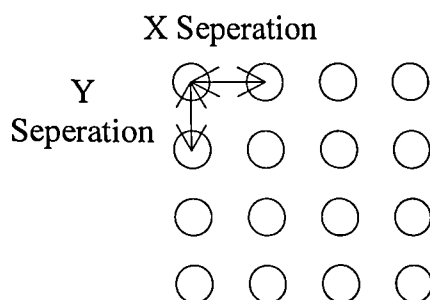


Figure 4.6 Graphical representation of the printing pattern used to determine droplet volume : separation characteristics of different surfaces

Two surfaces, acetone washed glass and APTS modified glass, had a defined pattern printed on them, with differing offsets between centre points, to determine the minimal point to point separation which could be achieved. The results from these experiments are shown in table 4.5.

Table 4.5 Dispense Characteristics of Small Volumes on Various Surfaces via a Biodot™ Cavro Printer - values of area (pixels²) and perimeter are in CCD camera pixel width units, where 1 pixel = 0.05 mm. The failure rate is determined as the percentage of droplets that fail to remain separate at the end of printing. AcW = acetone washed glass, APTS = vapour silanised glass. In all cases n = 8.

Surface	Volume (nl)	Separation (mm)	Area (mean)	Area (SD)	Perimeter (mean)	Perimeter (SD)	Failure (%)
AcW	120	2.5	93.72	4.88	28.83	1.50	0
AcW	120	2.0	95.7	6.49	29.19	1.81	0
AcW	120	1.5	96.27	6.38	29.93	1.89	0
AcW	120	1.0	94.46	3.64	29.71	1.23	0
AcW	90	0.8	719.4	85.32	105.3	7.21	60
APTS	120	1.5	74.26	15.91	22.41	3.59	0
APTS	90	1.0	63.9	4.63	19.35	1.14	0
APTS	90	0.8	125.56	26.51	39.02	10.97	25

Table 4.5 shows that for deposition of 120 µl droplets, the area, perimeter and associated standard deviations are very similar on acetone washed glass, demonstrating that the surface free energy of the glass is predictable and therefore considered reproducible. When the volume is reduced to 90 µl and the centre to centre separation is reduced to 0.8 mm, the droplets run together, and the printed array ceases to be clearly defined.

The array was also printed on an APTS modified surface. The results are also shown in Table 4.5. The results show that the droplet is more spherical than those generated on acetone washed slides as both the area and the perimeter of the droplets are reduced. This is due to the increase in surface free energy, as investigated by contact angle measurement (section 3.3.1) the minimum volume able to be printed was reduced to 90 µl, but the lowest minimum separation obtainable remained 1.0 mm.

As the dispensed volume was reduced, the separation between the surface and the needle tip, the offset height, became more critical, as the smaller the droplet, the less it protruded from the end of the needle. Printing was attempted with 60 nl, but was found to have a near 100% failure rate on all surfaces as the offset height was too critical and separation of the droplet from the needle could not be achieved.

4.3.8 Synthesis of CMD-FITC

To demonstrate the deposition of heterogeneous arrays, a system was need to which could be easily conjugated to CMD and for which an antibody is available.

Fluorescein was selected as an alternative low molecular weight analyte model, as it is of a similar molecular weight to anyltes of interest, particularly pesticides, it is available in an aminated form (5-((((2-amino ethyl)thio) acetyl)amino fluorescein, Molecular Probes, Leiden, Holland, code: A-457), and a commercial monoclonal antibody (monoclonal FL-D6, Sigma code: F5636) towards it is available. The atrazine-CMD system was not used, as the K4E7 antibody was not readily available in sufficient quantities.

CMD- fluorescein was synthesised as for CMD-Atrazine, with 5 mg of CMD being reacted with 1.75 mg of aminated fluorescein, using 2.5 mg/ml EDC and 1 mg/ml NHS and incubated at 20 °C for 1 hour. The reaction solution was then separated using a PD10 column.

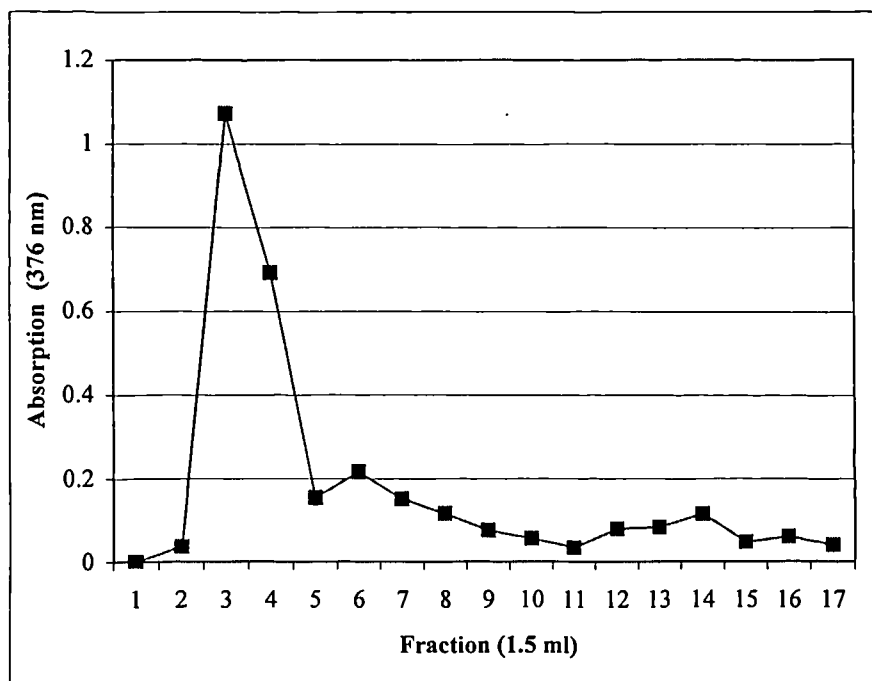


Figure 4.7 Elution profile of CMD-fluorescein from a PD10 column – the eluted fractions are assayed for the adsorption peak of FITC at 376 nm.

From the results of figure 4.6, fractions 3 and 4 were pooled and used for all subsequent experiments. The fact that the elution peak appears after the void volume of the column indicates that the fluorescein was successfully conjugated to the CMD.

4.3.9 Deposition of functional arrays via the Biojet

The Cavo™ experiments from section 4.3.7 have demonstrated that a low minimum volume and small centre to centre separation can be achieved with hydrophobic surfaces. Due to the need for precise z heights, the Cavo™ printer was not the best tool for producing printed arrays. A Biodot Biojet™ printing head was acquired and used for subsequent array deposition. As the Biojet™ actively expels droplets from a nozzle, the need for a precisely defined z offset is eliminated. In addition, the minimum droplet volume that can be dispensed was reduced to 8.3 nl, resulting in a higher density of printing than that which is possible with the Cavo™ printer.

To produce a multichannel surface that was compatible with the multiscan SPR platform, a line-based array was used. A printed array of CMD and CMD-reactant molecule conjugates were created. Six lines of CMD were printed onto APTS modified surfaces. To achieve this, the biojet was set to print overlapping droplets to produce horizontal lines that would avoid vertical run together. The parameters initially chosen are shown in table 4.6

Table 4.6: Printing parameters used with the Biodot Biojet printer for deposition of printed arrays

Droplet volume:	8.3 nl
X1 offset:	0.2 mm
Y1 offset:	0.0 mm
Repeat1 count:	16
X2 offset:	0.0 mm
Y2offset:	3.0 mm
Repeat2 count:	1
Z offset:	2.0 mm

The printing pattern used allowed the printing of more than one conjugated system to the silanised surface. This has been utilised to deposit two active areas of CMD-fluorescein and four control areas of CMD-BSA and CMD. (Figure 4.8).

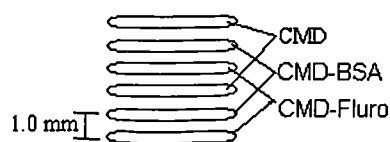


Figure 4.8 The printing pattern for the creation of the heterogeneous array – two lines of CMD were used as non-specific adsorption controls, two lines of CMD-BSA as an RD standard surface and two lines of CMD-FITC as an active areas.

The produced arrays were photographed via CCD camera at an angle of 30° to the horizontal. This allowed the droplets to be highlighted against the underlying substrate, as shown in figure 4.9. From this analysis, the effective deposition of defined areas was confirmed.

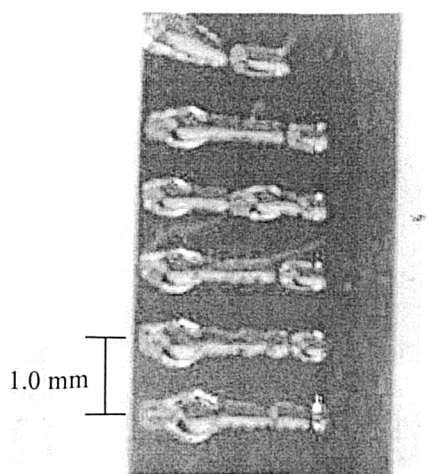


Figure 4.9 A printed array of CMD on silanised silver – a 0.1% (w/v) solution of CMD was printed on APTS modified glass, using the parameters set out in table 4.6.

Figure 4.9 shows that a defined pattern can be deposited onto a silanised surface, but that the system requires further optimisation. The expansion of the printed arrays to the left of the image may be caused by a retention of material at the nozzle of the Biojet™, which is dislodged at the beginning of the printing cycle. A pre-printing purge was investigated, but did not remove this effect. The unevenness and breaks in the printed line are believed to be due to inconsistencies on the underlying substrate.

4.3.10 Analysis of heterogeneous arrays

The deposited arrays were assayed using the multichannel SPR (MC-SPR) system to determine if the spatially resolved surface would retain a differential binding capacity across the heterogeneous array, and thereby demonstrate that pattern deposition can be used to create a complex optical biosensor interface. The assay was performed to determine if the anti-FITC antibody will react with CMD- fluorescein without cross reacting with, or producing a degree of non-specific binding to the CMD-BSA and CMD printed areas. The time scan of the assay is shown in figure 4.11.

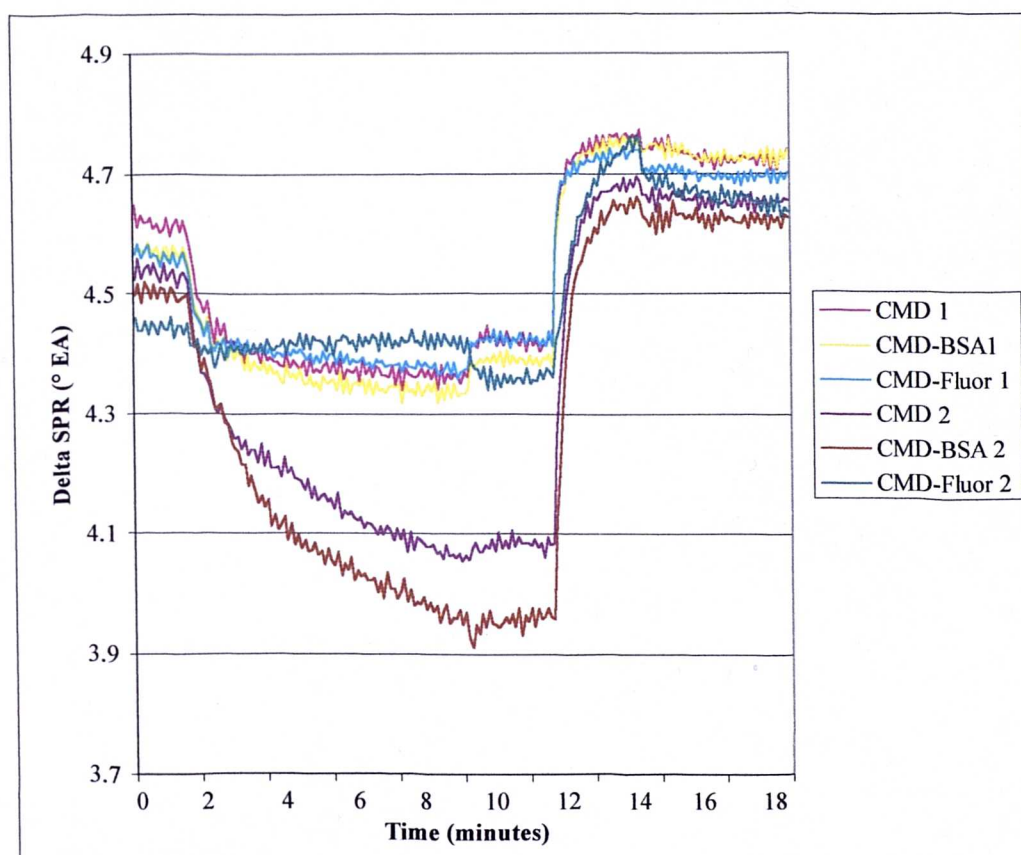


Figure 4.10 Interaction of anti-FITC IgG with a CMD- fluorescein / CMD-BSA / CMD heterogeneous printed array – a 20 minute time scan was initiated. At 2 minutes, the PBS buffer, pH 7.4, was replaced with a 100 µg/ml solution of anti-FITC in PBS, pH 7.4. At 12 minutes, this solution was replaced with the PBS buffer, pH 7.4. At 15 minutes, the buffer was replaced with a regeneration buffer of 0.1% SDS in water. At 18 minutes the regeneration buffer was replaced with PBS buffer, pH 7.4

The result from figure 4.11 was analysed. The change in angular response due to interaction of the to antiFITC IgG was determined by subtracting the point at 14 minutes from the point a 1 minute for each channel. This allowed the calculation of the Δ SPR between the base line for the printed array (1 minute) and the interaction of anitbody with the immobilised molecule, without bulk solution effects (14 minutes). The results are shown in table 4.7.

Table 4.7 Differential response of a heterogeneous printed array with CMD-fluorescence active channels and CMD / CMD-BSA control channels to antiFITC IgG

	CMD	CMD-Flur	CMD-BSA	CMD	CMD-Flur	CMD-BSA
Initial EA	4.724	4.651	4.684	4.721	4.636	4.652
IgG interaction	4.474	4.179	4.5	4.48	4.042	4.537
Regeneration	4.751	4.685	4.719	4.758	4.654	4.651
Δ SPR	0.25	0.472	0.184	0.241	0.594	0.115
Regeneration difference	-0.027	-0.034	-0.035	-0.037	-0.018	0.001

Table 4.7 Indicates that antiFITC-IgG specifically interacts with the deposited CMD-fluorescein, resulting in a Δ SPR of 0.533 ± 0.086 . The interaction of antiFITC-IgG with CMD is much lower (Δ SPR = 0.245 ± 0.009) and is further reduced with CMD-BSA (Δ SPR = 0.149 ± 0.048). From this it can be concluded that the printed array using reverse deposition has a differential interaction with the antibody, and that spatially resolved arrays combined with simple liquid cells have potential for multi-analyte detection.

This interaction with the control surfaces implies that the CMD alone is responsible for a degree of interaction, this may well be due to polymer entrapment of the extended matrix, which is less prevalent with the BSA loaded arrays. This system has been blocked with glycine, which allows the dextran interface to retain a negative charge. In this case, that may be the reason for the responses of the control channels, as the negative charge is retaining the antiFITC IgG by electrostatic interactions. Using an alternative blocking agent, such as ethylamine, which would result in the surface having a near neutral charge, could improve this.

To determine if the deposited interface was stable, a six channel CMD- fluorescein array was printed and assayed against antiFITC-IgG. The surface was regenerated and interacted 14 times, and the results are shown in figure 4.12

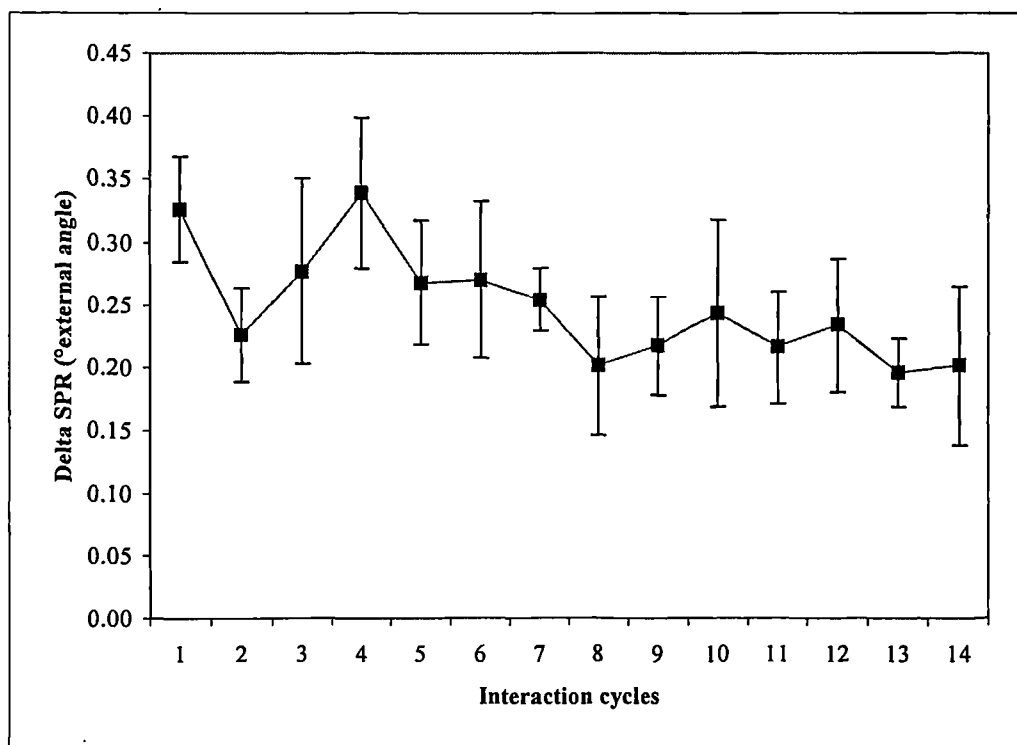


Figure 4.11. The effect of multiple regeneration cycles to the Δ SPR of printed CMD- fluorescein interacting – the assay used for figure 4.7 was repeated 14 times and the Δ SPR response was determined after each event. The error bars are the standard deviation of the four repeats.

Figure 4.12 shows that while the CMD interface degrades, it stabilises after 7 – 8 regeneration cycles. Whether this is a true degradation of the interface or a re-ordering of the interface is not known. If the signal remains stable, it is reasonable to presume that the effect is a re-order, as degradation would be a continuous process until the interface is completely degraded.

From the results presented for the analysis of printed arrays, it is evident that this method of array deposition produces a surface where the active areas are defined and separate, and that differential binding to this surface can be detected. The reduction in surface binding capacity under multiple regeneration cycles indicates that the surface stabilises and as such can be used for multiple assays.

4.4 Discussion and conclusions

4.4.1 Reverse deposition of CMD conjugates

The use of alternative systems, microtitre plate assay and SPR, to examine the effect of reverse deposition on surface functionality has resulted in interesting comparisons. For the HRP-polymer system, the SPR results indicate that reverse deposition results in proportionately less total material being immobilised than linear deposition. Conversely, the microtitre plate assay for HRP activity indicates that the reverse deposited interface has considerably more biological activity than the linearly deposited interface. While the microtitre based methods have proved to be invaluable in determining the activity of enzyme based system immobilised to polymers, it is important to remember that there could be substantial differences between silanised metal surfaces utilised for SPR studies and the polystyrene surfaces of microtitre wells.

These results are compounded by the further experiments examining the effect of linear and reverse deposition when applied to low molecular weight analytes. Atrazine is a molecule with a molecular weight of ~ 300 Da. Compared to the most common biological detection molecule, IgG, the ratio of molecular weights is 500 : 1.

When the discussion from Section 3.4 is considered, the effect of reverse deposition in the modification of the interface mesh size can be seen. The introduction of high molecular weight molecules to the interface prior to deposition may result in an increased mesh size, due to the association of the high molecular weight molecules with the polymer. This may result in a lower concentration of polymer at the transducer surface, but a substantially higher loading within the interface. This could account for the difference between the lower SPR response of RD interfaces but an increase in biological activity when assayed via the microtitre assay. This is in contradiction with the model presented by Witz, (1999) who reported that for an increase in polymer molecular weight, at high concentrations, the polymer interface restricts diffusion of reagents and recognition molecules into the polymer interface.

Conversely, when a low molecular weight molecule is incorporated into an RD interface, the problem of diffusion of high molecular weight analytes is similar to that

encountered when proteins interact with single polymer interfaces. The majority of the protein will be retained in the top section of the polymer interface, limited by a small mesh size from diffusing further into the polymer, as shown in figure 4.13 (Witz, 1999). While the attachment of a high molecular weight protein may increase the potential mesh size, the attachment of a low molecular weight protein may have little effect, with the result that the interface shows reduced activity compared to linearly deposited systems.

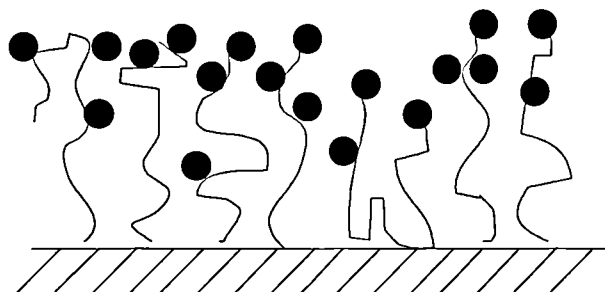


Figure 4.12: a representation of sequential immobilisation of protein - the polymer interface is deposited followed by the recognition molecule. Due to its size, the recognition molecule rapidly occupies binding sites at the surface of the interface, restricting movement of other recognition molecules and analytes further into the polymer layer.

By employing a system of conjugation from bulk solution and a subsequent single stage deposition to the optical transducer, a matrix can be created which is homogenous in three dimensions. This will result in a higher reproducibility across the biosensor interface and will increase the percentage of the evanescent field with which the biological element can interact, as represented in figure 4.14.

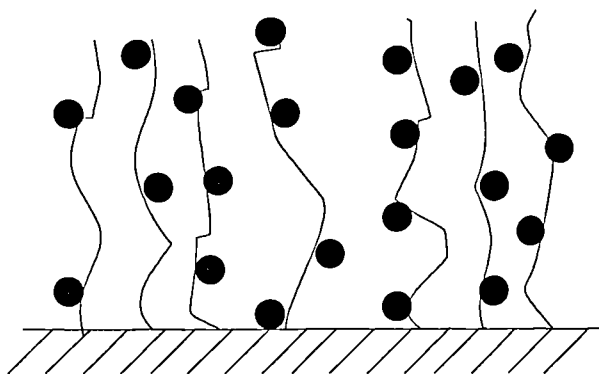


Figure 4.13: a representation of reverse deposition of a complete interface - by conjugating the polymer and biological recognition molecule in bulk solution prior to deposition to the transducer surface, the distribution of recognition molecules throughout the matrix is more homogenous than that for sequential deposition. The reverse deposited interface may also show increased porosity due to the average molecular weight increase forcing a greater spacing upon covalent linkage to the surface.

In the discussion of section 3.4, the studies of Lofas and Johnsson, (1990b) have been considered. They have stated that the use of high molecular weight polymers ($\sim 480,000$ MW) effects the layer thickness which is deposited, as the greater the molecular weight of a polymer, the further it can expand away from the surface which it is attached to. In the case of reverse deposition, the effect of pre-conjugating the protein to the polymer may have a similar effect, resulting in an expansion of the polymer away from the transducer surface. This would account for the reduced SPR response that is seen for RD systems. This relates to the studies of Kim and Zin, (1997), who determined that flexible side chains may increase the mesh size and potential loading of interfaces. In the experiments performed here, this equates to a higher degree of interaction with analytes in solution.

To compare this model to the results we have presented, the immobilisation of a high molecule weight component which then reacts with a low molecular weight analyte benefits from reverse deposition, as an interfaces which is homogenous throughout the membrane is achieved. If high molecular weight components are linearly immobilised into a pre-deposited polymer interface, the surface of the polymer will rapidly become inhibited by the interaction of molecules, restricting diffusion to the lower areas of the polymer matrix.

One of the benefits of RD for industrial applications is the potential time saving. For the laboratory-based system, RD represents a time saving of approximately 45 minutes to an hour when compared to LD, as assessed by in house comparison. Therefore, when applied to an industrial process, this system could result in substantial saving in time, and when combined with reductions in components to be immobilised, the financial saving could be significant.

4.4.2 Array printing via the Cavro

The use of Cavro printing was investigated for the deposition of arrays onto modified surfaces. It was found that the accuracy and reproducibility of a printed pattern increased with surfaces that were more hydrophobic than glass. APTS silanised glass proved to give the best results, showing the best reproducibility. The minimum volume able to be printed was reduced to 90 μl , and the lowest minimum separation obtainable was 1.0 mm. As the dispensed volume was reduced, the separation between the surface and the needle tip, the offset height, became more critical, as the smaller the droplet, the less it protruded from the end of the needle.

While Cavro printing has allowed us to determine the surface characteristics required for efficient array printing, it has also demonstrated that this is not an ideal system for deposition of arrays, due to the requirements for very flat and level surfaces. As Biojet printing became available for use, it superseded Cavro printing in all areas.

4.4.3 Heterogeneous array printing and analysis

Array based optical detection systems have been demonstrated previously, with the Biacore being the most successful (Karlsson *et al*, 1991; Jonsson *et al*, 1995). Johnston *et al* (1999) have demonstrated a multichannel planar SPR array based on a light pipe. This system was developed with the intention of being a stable portable instrument. While this system uses a probe based system, and is therefore suitable for sampling application, no further reports of the system have been published to date. The system presented here is a prototype for a multichannel biosensing system, which retains the traditional SPR arrangement, but uses precision deposition to create a

spatially defined heterogeneous array, whereas the Biacore uses a complex, multichannel flow cell attached to a homogenous SPR interface.

The use of biojet printing has been applied to the production of single droplet arrays, and has been shown by another researcher (S. Gillespie, personal communication) to be able to produce arrays of 400 droplets in a square centimetre. The use of the biojet printed has shown that arrays can be deposited reproducibly onto pre-modified surfaces, and that the subsequent surfaces can be interrogated via an array based SPR system. The two systems are interdependent. Without the array based SPR system, there is little point in deposition to the high degree of accuracy that the biojet allows. Without the printed arrays, the array based SPR system cannot be used to interrogated different assay point on the SPR surface, as clear resolution of points cannot be achieved. This system of deposition has the advantage that it can readily be applied to other surfaces, glass or silicon, with little or no modification over the system that has been used for the deposition to SPR surfaces.

The heterogeneous printed array was analysed via MC-SPR, and it has been shown that defined active areas can be detected in comparison to control areas. This has demonstrated that the printed surfaces are stable and remain spatially defined under operational conditions. It is interesting that the CMD-BSA areas show a lower Δ SPR than the plain CMD control. This may be due to the conjugate system introducing steric hindrance to non-specific binding, in a similar way to that described by Pavey and Olliff (1999) for mixed polymer interfaces. Alternatively, as the antibody is able to freely diffuse into the immobilised polymer layer, it may possibly become entrapped within the polymer matrix, due to molecular weight : mesh size similarities. This would result in a higher response for CMD than for CMD-BSA.

While these arrays were not interrogated using array based SPR systems in the current project, the use of CCD imaging for SPR detection would allow point arrays to be assayed effectively, as recently shown by Berger, et al (1998). This would be the next logical experiment as it would allow the development of two-dimensional arrays and increase the potential of the system to detect ~ 40 active areas in one assay. The complexity of this system is in the data processing, which would be a significant task

for a 2D array. Labview software is a versatile and adaptable platform that could be used to analysis data, using a system similar to the one used here, where a pixel is selected as the centre of the active area and the region around it is weighted for relative response. The computing power of PC's is beginning to be so great that this degree of data processing in real time is not unrealistic.

4.4.4 Conclusions

This series of experiments has demonstrated that the use of automated liquid handling systems can be applied to mass sensor fabrication, but to do so in a way which is readily applicable to industrial utilisation requires the use of alternative chemical systems for the deposited materials.

The use of a system, termed reverse deposition, to reduce surface modification to one or two steps, has demonstrated that the application of conjugation and purification from bulk solution can be used as the prerequisite for such a process. The presented results imply that the method of reverse deposition has distinct benefits when applied to the creation of interfaces for the immobilisation of active biological components, being both faster and more efficient than the alternative sequential deposition.

By combining SPR results with those of microtitre assays, it has been possible to determine something of the activity and interface structure than would be possible with either technique individually. The microtitre plate assay results show that the RD interface has considerably more activity than the corresponding sequential deposited surface. The initial indication of this is that more of the biological element is present within the RD interface.

The SPR results show the alternative result that the RD interface is in fact considerably less dense than the LD interface. This would indicate that although some biological material is present within the RD interface, it is not as efficient as LD.

The effective deposition of an interface using a method that could be readily adapted to industrial manufacturing has been demonstrated. The assays that have been used have shown that a higher activity can be achieved with apparently less biological

material. This is an indication that the immobilisation of the biologically active component results in an interface with better characteristics for the functioning of biological molecules in the case of reverse deposition than for linear deposition. The potential benefits in time and cost saving have been considered.

By examining some of the characteristics that allow biosensors to be produced commercially, this chapter has addressed some of the issues related to biosensor fabrication that are often overlooked at the research stage of a system. To further this area of research, experiments could be conducted to extend both RD systems and multichannel biosensing.

The next step for RD systems is the use of mixed polymer systems for RD interfaces, to discover if the benefits that were determined in Chapter 3 could be increased by application in an RD system. To complement this, better analysis of the deposited interfaces needs to be established. A technique which could be rapidly used is scanning confocal laser microscopy, which can identify fluorescent species within a matrix. By immobilising a fluorescently labelled molecule within vary matrices, the cross sectional distribution of molecules within RD and LD interfaces can be determined.

For the multichannel SPR system, development of the software and the transducer interface could result in a system that could both detect more analytes and be more use friendly. To achieve this, a printing system is needed that will allow a greater density of array points to to be deposited on the transducer surface. This could be achieved with the latest generation Biojet™, which has a minimum droplet deposition of 2.4 nl. This could result in arrays with a centre to centre separation as low as 400 microns. By developing the software to automatically detect the pixels that correspond to the midline of the centre point and the angle at which the SPR minima occurs, the system would be more user friendly. This would be a major development towards creating a turnkey system.

Chapter 5: Photomodulation of Enzymes

5.1 Introduction

The technological use of enzymes in washing powders, pharmaceutical products and as recognition molecules for use in analysis has become very common in the last three decades. (Mulchandani and Rogers, 1998).

The ability to modulate enzyme function, in effect being able to control turn over rate of an appropriate substrate, could have wide ranging benefits across many of the areas where enzymes are currently used. The effective modulation of proteins has implications for process control, biomaterials processing and “smart” biochemical sensors (Winter and Frecht, 1984; Hellinga and Marvin, 1998), and represents a direct application of molecular engineering to precisely modify protein function at a molecular level.

The photomodulation of proteins has attracted interest for biosensor applications (Rubin and Willner, 1994). Many such systems are based on the use of photochromic spiropyran dyes (Inouye, 1995), which under exposure to UV light, change not only colour, but also chemical structure. More significantly, under exposure to visible light, the reverse effect takes place. The following chapters examine the mechanism of photomodulation and present an explanation for differences in the degree of photomodulation that is observed for different protein systems. Two enzymes were studied initially: Glucose oxidase (GOx) and Horseradish peroxidase (HRP).

5.1.1 Modulation of biological activity and applications for sensor regeneration

Commercial biosensors generally utilise cheap disposable sensors external to the electronics required to process the signal. In cases where sensors, especially affinity sensors, can be regenerated, there is often a loss of sensitivity, due to both incomplete reversal of binding of the recognition molecule to its analyte and damage to the biological layer caused by the aggressive chemicals used in the regeneration process. To date, the methods used for the renewal of recognition molecules have been both imprecise and overtly aggressive towards the sensor. Commonly, either saturated salt solutions particularly 8 M urea (Guilbault and Luong, 1989), acid-glycine buffers

(Bier, Jockers and Schmid, 1994) or concentrated solvents, such as 85% ethanol in water, have been employed to regenerate biosensor interfaces. Proteases have been used to regenerate surfaces effectively over 600 times (Wijesuriya, 1994), but other systems have reported as much as a 10 % drop in sensitivity with every regeneration of the sensor surface (Wijesuriya, 1994).

5.1.2 Spiropyran Dyes

Spiropyran dyes are a class of compound containing two heterocyclic regions linked by a common tetrahedral sp^3 carbon atom. The two halves of the molecule are in two orthogonal parts, as shown in figure 5.1 (Durr and Bouas-Laurent, 1990). The benzopyran half is common to all spiropyran compounds. The heterocyclic half is variable, but is often built on an aromatic ring system, as for this project.

Absorption of light in the range 300 - 380 nm initiates the cleavage of the C-O bond in the benzopyran half of the molecule. This leads to the formation of the coloured 'open', or merocyanine, form of the dye, as opposed to the colourless 'closed', or spiropyran, form as shown in figure 5.1.

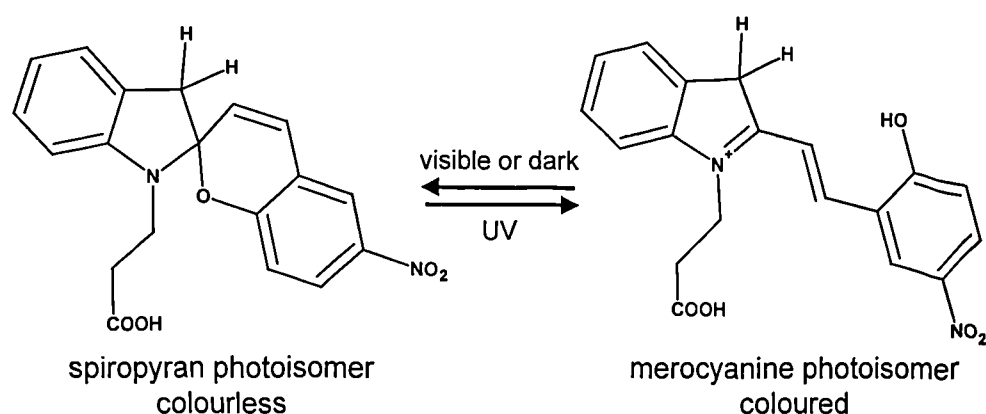


Figure 5.1. Schematic of the photo-isomerisation of the spiropyran dye (1'-(2-carboxyethyl)-3',3'-dimethyl-6-nitrospiro[2H-benzopyran-2,2'-indoline]). Visible illumination converts the red spiropyran form into the yellow merocyanine form and the schematic represents the merocyanine form after a cis-trans isomerisation of the central double bond and protonation of the oxygen group. UV illumination reverses the conversion. In addition, a slow dark conversion of the merocyanine to spiropyran form can occur.

5.1.3 The Role of Spiropyran Dyes in Bio-Modulation

The photomodulation of enzyme activity by direct attachment of a photochromic dye to the protein have been previously described, (Namba and Suzuki, 1975; Karube *et al*, 1976; Aizawa *et al*, 1977; Rubin and Willner, 1994; Zahavy *et al*, 1994; Liu *et al*, 1997). The most notable example of this is the photomodulation of papain by the photochromic dye azobenzene aldehyde that demonstrated an increase in activity of ~600% compared to the native protein (Westmark *et al*, 1993). This mechanism of photomodulation was not widely accepted as it was stated that the azobenzene aldehyde was poorly soluble and could act as an enzyme inhibitor, particularly for serine proteases.

A simple and relatively non-aggressive method for attaching photochromic dyes to both proteins and supporting matrices (Arai *et al*, 1996), might find broad application for both the labelling and modulation of biological molecules. One such method which has been used involves the covalent attachment of a class of photochromic dyes, spiropyrans (Gugliemetti, 1990), to a biologically active component, via a carboxyl side chain as shown in figure 5.1. The carboxylic acid side chain allows the use of water-soluble conjugation chemistries, such as EDC-NHS, as described in Chapter 3, which enables the rapid conjugation of proteins with spiropyrans.

Exposure to UV light induces a change in chemical conformation of a spiropyran conjugated to a protein. (Westmark *et al*, 1993). This change in conformation is accompanied by a shift in charge/polarisation (Cooper *et al*, 1999). Theoretically this has the potential to disrupt the tertiary structure of the protein, by causing distortion of the protein structure and thus induce a subsequent change of shape in the binding site of the protein. In doing so this disrupts the function of the protein. Once this has been achieved the protein-dye complex could be illuminated with visible light, to return the spiropyran dye to its original state, and allow the protein to revert to its native conformation, thus leaving the active site available to function as before (Willner *et al*, 1993). The effect of this structural disruption on the binding affinity of the protein has the potential to switch the protein between an active and inactive form (Rubin and Willner, 1994). While this might not be as effective as some direct chemical methods for renewal of active sites, it may be less damaging to the protein for multiple regeneration cycles.

5.1.4 Aims

The aims of the work described in this chapter was to synthesis a well-characterised form of spiropyran, and then attempt to utilise the unique features of photochromic dyes to modulate two model enzymes. By utilising the change in charge and molecular shape which accompanies a switch from the spiropyran to merocyanine form, it is intended to examine potential disruption to the chemical or physical structure of the two example enzymes. The enzymes initially chosen for this study were glucose oxidase (EC 1.1.3.4) and horseradish peroxidase (EC 1.1.11.7) as they are historically central enzymes in biosensor technology (Hall *et al*, 1996; Poayard *et al*, 1998; Sun *et al*, 1998). And their activity can be assayed using a colourometric reagent, and are readily available.

Subsequent experiments (Chapters 6 and 7) will explore the photomodulation of other biochemical systems, the peroxidase super family and antibodies, to determine whether the conjugation of spiropyran dyes to proteins have a predictable effect.

5.2 Methods

5.2.1 Synthesis of the spiropyran precursor, 1-carboxymethyl-2,3,3-trimethylindolenium iodide

As a precursor for the synthesis of the carboxylated spiropyran, the compound 1-carboxymethyl-2,3,3-trimethylindolenium iodide was required. The reaction is based on a nucleophilic substitution (SN2 reaction) between the iodine of iodopropionic acid and the nitrogen atom of 2,3,3-trimethylindolenium (Thakur and Hosangadi, 1996). The dye was synthesised using the method of Aizawa *et al* (1977).

An equimolar amount (7.55g) of 3-iodopropionic acid (Sigma code: I-1,045-7) was added to 6.00g of 2,3,3-trimethylindolenium iodide (Sigma code: T-7,680-5). This mixture was heated at 80°C under reflux for 3 hours and then 93 ml of 20% v/v ethanol in toluene was added to the mixture. This solution was heated at 100°C under reflux for 1 hour and left overnight at room temperature. The purple solid that precipitated from the solution was collected, and the solution was retained for further crystallisation. The collected purple solid was crushed and then washed with 5% ethanol in toluene, until the filtrate became pale yellow. The filtrate was retained for further crystallisation.

In order to facilitate cyclisation to the desired spiropyran, the solid obtained was further refluxed at 100°C with 20% v/v ethanol in toluene, using sufficient solvent to dissolve all the material. This was left overnight at 4°C to recrystallise. The crystals were filtered off and dried to give a white crystalline product, which was stored in the dark at room temperature.

A solution of the product was made in 100 % ethanol and spotted onto an aluminium oxide TLC plate (aluminium oxide 60 F₂₅₄, neutral type E, Merck code: A 5581). The initial reaction mixture was also spotted onto the plate as a comparison. The plate was then run using 20% ethanol in toluene as a liquid phase. The resulting positions of compounds were viewed under UV light (245 nm) and the R_f values determined.

5.2.2 Synthesis of carboxylated spiropyran

The method used to synthesis the spiropyran was based on the method of Namba and Suzuki (1975), with the exception that 1-carboxyethyl-2,3,3-trimethylindolenium iodide was used as the spiropyran precursor in the place of 1-carboxymethyl-2,3,3-trimethylindolenium iodide. The reaction is shown in figure 5.2.

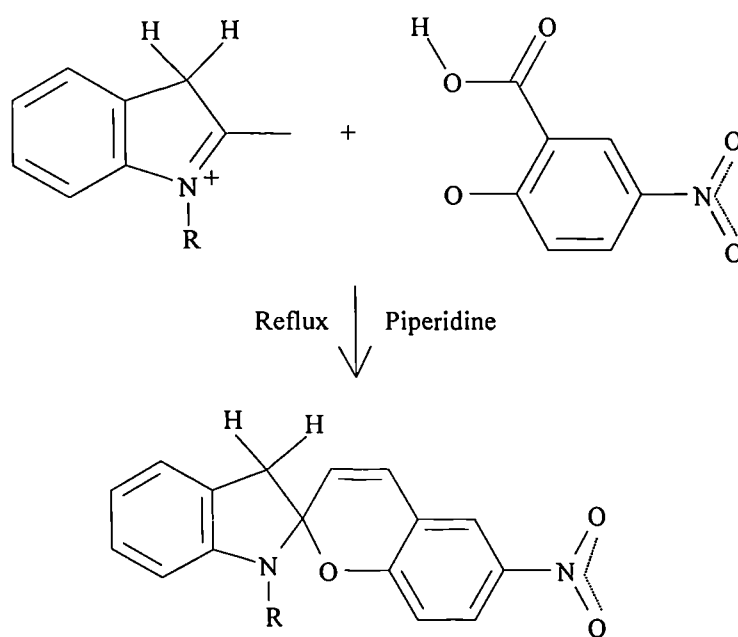


Figure. 5.2 The Reaction Sequence to Synthesis a Spiropyran Dye – where R = (CH₂)₂ COOH

Five hundred milligrams (1.4 mmol) of 1-carboxymethyl-2,3,3-trimethylindolenium iodide (Section 5.2.1) was suspended in 160 ml of methyl ethyl ketone (Sigma code: B-7917), and after the addition of 12.5 ml of piperidine (Sigma code: P-5881) the solution was heated under reflux at 110 °C for three hours.

After the addition of 250 mg of 5-nitrosalicylaldehyde (Sigma code: 43,408-6) the solution was heated under reflux at 110 - 120°C for 30 min. The mixture was left overnight at room temperature to allow the carboxylated spiropyran dye to precipitate.

The precipitate was filtered and washed under a vacuum with 50 ml of water and left to dry. It was stored in the dark at room temperature.

A solution of the product was made in 100 % ethanol and 25 μ l spotted onto an aluminium oxide TLC plate (aluminium oxide 60 F₂₅₄, neutral type E, Merck code: A 5581). The initial reaction mixture was also spotted onto the plate as a comparison. The plate was then run using 20% ethanol in toluene as a liquid phase. The resulting positions of compounds were viewed under UV light (245 nm) and the positions measured.

5.2.3 Photochromic activity of SP-COOH in ethanol

To demonstrate the successful synthesis of SP-COOH and to determine the photochromic activity, the following experiments were performed. A 1 mg/ml solution of the spiropyran (SP) of interest was made using 100% ethanol as the solvent. The M350 UV-Visible spectrometer was zeroed at 800nm, using 100% ethanol as the blank.

A 3 ml aliquot of the SP solution was placed in a quartz cuvette (path length: 1cm) and assayed with the spectrophotometer set in scan mode, between 400 and 650 nm. This was considered the base line profile of photochromic activity due to ambient light.

The cuvette was removed from the spectrophotometer and illuminated with intense UV light (UVG-54, UV products Ltd, San Gabriel, CA. Peak output: 245 nm, 0.12 amps at 220 volts) for 15 minutes. The cuvette was then returned to the spectrophotometer and scanned every 2 minutes to observe the fade back of the photochromic effect. The absorption of the peak at 484 - 492 nm is the photochromic activity of the SP.

To observe the effect of differing illumination, the cuvette was illuminated for 5 minutes with UV light (245 nm) and then for 5 minutes with visible light (tungsten filament, 80 W). The absorption profile was recorded after each illumination cycle.

5.2.4 Spiropyran - protein conjugation

To conjugate the protein to the SP-COOH, 10 mg of SP-COOH was dissolved in 10 ml of 50% ethanol in 0.1 M MES, pH 7.1. This was achieved by dissolving the dye in 5 ml of 100% ethanol and then diluting with 5 ml of 0.1 M MES. 5 mg of protein was dissolved in 10 ml 0.1 M MES (pH 7.1) containing up to 50% ethanol if required for solubility.

The protein solutions of interest and the dye were mixed together and 300 mg of 1-ethyl-3-(3-dimethylaminopropyl) carbodimide (EDC) was added and stirred until dissolved. The reaction mixture was allowed to incubate for 4 hr, with gentle mixing at 20 °C. (Hermanson *et al*, 1992)

A Sephadex PD 10 column (Pharmacia, Uppsala, Sweden. exclusion limit 5×10^3 molecular weight, code number: 17-0851-01) was equilibrated with ten 2.5 ml aliquots of 25% ethanol in 0.1 M MES, pH 7.1. A 2.5 ml aliquot of the dye-protein reaction mixture was applied to the PD 10 column. If the dye has successfully linked with the protein, the photochromic fraction will pass through the column and be present in the 4th or 5th 1 ml fraction that is eluted from the column, which represents the void volume of the column.

The fractions that passed through the PD10 column were assayed for by absorption at 548 nm, the absorption maximum of the spiropyran moiety.

5.2.5 Protein assay of dye-protein conjugates

The common method for non-destructive protein assay is to measure the absorption of a protein solution at 280 nm, due to the aromatic amino acid residues present within the protein. As the spiropyran dye adsorbs strongly under UV, the concentration of spiropyran conjugated proteins cannot be determined by this method, as the absorption of spiropyran masks the absorption due to the protein. Determination of

protein content was achieved by a modified Folin Lowry assay (Sigma code: 690-A). Briefly, a sample of the protein solution is made up to 1 ml with RO water. A 1 ml aliquot of RO water was used as a blank. With constant mixing, 1 ml of Folin's reagent was added to each solution. The solutions were incubated at 20 °C for 40 minutes, then 0.5 ml of Lowry's reagent was added with mixing. Solutions were allowed to incubate for a further 20 minutes at 20 °C. At the end of incubation the samples were read against a blank at 740 nm.

5.2.5 Determination of retention of biological activity by SP-protein conjugates

5.2.5.1 SP-GOx conjugate

Glucose oxidase activity was determined indirectly by the reaction of the H_2O_2 produced by the GOx with 2,2' azino-bis-ethylbenzthiazoline-6-sulfonic acid (ABTS) (Sigma code: A-1888) in the presence of horseradish peroxidase. Solutions of 20 ml of 0.5 mg/ml glucose oxidase in 0.1 M MES (pH 6.8), 50 ml of 5 mg/ml D-glucose (Sigma Code: G-8270) in 0.1 M MES (pH 6.8) and 50 ml of horseradish peroxidase (Type II from horseradish, EC code 1.11.1.7, Sigma code: P-8250) in 0.1 M MES (60 units/ml) were made. A solution of ABTS (Sigma Code: A-1888) was prepared by the dilution of 1.0 ml of 6 mg/ml stock solution to 100 ml with 0.1 M MES.

1.0 ml of ABTS, 0.05 ml peroxidase solution and 0.5 ml glucose solutions were pipetted into a 3 ml cuvette, stirred and allowed to equilibrate at 25°C for 20 minutes. 0.05 ml of the enzyme solution of interest was added to the assay medium. A time scan was initiated via the spectrophotometer software, and the sample access shutter of the spectrophotometer was then opened, and the cuvette illuminated by light of the required wavelength. After 16 seconds, the door was closed a reading taken over 4 seconds and the door reopened. This cycle continued every 20 seconds for three minutes.

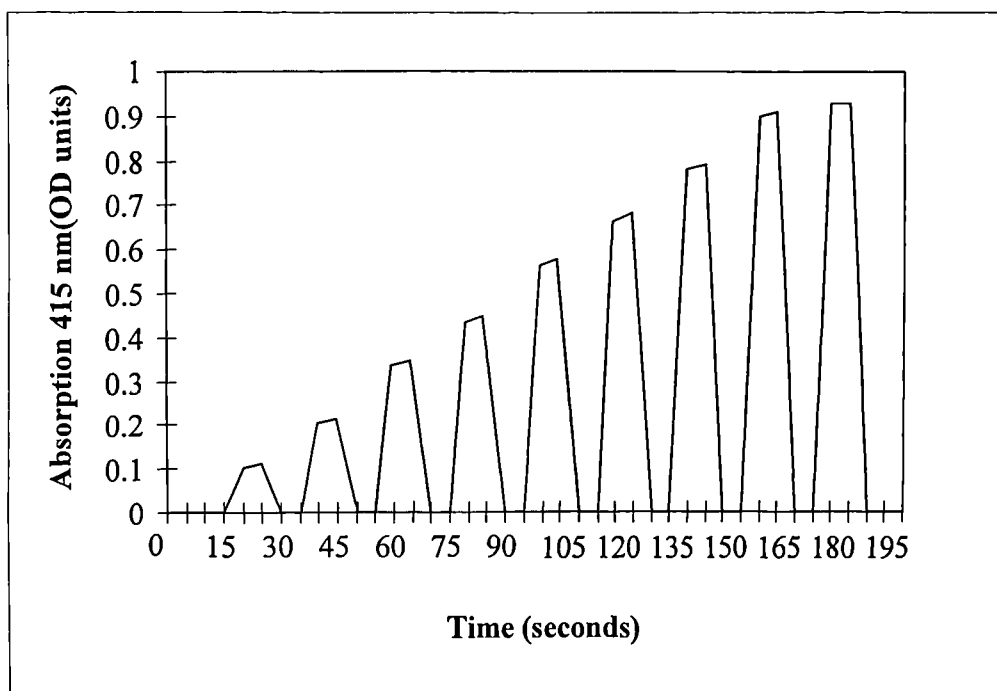


Fig. 5.3 A Representation of an ‘open door’ UV/visible Spectrophotometer Time Scan Print Out

The point readings determined at twenty second intervals (figure 5.3) were graphed and from this, the rate of reaction and the shift in activity resulting from illumination by different wavelengths of light was determined. Three repeats of each condition were run and the mean values calculated.

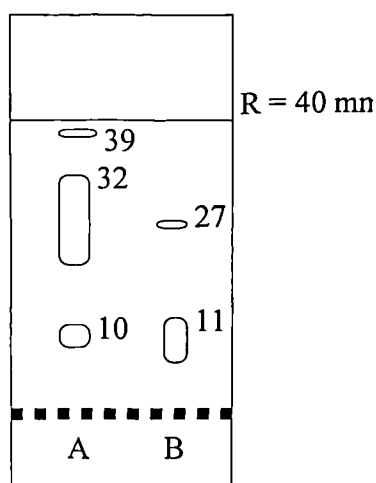
5.2.5.2 SP-HRP conjugate

The assay used was identical to that used in 5.2.5.1, with the exception that a known concentration of GOx (0.5 mg/ml) was used and the assay was initiated by the addition of 0.05 ml of 60 units/ml HRP to determine the activity of the native protein. A SP-HRP conjugate was synthesised and the assay was performed as 5.2.5.1, using different illuminations to modulate the protein.

5.3 Results

5.3.1 Synthesis of 1-carboxymethyl-2,3,3-trimethylindolenium

1-carboxymethyl-2,3,3-trimethylindolenium iodide the precursor for the synthesis of SP-COOH, was synthesised as described in section 5.2.1. A sample of the reaction mixture was run on an aluminium oxide TLC plate, with a sample of the precursor species 3-iodopropionic acid as a comparison.



A = 3-iodopropionic acid

B = reaction mixture

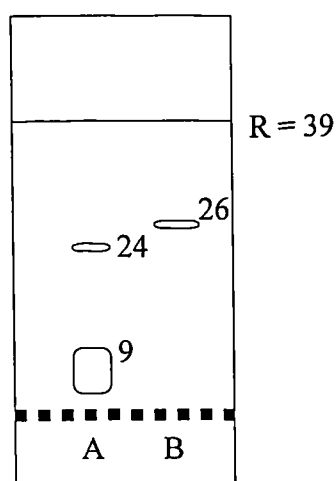
Leading edge distances are shown in mm.

Figure 5.4 Representation of TLC plate of 1-carboxymethyl-2,3,3-trimethylindolenium and its precursor - The aluminium oxide plate was loaded with ~ 25 μ l of the precursor and synthesised compound, allowed to dry and run in 20% ethanol in toluene. The bands shown are those seen under UV light (245 nm). The TLC plates were treated to fluoresce in the excitation range 230 - 260 nm wavelength. All values are stated as millimetres.

Figure 5.4 shows that the 1-carboxymethyl-2,3,3-trimethylindolenium iodide had considerably different R_f 0.675 and 0.275 (27 and 11 mm), values than the 3-iodopropionic acid, 0.975, 0.8 and 0.25 (39, 32 and 10 mm), and also showed a more pronounced, purple colouration. The band at R_f 0.275 (11 mm) is believed to be 1-carboxymethyl-2,3,3-trimethylindolenium, with the band at R_f 0.675 (27 mm) being impurities in the product. The range of bands shown for 3-IPA indicates the level of impurity that is present in the precursor. The reason three bands are seen for 3-IPA and only two for the reaction solution may be that the impurities are unstable volatiles and have been broken down during reflux.

5.3.2 Synthesis of Carboxylated Spiropyran

The 1-carboxymethyl-2,3,3-trimethylindolenium iodide synthesised in section 3.6.1 was used as the precursor for the synthesis of carboxylated spiropyran. To determine that SP-COOH had been synthesised, a sample of the reaction mixture was run on an aluminium oxide TLC plate, with a sample of 1-carboxymethyl-2,3,3-trimethylindolenium for comparison.



A = 1-carboxymethyl-2,3,3-trimethylindolenium iodide

B = SP-COOH

Leading edge distances are shown in mm.

Figure 5.5 Representation of a TLC plate of SP-COOH and its precursor - The aluminium oxide plate was loaded with ~ 25 μ l of the precursor and synthesised compound, allowed to dry and run in 20% ethanol in toluene. The bands shown are those seen under UV light (245 nm). The TLC plates were treated to fluoresce in the excitation range 230 - 260 nm wavelength. All values are stated as millimetres.

Figure 5.5 clearly shows that the SP-COOH had a different R_f value 0.666 (26 mm) to the 1-carboxymethyl-2,3,3-trimethylindolenium iodide, 0.231 and 0.615 (9 and 24 mm), and also showed a different colouration (deep purple) under illumination with UV light. The change in colouration is due to the synthesis of the extended delocalised system of the merocyanine form and therefore strong evidence that spiropyran had been successfully synthesised. Due to limited access to further analytical techniques, this was accepted as proof of effective synthesis of SP-COOH.

The final yield of this reaction was only 5.3% of starting weight. The published yield for this reaction is > 90% (Aizawa *et al*, 1977). The loss of material in this synthesis is due to

inefficient washing steps and incomplete crystallisation of product. By reducing the ethanol content of the wash to 3%, the loss due to solvation of the product would be reduced. To achieve higher recovery, rotary evaporation would be needed.

5.3.3 Photochromic activity of SP-COOH in ethanol

The photochromic activity of the synthesised spiropyran was assayed by making a solution of the dye in 100% ethanol and scanning the sample between 400 and 650 nm with a UV/visible spectrophotometer. To determine the natural fade back of the merocyanine form to the spiropyran form, a 1 ml aliquot of 1 mg/ml SP-COOH in ethanol was illuminated for 15 minutes with UV light. The sample was scanned and then removed from the spectrophotometer and exposed to ambient light. The sample was then scanned every two minutes until the absorption profile stabilised.

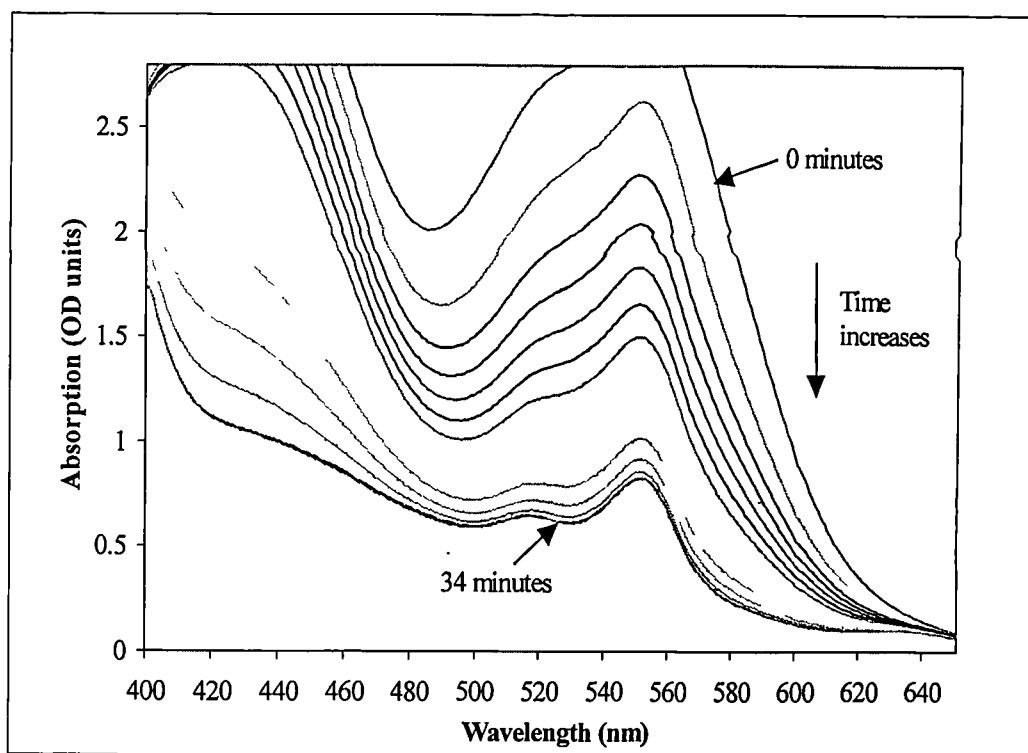


Figure 5.6 Fade back of the merocyanine form of SP-COOH to the spiropyran form - 1.0 ml of 1 mg/ml SP-COOH in ethanol was illuminated for 15 minutes with UV light and allowed to fade back to the spiropyran form. The absorption profiles were recorded at two minute intervals.

Figure 5.6 shows that the absorption peak at 548 nm is greater than 3 with 15 minutes UV illumination. The fade back is initially rapid, but becomes much slower as the spiropyran reaches equilibrium under ambient lighting conditions. The last three time points (30 – 34 minutes) show very little change in absorption.

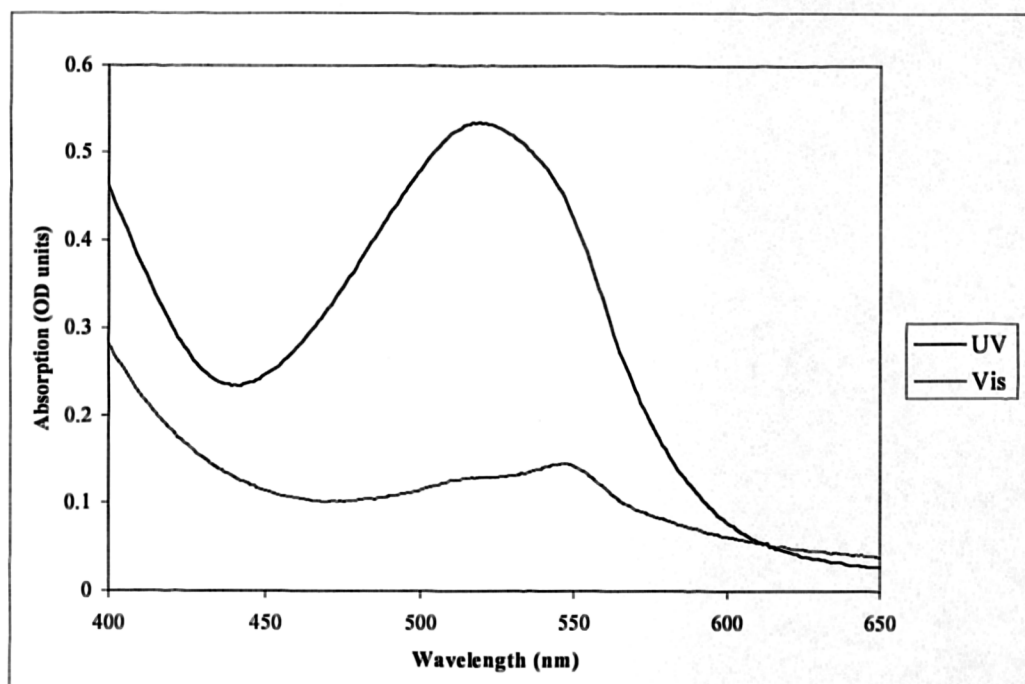


Figure 5.7 The absorption of SP-COOH in ethanol under visible and UV illumination – the sample, containing 100 $\mu\text{g/ml}$ SP-COOH in ethanol, was illuminated with either UV (245 nm) or visible (Tungsten, 80 watt) light for five minutes before being assayed for adsorption.

Figure 5.7 shows the absorption of SP-COOH in ethanol under visible and UV illumination, but where the sample is illuminated with visible light as opposed to being allowed to fade back naturally. When compared to the profiles shown in figure 5.6, the maximum absorption of the SP-COOH is lower in figure 5.7. This may be due to the fact that this sample was illuminated for a much shorter period of time. The subsequent back illumination with visible light reduces the absorption at 540 – 560 nm. This shows that the steady state achieved in figure 5.6 is an equilibrium created by the broad range of wavelengths present in ambient light, but that illumination with strong visible light can drive the dye further towards the spiropyran form.

5.3.4 Synthesis SP-Gox

SP-Gox was synthesised as a prerequisite to the subsequent photomodulation experiments. The elution profile of the conjugate from a PD10 column is shown in figure 5.10, from this result, fractions 3 and 4 were pooled and used for subsequent experiments.

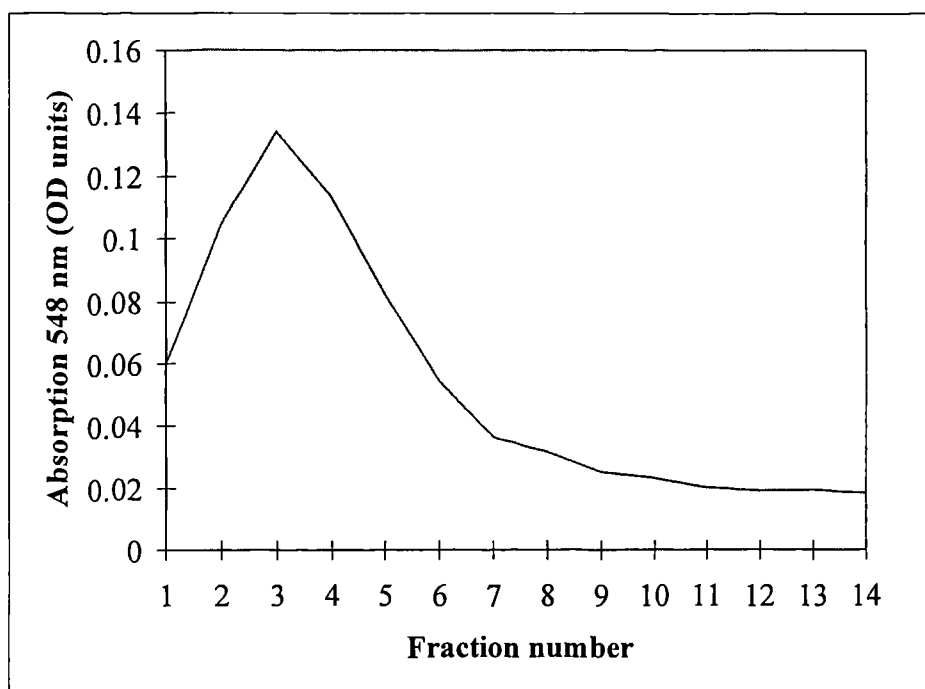


Figure 5.8 Elution profile of SP-GOx from a PD10 column – fraction volume 1.5 ml. The adsorption of spiropyran at 548 nm was used to detect both the conjugated SP-GOx and the unconjugated SP-COOH. A second peak for SP-COOH is not clearly defined, as the spiropyran has been retained within the PD10 column, as shown by the colouration of the column.

Figure 5.8 shows the elution peak of the SP-GOx being eluted immediately after the void volume of the PD10 column. There is no evidence of a second peak for unconjugated spiropyran, which is either due to all available spiropyran being conjugated to the protein, or to the unconjugated spiropyran being retained within the column matrix, which showed a distinct colouration. Fractions 2, 3 and 4 were pooled, and the solution then assayed for protein content and spiropyran concentration. This indicated that the spiropyran : GOx ratio was 4:1, which indicates that only 30% of available amines within the protein structure are available to covalently attach to GOx under the chosen conditions.

5.3.5 The activity of SP-Gox compared to native GOx under visible and UV illumination

To determine whether spiropyran (SP) dyes can be used for the modulation of protein function, the SP dye must be linked to the protein using a simple, non-aggressive procedure to avoid any disruption to protein structure. EDC reactions have been used to covalently attach spiropyrans to proteins via the carboxyl group of the carboxylated spiropyran (SP-COOH) and the amino groups present on lysine residues and N-terminal amines of the protein primary structure. To determine whether the spiropyran dye can affect the activity of the enzyme, a comparison of the glucose catabolism of native and SP coupled proteins under the influence of UV and visible light was conducted

Glucose oxidase (GOx) (Type VII-S from *A. niger*, EC code 1.1.3.4, Sigma code: G-7016) catalyses the aerobic oxidation of glucose to D-gluconate and hydrogen peroxide. Enzyme activity was assayed using a coupled assay (Szutowicz, *et al*, 1984) comprising glucose and glucose oxidase (EC 1.1.3.4 from *Aspergillus niger*, code: G 7016, Sigma, UK) to produce hydrogen peroxide as a substrate for horseradish peroxidase (HRP) to convert the indicator dye 2,2' azino bis (3 ethyl) benzthiazoline-6-sulfonic acid (ABTS) (Sigma code: A-1888), as shown in figure 5.9 (Makinen and Tonovuo, 1982) from a colourless to a coloured form with the reaction monitored by optical adsorption at 415nm in a spectrophotometer (Camspec model M350).

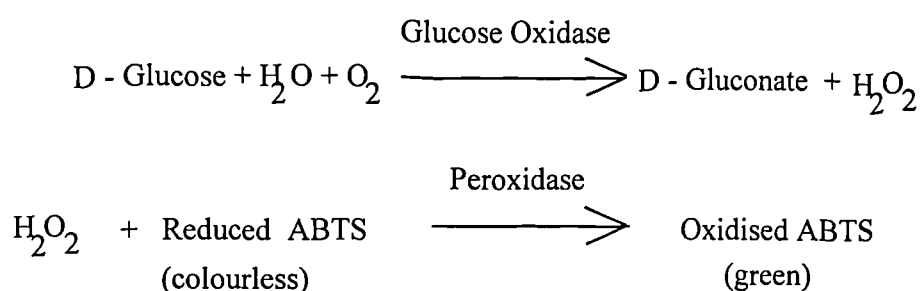


Figure. 5.9 The reaction mechanism of the glucose oxidase assay

The oxidation of ABTS produces a green-blue coloration that has an extinction coefficient of 36.8 OD units at 415 nm for a 1 mM solution. Assuming linearity, this equates to an $\text{Abs}_{415 \text{ nm}}$ of 0.271 for 100 μmol solution of oxidised ABTS with a path length of 1 cm.

By comparing the activity of the SP-Gox conjugate with the activity of equivalent concentrations of unmodified glucose oxidase, the percentage of activity lost in binding to the spiropyran was determined. This was achieved by incubating a known concentration of glucose with a known concentration of either native glucose oxidase or SP-Gox under both UV and visible illumination and determining the rate of oxidation of ABTS that occurs. Direct comparison of results should determine the loss of activity upon binding of SP.

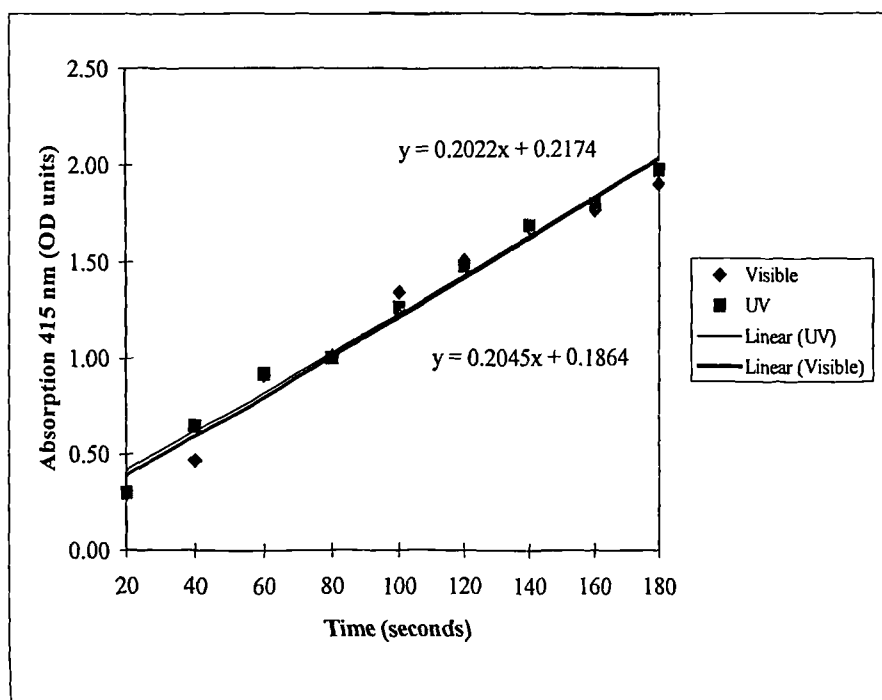


Figure. 5.10 The effect of UV and visible illumination on native glucose oxidase. – The example comprised GOx at a concentration of 5 µg/ml in 100 mM MES buffer, pH 6.8. The data points are specific absorbance measurements and the lines represent linear regressions and used to calculate the specific enzyme activity of the native GOx under the different illumination.

The results of the assay show that the native GOx was very active, shown by the degree of oxidation that has occurred. The effect of visible or UV illumination on GOx (Figure 5.10) was that no discernible variation on activity could be determined between the two conditions. This was support by the fact that the specific activity of the two samples was 0.352 enzyme units per mg for UV illumination and 0.337 enzyme units per mg for visible illumination.

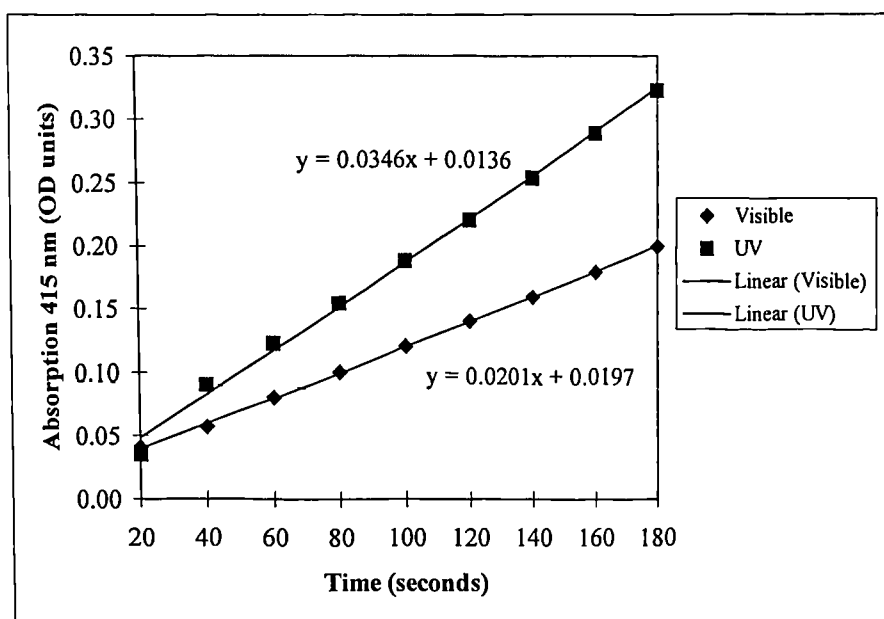


Figure. 5.11 The effect of UV and visible illumination on SP-glucose oxidase - The example comprised SP-GOx at a concentration of 20 $\mu\text{g/ml}$ in 100 mM MES buffer, pH 6.8. The data points are specific absorbance measurements and the lines represent linear regressions and used to calculate the specific enzyme activity of the native SP-GOx under the different illumination.

The effect of visible or UV illumination on SP-Gox (SP:Gox $\sim 4:1$) (figure 5.11) was that the visibly illuminated samples show $\sim 42\%$ reduction on activity when compared to the rate measured for UV illumination. These results show a change in activity between native and modified GOx. This change suggests an inhibition of SP-GOx under illumination with visible light, shown by a reduction in activity compared to SP-GOx illuminated by UV light.

The specific activity of the samples was 544.8 enzyme units per mg for native GOx and 278.6 enzyme units per mg SP-GOx. This shows that the conjugation of carboxylated spiropyran to GOx results in a reduction in activity of approximately $\sim 49\%$. This reduction in activity is probably due to inappropriate crosslinking during the conjugation process that has disrupted the active site of the protein.

5.3.6 Synthesis of SP-HRP

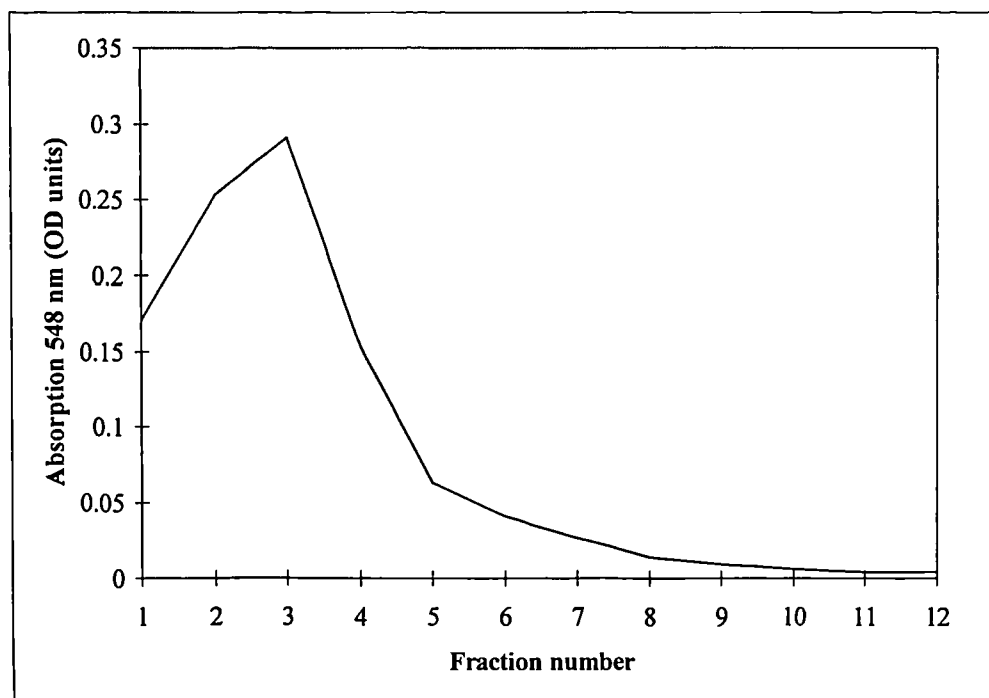


Figure 5.12 Elution profile of SP-HRP from a PD10 column – fraction volume 1.5 ml. The adsorption of spiropyran at 548 nm was used to detect both the conjugated SP-HRP and the unconjugated SP-COOH. A second peak for SP-COOH is not clearly defined, as the spiropyran has been retained within the PD10 column, as shown by the colouration of the column.

Figure 5.12 shows the absorption peak of the SP-HRP being eluted immediately after the void volume of the PD10 column. There is no evidence of a second peak for unconjugated spiropyran, which is either due to all available spiropyran being conjugated to the protein, or to the unconjugated spiropyran being retained within the column matrix, which was evident by colouration of the column. Fractions 2, 3 and 4 were pooled, and the solution then assayed for protein content and spiropyran concentration. This indicated that the spiropyran : HRP ratio was 6:1.

5.3.7 The activity of SP-HRP compared to native HRP under visible and UV illumination

As a control for the photomodulation of the SP-HRP conjugate, the assay was performed under visible and UV illumination using the native protein at a concentration of 2 µg/ml. The enzyme activity produced was determined as for 5.2.5.2, and is shown in figure 5.15.

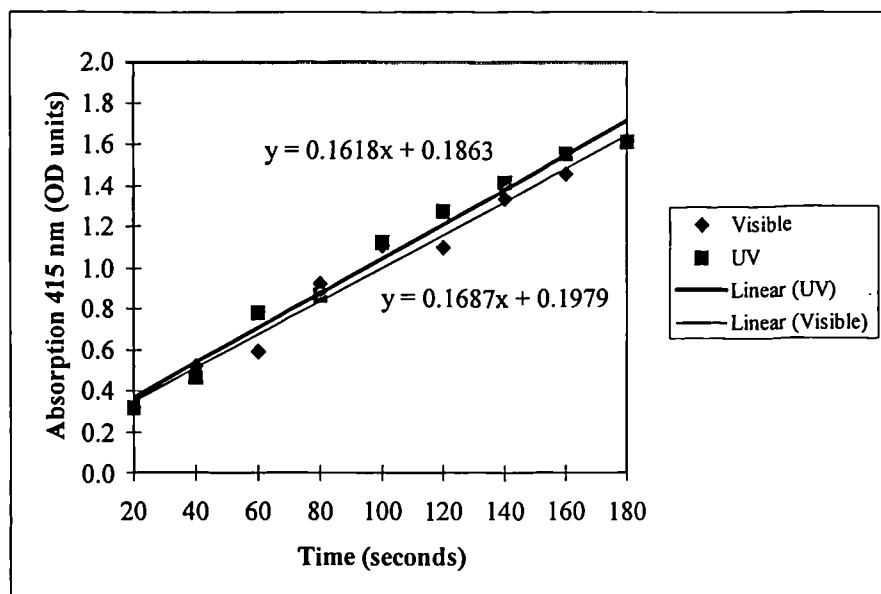


Figure 5.13 The effect of UV and visible illumination on native HRP - The example comprised HRP at a concentration of 1 µg/ml in 100 mM MES buffer, pH 6.8. The data points are specific absorbance measurements and the lines represent linear regressions and used to calculate the specific enzyme activity of the native HRP under the different illumination.

The results of the assay (figure 5.13) show that the native HRP was very active, shown by the degree of oxidation that has occurred. The effect of visible or UV illumination on HRP shown in figure 5.13, was that no discernible variation on activity could be determined between the two conditions. This was support by the fact that the specific activity of the two samples was 0.644 enzyme units per mg for UV illumination and 0.651 enzyme units per mg for visible illumination.

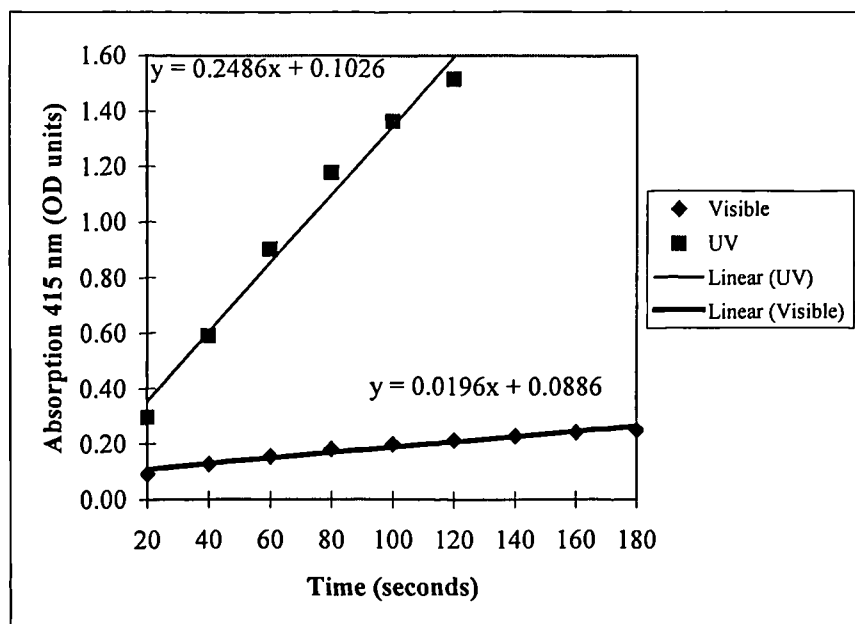


Figure 5.14 The effect of UV and visible illumination on SP-HRP - The example comprised SP-HRP at a concentration of 1.8 $\mu\text{g/ml}$ in 100 mM MES buffer, pH 6.8. The data points are specific absorbance measurements and the lines represent linear regressions and used to calculate the specific enzyme activity of the native SP-HRP under the different illumination.

This data shows reduction in rate of the SP-HRP (figure 5.14) under visible illumination of ~88%. This was considerably more variation than the GOx study. These results show a change in activity between native and modified HRP. This change suggests an inhibition of SP-HRP under illumination with visible light, shown by a reduction in activity compared to SP-HRP illuminated by UV light.

The specific activity of the samples was 2166.4 enzyme units per mg for native HRP and 440.6 enzyme units per mg SP-HRP. This shows that the conjugation of carboxylated spiropyran to HRP results in a reduction in activity of approximately ~ 89 %. This reduction in activity is probably due to inappropriate crosslinking during the conjugation process that has disrupted the active site of the protein.

5.4 The effect of variation of conjugation time on photochromic activity

Following from the previous experiments, an assay was designed to determine the effect of the ratio of SP to protein on photochromic modulation of protein activity. Variation of spiropyran conjugation is achieved by creating a large volume synthesis as for section 5.2.3 and removing 2 ml aliquots at 20 minute intervals. These aliquots were immediately separated by PD10 column, as for section 5.2.3. The ratio of dye to protein was determined by the ratio of the absorption at 548 nm and protein content determined from the Folin Lowry assay.

5.4.1 Variation of SP content to glucose oxidase

To determine the effect of variable spiropyran loading on GOx activity, a conjugation of SP-COOH with GOx was initiated. At 20, 40, 60, 90 and 120 minutes, 2 ml aliquots were taken and the conjugate and unreacted species were separated via a PD10 column. The collected aliquots were assayed for activity under UV and visible illumination, the results are shown in figure 5.17.

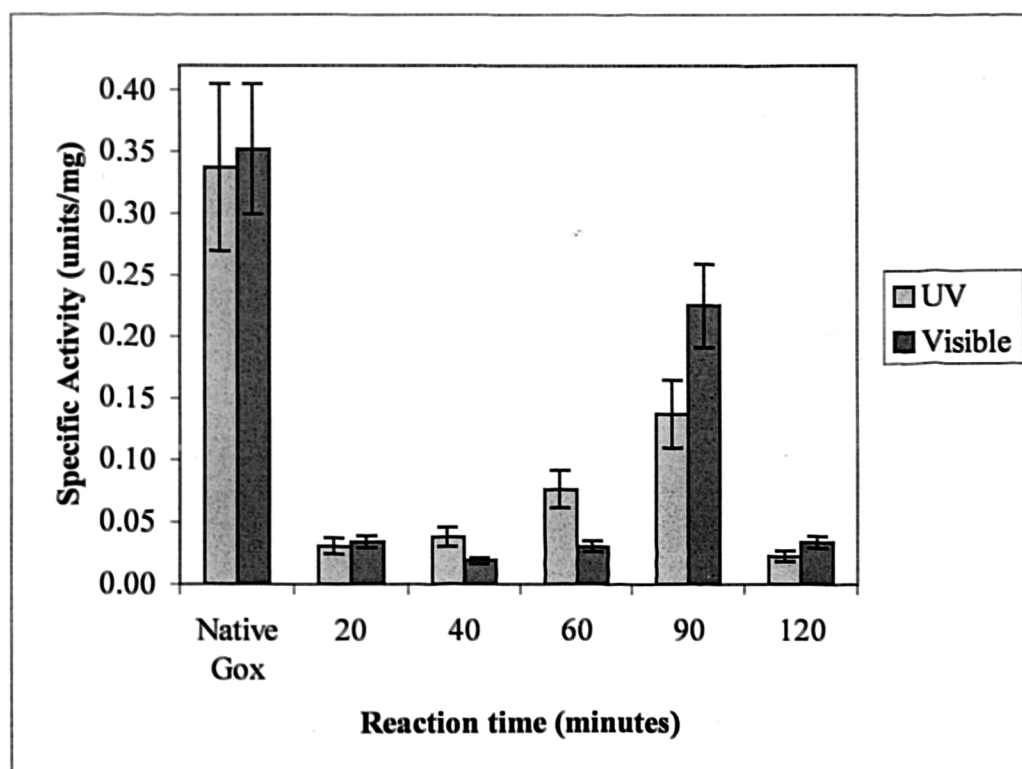


Figure 5.15 Effect of conjugation reaction time on the photo-modulation of enzyme activity of Glucose oxidase - spiropyran dye (SP-GOx) conjugates. Specific activities of the SP-GOx conjugates were determined via a spectrophotometric enzyme assay under either UV or visible illumination. The dye:enzyme ratios were determined spectrophotometrically and are shown in Table 5.1. Error bars represent the standard deviation of three repeats.

Figure 5.15 summarises the specific enzyme activities for a range of SP-GOx conjugates obtained from various lengths of conjugation reactions. For the controls consisting of native GOx under visible and UV illumination, similar specific activities are seen, as expected. It is apparent that for the synthesised SP-Goxs specific activities under both UV and visible illumination are significantly reduced, For the 40 minute incubation, 1:2.5 enzyme:dye ratio, a reduction of 88% in enzyme specific activity is seen under UV illumination compared to native enzyme and under visible illumination, a reduction of specific activity of 94% versus the native is observed. The 90 minute incubation is an exception, as it shows an increase in specific activity compared to the other conjugates. This is thought to be an artefact of the of the enzyme activity assay, giving a false result.

These results show that the effect of photomodulation under visible illumination can be significant for SP-GOx, but that the overall reduction in enzyme activity after SP conjugation may be too great for the enzyme to be used in an assay format. It is unknown whether the process of conjugation or the covalent attachment of the spiropyran to the protein is the principle cause of the loss in activity.

5.4.2 Variation of SP content to HRP activity

To determine the effect of variable spiropyran loading on HRP activity, a conjugation of SP-COOH with HRP was initiated as above. At 20, 40, 60, 90 and 120 minutes, 2 ml aliquots were taken and the conjugate and unreacted species were separated via a PD10 column. The collected aliquots were assayed for activity under UV and visible illumination, the results are shown in figure 5.16.

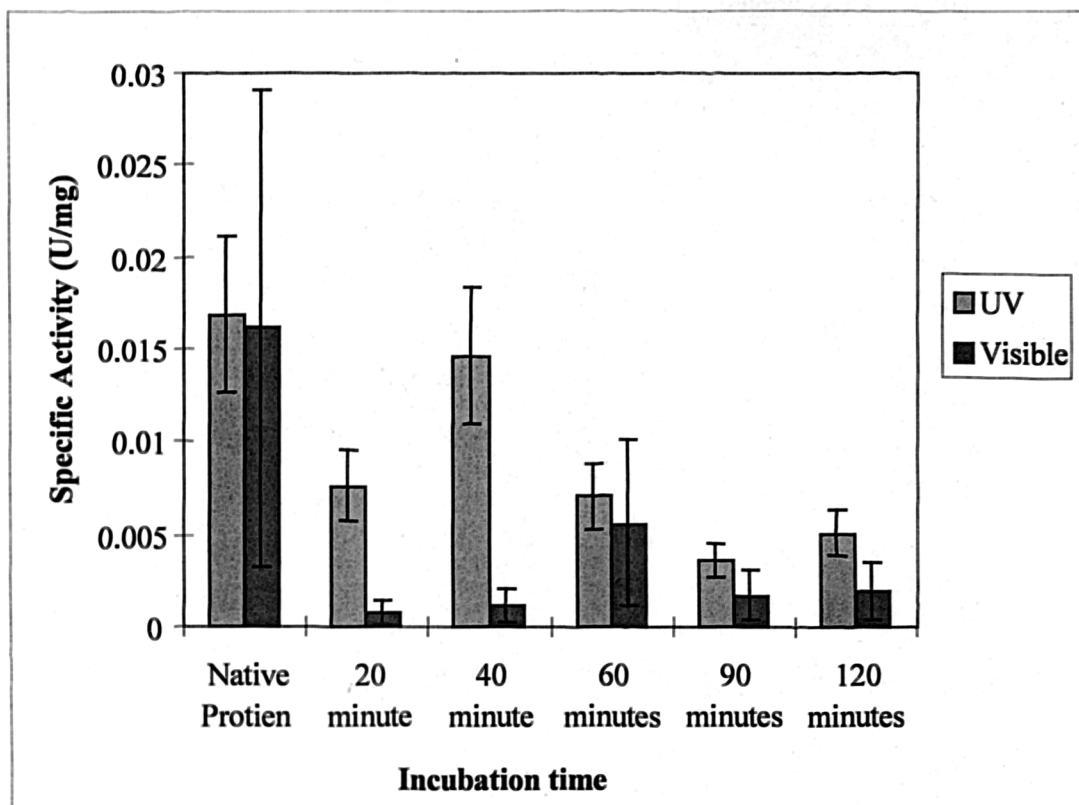


Figure 5.16 Effect of conjugation reaction time on the photo-modulation of enzyme activity of spiropyran dye - horseradish peroxidase (SP-HRP) conjugates. Specific activities of the SP-HRP conjugates were determined via a spectrophotometric enzyme assay under either UV or visible illumination. The dye:enzyme ratios were determined spectrophotometrically and are shown in Table 5.1. Error bars represent the standard deviation of three repeats.

The direct comparison of incubation time to dye loading is shown in table 5.1. From this it can be seen that the dye loading increases rapidly up to 60 minutes for both proteins, and then plateaus. This implies that the majority of the amines are occupied at 1 hour. Any further activity that occurs after this time will involve the crosslinking within or between protein structures. This may account for the reduction in HRP activity that is seen after 60 minutes.

Table 5.1: the increase in protein dye loading as a function of incubation time -

Time (mins)	SP:Gox	SP:HRP
0	0:1	0:1
20	1.3:1	6.5:1
40	2.5:1	8.5:1
60	3:1	8:1
90	3:1	8:1
120	3:1	9:1

Table 5.1 also shows that the dye loading is much less for GOx than for HRP, although GOx has more potential binding sites (14 compared to 9). While the dye loading of HRP is complete at 120 minutes, for GOx it is less than 30%. This may be due to the surface area : volume ratio of GOx, with a large percentage of the lysine residues being involved in the interior of the protein and therefore are not available to be covalently attached to. This may account for the difference in modulation between SP-GOx and SP-HRP.

Figure 5.16 summarises the specific enzyme activities for a range of SP-HRP conjugates obtained from various lengths of conjugation reactions. For the controls consisting of native HPR under visible and UV illumination, similar specific activities are seen, as expected. It is apparent that for SP-HRP produced via long conjugation reaction times, greater than 40 minutes, specific activities under both UV and visible illumination are significantly reduced.

Since the degree of conjugation does not increase, the formation of carbodiimide cross-linked enzyme aggregates may account for this observation. For reaction times of 20 and 40 minutes, a significant variation of enzyme specific activity is seen between UV and visible illumination. For the 40 minute incubation, 1:8.5 enzyme:dye ratio, a reduction of 13% in enzyme specific activity is seen under UV illumination compared to native enzyme and under visible illumination, a reduction of specific activity of 93% versus the native is observed. The reduction in specific activity for the SP-HRP under visible compared to UV illumination is 92%. At present, it is not understood why the SP-HRP produced via a 20 minute reaction, 1:6.5 enzyme:dye ratio, demonstrates a reduced specific activity under UV illumination compared to both native HRP and SP-HRP produced via a 40 minute reaction.

5.5 Discussion and Conclusions

5.5.1 Synthesis of SP-COOH

The organic synthesis of SP-COOH demonstrated that while the synthesis of the dye is simple to perform, the purification of the synthesised compound is more complex. Within this project, a series of washing steps has been used to remove precursors from the synthesised and solidified dye. When the dye was subsequently used within conjugation reactions, insoluble coloured solids were produced when the dye was dissolved.

This method differs from the standard method in using 1-carboxyethyl-2,3,3-trimethylindolenium iodide was used as the spiropyran precursor in the place of 1-carboxymethyl-2,3,3-trimethylindolenium iodide. This increases the linker length between the carboxyl group and the spiropyran, and as such may increase the freedom of rotation of the spiropyran when conjugated to proteins. The yield of the dye was 5 %, compared to > 90 % for the published method (Aizawa *et al*, 1977). The synthesised spiropyran contained a percentage of insoluble by-product present in the final product, but there is little soluble impurity, as the TLC separation would have shown any soluble by-product.

To improve the synthesis, a re-crystallisation and filtration step would reduce the amount of insoluble by-product. To improve the yield of the synthesis, the solvent used for the washing stage, 5% ethanol in toluene, could be modified. Reducing the ethanol to 3% would reduce the loss of product due to inappropriate solvation.

5.5.2 Synthesis and Photomodulation of SP-Protein conjugates

Glucose oxidase was a logical protein to initially photomodulate. The fact that GOx was a novel system combined with the relatively high activity, low cost and large body of data concerning GOx lead to it being the first choice for spiropyran conjugation. At the start of the project, there were no reports that GOx had been used for this type of experiment, but it has since been described by Willner and Willner (1997). No comparison with these results is possible, as they do not clearly state the degree of photomodulation that has been achieved. The nature of the GOx activity assay that was used required that a second enzyme, horseradish peroxidase, be used to convert the hydrogen peroxide generated by the GOx into

a measurable product, using a colourmetric reagent, for these experiments ABTS. The indications from SP-GOx are that the protein function has been down regulated by as much as 30% in the presence of strong visible light. This may be due to change in molecular dipole as the dye switches from its open (merocyanine) form to the closed (spiropyran) form, which causes an interaction with the protein structure, resulting in disruption of the protein active site.

From this it was a natural progression to retain the assay format and conjugate the second enzyme of the glucose oxidase assay, HRP, to spiropyran, allowing the assay format to be retained. To this time, there are no reports in the literature of HRP having been used for spiropyran conjugation. The work reported here has been recently published (Weston *et al*, 1999) The results for the conjugate with an enzyme:dye ratio of 1:8.5 shows a reduction of 92% in the enzyme reaction rate when illumination was changed from UV to visible, i.e. from merocyanine photoisomer to spiropyran photoisomer.

Figures 5.16 and 5.17 summarise the specific enzyme activities for a range of SP-protein conjugates obtained from various lengths of conjugation reactions. For the controls consisting of native proteins under visible and UV illumination, similar specific activities are seen, as expected. It is apparent that for conjugates produced via long conjugation reaction times, greater than 40 minutes, specific activities under both UV and visible illumination are significantly reduced. The results demonstrated that both glucose oxidase and HRP, when conjugated to SP-COOH showed a reduction in activity when illuminated with strong visible light, but showed no loss of activity when illuminated with UV light.

The observed amount of the conjugated photochromic dye that is switched from the merocyanine to the spiropyran form upon visible illumination SP-HRP was determined. This suggested that only ~ 30% of the attached dyes have switched forms under the appropriate illumination. Therefore the reduction in specific activity observed may only be due to the switching of 2-3 dye molecules. This indicates that only a small number of the bound dyes are involved in the modulation of protein function and suggest that modulation occurs due to close interaction of the dyes with the active site of the protein, either via direct steric effects or via local distortion of the protein around the active site.

The photomodulation of covalently conjugated spiropyran-protein systems has been demonstrated with a variety of spiropyrans and proteins, as shown in Table 1.1. While all of the protein systems modulated with spiropyran dyes show a degree of modulated activity, none demonstrates the change in activity that HRP has done within these experiments.

5.5.3 The mechanism of photomodulation

The effect of photo induced isomerisation of spiropyran dyes on protein structure has not been fully defined. Proposed mechanisms for photo-modulation of protein function range from direct influence of the photochromic dye on the activity site (Harada *et al*, 1994) to distortion of the protein tertiary structure (Pieroni and Fissi, 1992; Willner and Willner, 1997). It has been reported by Montagnoli and Pieroni (1983) that when illuminated with UV light the spiropyran dye exists in the merocyanine form, which introduces a distinct polarity to the molecule. It was proposed that this polarity change may have such a great effect on protein structure that as few as one spiropyran molecule may be all that is needed to disrupt the secondary structure of a polypeptide.

Studies performed on polypeptides have shown how the spiropyran dyes interact with secondary structures, particularly α helices. Cooper *et al* (1999) examined the effect which photochromic modulation had on a range of polypeptides, and determined two points: Firstly, the spiropyran dyes attached to side chains interact with the solvent surrounding the molecule. The solvent stabilised the polar, merocyanine form of the dye, and this increased the hydrogen bonding within the polypeptide. In the spiropyran form, the lower polarity of the dye prevented entry of the solvent into the peptide backbone, which was subsequently destabilised. Secondly, the interaction of the merocyanine form with the α helices results in the extension of hydrogen bonds and an increase in flexibility of the of the peptide backbone, resulting the α helix structure being poorly conserved.

From the results presented in this chapter, the following hypothesis is proposed: as the molecular weight of a protein increases the extent and complexity of the tertiary structure generally increases. In turn, this often increases the stability of the protein. Conversely, as protein molecular weight decreases, the stability can decrease. In terms of the potential to photomodulate a particular protein, the higher the molecular weight, the lower the potential

degree of photomodulation that can be achieved. This simply implies that the more stable a protein is, the more difficult it is to perturb the structure.

Comparison of the two enzymes that were photomodulated here reveals two features of importance. Firstly, horseradish peroxidase is an enzyme that contains virtually no β sheet, consisting of nearly all α helices, whereas GOx is a more conventional enzyme, having both β sheet, and α helices present. This feature of HRP, and indeed of the peroxidase super family (Banci, 1997), has led to the development of a hypothesis of the mode of action of photomodulation.

5.5.4 A proposed hypothesis for the photomodulation of spiropyran modified proteins

If a molecule contains a large percentage of α helices, it is likely to be modulated by the interaction of the spiropyran form of the spiropyran dye. It is unlikely that the amount of α helix present within a protein structure is the only feature that is involved in the process of photomodulation.

It is suggested that the effect of the change in polarity of the spiropyran dye and the molecular weight of the protein have a significant effect on the degree of photomodulation that is observed. The hypothesis that will be tested is this: the effect of the shape : polarity variation which occurs when the photochromic species is driven from the merocyanine to the form creates an interaction with the protein to which it is attached. If the spiropyran is attached to an α helix, the resulting spiropyran isomerisation may result in a disruption of the water molecules associated to the protein. This disruption may effect the hydrogen bonding which maintains the secondary structure of the protein, which could have an effect distal from the site of modulation by affecting the tertiary structure of the protein. As the molecular weight of the protein increases, the covalent attachment points of the spiropyran dye become more separated, and the possibility of a cumulative effect of several photomodulation events is reduced. Therefore, as molecular weight increase, the degree of photomodulation that can be achieved is reduced.

5.5.5 Conclusions

To conclude, the first photo-modulation of the important redox enzyme horseradish peroxidase has been observed. The degree of photo-modulation reported here, 92% reduction in enzyme activity under visible illumination compared to UV illumination matches the largest degree of photo-modulation previously reported in the literature for a spiropyran dye. The observation that only a small fraction of the conjugated photochromic molecules are photo-switched to cause the reduced activity suggests that for the studied system, the dyes influence the enzyme activity via local interaction which may be distal from the enzyme active site.

To test the proposed hypothesis two protein systems with varying molecular weights, the peroxidase super family and an antibody / Fab system, will be conjugated with spiropyran dyes and photomodulated in Chapters 6 and 7.

Chapter 6: The effect of protein molecular weight on photochromic activity

6.1 Introduction

Chapter 5 has shown that the photomodulation of two differing enzymes results in a distinct difference in the degree of photomodulation that can occur. Spiropyran modified horseradish peroxidase has shown a down regulation which is comparative to the largest decrease in activity due to photomodulation by spiropyran dyes currently presented in the literature, which is ~ 60% for concanavalin (Wilner, *et al*, 1993). The reason behind this high degree of modulation has been considered, and within this chapter the possible mechanism of photomodulation is expanded and the hypothesis that was proposed in section 5.5.3 is tested.

6.1.1 Molecular weight as the restricting factor to photomodulation

The hypothesis presented in Chapter 5 states that photochromic modulation effects increase as the molecular weight of the modified protein decreases. To test this hypothesis a range of proteins with common secondary structures and an ability to utilise the same substrates but with differing molecular weights was needed.

The super family of peroxidase enzymes (E.C. 1.1.11.7) contains enzymes ranging from ~ 35 kDa to ~100 kDa (Banci, 1997) The peroxidase family is a group of enzymes which all show a conserved active site, yet have molecular structures which are more or less extended (Welinder *et al*, 1992). While the extent of the protein backbone varies greatly, there are common features that are conserved (Henrissat, 1990; Li and Poulos, 1994). The principal conserved residues of the enzymes are Arg48, His52, Asn 82, His 175 and Asp 235, which appear to be central in peroxidase specific catalysis. Asp106, Gly 129 and Arg130 form a buried salt bridge central to the conformation of the enzyme. A further 22 amino acids are nearly invariant, and constitute the conserved structural framework of the enzyme (Welinder *et al*, 1992).

At the level of tertiary structure, the enzymes throughout the peroxidase family all have a structure that is similar, being predominantly composed of 10 dominating α helices (Welinder *et al*, 1992) with very little β sheet being present. This feature may be a principal reason why photomodulation is so effective with peroxidases, as the structural disruption caused by the

creation of the spiropyran dipole may have a greater effect on the secondary structure of α helices than of β sheets, as discussed in Chapter 5.

The enzymes chosen for this study were HRP, lactoperoxidase and myeloperoxidase. These are the three most commonly available peroxidases, and represent a wide spread of molecular weights, 43, 77 and 102 kDa respectively (Banci, 1997; Henriksen *et al*, 1998). Microperoxidase was also obtained as part of this study as it has the conserved active site present in the peroxidase super family. The molecular weight of microperoxidase is only 1.2 kDa, and it is therefore a catalytic peptide, not having an extended molecular structure as the other enzymes do. It is possible to use the same substrates (H_2O_2 and the colourimetric co-substrate ABTS) and assay format for all enzymes used.,

6.1.2 Aims

The aim of this chapter is to investigate the hypothesis proposed in Chapter Five, by selecting members of a protein family with similar structures and activities, but varying molecular weights. The activity of the native and SP conjugated proteins will be compared, and the hypothesis will be revised according to the results obtained.

6.2 Methods

6.2.1 Conjugation of enzymes to SP-COOH

The enzymes used for these experiments were Horseradish peroxidase, Lactoperoxidase (Fluka, Poole Dorset, product code: 61328), Myeloperoxidase (Sigma, Poole Dorset, product code: M 6908) and Microperoxidase (Biozyme Laboratories Ltd, Gwent, Wales. product code: MPO1). The enzymes were conjugated to SP-COOH utilising EDC chemistry as described in chapter 5. The enzymes were diluted to 2 mg/ml with 100 mM MES (pH 6.8). 500 µg of carboxylated spiropyran was dissolved in 0.25 ml of absolute ethanol and then diluted to 1 ml with 100 mM MES (pH 6.8). The two solutions were combined resulting in a final mixture of 1 mg/ml enzyme 250 µg/ml SP-COOH in 12.5% EtOH in 100 mM MES. This solution was activated by the addition of 1 mg/ml EDC and allowed to incubate at 20°C for 1 hour. A 1 hour incubation is used as it has been shown to be the optimum incubation time for interaction with protein (section 5.4) The number of spiropyran dyes which attach to the proteins of interest will vary in each case, as the number of spiropyran binding sites will vary.

At the end of incubation the protein conjugate solution was passed through a PD10 column (Pharmacia, Uppsala, Sweden) and the eluted fractions assayed for the presence of photochromic dye by measuring Abs_{548nm}. The protein conjugated spiropyrans are eluted in the void volume of the column, with any unbound spiropyran being retained within the column matrix. The ratio of spiropyran to protein is determined by the ratio of the Abs_{548nm} of the pooled fractions and of the protein concentration determined by the Folin Lowry method.

6.2.2 Assay of enzyme activity

Enzyme activity was assayed as described in section 5.2.5, with the modification that the reaction buffer used was modified to pH 6.4, using a 100 mM MES buffer. This buffer was found to be suitable for all the enzymes, and was used for all assays. The colourimetric reagent used was ABTS, assayed for absorption at a wavelength of 415 nm. Photomodulation of the enzymes was as described in section 5.2.5.

6.3 Results

6.3.1 Synthesis of spiropyran-protein conjugates

The effective conjugation of carboxylated spiropyran with the peroxidase enzymes is central to the subsequent photomodulation experiments. The spiropyran protein conjugates were synthesised and separated via elution through a Sephadex PD10 column. The resulting elution profiles and dye : protein ratios are shown below.

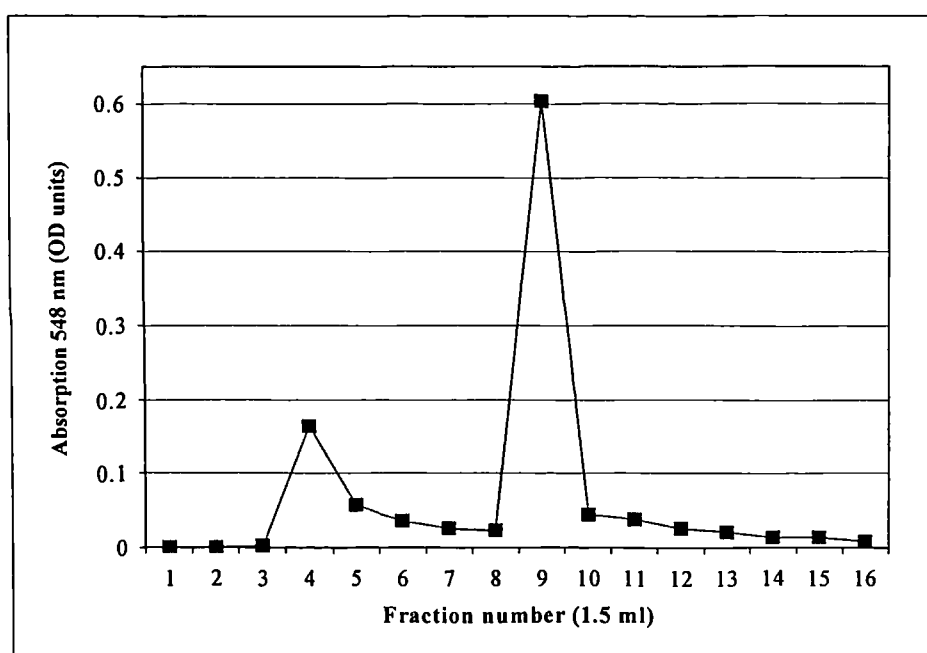


Figure 6.1: Elution profile of SP-HRP from a PD10 column (1.5 ml fractions).

The two absorption peaks, shown at fractions 4 and 9 in figure 6.1, show the SP-HRP conjugate (fraction 4) eluted in the void volume of the column and the unconjugated SP-COOH (fraction 9) retained longer on the column. The ratio of SP : HRP is ~6:1 as determined by the spiropyran concentration ($Abs_{548\text{ nm}}$) and the protein concentration determined by a Folin Lowry assay.

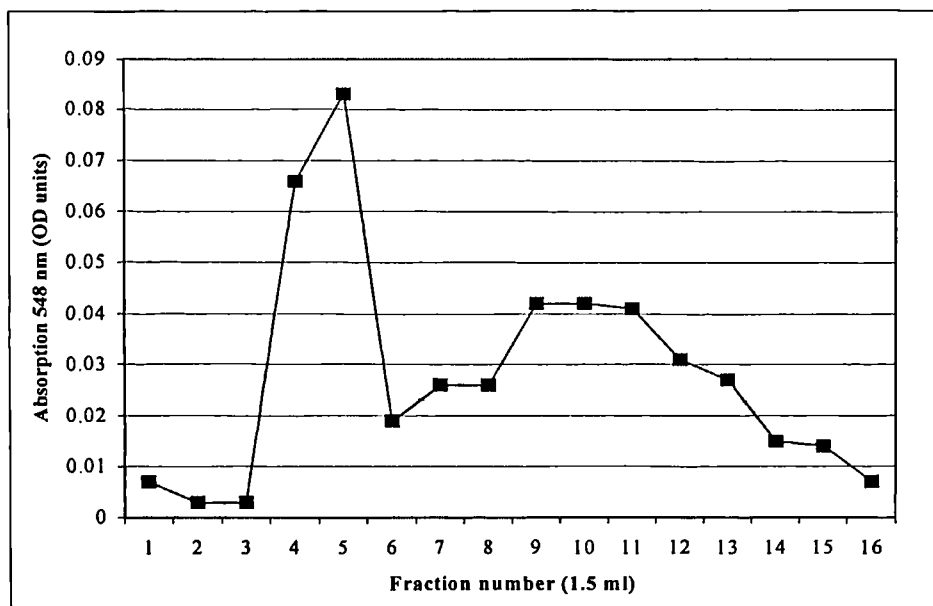


Figure 6.2: Elution profile of SP-Lpod from a PD10 column (1.5 ml fractions)

From the results of figure 6.2, fractions 4 and 5 were retained and used for subsequent photomodulation assays. While fractions 4 and 5 are the conjugated SP-LPod, the unconjugated SP-COOH can be seen as a second broad peak. The ratio of SP : LPod is ~14:1 as determined by the spiropyran concentration ($Abs_{548\text{ nm}}$) and the protein concentration determined by a Folin Lowry assay.

The elution profile of SP-myeloperoxidase from a PD10 column is shown in figure 6.3.

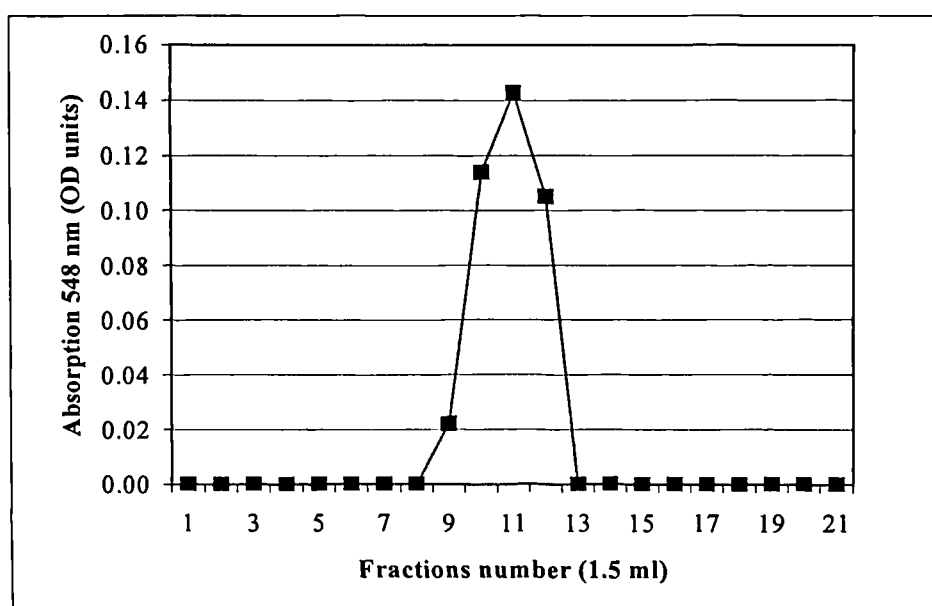


Figure 6.3: Elution profile of SP-myeloperoxidase from a PD10 column (1.5 ml fractions)

From the elution profile of , SP-myeloperoxidase no peak was observed at fractions 4 and 5 where the protein peak is expected. The unconjugated SP-COOH has been eluted in fractions 9 – 11, as shown for the elution profile of SP-HRP (figure 6.1). Therefore, the small amount of myeloperoxidase that is present in the conjugation solution was not detected, and therefore the SP-myeloperoxidase system could not be taken further.

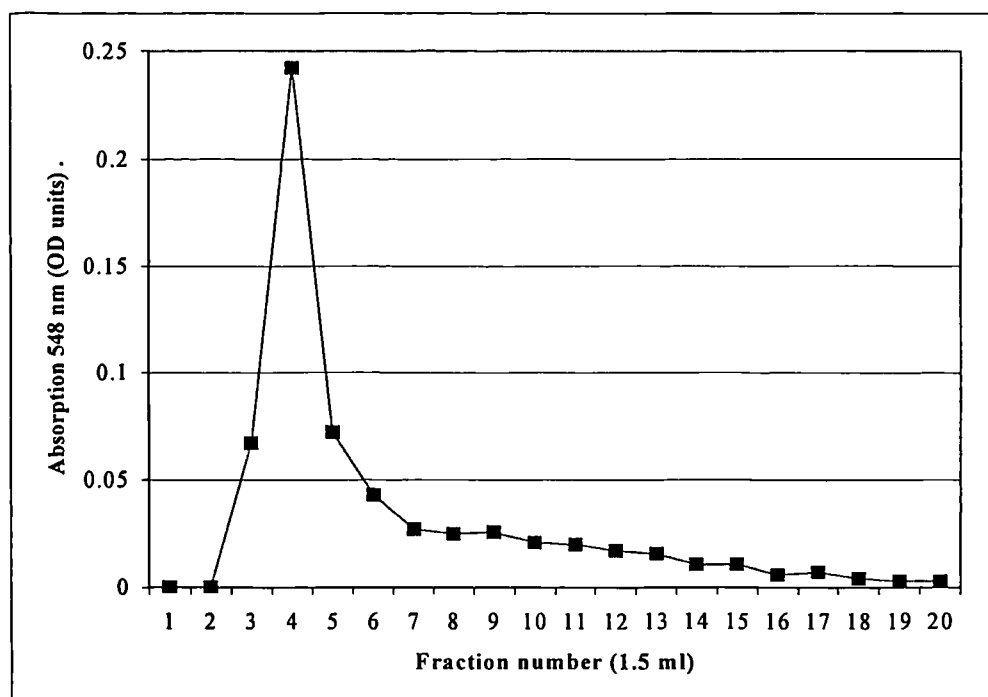


Figure 6.4: Elution profile of SP-microperoxidase from a PD10 column (1.5 ml fractions)

From the elution profile of SP-microperoxidase (figure 6.4), fractions 3 to 5 were the elution of the SP-microperoxidase. While microperoxidase is only a 1.2 kDa peptide, the SP-COOH has a molecular weight of 381, therefore the conjugate and unconjugated SP should be clearly defined as separate peaks. The lack of a second peak indicates that almost all of the SP-COOH has been conjugated to the microperoxidase. The ratio of SP : microperoxidase is ~3:1 as determined by the spiropyran concentration ($Abs_{548\text{ nm}}$) and the protein concentration determined by a Folin Lowry assay.

6.3.2 Photomodulation of HRP

The photomodulation of HRP was performed, using the introduction of H_2O_2 and without relying on the interaction of GOx with glucose as described in Chapter 5. This experiment has been performed as a base line for comparison with the other enzymes.

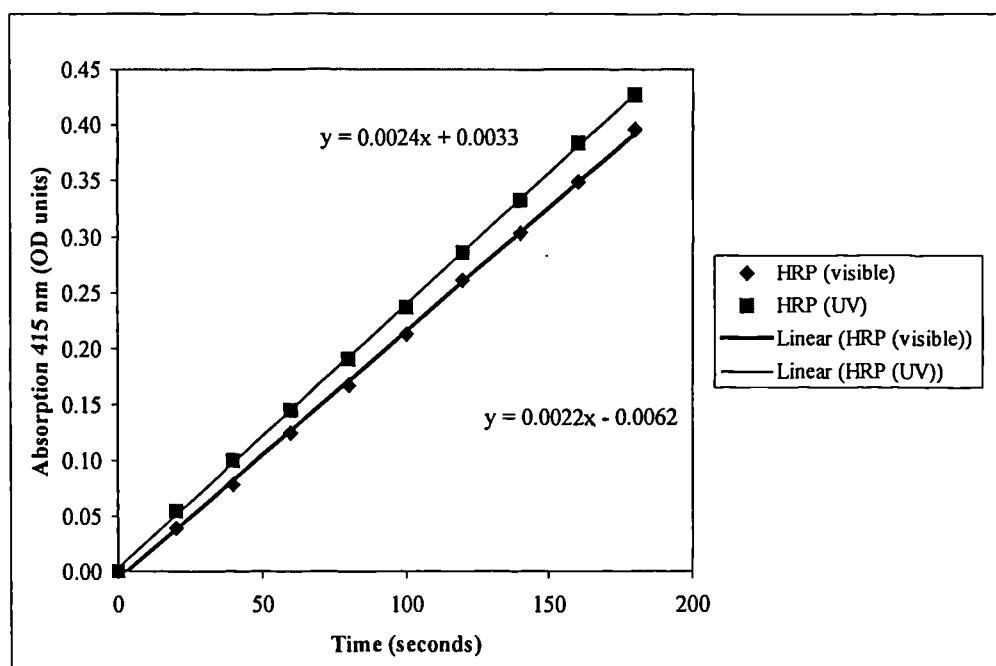


Figure 6.5: The effect of UV and Visible light on native HRP – 180 second incubation, with readings taken every twenty seconds. Illumination was either UV (245 nm) or visible light (Tungsten, 80 W) from a distance of 10 cm.

These results (figure 6.5) indicate that the native protein is stable under both UV and visible illumination, having a similar linear increase of absorption over the time course of the assay. As with the previous experiments (Chapter 5), the activity of the UV illuminated SP-HRP is similar to that for the native protein.

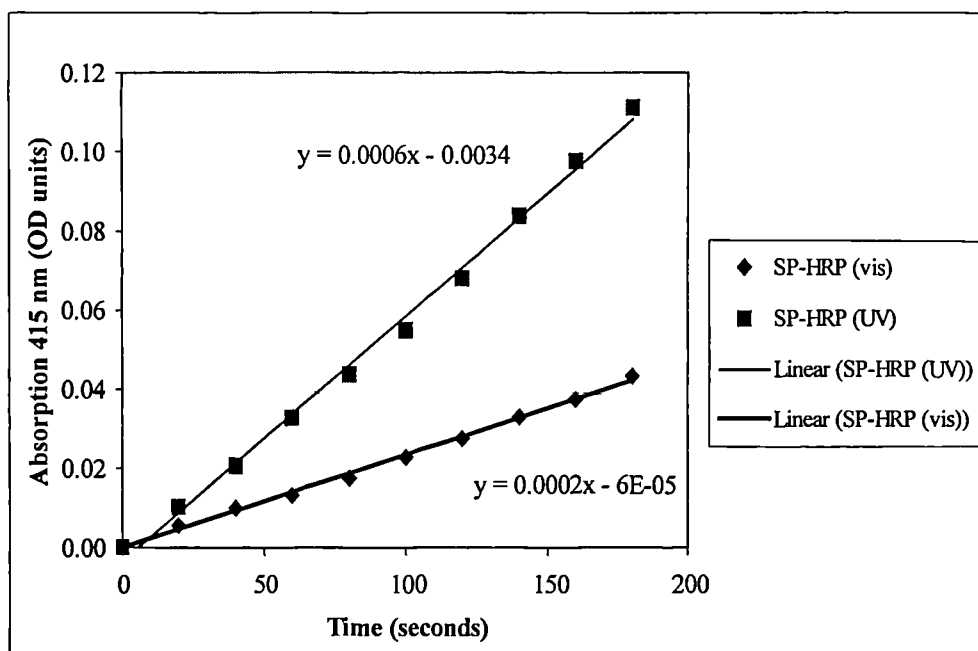


Figure 6.6: The effect of UV and Visible light on native SP-HRP - 180 second incubation, with readings taken every twenty seconds. Illumination was either UV (245 nm) or visible light (Tungsten, 80 W) from a distance of 10 cm.

Under visible illumination, the SP-HRP shows a reduction in activity ~ 60% compared to the activity under UV illumination. This result shows a reduction of ~ 30% compared to the results for the previous assay (Chapter 5). This may be due to the modification in the assay format, introducing H_2O_2 as opposed to utilising H_2O_2 generated from glucose oxidase.

The specific activities of the native proteins under both UV and visible light were calculated as 89.0 and 125.5 molar EU for native HRP and 46.0 and 76.6 molar EU for SP-HRP respectively. This indicates that the conjugation of the spiropyran to the protein has reduced the enzyme activity by ~ 50% for UV illumination and 40% for visible illumination

6.3.3 Photomodulation of lactoperoxidase

The enzyme lactoperoxidase was chosen as a possible enzyme for photomodulation, as it reacts with the same substrates as HRP, yet has a considerably higher molecular weight (72 kDa). Through the use of lactoperoxidase, it is intended to demonstrate that the increase in molecular weight results in a reduction in the photomodulation effect.

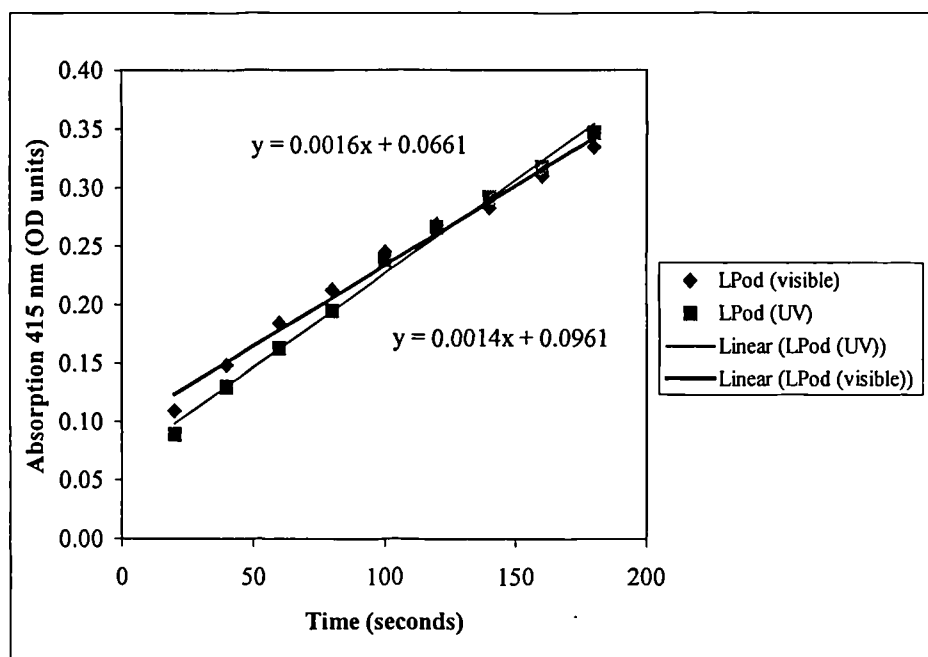


Figure 6.7 The effect of visible and UV light on native Lpod - 180 second incubation, with readings taken every twenty seconds. Illumination was either UV (245 nm) or visible light (Tungsten, 80 W) from a distance of 10 cm.

The variance in trend between the activity of Lpod (figure 6.7) under visible and UV illumination may be due to either protein variability, or due to a weakness in the assay design. Due to the beginning of a plateau for the visibly illuminated Lpod, it can be concluded that the assay is not completely optimised, and this is effecting the derived trend.

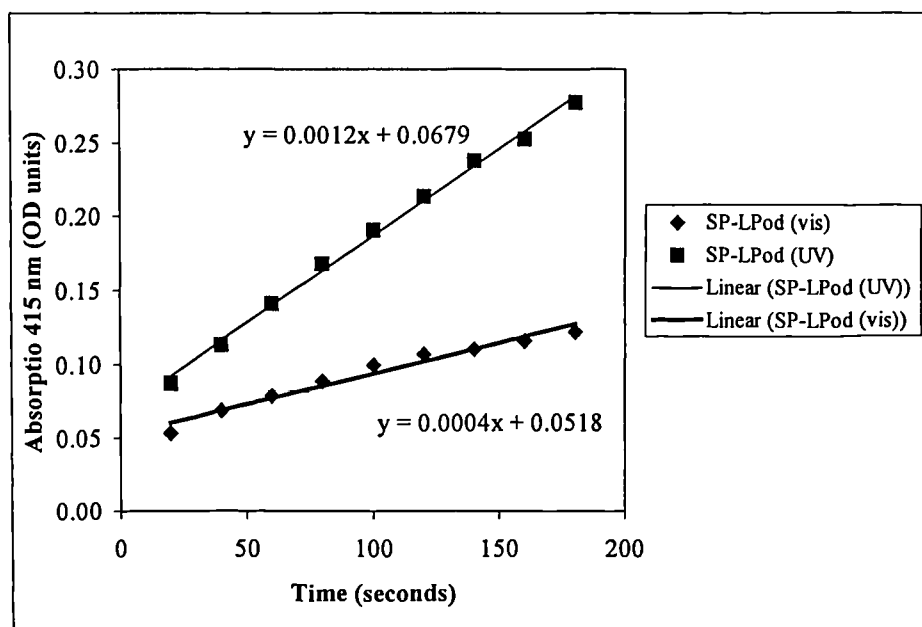


Figure 6.8 The effect of visible and UV light on SP-Lpod - 180 second incubation, with readings taken every twenty seconds. Illumination was either UV (245 nm) or visible light (Tungsten, 80 W) from a distance of 10 cm.

The activity of the UV illuminated SP-Lpod is similar to that for the native protein. Under visible illumination, the SP-Lpod shows a reduction in activity of ~ 60%, which is comparable to the result observed for SP-HRP under visible illumination. This is an unexpected result, when considered within the context of the hypothesis developed in Chapter 5, as the molecular weight of Lpod is considerably higher than that of HRP (72 KDa compared to 42 KDa). The number of spiropyrans conjugated to the protein has increased to ~14:1, compare to ~6:1 for SP-HRP.

The specific activities of the native proteins under both UV and visible light were calculated as 140.1 and 151.1 molar EU for native Lpod and 159.7 and 276.9 molar EU for SP-Lpod respectively. This indicates that the effect of spiropyran conjugation to the protein has not reduced the activity but may have increased it, perhaps by stabilising the protein structure.

This implies that the effect of the conjugation of spiropyran dye to the molecule has an effect on the activity of the protein, this may be caused an interaction at the active site, due to spiropyran attachment points which are not present in other members of the peroxidase super family. The fact that SP-Lpod has more than twice the number of spiropyran dyes attached to

the protein than SP-HRP. The result of this increase, and the increased number of molecular dipoles which it introduces, is unknown, therefore more study of this effect is needed.

6.3.4 Photomodulation of myeloperoxidase

As low concentrations of myeloperoxidase were used in this assessment no activity could be registered for this enzyme. Enzyme cost was prohibitive, and a greater amount of myeloperoxidase was not available for further research.

6.3.5 Photomodulation of microperoxidase

The peroxidases utilised herein were all of high molecular weight. To examine the effect of spiropyran modulation on small molecular weight enzymes, the enzyme microperoxidase (derived from horse heart, product code: MPO1. Biozyme Laboratories Ltd, Gwent, Wales) was chosen. Microperoxidase is a 10 amino acid peptide that has sequence homology (residues 10 – 21) with cytochrome c. This sequence contains three lysine residues, and therefore contains four potential binding sites for SP-COOH. The effect of spiropyran conjugation and photomodulation in relationship to microperoxidase has been examined.

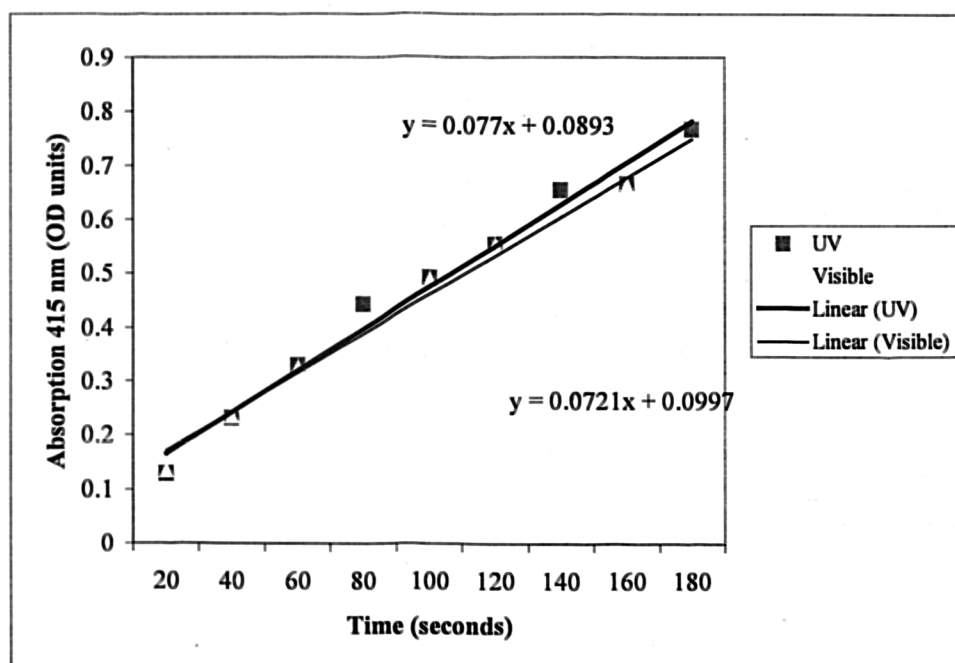


Figure 6.9 The effect of visible and UV light on native Micropod - 180 second incubation, with readings taken every twenty seconds. Illumination was either UV (245 nm) or visible light (Tungsten, 80 W) from a distance of 10 cm.

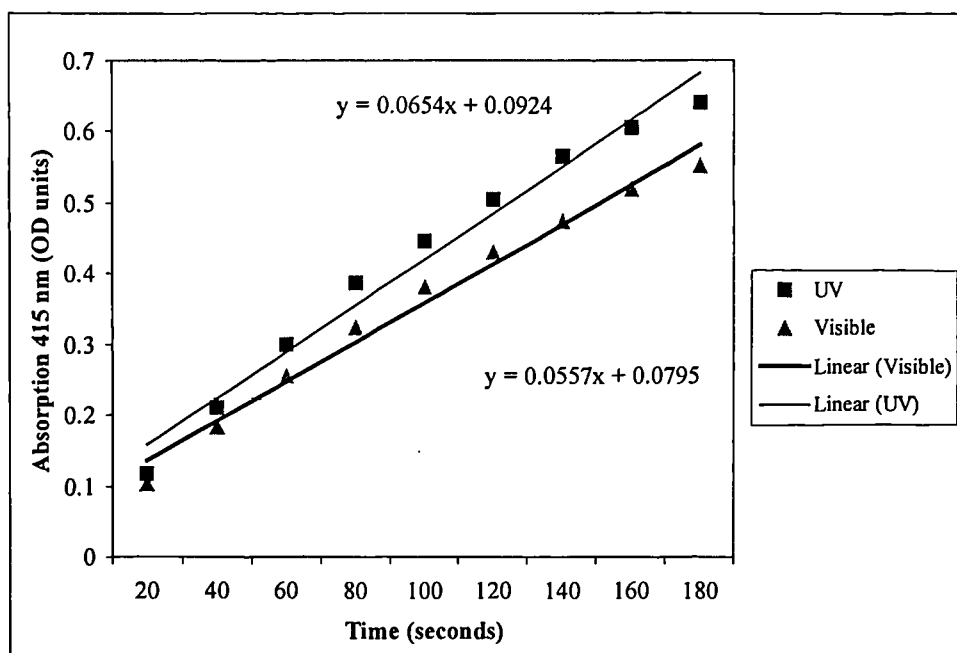


Figure 6.10 The effect of visible and UV light on SP- Micropod - 180 second incubation, with readings taken every twenty seconds. Illumination was either UV (245 nm) or visible light (Tungsten, 80 W) from a distance of 10 cm.

The activity of the UV illuminated SP-micropod is similar to that for the native peptide. Under visible illumination, the SP-micropod shows a reduction in activity of ~ 15%. This is an unexpected result, when considered within the context of the hypothesis developed in Chapter 5, as the molecular weight of microperoxidase is very low compared to that of HRP (1.2 kDa compared to 42 kDa). The specific activities of the native peptide under both UV and visible light were calculated as 69.5 and 45.1 molar EU for native micropod and 71.0 and 82.5 molar EU for SP- micropod respectively. The number of spiropyrans conjugated to the peptide has decreased to ~3:1, compare to ~6:1 for SP-HRP. Therefore, the ratio of spiropyrans to molecular weight implies that the effect of photochromic switching on SP-microperoxidase should be much greater than the result obtained for the photomodulation of SP-HRP.

From these results it appears that the influence of spiropyrans modulation on the activity of microperoxidase is minimal. This is unexpected, as the SP should dominate the microperoxidase activity at the ratio of 3 SP molecules to each microperoxidase molecule, and as such should result in a large change in activity under alternative illumination. The lack of clear photomodulation effect may be due to the low molecular weight of microperoxidase, and the fact that a peptide with so few amino acids will form a very simple secondary structure. This fact may be the reason why microperoxidase is not susceptible to the mode of action that has been suggested for spiropyrans modulation of larger proteins.

6.4 Discussion and Conclusions

Experiments have been conducted to test the hypothesis that there is a relationship between the molecular weight of a protein and the degree to which it can be photomodulated. Peroxidases were chosen for this study as they had already been identified as a group of enzymes that may show a high degree of modulation when conjugated to spiropyran dyes. Conservation within the central amino acids and common features within the molecular superstructure of the peroxidase active sites allowed the use of the same substrate, ABTS, for all the enzymes examined.

6.4.1 The photomodulation of various peroxidases

HRP was used as a control compound within this study, and was found to respond in a very similar way to the HRP assay in chapter 5, where the HRP catalysed the oxidation of ABTS and H_2O_2 generated by glucose oxidase. The use of chemical H_2O_2 did not appear to effect the assay. SP-HRP showed a reduction in activity of $\sim 60\%$ under visible illumination compared to the enzyme activity of SP-HRP under UV illumination. As for the results presented in Chapter 5 the specific activities of the relative protein assays indicate that conjugation of the spiropyran to the protein has reduced the enzyme activity by $\sim 50\%$.

Lactoperoxidase was easily conjugated to carboxylated spiropyran, and was assayed using the protocol that was applied to HRP and SP-HRP. The UV and visibly illuminated lactoperoxidase showed very similar enzyme activities. The activity of the UV illuminated SP- lactoperoxidase is similar to that for the native protein. Under visible illumination, the SP- lactoperoxidase shows a reduction in activity of $\sim 60\%$, which is comparable to the result observed for SP-HRP under visible illumination.

This is an unexpected result, when considered within the context of the hypothesis developed in Chapter 5, as the molecular weight of Lpod is considerably higher than that of HRP (72 kDa compared to 42 kDa). If the hypothesis was correct, the activity of the SP- lactoperoxidase under visible illumination should have shown less reduction than the comparable SP-HRP assay. The fact that the specific activities of the native protein under both UV and visible light were lower than the SP- lactoperoxidase may indicate that the effect

of spiropyran conjugation to the protein has not reduced the activity but may have increased it, perhaps by stabilising the protein structure.

The synthesis of the spiropyran-myeloperoxidase conjugate was not successful, and as such no information about the modulation of SP-myeloperoxidase was obtained. Myeloperoxidase was the most expensive of the enzymes used, and it was this high cost to weight difference which prevented it from being further investigated. The fact that myeloperoxidase had the highest molecular weight of the peroxidases that were examined (102 kDa), means that there is still an interest in the future use of the enzyme.

Microperoxidase was perhaps the most interesting enzyme that was conjugated to spiropyran. The low modulation of microperoxidase indicates that there may be a minimal molecular weight that is capable of effective photomodulation. Therefore, it is reasonable to presume that the disruption of interaction of tertiary structures is a principal component of photomodulation by spiropyrans. Microperoxidase, being of insufficient molecular weight to possess an extended tertiary structure, maybe resistant to photoswitching, even if the ratio of SP to amino acids implies that a high degree of modulation should occur.

The hypothesis concerning the mode of action of spiropyran dyes on molecular structure has an alternative concept of why photomodulation occurs, which is more complex, yet more thorough, than the existing concepts of steric hindrance which do not express how the steric hindrance occurs. If indeed molecular weight has a stabilising effect on the active site of the protein, by providing extended molecular scaffolding through the protein, then steric hindrance would be unpredictable, only being applicable to systems where binding of the photochromic dye occurs at or near the active site of the protein. In the case of peroxidases, there are no conserved lysine residues within the active site of the super family (Welinder *et al*, 1992) therefore the similarity in degree of photomodulation must be due to another process.

The concept that photochromic switching can destabilise the protein fits well with the experimental evidence that has been collected. While the change of form of the spiropyran is the central event in photomodulation of activity, what is it about the change in form that effects the protein? The established hypothesis is that the rotation around the centre of the spiropyran moiety results in steric hindrance of the active site of the protein. The high degree

of photomodulation obtained from the peroxidases might be why these enzymes do not fit within the theory suggested for the mode of action of photomodulation of enzymes. The fact that the peroxide super family is a group of enzymes which contain a high percentage of α helices which may result in a degree of modulation greater than that expected for other enzymes of a comparable molecular weight.

6.4.3 Conclusions

From the results we have obtained, it appears that as molecular weight increases, the degree of photomodulation that can be achieved decreases. While this contradicts the published data, the hypothesis that supports it is logical: protein structure exists at three levels, the primary amino acid sequence, secondary structures, α helices and β sheets, and tertiary structures, such as helix-turn-helix and Greek key motifs. It is the tertiary structure of the protein that allows active sites to be held in the correct conformation to be active. Beneath this, it is the primary structure that allows the secondary structure to form, and the secondary structures that form tertiary motifs. By inducing variation in the secondary structure, the tertiary motif is perturbed. This effect leads to loss of conformation of the active site of the protein.

The experiments presented in this chapter have shown that photomodulation occurs within other members of the peroxidase superfamily aside from HRP. Unfortunately, the hypothesis that the effect of photomodulation is greater with smaller molecular weight proteins has not been effectively demonstrated. It appears that features of the peroxidase super family which allow SP-HRP to show reduced activity (~70% under visible illumination) are also the reasons that peroxidases do not generally perform as would proteins with a higher percentage of β sheet. This result does not confirm the hypothesis that molecular weight of protein has a direct influence on the degree of photomodulation that occurs, it does not refute it.

As photomodulation has potential benefits beyond the use of enzyme modulation, this system has been applied to another affinity system. In Chapter 7 the effect of photomodulation on IgG and the corresponding Fab fragment is examined.

Chapter 7: Photomodulation of Antibodies

7.1 Introduction

Photomodulation systems have shown in Chapters 5 and 6 that the use of enzyme conjugated spiropyran can achieve a high degree of photoreduction in enzyme activity. To develop the investigation of photomodulation of proteins, the techniques previously used have been applied to antibody-antigen systems. Carboxylated spiropyran has been conjugated to antibody systems, and the photomodulation of immunoaffinity has been investigated.

7.1.1 The application of antibody technology to diagnostics

Immunoglobulins, or antibodies, are specific bioactive molecules, and are extensively used in commercial systems, particularly medical diagnostic kits such as enzyme linked immunosorbent assays (ELISAs). There has been considerable interest in the use of antibodies for biosensors (Killard *et al* 1995, Boncheva *et al*, 1999).

Regeneration of antibodies (the active dissociation of the bound antigen) is commonly achieved using low pH glycine-hydrochloric acid buffers, but a loss in antibody activity is associated with this method (Suzuki *et al*, 1999). The use of photochromic modulation, as described in Chapters 5 and 6, when applied to antibodies to reverse antigen binding represents a distinct advantage over existing methods, as the reduction in antibody activity of the antibodies should be minimal, and thus it may be reusable. The application of this technology has the potential to be extended to techniques such as immunoaffinity chromatography and optical biosensor systems, such as the BIAcoreTM (Lofas and Johnsson, 1990; Lofas *et al*, 1993).

Previously the photoregulation of antigen-antibody interactions has been investigated, and Hohsaka, *et al* (1994) and Sisido, *et al* (1998) have shown that modulation is possible by utilising the special case of a photochromic antigen. Wilner, *et al* (1991) considered that photochromic modulation was inappropriate for the regeneration of antibodies systems as their molecular mass (~150 kDa) was too large to be modulated by the action of photochromic groups.

7.1.2 Antibody structure and function

Antibodies are complex proteins, the simplest of which is immunoglobulin G (IgG). IgG is derived from two light and two heavy chains interconnected by disulphide bonds. The IgG molecule is divided into three distinct regions: The cellular binding domain (Fc region) composed of the interacting heavy chains, and two antigen binding regions (Fab regions) derived from a combination of a light and heavy chain (Killard *et al* 1995).

IgG has an average molecular weight of 150 kDa, but the active site of the antibody is restricted to two relatively small regions situated between the heavy and light chains of the antibody. This region can be partially isolated by removal of the Fc region of the antibody, by papain hydrolysis, thus creating the isolated arm containing the constant and variable light and heavy chains, know as the Fab fragment. This is the smallest antibody fragment that can be created by chemical reduction, and is shown in figure 7.1.

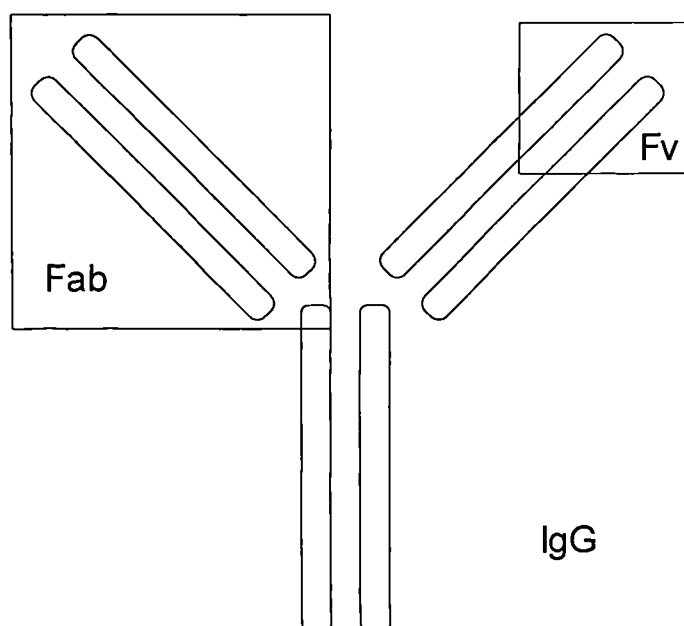


Figure 7.1: A representation of the IgG molecules and the reduction in size of the relevant fragments. The whole IgG molecule is shown in comparison to the relative size of Fab and Fv fragments.

It is possible to create a smaller fragment composed of only the variable region of the antibody. This achieved by determining the amino acid sequence of the antigen binding site

and the subsequent insertion and expression of a created gene from vector organisms, such as *E. coli* and *S. cerevisia* (Kramer, 1998). The two predominant forms of fragment produced by expression systems are Fab and Fv fragments (Lu, *et al*, 1996), composed of variable light (V_L) and heavy chains (V_H) only. These fragments contain the six hyper hypervariable loops, three each from the V_H and V_L chains, mounted on a framework of β strands (Cheetham, 1988).

While expressed Fab fragments are effectively similar to papain cleaved Fab fragments, they are considered to be more stable, as they have been designed to not rely on the molecular architecture which is present from the IgG molecule. Fv fragments are, conversely, unstable as there is limited molecular architecture to maintain the structure of the active site. The use of single chain Fv (scFv) fragments overcomes this problem as the use of a folded single chain removes the reliance on interchain stability (Kramer and Hock, 1996; Dougan, *et al*, 1998).

Smaller antibody fragments may be ideally suited to photomodulation. Reduced stability of the smaller structure may allow spiropyran dye to further destabilise the antigen binding site (as was shown for enzyme modulation in Chapters 5 and 6) and therefore result in reversible antigen binding. If the extended molecular architecture of antibodies is responsible for ineffective photomodulation of IgG, then the use of Fab and smaller fragments may increase photomodulation effects, eventually resulting in reversible binding of antigen.

7.1.3 Aims

Within this chapter, the modulation of antibody molecules and created antibody fragments (Fabs) will be examined. It is suggested in Chapter 5 that the molecular weight of a protein is a fundamental aspect in the efficiency of its photomodulation.

Further to this, the conjugation of spiropyrans to immobilised antibodies will be examined on microtitre plates. This method represents a novel approach to the photomodulation of protein systems, allowing a high throughput of repeats but also introducing a method that is relevant to biosensor surfaces, due to the immobilisation of the biological element. The use of a simplified conjugation may also limit interference between the immobilised IgG and the

subsequent conjugation of SP-COOH to the IgG. This intern may help to reduce the variation that is seen in photomodulation experiments in solution.

While it may be difficult to demonstrate the direct reversal of antibody-antigen interaction, the principle of the photomodulation of antibodies may be demonstrated by the reduction of antigen binding capacity by the antibody. This will provide an effective demonstration that the principle that photomodulation of antibodies is possible.

7.2 Methods

7.2.1 Immobilisation of protein to modified microtitre plates

Pre-modified microtitre plates were used to determine if covalent attachment and *in situ* modification of proteins could be achieved on a solid surface. The protein of interest was attached to the surface and modified by conjugation with the carboxylated spiropyran.

To improve the binding capacity of the microtitre plates, a carboxylated dextran (CMD) matrix was attached to the surface of aminated microtitre plates. A 0.1% w/v solution of CMD (Fluka, code: 27560) was made in RO water. This solution was activated by the addition of 2.5 mg/ml EDC and 1.0 mg/ml NHS, as described in Chapter 2. Aliquots of 100 µl of the activated solution were pipetted into each well of an aminated microtitre plate incubated at 20 °C for 1 hour. At the end of incubation the plate was washed three times in RO water.

A 100 µg/ml solution of the protein of interest was made in 100 mM MES buffer, pH 6.7. This solution was activated by the addition of 1 mg/ml EDC. 100 µl of the activated solution was pipetted into each well of an aminated microtitre plate incubated at 20 °C for 40 minutes. At the end of incubation the plate was washed once in RO water, once in 0.05 % Tween 20 solution and three times in RO water. Aliquots of 100 µl of 100 mM glycine were pipetted into each well and allowed to incubate for 25 minutes at 20 °C. This is a blocking step which neutralises any activated carboxyl groups which may remain within the dextran matrix.

7.2.2 Conjugation of spiropyran dyes to immobilised proteins

A 1 mg/ml solution of carboxylated spiropyran was made in 25% EtOH and 75% 100 mM MES buffer, pH 6.7. This solution was activated by the addition of 1 mg/ml EDC. 100 µl of the activated solution was pipetted into each protein modified well prior to the glycine blocking step and incubated at 20 °C for 40 minutes. At the end of incubation, the antibody solution was removed and the microtitre wells were washed four times in 0.1 M MES buffer.

7.2.3 Creation of Fab fragments

Monoclonal anti-fluorescein isothiocyanate (FITC) IgG clone (sigma code: P5636) was diluted to 5 mg/ml with sodium acetate buffer, pH 5.5. Cysteine (sigma code: C-7755) and EDTA (sigma code: E-9884) were added to a final concentration of 50 mM and 1 mM respectively to this solution. 200 µg of papain (sigma code: P-3250) was added to the solution. The reaction vessel was sealed and incubated in a water bath at 37 °C for 10 hours. At the end of incubation, iodoacetemide (sigma code: I-6125) was added to the solution to a final concentration of 75 mM. This allows the charge on the cysteine residues to be favourable for papain digestion. The solution was allowed to incubate for a further 30 minutes at 20 °C. (Harlow and Lane, 1988)

A protein G column (product code: Pharmacia, Uppsala, Sweden) was used to remove the Fc fragments and papain from the reaction mixture. The eluted protein, comprising the Fab fragment of anti-FITC IgG, was assayed by absorption at a wavelength of 280 nm to determine protein content.

7.2.4 Assay for photochromic modulation of antibody and Fab affinity

Four microtitre strip wells (8 wells per strip) were placed into each of two strip well plates. These strip wells were modified so that each plate had eight wells covalently attached to native IgG, native Fab, SP-IgG and SP-Fab respectively. The two plates were flooded with 100 mM phosphate buffer, pH 7.4, and illuminated with either visible light (tungsten filament, 80 W) or UV light (UVG-54 UV lamp peak output 245 nm. UV Products Inc., San Gabriel, CA, USA,) for 15 minutes. The buffer was removed from the plates, and 100 µl of 100 µg/ml FITC-horseradish peroxidase (FITC-HRP) in 100 mM phosphate buffer, pH 7.4, was pipetted into each well. The plates were allowed to incubate under the appropriate illumination for 25 minutes. At the end of incubation, the plates were washed in RO water, 0.1% Tween 20 solution and three times in RO water. The affinity of the respective conditions was determined by an OPD assay for HRP activity assayed for by absorption at a wavelength of 495 nm with a Dynex CX microtitre plate reader (Jencons Lab Supplies, Bucks, UK), as described in section 3.3.3.

7.3 Results

7.3.1 The photomodulation of immobilised native and SP modified HRP

As a prelude to the modulation of immobilised antibodies, the photomodulation of an immobilised enzyme was performed. An HRP based system was assessed as a model to determine whether an immobilised protein could demonstrate photomodulation of protein function. HRP was chosen as a model protein, as it is well characterised within this thesis in terms of SP-HRP photomodulation in free solution, see Chapter 5 and 6, and shows a high degree of modulation under those conditions.

The activity of the immobilised protein was estimated using o-phenyl diamine (OPD) (sigma code: P-1526) as a substrate, which was found to be more suitable for microtitre assays than ABTS, having a slower reaction and resulting in better reproducibility. While enzyme activity assays do not give a direct measurement of the protein attached to the interface, it provides an indication of the activity retained by the protein. The plate was read at 495 nm to increase the sensitivity of product detection at physiological pH (the OPD product has a different absorption maximum at higher pHs). The plate was only assayed under visible light, as it is the potential variance due to photomodulation under these conditions that is of interest.

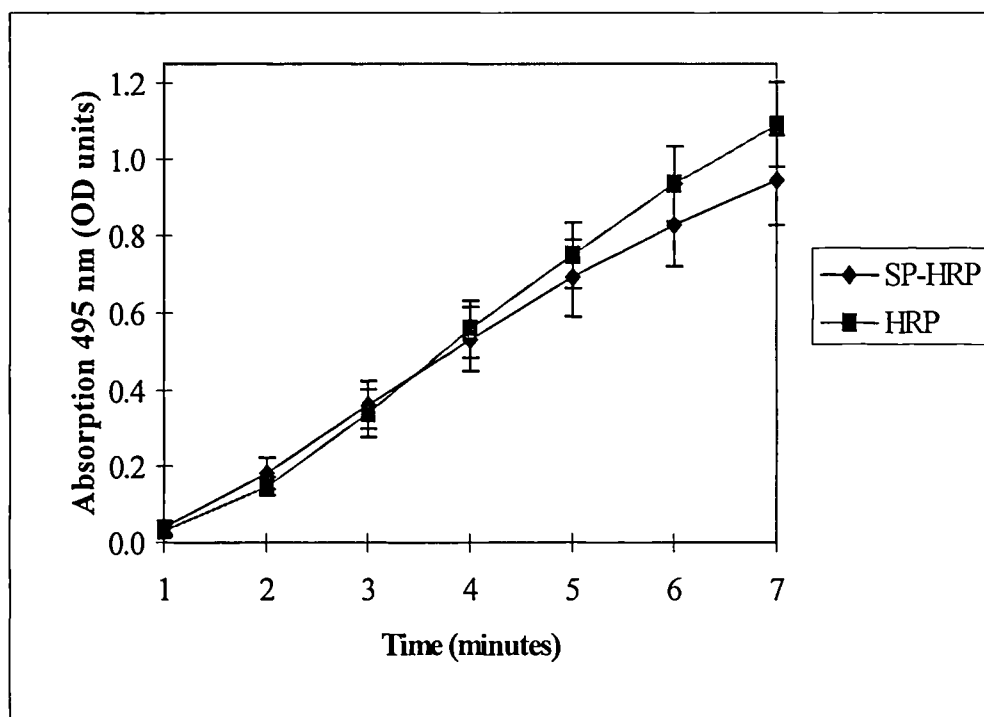


Figure 7.2 The activity of immobilised native and SP- HRP under visible illumination – Illumination was provided by a tungsten light (80 watt) at 10 cm, using a 1 cm deep water bath as a thermal buffer. The plate was read each minute for 7 minutes. The error bars show the standard deviation of 8 repeats. The spiropyran modified HRP (SP-HRP) shows a reduction in activity of ~15% compared to the unmodified enzyme (HRP)

Figure 7.2 indicates that a reduction of SP-HRP activity does occur when the protein is immobilised to an extended matrix. This result shows that the immobilised SP-HRP has ~15% decrease in activity compared to native HRP. When compared to the results for SP-HRP in solution (reduction in activity of > 70%) it is evident that immobilisation to a solid support has a distinct effect on photomodulation. This implies that immobilisation to a solid support reduces the ability for the protein structure to be perturbed by the effects of the conjugated spiropyran dye, possibly as a result of steric hindrance from the extended matrix or via the immobilisation utilising amine groups usually involved in SP conjugation. This experiment has demonstrated that immobilisation and *in situ* modification of proteins and their subsequent photomodulation can be achieved in a microtitre assay. The immobilisation of antibodies to a solid support and subsequent conjugation to carboxylated spiropyran may have a reduced affinity compared to an antibody assay in solution, but an immobilised antibody can be easily assayed for binding of an antigen-enzyme complex, which was the reason why this approach was adopted.

7.3.2 The photomodulation of native and SP-modified anti-FITC IgG

Initial experiments were conducted to identify an antibody which could be easily immobilised and conjugated to the spiropyran whilst retaining maximal activity. Anti-human IgG, anti-HRP IgG and rabbit anti-mouse IgG were examined for use in the assay format. All of these antibodies proved to be unstable when subjected to conjugation conditions, retaining little or no antigen binding capacity. This effect may have been due to the crosslinking agent EDC, creating covalent bonds at or near the antigen binding site, resulting in a loss of affinity for the IgG. The monoclonal antibody, anti-FITC IgG (sigma code: F-5636) was found to retain a high degree of activity when covalently attached to a solid support.

The assays to determine change in affinity of native and SP modified FITC IgG were performed under UV and visible illumination conditions as described in section 7.2.4. The results of each illumination condition were determined. Mean response and standard deviations are shown in figure 7.3

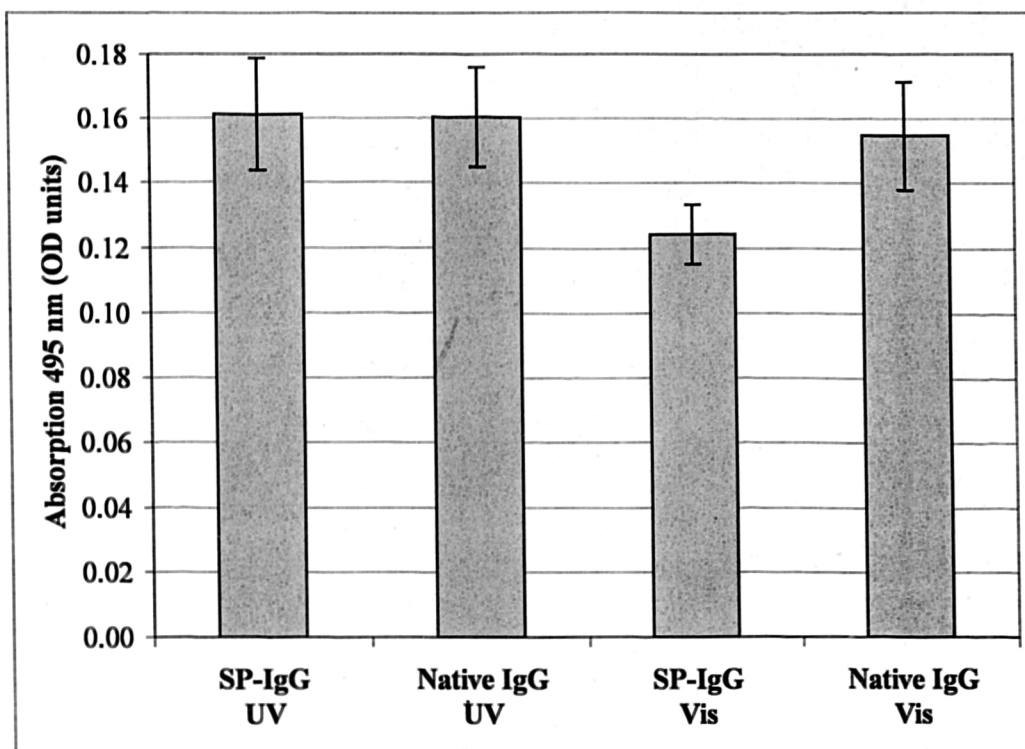


Figure 7.3: The effect of Photomodulation on Native and SP modified IgG under UV and visible illumination. – the OPD assay was allowed to incubate for 10 minutes at 20 °C before being stopped by the addition of 100 μ l of 1.6 M HCl. The error bars represent +/- 1 standard deviation of the mean.

The results (figure 7.3) indicate that there is no discernible difference between the spiropyran modified IgG (SP-IgG) and native IgG under UV illumination. Under visible illumination, the native IgG has a reduction in binding of ~ 3% compared to native IgG under UV illumination. The spiropyran modified IgG has a reduction in binding of ~ 23% compared to SP- IgG under UV illumination.

The effect of photomodulation of SP-IgG under visible illumination shows a considerable reduction in antigen binding capacity from that of either native IgG or SP-IgG under UV illumination. This indicates that the effect of the spiropyran dye in the spiropyran form has an effect on the antibody, but that in the merocyanine form, no negative effect is present. As native IgG shows little reduction in affinity under visible illumination this suggests that the response is not an artefact of the light source. This result is in agreement with previous experiments performed with model enzyme systems in solution, presented in Chapter 5.

7.3.3 The creation of Fab fragments from anti-FITC IgG

To extend the experiment in section 7.3.2, and to examine the effect of reduced molecular weight on photochromic modulation, Fab fragments were created from the monoclonal anti FITC IgG. To create Fab fragments from anti-FITC IgG, the antibody was digested with papain, and the resulting solution was purified using a protein G column to remove the generated Fc fragments.

The protein G column eluant was assayed for protein content by absorption at 280 nm, and the elution of Fab indicated that the papain digestion had been highly successful, resulting in > 95% of the Fab being recovered. The commercial antibody contains a high percentage of unspecified protein (IgG concentration = 10.5 mg/ml, total protein concentration = 25.2 mg/ml). It appeared from the results of the eluant from the protein G column that a high percentage of this protein was removed along with the Fc fragments. It has been reported that protein G has an affinity for other proteins, particularly albumins (Soe, *et al*, 1999), which may be problematic for the purification of IgG, but has proved beneficial for purifying the generated Fab fragments.

7.3.4 The comparative photomodulation of IgG and Fab

The previous experiment has demonstrated that the reduction in binding affinity of antibodies can be achieved by *in situ* conjugation with SP-COOH and the subsequent exposure to visible light. To extend this, assays to determine change in affinity of native and SP modified FITC IgG and the corresponding Fab fragments were performed under UV and visible illumination conditions. The results of each condition were determined and mean response and standard deviation are shown in figure 7.4

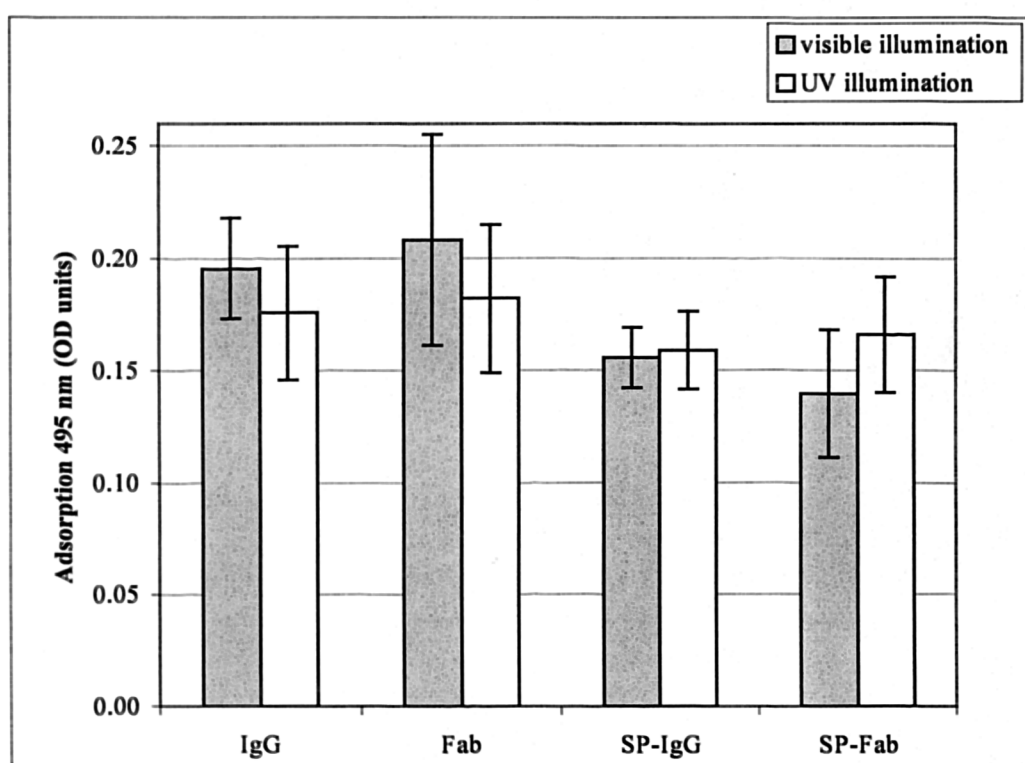


Fig. 7.4: The effect of Photomodulation on Native and SP modified IgG and the corresponding Fab fragment under UV and visible illumination. - The OPD assay was allowed to incubate for 10 minutes at 20 °C before being stopped by the addition of 100 μ l of 1.6 M HCl. The visible illumination of the SP-IgG indicates a reduction in antigen binding compared to the native IgG, a response that is increased with the Fab and SP-Fab fragment. Conversely, the UV illumination of the IgG and Fab shows little difference in antigen binding between the SP and native proteins.

The native IgG and Fab fragments showed negligible reduction in antigen binding under exposure to either light source. This indicates that conjugation to spiropyrans has an effect on protein activity that is not associated to protein denaturation caused by the source of

illumination. To better express the effect of photomodulation on the IgG and corresponding Fab's, the results of the visible and UV assays have been expressed as a ratio in table 7.1.

Table 7.1: Variation in activities between visible and UV illumination of IgG, Fab and the spiropyran modified proteins expressed as ratios and percentage change

Antibody	visible : UV response	% variation
IgG	1.113 : 1	+10.3
Fab	1.144 : 1	+12.5
SP-IgG	0.978 : 1	-3.4
SP-Fab	0.841 : 1	-15.8

The effect of visible light on spiropyran modified IgG and Fab shows that there is a reduction in relative activity from that of SP IgG and Fab under UV illumination, of 13.7% for SP-IgG and 28.3% for SP-Fab. This may be accounted for by the Fab having approximately 30% the molecular weight of the IgG.

7.4 Discussion and conclusions

7.4.1 The photomodulation of immobilised native and SP modified HRP

The use of HRP as a model system demonstrated that *in situ* modification of immobilised proteins was possible, but that the degree of photomodulation that was obtained was reduced compared to the same protein system in solution. Ustamehmetoglu (1999) has shown that the matrix that the spiropyran is contained within may have a considerable effect on the switching of the spiropyran dyes. In particular, the rate of isomerisation can be varied by the concentration of the polymer (CMD) attached to the solid support, and this may be the reason that lower levels of photomodulation are seen with the immobilised SP-HRP.

While the use of immobilisation of proteins to a solid support may reduce their activity, the convenience of the assay format makes the method viable, as the assay is far easier to perform than an antibody assay in free solution. From these initial results, an assay system utilising antibodies and Fab fragments was developed.

7.4.2 The photomodulation of native and SP-modified anti-FITC IgG and Fab

The results of the antibody assays clearly show that the affinity of spiropyran-modified IgG and Fab fragments is reduced under illumination with visible light, but show no noticeable reduction in affinity when exposed to UV light. The mechanism of photomodulation of proteins is not fully understood, and the effect at a molecular level is the subject of debate. One of the common hypotheses used to account for the effect of photomodulation is that the attached dye causes steric hindrance in one form but not in the other (Westmark, *et al*, 1993; Willner, *et al*, 1993). When considered in relation to defined binding sites on proteins, this theory is possible. It fails to account for the difference in affinity between SP-IgG and SP-Fab, as the binding sites of the whole antibody and the fragment are identical, and under UV illumination spiropyran modified IgG and Fab have similar binding affinities for FITC- HRP. Under visible illumination, the SP-IgG shows a slight reduction in binding affinity, with the SP-Fab having twice the reduction in binding affinity.

In an attempt to explain this difference in affinity, it was hypothesised in Chapter 5 that the photomodulation is due to the isomerism of the spiropyran dye resulting in a change in polarity between the spiropyran and merocyanine forms of the dye. This charge difference

would disrupt the hydration shell around the protein which has a role in stabilising the secondary and tertiary structures within the protein (Cooper *et al*, 1999). The proposed hypothesis states that this effect may result in an increased effect in modulation with smaller proteins, as the destabilisation can be effective on a proportionally larger part of the protein. It appears that this effect occurs between IgG and the corresponding Fab fragment within these experiments.

When we compare antibody systems to the peroxidases that were spiropyran modified in Chapters 5 and 6, the differences in structure become evident. Peroxidases are characterised by having a very low percentage of β sheet. Conversely, antibodies have a very low percentage of α helix, being composed primarily of anti-parallel β -pleated sheet (McConnell *et al*, 1981). In Chapter 5, the hypothesis that was presented focused on a created instability within α helix, which was then further tested within Chapter 6. The results presented here indicate that the disruption of hydrogen bonding may be a common effect, and is equally applicable to β sheet and α helix.

To further extend this area of study, the application of this technique to Fv fragments would consider the effect of photomodulation on smaller antibody fragments. The creation of antibody fragments, particularly engineered scFv fragments (Kramer, 1998), would allow the possible inclusion of increased spiropyran conjugation points. In theory, this would allow a higher degree of modulation of affinity, finally resulting in a photo-reversible antibody fragment. The potential disadvantage of this method is that if the number of covalently attached spiropyran groups becomes too great, the protein may be irreversibly modified under visible illumination.

7.4.3 Conclusions

To conclude, the photomodulation of antibodies is possible and practical, as these experiments have shown. We believe that smaller antibody molecules, and ultimately the use of fragments engineered to have a comparatively low molecular weight and to incorporate the optimum number of spiropyran molecules, will result in an antibody system which can be modulated enough to show dissociation of the antigen.

8. Final discussion, conclusions and future work

8. 1 Final discussion

The research presented in this thesis has examined several areas of molecular engineering. All of the areas examined have a relevance to biosensor technology, either for the fabrication process, or for the modulation of the immobilised biological molecule to create sensor interfaces which can be regenerated without the use of harsh chemical washes. The central points of this research are presented in this chapter as a summary of individual chapters

8.1.1 The use of polymers to modify transducers

The use of carboxylated polymers as transducer modifying agents has been investigated to determine if the current polymer of choice, carboxymethyl dextran (CMD), is the most suitable system. CMD is used extensively as a modifying agent for optical transducers, and is stated to act both as a method for concentrating recognition molecules at the transducer interface and as a method of reducing non-specific binding to the transducer (Piehler *et al*, 1996).

To examine CMD as a component, a similar molecule, carboxymethyl cellulose (CMC) was used as an alternative. It was found that CMD showed higher loading of protein to the surface, and therefore was preferable to CMC. The homogeneity of the two systems, as determined by AFM, was very similar, demonstrating that carboxylated glucose polymers attach to functionalised surfaces in a similar manner. Corresponding SPR measurements also indicate that similar amounts of the two polymers attach to surfaces, but the subsequent protein loading was higher on CMD than CMC. The CMD and CMC were deposited to aminated microtitre wells to determine if the activity of the proteins immobilised to the polymers showed any differences. The results of this showed that the trend determined from the SPR studies was maintained, with the CMD interface retaining higher activity in proportion to the amount of immobilised enzyme.

To extend this study, mixed polymer interfaces, with varying ratios of CMD to CMC were deposited to aminated microtitre wells. The subsequent protein loading to these wells indicated that by varying the ratios of polymers in bulk solution, the protein loading to the

wells could be varied. It is suggested that this is due to the polymer packing changing the porosity of the interface, a concept that is supported by the research of Andrade (1994).

To extend this area of enquiry, a straight chain aliphatic polymer, carboxylated polynoxylin (CPN) was synthesised as an additive to transducer interfaces and included as a component in mixed polymer interfaces. The introduction of CPN into the interface matrix showed that a small amount (< 10%) of a structurally different polymer could have large effects on the protein loading of an interface. The reason for this effect may be an increase in mesh size of the interface, resulting in a reduction of diffusion limited access of molecules to immobilisation points within the matrix.

As the use of such polymer-modified biosensors in real-world situations is of principal interest, an assay was developed to investigate the biological stability of interface components that appears to have been overlooked in the published literature. Using a minimal salts media with the polymer components being used as the principal carbon source, it was found that CMD was readily degraded, followed by CMC. This was the expected result, as dextran is a bacterial storage product and cellulose is a common natural substrate. CPN appeared to show minimal degradation, with potential antimicrobial properties. From this, a second experiment using mixed systems was used, and it was found that a small percentage of CPN has a distinct antimicrobial effect and as such can be a protecting agent for CMD and CMC. The use of polynoxylin as an antimicrobial has been reported for medical purposes (Gorman *et al*, 1988; Lynch *et al*, 1991), but not in an environmental monitoring role.

From these results, a hypothesis was suggested that proposed that the amount of a particular molecule that can be immobilised to an interface is a function of the polymer or polymer blend within the interface. The use of a single glucose polymers and mixed glucose / aliphatic polymers have shown that the degree of surface loading that is achieved can be controlled. To further investigate this, a method of determining the polymer ratio that is immobilised onto the surface is needed. The use of confocal laser microscopy with polymers that have been modified to contain a fluorescent species is a technique that has been used to examine polymer layers. Fluorescein isothiocyanate and tetramethyl rhodamine isothiocyanate-conjugated probes were used in conjunction with scanning confocal laser microscopy by Wolfaardt *et al* (1998), to detect and quantify lectin binding to a variety of glycoconjugates. Confocal laser microscopy has also been used to determine the structural complexity of fully

hydrated living biofilms and determine the distribution of individual species within biofilms. This has shown the significance of structural heterogeneity on mass transfer in biofilms (Lawrence *et al*, 1998; Stoodley *et al*, 1999). This method could be applied to the investigation of biosensor interfaces to determine how fluorescently labelled molecules migrate into interfaces, and whether the models proposed for RD and LD deposition are correct. While the system is usually applied to matrices with a greater thickness, it may still be beneficial for polymer interfaces such as these with a thickness of ~ 300 nm.

8.1.2 Advanced and novel transducer fabrication techniques

The examination of dextran and alternative polymer systems has shown that single polymer systems have distinct characteristics when covalently attached to surfaces and demonstrate varying protein loading levels. The examination of mixed polymer systems has introduced the concept of variable surface loading as a function of the ratios of the polymers that are deposited onto the surface, and this implies that the potential loading of an interface can be predetermined by controlling the polymer mix. For an analyte of a known molecular weight, this would allow the creation of interfaces that were selective in relation to access to molecules below a given molecular weight. To further this area of interest, methods for deposition of printed arrays were examined.

A novel approach to interface production was proposed in the form of reverse deposition. A comparison of the created reverse and linearly deposited interfaces demonstrated that the interface characteristics could be modified to suit either low or high molecular weight systems. It has been shown that for immobilised high molecular weight recognition molecules to interacting with small molecular weight molecules that RD is beneficial as it allows a greater number of recognition molecules to interact with the evanescent field of optical biosensors. Conversely, when the opposite is used, where a small molecular weight molecule is immobilised to the matrix and reverse deposited, the subsequent interaction with a high molecular weight analyte produces a lower response than a linearly deposited surface. The reason behind these results is due to diffusion limitation into the extended polymer matrix, a feature that may be overcome by using a combination of polymers in RD interfaces, by altering the mesh size of the matrix, as stated above. The application of this method to biosensor technology is twofold. Firstly, the cost of fabrication could be reduced due to the

potential time and materials saved by using reverse deposition, and secondly, the produced biosensors may be more sensitive, as a high percentage of the molecular recognition occurs within the evanescent wave.

Further research into this area could be easily allied to that of the mixed polymer interfaces, suggested in section 8.1.1. SPR could be used to determine the kinetics of molecular interactions, and therefore examine the diffusion of molecules into polymer interfaces.

8.1.3 Deposition and analysis of printed arrays

To demonstrate that the methods and concepts that have been developed are applicable to advanced biosensor design, reverse deposited interfaces have been print for use with a multi-channel SPR (MC-SPR) assembly that was created part of an EU project*, which partially funded this research. Methods were devised to print heterogeneous arrays of antigens on to APTS-modified surfaces. An array of control surfaces, active molecule and proteins were printed onto a pre-prepared SPR surface. These arrays where then analysed via MC-SPR, and the printed arrays showed differential binding of IgG to the area containing the specific antigen, with low levels of binding observed to the other areas. This confirms that a multichannel optical biosensor can be created by precision printing of active areas, and subsequently used in conjunction with simple fluidic systems, such as a static liquid cell.

These experiments have shown that specific biosensors with the potential to have a range of activities are achievable with existing technologies. The arrays that have been used here only utilise printed arrays of 6 elements, with an active surface of 1 cm², as the gasket seal encroaches on this area. By increasing this area to 1.5 cm², the printed array could be increased to 12 or 15 elements, as the area required to seal a liquid cell would be reduced compared to the active area. To further extend this research, the use of CCD cameras is the next step in developing multianalyte SPR systems. The use of a CCD camera will allow droplets to be deposited, therefore increasing the number of points which can be analysed from 5 or 6 elements to 25 or 36. The disadvantage of this system is that the amount of data to

* EU project title: Measurement of priority metabolites using optoelectronic biosensors derived from antibody and molecular receptor libraries. Project reference: ENV4-CT96-0333

be processed increases proportionally, therefore the restriction on this system is the software, and perhaps more importantly, the computer processing power that is available.

8.1.4 The photochromic modulation of protein activity

The published literature has demonstrated the photomodulation of a variety of protein systems by using a range of photochromic compounds. The application of photochromic modulation has been examined in the current research, and a study of the varying degrees of photomodulation that can be achieved from enzymes within a super family, namely the heme oxidases have been studied. From the published data and experimental results, a theory has been developed to explain the mode of action of photomodulation of protein systems.

It is proposed that the effect that was observed was not a result of steric hindrance of the protein, but was in fact due to the effect of the shape : polarity variation which occurs when the photochromic species is driven from the merocyanine to the spiropyran form. This results in a disruption of the water molecules associated to the protein. This disruption may effect the hydrogen bonding which helps to maintain the secondary structure of the protein, which could have an effect distal from the site of modulation by affecting the tertiary structure of the protein. As the molecular weight of the protein increases, the covalent attachment points of the spiropyran dye become more separated, and the possibility of a cumulative effect of several photomodulation events is reduced. Therefore, as molecular weight increase, the degree of photomodulation that can be achieved is reduced.

This theory extends the current thinking concerning photomodulation of proteins, and introduces the concept that the degree of photomodulation can be predicted for a particular protein, on the basis of molecular weight and secondary structure. When this theory was applied to the enzymes examined and to the published results, it was evident that the heme oxidases do not fit the model. The reason behind this result may be due to the high α helix content that is present within the heme oxidases, which allows for a degree of photomodulation far higher than that observed for other proteins.

To extend the area of photomodulation, the application of the system has been applied to an antibody system, anti FITC-IgG. This has been achieved by developing a method for the

conjugation of proteins to spiropyrans after the protein has been covalently attached to a solid support, a pre-modified microtitre well. The subsequent modulation of antibodies demonstrated that the capacity of IgG could be reduced by ~ 16% when attached spiropyrans were in the spiropyran form, with no discernible effect being seen when the spiropyran was in the merocyanine form. Following from this, the Fab fragment of anti FITC-IgG was created by papain hydrolysis, and the subsequent modulation resulted in a reduction in affinity of ~ 23%.

These results allow the consideration of the effect of spiropyran dye switching on the structure of proteins. In Chapter 5, the hypothesis that was presented focused on a created instability within α helices, caused by effecting the hydration shell around the protein when photochromic isomerisation occurs (Cooper, *et al*, 1999). This hypothesis then further tested within Chapter 6 using peroxidases, which are characterised by having a very low percentage of β sheet. The experiments presented in Chapter 7 examined the effect of covalent attachment of spiropyrans to IgG and the corresponding Fab fragments. Antibodies have a very low percentage of α helix, being composed primarily of anti-parallel β -pleated sheet (McConnell, *et al*, 1981). The initial hypothesis was revised due to the combined evidence of the enzyme and antibody experiments. The results of these experiments indicated that the disruption of secondary structure may be a broad based effect of photomodulation of spiropyran dyes, and is equally applicable to β sheet and α helix.

To continue the existing area of study, a series of experiments are needed to examine the degree of photomodulation of proteins with decreasing molecular weight, but similar functionality. The use of the peroxidase super family has proved to be inconclusive, due to the common protein architecture with extensive α helix biasing the results of photomodulation experiments. The logical choice for an extended study of this type would be to select an IgG, Fab and Fv fragment for the same molecule and conjugate then with spiropyran dyes and observe the effect of photomodulation. To take this one step further, an existing scFv library could be used to examine the effect of insertions of binding sites for the spiropyran dye. From this, the location and number of spiropyrans attached to the scFv can be studied and the hypothesis reviewed to take into account the location of the covalently attached spiropyran in relation to the separation from the active site of the antibody. This system would also allow

for spiropyrans to be attached near or at the antigen-binding site, to determine if this reduces or destroys the activity of the antibody by specific interaction with the binding site.

The photochromic modulation of proteins is still undefined in terms of mode of action. A plausible hypothesis has been proposed and investigated which advances the current concepts concerning photomodulation, and has shown for the first time that the photomodulation of antibody systems is possible. The advantage of this system compared to the use of photochromic antigens, is that it is a generic approach and as such applicable to all antibody systems.

8.1.5 The application of generic technologies

Across the two areas that have been examined, surface modification (polymer modified interfaces) and protein engineering (spiropyran conjugation and the subsequent photomodulation of proteins), the use of common methods and techniques has been emphasised. Predominant amongst these areas has been the use of carbodiimide chemistry, in the form of EDC-NHS reactions, to form peptide bounds between amine and carboxyl groups. This chemistry has been shown to be effective at conjugating proteins to spiropyrans, proteins to polymers, polymers to silanised metals and glass, polymers and proteins to aminated polystyrene. While the use of EDC-NHS resulted in the cross linking of proteins, and their subsequent sedimentation from solution, the use of EDC alone did not result in this effect. For each situation, with little variation of method, effective and non-reversible covalent linkages have been achieved, thus demonstrating the true generic nature of this chemistry.

The application of established technologies, in the form of microtitre assays, as both a stand-alone system and as a comparative method for SPR analysis, has again demonstrated the application of generic technologies for novel purposes. Central to this was the use of aminated microtitre plates as a solid support for the subsequent immobilisation and spiropyran conjugation of antibodies and antibody fragments. The use of microtitre plates provides a system that is able to screen a large number of variations quickly with multiple repeats. While this has been used extensively in medical analysis, its application to biological surface science has provided a useful comparative technique to AFM and SPR analysis.

8.2 Future work

While the areas investigated have resulted in novel research and furthered the knowledge of both photochromic chemistries and sensor fabrication, it has also highlighted other areas that could be investigated:

8.2.1 Characterisation of Active Surface

While a degree of study has been performed via the atomic force microscope and by contact angle measurement to examine the structure and characteristics of surfaces and interfaces, many questions still remain unanswered. The application of established and emerging technologies will enable a far greater understanding of the interfacial interactions than currently exists. Principle amongst these techniques is:

Electron Microscopy – EM has historically being applied to prepared, rigid targets. For certain samples, the resolution of the electron micrographs can be greater than AFM images. The disadvantage of electron microscopy as a method of analysis is that it requires extensive sample preparation prior to imaging, including total dehydration and the use of an appropriate label, usually an evaporated gold film. Both of these features would introduce artefacts into the derived image.

Studies of immobilised films have been conducted (Duschl *et al*, 1996; Moller *et al*, 1998; DuChesne, 1999). Of particular relevance to potential future work is the research of Sarwade and Singh (1999) who have studied the morphology of photooxidative degraded films of ethylene-propylene copolymer by scanning electron microscopy. This technique could be applicable to study the effects of mixed polymer interfaces to determine the nature of degradation and the effect CPN has within the matrix.

Scanning electrochemical microscopy (SEcM) – While EM and AFM can characterise a physical surface down to sub-angstrom resolutions, it does not indicate anything of the biochemical nature of the surface. The SEcM is a scanning probe technique that can determine the local electrochemical nature of surfaces. Studies have been performed with self-assembly monolayers (Turyan and Mandler, 1998) for biomaterials corrosion (Gilbert *et al*, 1998) and to analysis of sensor surfaces (Strike *et al*, 1999). The potentials for examining the

microstructure of extend interfaces and immobilised enzymes exist (Shultze et al, 1999). Shao and Mirkin (1997) studied the diffusion of ionic species between an aqueous and organic phase, but a similar system would be applicable to examine the diffusion of ionic species into polymer films. This would allow an extended study on the effect of mixed polymers on the diffusibility of molecules into the matrix.

Advanced SPR Analysis – the initial SPR studies that have been conducted is only a small amount of what can be achieved from SPR analysis. To further extend this area of research, a variety of areas can be examined. McGurk *et al*, (1999) have applied a combined AFM-SPR system to the analysis of engineered surfaces, including a range of hydrophilic polymer brush surfaces and protein. This has allowed a comparison of the force of adhesion, obtained from AFM, and adsorption trends onto these surfaces, observed with SPR. Edwards (1999) has extended SPR analysis to measure rate constants of the associated reaction occurring during biomolecular interaction. A technique similar to this could be applied to both polymer and spiropyran systems to construct models of the molecular interactions of both systems. Further to this, Kaganer et al (1999) have used SPR to analyse the interaction of antibodies with photochromic antigens. A variation of this system would allow the examination of interaction of SP-modified antibody – antigen interaction.

By using a combination of these techniques it would be possible to extend the research concerning the nature of interfaces and how they interact with the underlying surface and molecules which are attached to them. Several hypotheses have been proposed within this current work concerning the interaction of different polymers and methods of depositing interfaces. From this point, the examination of these hypotheses, particularly concerning how interfaces perform on different substrates, and whether polymer blends and molecules of a given molecular size can have predictable interactions, is a principle area of further research.

8.2.2 Advanced sensor fabrication

While this project has examined a variety of methods for the commercial manufacture of biosensors, it has not attempted to transfer any of the technologies to high throughput manufacturing. The use of multiple component printing systems, such as the 8 dispenser Biojet™ systems now available from Biodot (Cambridge, UK), would allow the printing of complex patterns in a single process, such as those discussed in chapter 4. Another potential

area of interest in the ability to print different solutions and volumes onto a defined area. This would allow the creation of printed arrays that have analyte concentration gradients, which would allow detection variation dependent on receptor concentration, therefore increasing the active range of the sensor.

To extend the chemistry and surface science of biosensors, the use of both alternative carboxylated polymers, both polysaccharides and linear carbon backbones, should be investigated further. The research performed in this thesis has begun to investigate the variation in surface characteristics that can be achieved using both novel polymer systems and mixed polymers.

8.2.3 Photomodulation of Affinity Systems

The photomodulation of enzymes has been clearly demonstrated, and to an extent the modulation of antibody systems has demonstrated that it is possible to effect systems with high affinity. The two principle areas of interest for further research would be the reversal of binding of antigens and the photo dissociation of biotin-avidin interactions.

The importance of photomodulation to these systems primarily relates to the area of diagnostic systems, as they are both commonly used in immunoassays. The use of photo dissociation would allow the regeneration of the active biological recognition molecule, the case of antibodies, and of the immobilised surface in the case of avidin-biotin interactions. While traditional microtitre tests are inexpensive, more advanced analytical systems, particularly SPR and waveguide based systems, use expensive transducers. In these cases, surface regeneration that would retain a high level of activity would be cost effective. The potential exists for optical biosensors to be photomodulated by applying a light source of the appropriate wavelength through the transducer, thereby reducing regeneration to the flick of a switch. This thesis has examined the photomodulation of antibodies and has shown that the potential for reversible binding exists. The use of Fab and single-chain fragments has been discussed. The use of novel antibodies may be an alternative to modifying existing systems, Camelid antibodies (Decanniere *et al*, 1999; Muyldermans and Lauwereys, 1999) may be particularly suitable. Camelid antibodies have an inherently stable structure, as the molecule is made of two heavy chains as opposed to a heavy and a light chain. This extended structure stabilises the antigen binding site. Camelid antibodies may be suitable for photomodulation,

as this extended system may still be able to be photomodulated, but retain a high degree of affinity.

To further examine these areas beyond the methods that have been applied here, other technologies are needed. Molecular modelling can be used to examine the theoretical effect of spiropyran photomodulation, and is able to modify conditions to determine the optimum photomodulation that can be obtained. Kinetic analysis and calorimetry could be used to elucidate the mechanism of photomodulation. Further to this, studies of solubility and stability of the various forms in organic solvents would indicate the involvement of water in the photomodulation process.

8.2.4 Optical Control of Bioreactors

While the use of photochromic modification of proteins has been shown to be effective for use with a wide range of enzyme systems, the use of this has not been fully explored. While the concept of utilising optical modulation in mixed enzyme fermentation systems is an attractive concept, it would be hard to achieve due to the high densities which are achieved in fermentation vessels, resulting in very short transmission pathways of light.

An approach that can be utilised to avoid the problems of bulk fermentation reactors is to use one of the more advanced designs. While hollow fibre based systems, such as the hepatic bioreactor systems (Marquis, 1995; Gerlach, 1997) have been shown to be an effective method for the development of mammalian cell culture (Deshusses *et al*, 1997). An alternative method, which may hold the answer to photomodulation of enzyme reactors would be the use of optical fibres to immobilise spiropyran modified enzymes. This method would have two benefits. Firstly, the optical fibre would allow a convenient method to modulate the immobilised protein, and secondly, the surface area provided by the optical fibres would allow a high level of surface loading per volume of the reactor. This system would have benefits in areas where both high through put of media and the ability to control the activity of the immobilised biological component are needed, such as bioremediation. This system allows the activity of the reactor to be modulated in relation to the concentration of the initial media, therefore allowing the product concentration to remain constant, which may be important in a GMP environment.

8.3 Final conclusions

The use of molecular engineering has proved to be both interesting and relevant in the field of biosensor technology, and the application of the principles has resulted in the following conclusions:

- Differing combinations of polysaccharide and synthetic polymers in immobilised thin films result in differing surface morphologies as determined by AFM
- The capacity of the various immobilised thin films to covalently bind protein, as determined by SPR, has been shown to vary as a function of the constituent polymers
- The use of reverse deposition can be beneficial, as it allows the creation of a more homogenous biosensor interface with higher loading of a recognition molecule, and subsequently can increase the sensitivity of the sensor. Reverse deposition is also compatible with existing mass manufacturing technology.
- The use of spiropyran dye to modulate enzyme function of a novel system, horseradish peroxidase, has been demonstrated. A hypothesis of the method of photomodulation was presented.
- This hypothesis was tested with the peroxidase super family of proteins. The results demonstrated that the degree of modulation was not significantly different with proteins of different molecular weights. It is believed this is due to the secondary structure of peroxidases. The hypothesis was revised in light of these results.
- The photomodulation of antibody affinity was explored using IgG and the corresponding Fab fragment. This showed that the smaller the

molecule the greater the degree of modulation that could be achieved. A method using Fv fragments has been proposed.

The areas of interest that this project has addressed have proved to be both interesting and have generated many more questions to be investigated. Of the areas that have been examined, any of them could have been expanded into comprehensive projects in their own right. Section 8.2 has addressed the logical progression of the research that has been presented, and also proposes some ambitious applications of molecular engineering. The potential for applying molecular engineering principles to biosensor interfaces and other areas of bio and surface science are huge. Hopefully the findings of this thesis will lead to further research into the broader field of molecular engineering.

References

- Aizawa, M., Namba, K. and Suzuki, S. (1977) Photo control of enzyme activity of α -amylase, *Archives of Biochemistry and Biophysics*, **180**, 41-48
- Alvarez-Icaza, M. and Bilitewski, U. (1993). Mass Production of Biosensors. *Analytical Chemistry*, **65** (11), 525 - 533
- Andrade, J, Hlady, V and Wei, A. (1992). Adsorption of complex proteins at interfaces *Pure and applied chemistry*, **64** (11) 1777 - 1781
- Andrade, J Hlady, V, Wei, A, Ho, C, Lea, A, Jeon, S., Lin, Y. and Stroup, E. (1992) Proteins at interfaces: principles, multivariate aspects, protein resistant surfaces and direct imaging and manipulation of adsorbed proteins. *Clinical Materials*, **11**, 67 - 84
- Andrade, J. (1994). Polymers have intelligent surfaces: polymer surface dynamics. *Journal of intelligent material systems and structures*, **5**, 612 – 618
- Arai, K., Shitara, Y. and Ohyama, T. (1996). Preparation of photochromic spiropyrans linked to methyl cellulose and photoregulation of their properties. *Journal of materials chemistry*, **6**(1), 11 - 14
- Ariga, K and Okahata, Y (1989) polymerised monolayers of single- double and triple-chain silane amphiles. *JACS*, **111**, 5618 - 5622
- Baldini F. and Bracci, S. (1993). Optical-fibre sensors by silylation techniques. *Sensors and Actuators B*, **11**, 353 - 360
- Banci L. (1997). Structural properties of peroxidases. *Journal of biotechnology*, **53**, 253 – 263
- Barrow, D. Cefai, J. and Taylor, S. (1999). Shrinking to fit. *Chemistry and industry*, **15**, 591 – 594
- Bastos-Gonzalez, D, Ortega-Vinuesa, L, Nieves, F and Hidalgo-Alvarez, R. (1995). Carboxylated latexes for covalent coupling antibodies *Journal of colloid and interface Science*, **176**, 232 – 239
- Berger, C. Beurner, T, Kooyman, R. and Greve, J. (1998) SPR Multisensing *Analytical Chemistry*, **70**, 703 - 706
- Bier, F.F, Jockers, R. And Schmid, R.D. (1994). Intergrated optical immunosensor for s-Triazine Determination: Regeneration, Calibration and Limitations. *Analyst*, **119**, 437 - 441
- Blenkharn, J. (1985). Biological activity of polynoxylin – an insoluble urea-formaldehyde condensation product. *Journal of clinical and*
- Boncheva, M, Scheibler, L, Lincoln, P, Vogel, H, and Akerman, B (1999) Design of oligonucleotide arrays at interfaces. *Langmuir*, **15** (13), 4317 - 4320

- Buckle, P. Davies, R. Kinning, T. Yeung, D. Edwards, P. Pollard-Knight, D. and Lowe, C. (1993)** The resonant mirror: a novel optical sensor for direct sensing of biomolecular interactions II: applications. *Biosensors and bioelectronics*, **8**, 355 – 363
- Cass, A, Davis, G, Francis, G, Hill, H, Aston, W, Higgins, J, Plotkin, E, Scott, L, and Turner, A. (1984)** Ferrocene-mediated enzyme electrode for amperometric determination of glucose. *Analytical Chemistry*, **56**, 667 – 671
- Carlsson J, Mosbach K and Bulow L. (1996)** Affinity precipitation and site-specific immobilization of proteins carrying polyhistidine tails. *Biotechnology and bioengineering* **51** (2), 221 - 228
- Catimel, B Nerrie, M, Lee, F, Scott, A, Ritter, G, Welt, S, Old, L, Burgess, A and Nice, E. (1997)** Kinetic analysis of the interaction between the monoclonal antibody A33 and its colonic epithelial antigen by the use of an optical biosensor: a comparison of immobilisation strategies. *Journal of Chromatography A*, **776**, 15 - 30
- Catimel, B. Scott, A. Lee, F. Hanai, N. Ritter, G. Welt, S. Old, L. Burgess A. and Nice E. (1998)** Direct immobilisation of gangliosides onto Au-CMD sensor surfaces by hydrophobic interaction. *Glycobiology*, **8**, (9), pp 927 - 938
- Chang, I, Lin, J, Andrade, J and Herron, J. (1995).** Photoaffinity labeling of antibodies for applications in homogeneous fluoroimmunoassays. *Analytical Chemistry*, **67**, 959 - 966
- Cheetham, J. (1988).** Reshaping the antibody combining site by CDR replacement – tailoring or tinkering to fit? *Protein Engineering*, **2** (3) 170 - 172
- Chidsey, C and Loiancono, D. (1990).** Chemical functionality in SAM's: structural and electrochemical properties. *Langmuir*, **6**, 682 - 691
- Cooper, T, Natarajan, L and Miller, C. (1999)** Control of ring substitution of the conformation change dynamics in photochromic polypeptides. *Photochemistry and photobiology*, **69**(2), pp 173 - 176
- Corriu, J, Moreau, J, Thepot, P and Man, M. (1992).** New Mixed organic-inorganic polymers: hydrolysis and polycondensation of bis(trimethoxysilyl)organometallic precursors. *Chemical Materials*, **4**, 1217 –1224
- Cowen, S. (1999).** Chip service. *Chemistry and industry*, **15**, 584 - 586
- Csempesz, F, Csaki, K Kovacs, P and Nagy, M. (1995)** Simultaneous competitive adsorption of polymers from tertiary solutions at solid/liquid interfaces. *Colloids and Surfaces A*, **101**, 113 - 121
- Cullen, D.C. and Lowe, C.R. (1994).** AFM Studies of Protein Adsorption. *Journal of Colloid and Interface Science*, **166**, 102 – 108
- Davies, J (1994).** SPR – the technique and its applications to biomaterial processes. *Nanobiology*, **5**, 5 – 16

- Debono, R.F., Loucks, G.D., Manna, D.D. and Kruli, U.J. (1996).** Self-assembly of short and long-chain n-alkyl thiols onto gold surfaces. *Canadian Journal of Chemistry*, **74**, 677 – 688
- Deshusses, M, Chen, W, Mulchandanj, A and Dunn, J. (1997)** Innovative Bioreactors. *Current Opinion in Biotechnology*, **8**, 165 - 168
- Disley, D.M. Blyth, J, Cullen, D, You, H, Eapen, S and Lowe, C. (1998)** Covalent Coupling of IgG to PVA-P(AA) graft polymer as a method for fabricating the interfacial-recognition layer of a SPR immunosensor. *Biosensors and Bioelectronics*, **13 (3-4)**, 383-396
- Dougan, D. Malby, R. Gruen, L. Kortt, A. and Hudson, P. (1998).** Effects of substitutions in the binding surface of an antibody on antigen affinity. *Protein Engineering*, **11 (1)** 65 – 74
- DuChesne, A (1999)** Energy filtering transmission electron microscopy of polymers - Benefit and limitations of the method. *Macromolecular Chemistry and Physics*, **200 (8)**, 1813 - 1830
- Dubois, L, Zegeraski, B and Nuzzo, R. (1990).** Fundamental studies of microscopic wetting on organic surfaces: interaction of secondary adsorbates with chemically textured organic monolayers. *JACS*, **112**, 570 – 579
- Duschl, C, Liley, M, Lang, H, Ghandi, A, Zakeeruddin, S, Stahlberg, H, Dubochet, J, Nemetz, A, Knoll, W and Vogel, H. (1996)** Sulphur-bearing lipids for the covalent attachment of supported lipid bilayers to gold surfaces: A detailed characterisation and analysis. *Materials science and Engineering C- Biomimetic materials sensors and systems*, **4 (1)**, 7 - 18
- Dvornic, P.R. and Tomalia, D.A. (1996)** Recent Advances in dendritic polymers *Current Opinion in Colloid and Interface Science*, **1**, 221 - 235
- Edwards, D. (1999).** Estimating rate constants in a convection-diffusion system with a boundary reaction. *IMA journal of Applied Mathematics*, **63 (1)**, 89 - 112
- Frantz, P. And Granick, S. (1992).** Surface preparation of silicon for polymer adsorption studies. *Langmuir*, **8**, 1176 – 1182
- Galan-Vidal, C.A., Munoz, J. Domingues C. and Alegret S. (1995).** Chemical sensors, biosensors and thick film technology. *Trends in analytical chemistry*, **14 (5)**, 225 - 231
- George AJT and Epenetos AA, (1996).** Advances in antibody engineering. *Expert opinion on therapeutic patents*, **6 (5)**, 441 – 456
- Gerlach, J. (1997).** Long-term liver cell cultures in bioreactors and possible application for liver support. *Cell biology and toxicology*. **13**, 349 – 355
- Gilbert, J, Zarka, L, Chang, E, and Thomas, C. (1998)** The reduction half cell in biomaterials corrosion: Oxygen diffusion profiles near and cell response to polarised titanium surfaces. *Journal of Biomedical Materials Research*, **42 (2)**, 321 - 330

Goodrow, M and Hammock, B (1998) Hapten design for compound-selective antibodies: ELISAS for environmentally deleterious small molecules. *Anal. Chim. Acta.* **376** (1), 83-91

Gorman, S. McCafferty, D. Woolfson, A and Kennedy, G. (1988). Reduced adherence and inhibition of hyphal development of candida albicans by the antimicrobial agent polynoxylin *Letters in applied microbiology*, **6**, 145 – 148

Green, R., Davies, J., Davies, M., Roberts, C. and Tendler, S. (1997). SPR for real time in situ analysis of protein adsorption to polymer surfaces. *Biomaterials*, **18**, 405 – 413

GuergovaKuras M, SalcedoHernandez R, Bechmann G, Kuras R, Gennis R and Crofts A (1999) Expression and one-step purification of a fully active polyhistidine-tagged cytochrome bc(1) complex from Rhodobacter sphaeroides *Protein expression and purification*, **15** (3) 370 380

Guglielmetti, R. (1990). 4n+2 Systems: Spiropyrans. *Photochromism: Molecules and Systems*, chp. 8, pp 314 – 320

Guilbault, G.G and Luong, J.H.T (1989). Immobilisation methods for piezoelectric biosensors. *Biotechnology*, **7**, 349 – 351

Hall, C, Datta, D and Hall, E. (1996). Parameters which influence the optimal immobilisation of oxidase type enzymes on methacrylate copolymers as demonstrated for amperometric biosensors. *Analytica Chimica Acta*, **323**, 87 - 96

Hall D.R. and Winzor D.J. (1997). Use of a Resonant Mirror Biosensor to Characterise the Interaction of Carboxypeptidase A with an Elicited Monoclonal Antibody. *Analytical Biochemistry* **244**: 152-160.

Hall, E., Gooding, J, Hall, C and Martens, N. (1999). Acrylate polymer immobilisation of enzymes. *Fresenius journal of analytical chemistry*, **364** (1-2), 58 – 65

Harada, M.; Sisido, M.; Hirose, J.; Nakanishi, M. (1994). Photocontrolled uptake and release of photochromic haptens Mab's: evidence of photoisomerization inside the hapten binding site. *Bull. Chem. Soc. Jpn.* **67**, 1380-1385

Harlow, E. and Lane, D. (1988) *Antibodies – a laboratory manual*, 626 - 629

Hayden MS, Gilliland LK and Ledbetter JA (1997). Antibody engineering. *Current Opinion in Immunology*, **9** (2), 201-212

Hayes, J, Kenmore, M, Badley, A and Cullen, D. (1998) AFM study of antibody adsorption to polystyrene microtitre plates. *Nanoobiology*, **4**, 141 - 151

Hayes, W, Kim, H, Yue, X, Perry S, Shannon C. (1997). Nano-scale patterning of surfaces using self assembly chemistry. 2. Characterisation and electrochemical behaviour of two-component organothiol monolayers on gold surfaces. *Langmuir*, **13**, 2511 - 2518

Heideman, R Kooyman, R and Greve, J (1993). Performance of highly sensitive optical waveguide Mach-Zender interferometer immunosensor. *Sensors and Actuators B*, **10**, 209 – 217

Hellinga, H. and Marvin, J. (1998) Protein engineering and the development of generic biosensors *Trends in Biotechnology*, **16**, 183 - 189

Henriksen, A. Schuller, D. Meno, K. Welinder, K. Smith A. and Gajhede M. (1998) Structural interactions between HRP and the substrate benzhydroxamic acid determined by X-ray crystallography. *Biochemistry*, **37**, 8054 – 8060

Henrissat, B. Saloheimo, M. Lavaitte S. and Knowles J. (1990). Structural homology among the peroxidase enzyme family revealed by hydrophobic cluster analysis. *Proteins*, **8**, 251 - 257

Hermanson, Mallia and Smith (1992). *Immobilised Affinity Ligand Techniques* , 210 - 214

Hoffman, W. and O'Shannesy, D. (1988). Site specific immobilisation of antibodies by their oligosaccharide moieties to new hydrazide derivatised solid supports, *Journal of Immunological Methods*, **112**, 113 - 120

Hohsaka, T. Kawashima, K. and Sisido, M. (1994) Photoswitching of NAD⁺ - mediated reaction through photoreversible antibody – antigen reaction. *JACS*, **116**, 413 – 414

Howell, S. Kenmore, M. Kirkland M. and Badley R. (1998). High-density immobilisation of an antibody to a CMD-linked biosensor surface. *Journal of molecular recognition*, **11**, 200 - 203

Howland, R. and Benatar L. (1997). *A practical guide to scanning probe microscopy*, 7 – 17 (Park scientific instruments)

Huan, S.C., et al (1996). Site Specific Immobilisation of Mab's using spacer-mediated antibody attachment. *Langmuir*, **12**, 4292 - 4298

Hutchinson, A. (1995). Evanescent Wave Biosensors. *Molecular Biotechnology*, **3**, 47 - 54

Jaffrezic-Renault, N and Martelet, C (1997). Semiconductor based microbiosensors. *Synthetic materials*, **90**, 205 – 210

Johnston, K, Mar, M and Yee, S. (1999). Prototype of a multi-channel planar SPR probe. *Sensors and Actuators B*, **54**, 57 - 65

Jones, R. (1997). Polymer interfaces and the molecular basis of adhesion. *Current opinion in solid state and materials science*, **2 (6)**, 673 – 677

Jonsson, U, Olofsson, G, Malmqvist, M and Ronnberg, I. (1985). Chemical Vapour depositions of silanes *Thin solid films*, **124**, 117 – 123

Jonsson, B, Lofas, S, Edstrom, A, Hansson, A, Lindquist, G, Hillgren, R and Stigh, L (1995). Comparison of methods for immobilisation to carboxymethyl dextran sensor surfaces by analysis of specific activity of monoclonal antibodies
Journal of Molecular recognition, **8**, 125 - 131

Kaganer, E, Pogreb, R, Davidov, D and Willner, I (1999) Surface plasmon resonance characterisation of photoswitchable antigen-antibody interactions. *Langmuir*, **15 (11)**, 3920 - 3923

Karlsson, R, Michealson, A. and Mattson, L. (1991). kinetic analysis of Mab-anitgen interactions with a new biosensor based analytical system. *Journal of immunological methods*, **145**, 229 - 240

Karube, I. Nakomoto Y. and Suzuki, S. (1976) Photocontrol of urease activity in spiropyran collagen membrane, *Biochemica Biophysica Acta*, **445**, 774 – 779

Karube, I., Nomura, Y. and Arikawa, Y. (1995). Biosensors for Environmental control
Trends in Analytical Chemistry, **14 (7)**, 295 - 299

Killard A. Deasy, B, O'kenedy R. and Smyth, M. (1995). Antibodies production, function and applications in biosensors. *Trends in analytical chemistry*, **14** no.6 pp 257 - 266

Kim, H and Zin, W. (1997) Molecular packing of poly(azomethine)s having flexible (n-alkyloxy)methyl side chains in films. *Polymer Bulletin*, **39**, 701 - 705

Kossek, S., Padeste, C, Tiefenauer, L, and Siegenthaler, H. (1998), Localisation of individual biomolecules on sensor surfaces. *Biosensors and bioelectronics*, **13 (1)**, 31 - 43

Kuby, J. (1991). *Immunology*, 2nd edit Freeman Press, 157 - 158

Kuhn, H. (1988). Molecular Engineering – facts and aims. *Journal de Chimie Physique et de physico – chimie biologique*, **85**, (11-12) 991-993

Kurihara, K (1997) Direct measurement of surface forces as a novel means of investigating supramolecular assemblies. *Advances in Colloid and Interface Science*, **71 – 72**, 243 - 258

Kurthen, C. and Nitsch, W. (1991) Orientation of monolayers by convection *Advanced Materials*, **3 (9)**, 445 - 447

Kramer, K. (1998) synthesis of pesticide specific single chain Fv utilising the recombinant phage antibody system *Analytical letters* **31**, 1, pp 67 – 92

Kramer K. and Hock, B. (1996). Recombinant antibodies for pesticide detection
Immunoassays for residue analysis ACS, 470 - 484

Kriz, D, Ramstrom, O, Svensson, A and Mosbach, K. (1995). Introducing biomimetic sensors based on molecular imprinted polymers as recognition elements. *Analytical chemistry*, **67**, 2142 - 2144

- Laibinis, P, Hickman, J., Wrighton, M. and Whitesides, G. (1989).** Orthogonal SAM's: alkanethiols on gold and alkane carboxylic acids on alumina. *Science*, **245**, 845 - 847
- Lam K, Salmon S, Hersh E, Hraby V, Kazmirski W and Knapp R. (1991).** A new type of synthetic peptide library for identifying ligand-binding activity. *Nature*, **354**, 82 - 86
- Lareginie P, Samat, A and Guglielmetti, R. (1996)** Structure-visible absorption relationship in the photochromic spiro[indoline-naphthoxazine] series. *Journal of Physical Organic Chemistry*, **9**, 262 – 264
- Lawrence, C. and Geddes, N. (1998).** SPR for biosensing. *Handbook of Biosensors and Electronic Noses*, 149 – 154
- Lawrence, J, Nie, T, Swerhone, G (1998).** Application of multiple parameter imaging for the quantification of algal, bacterial and exopolymer components of microbial biofilms. *Journal of microbiological methods*, **32 (3)**, 253 - 261
- Lesho, M.J. and Sheppard, N.F. (1996).** Adhesion of polymer films to oxidised silicon and its effect on performance of a conductometric pH sensor. *Sensors and Actuators B*, **37**, 61 -66
- Li, H. and Poulos, T. (1994).** Structural variation in heme enzymes: a comparative analysis of peroxidase and P450 crystal structures. *Structure*, **2**, 461 – 464
- Lidin, S, Jacob, M and Andersson, S. (1995)** A mathematical analysis of rod packings *Journal of solid state chemistry*, **114**, 36 - 41
- Liedberg, B. and Lundstrom, I. (1993).** Principles of biosensing with an extended coupling matrix and surface plasmon resonance. *Sensors and Actuators B*, **11**, 63 – 72
- Lin, J-N, Change, I, Herron, J and Christensen, D (1991).** Comparison of site-specific coupling chemistry for antibody immobilisation on different solid supports. *Journal of Chromatography*, **542**, 41 - 54
- Lofas, S. (1995).** Dextran modified self-assembled monolayer surfaces for use in biointeraction analysis with surface plasmon resonance. *Pure and Applied Chemistry*, **67**, 829 - 834
- Lofas, S. and Johnsson, B. (1990)** A novel hydrogel matrix on gold surfaces in surface plasmon resonance sensors for fast and efficient covalent immobilisation of ligands *Journal of the Chemical Society, Chemical Communications 1990* 1526 - 1528
- Lofas, S, Johnsson, B., Tegendal, K. and Ronnberg, I. (1993).** Dextran modified gold surfaces for SPR sensors. *Colloids and Surfaces B: biointerfaces*, **1**, 83 - 89
- Lu, B. Smyth, M.R. and O'kenedy, R. (1995).** Oriented immobilisation of Fab' fragments on silica surfaces. *Analytical Chemistry*, **67**, 83 - 87
- Lu, B., Smyth, M.R. and O'kenedy, R. (1996).** Oriented immobilisation of Ab's and its applications in immunoassay and immunosensors. *Analyst*, **121**, 29R - 32R

- Lui, W., Han, X. Liu, J. And Zhou, H. (1994).** Structure and properties of AB cross-linked polymers. *Interpenetrating polymer networks*, 571 - 594
- Lynch, M. MacDermott, J. Byrne, D. and Hamilton Stewart, P. (1991)**
Use of an antibacterial powder spray to prevent prostatectomy urinary infection
Journal of the royal society of medicine, **84**, 667 - 668
- Macas J, Nouzova M, Galbraith, D (1998).** Adapting the Biomek(R) 2000 laboratory automation workstation for printing DNA microarrays. *Biotechniques*, **25 (1)**, 106 - 110
- Magonov, S and Reneker, D (1997)** Characterisation of polymer surface with AFM. *Annual review of Materials Science*, **27**, 175 - 222
- Makinen, K, and Tonovuo, J. (1982)**
Observations in the use of Guaiacol and 2,2' azino-bis-ethylbenzthiazoline-6-sulfonic acid as peroxidase substrates
Analytical Biochemistry, **126**, 100 - 108
- Marco, M. P. and Barcelo, D. (1996),** Environmental applications of analytical biosensors
Measurement in Science and Technology, **7**, 1547 - 1562
- Marquis, C. (1995).** Engineering issues in applied mammalian cell culture. *Australian Biotechnology*, **5 (2)**, 87 – 91
- Mateson R. and Little, M. (1988).** Strategy for the immobilisation of monoclonal antibodies on solid-phase supports. *Journal of chromatography*, **458**, 67 - 77
- McConnell, I, Munro, A and Waldman, H.(1981)** The Immune system, *Blackwell Scientific Publications*, **chp 1**, 25 - 30
- McGurk, S, Green, R, Sanders, G, Davies, M, Roberts, C, Tendler, S and Williams, P. (1999)** Molecular interactions of biomolecules with surface-engineered interfaces using atomic force microscopy and surface plasmon resonance. *Langmuir*, **15 (15)**, 5136 – 5140
- Moller, K, Bein, T and Fischer, R. (1998)** Entrapment of PMMA polymer strands in micro- and mesoporous materials. *Chemistry of Materials*, **10 (7)**, 1841 - 1852
- Moore, W. (1978)** *Physical Chemistry*, 495 – 496, Longman Press
- Mulchandani. A and Rogers, K. (1998)** *Enzyme and microbial biosensors*, Humana press, 199 - 203
- Nascimento,_VB, Angnes,_L (1998).** Screen-printed electrodes. *QUIMICA NOVA*, **21, (5)**, 614-629
- Newman, J Turner, APF and Marrazza, G. (1992)** Inkjet printing for the fabrication of amperometric glucose biosensors. *Analytica Chemica Acta*, **262**, 13 - 17
- Newman, J.D. and Turner, A.P.F. (1994)** Biosensors: the analyst's dream? *Chemistry and Industry*, **16 May, 1994**, 374 - 378

Oh, S. (1993). immunosensors for food safety. *Trends in Food Science and Technology*, **4**, 98 - 103

O'Shannessy, D. Brigham-burke, M. Soneson, K. Hensley, P. and Brooks, I.(1993). Determination of rate and equilibrium binding constants for macromolecular interactions using SPR. *Analytical Biochemistry*, **212**, 457 - 468

Ottova, A. Tvarozek, V. Racek, J. Sabo, J. Ziegler, W. Hianik T. and Tien H. (1997). Self assembled BLMs: biomembrane models and biosensor applications. *Supramolecular science*, **4**, 101 – 112

Owens, D R, Vora, J. and Dolben, J (1991). Human Insulin and Beyond : Semisynthesis and recombinant DNA technology reviewed. *Biotechnology of Insulin Therapy*: Ed: John C Pickup, Blackwell Scientific Publications:24-41

Pale-Grosedemange, C. Simon, S. Prime, K. and Whitesides, G. (1991)
Formation of SAM's by chemisorption of derivatives of oligo(ethylene glycol) of structure $\text{HS}(\text{CH}_2)_{11}(\text{OCH}_2\text{CH}_2)_m\text{OH}$ on gold

Pavey, K. and Olliff, C. (1999). SPR analysis of the total reduction of protein adsorption to surfaces coated with mixtures of long and short chain PEO block co-polymers. *Biomaterials*, **20**, pp 885 - 890

Piehler, J Brecht, A Geckler, C and Gauglitz, G (1996). Surface modification for direct immunoprobes. *Biosensors and bioelectronics*, **11** no. 6/7 pp 579 – 590

Pierrat, O, Lechat, N, Bourdillion, C and Laval, J (1997). Electrochemical and SPR characterisation of the step by step self-assembly of a biomimetic structure onto an electrode surface. *Langmuir*, **13**, 4112 - 4118

Plant, A, Brigham-Burke, M, Petrella, E and O'Shannessy, D. (1995). Phospholipid /alkanethiol bilayers for cell-surface receptor studies by SPR. *Analytical Biochemistry*, **226**, 342 – 348

Poyard, S, Jaffrezic-Renault, N, Martelet, C, Cosnier, S and Labbe, P. (1998)
Optimisation of an inorganic / bio-organic matrix for the development of new glucose biosensor membranes. *Analytica Chimica Acta*, **364**, 165 - 172

Quici S, Manfredi A, Pozzi G, Cavazzini M and Rozzoni A (1999) Ditopic receptors capable of hydrogen bonding: Synthesis and complexation behaviour of diaza crown-ethers having melamine sidearms. *Tetrahedron*, **55** (34), 10487 - 10496

Ramachandran, T, Madhukar, A, Chen, P and Koel, B. (1998). Imaging and direct manipulation of nanoscale 3D features using the noncontact AFM. *Journal of vacuum Science Technology*, **16**(3) 1425 – 1429

Rimmel G and Bauerle P (1999). Molecular recognition properties of crown ether-functionalized oligothiophenes. *Synthetic metals*, **102** (1-3), 1323 - 1324

- Robinson, G. (1995).** The Commercial development of planar optical biosensors *Sensors and Actuators B*, **29**, 31 – 36
- Rubin, S. and Willner, I. (1994)** Photoregulation of the activities of proteins, *Molecular Crystals and Liquid Crystals*, **46**, 201-205
- Salamon, Z, Brown, M and Tollin, G. (1999)** Plasmon resonance spectroscopy: probing molecular interactions within membranes. *Trends in Biochemical Sciences*, **24 (6)**, 213 – 219
- Sarwade, B and Singh, R (1999)** Morphology of photodegraded heterophasic ethylene-propylene copolymers. *Journal of Applied polymer Science*, **72 (2)**, 215 – 225
- Sasaki, S. Nagata, R Hock, B and Karube, I. (1998).** Novel surface plasmon resonance sensor chip functionalisation with organic silica compounds for antibody attachment. *Analytica Chimica Acta*, **368**, 71 – 76
- Scouten, W.H., luong, J.H.T. and Brown, R.S. (1995).** Enzyme or protein immobilisation techniques for applications in biosensor design. *Trends in Biotechnology* **13**, 178 – 185
- Schultze, J, Morgenstern, T, Schattka, D and Winkels, S. (1999)** Microstructuring of conducting polymers. *Electrochimica Acta*, **44 (12)**, 1847 - 1864
- Semanova, M and Savilova, L. (1998)** The role of biopolymer structure in interactions between unlike biopolymers in aqueous medium, *Food Hydrocolloids*, **12**, 65 - 75
- Seo, K. Brackett, R. Hartman N. and Campbell, D. (1999).** Development of a rapid response biosensor for detection of Salmonella Typhimurim. *Journal of Food Protection*, **62**, no. 5, pp 431 - 437
- Shao, Y and Mirkin, M. (1997)** Scanning electrochemical microscopy (SECM) of facilitated ion transfer at the liquid/liquid interface. *Journal of Electroanalytical Chemistry*, **439 (1)**, 137 - 143
- Sisido, M., Harada, M., Kawashima, K., Ebato, H. & Okahata, Y. (1998)** Photoswitchable peptide antigens on solid surfaces, *Biopolymers*, **47**, 159-165
- Stamm, Ch and Lukosz, W. (1996).** Intergrated optical difference interferometer as immunosensor. *Sensors and Actuators B*, **31**, 203 - 207
- Steele, A, Goddard, D, Beech, I, Tapper, R, Stepleton, D and Smith J. (1998).** AFM imaging of fragments from the Martian meteorite ALH84001. *Journal of Microscopy*, **189**, 2 – 7
- Stevenson D (1999)** Molecular imprinted polymers for solid-phase extraction. *Trends in analytical chemistry*, **18 (3)**, 154 – 158
- Stoodley, P, Boyle, J, DeBeer, D and LappinScott, H (1999).** Evolving perspectives of biofilm structure. *Biofouling*, **14 (1)**, 75 - 95

Strike, D, Hengstenberg, A, Quinto, M, Kurzawa, C, KoudelkaHep, M, and Schuhmann, W. (1999) Localised visualisation of chemical cross-talk in microsensor arrays by using scanning electrochemical microscopy. *Mikrochimica Acta*, **131** (1-2), 47-55

Sun, J, Fang, H and Chen, H (1998) Immobilisation of HRP on a SAM modified gold electrode for the detection of hydrogen peroxide. *Analyst*, **123**, 1365 - 1366

Suzuki, M. Nakashima Y. and Mori, Y (1999). SPR immunosensor integrated two miniature enzyme sensors. *Sensors and Actuators B*, **54**, 176 – 181

Szutowicz, A. Kobes, R and Orsulak, P (1984). Colourametric assay for monoamine-oxidase in tissues using peroxidase and 2,2'-azinodi(3-ethylbenzthiazoline-6-sulfonic acid) as chromogen. *Anal. Biochem.* **138**, 86-94

Takeuchi T and Matsui J (1996). Molecular imprinting: An approach to "tailor-made" synthetic polymers with biomimetic functions. *Acta polymerica*, **47** (11-12) 471 - 480

Tan Z and Remcho V (1998) Molecular imprint polymers as highly selective stationary phases for open tubular liquid chromatography and capillary electrochromatography. *Electrophoresis*, **19** (12) 2055 - 2060

Thakur, S and Hosangadi, B. (1996)
Synthesis of photochromic spiroindolinopyrans with extended conjugation
Tetrahedron, **52** no. 26, pp 8755 – 8762

Timkovich, R. (1977). Detection of the stable addition of carbodiimide to proteins
Analytical Biochemistry, **79**, 135 – 143

Tisone, T. (1998) Dispensing systems for miniaturised diagnostics. *IVD Technology*, May/June 1998, 40 – 46

Tomalia, D.A. and Esfand, R.(1997) Dendrons, dendrimers and dendrigrafts
Chemistry and Industry, 2nd June 1997, 416 - 420

Treloar, P, Christie, I and Vadgama, P (1995). Engineering the right membranes for electrodes at the biological interface. *Biosensors and bioelectronics*, **10**, 195 - 201

Turner, A. Karube, I. and Wilson, G. S. (1987). *Biosensors: Fundamentals and Applications*. Oxford University Press, Oxford.

Turner, APF, Newman, J. and White, S. (1995). Fabrication technologies for membranes
Sensor 95, 619 - 624

Turyan, I and Mandler, D. (1998) Two-dimensional polyaniline thin film electrodeposited on a self-assembled monolayer. *JACS*, **120** (41), 10733 - 10742

Ustamehmetoglu (1999). Matrix effect on the electrochromism of spirochromics
Polymers for advanced technologies, **10**, 164 - 168

- Verma R, Boleti E and George AJT (1998).** Antibody engineering: Comparison of bacterial, yeast, insect and mammalian expression systems. *Journal of Immunological methods*, **216** (1-2), 165-181
- Watson, J.D., Gilman, M., Witowski, J. and Zoller, M. (1992).** *Recombinant DNA* (2nd edit.) 63 - 77
- Wei, Herron and Christensen, (1992).** *Biosensor Design and Application*, Chapter 10, 108 - 112
- Weiping, Q, Bin X, Chunxiao, W, Danfeng, Y, Fang, Y, Chunwei, Y and Yu, W. (1999)** Controlled site-directed assembly of antibodies by their oligosaccharide moieties onto APTES derivatised surfaces. *Journal of Colloid and Interface Science*, **214**, 16 - 19
- Weisenhorn, A.L., et al (1993).** Deformation and height anomaly of soft surfaces studied with an AFM. *Nanotechnology*, **4**, 106 – 113
- Welindr, K. Mauro, M. and Norskov-Lauritsen, L. (1992).** Structure of plant and fungal peroxidases. *Biochemical Society Transactions*, **20**, pp 337 - 340
- Westmark, P. Kelly J. and Smith D. (1993)** Photoregulation of enzyme activity. *Journal of the American Chemical Society*, **115**, 3416 – 3419
- Weston, D, Fowler, D. Cullen D. and Taylor F. (1999)**
Evaluation of Biosensor Components for Environmental Monitoring
Biosensors and Bioelectronics, in press.
- Wijesuriya, D. (1994).** Regeneration of immobilised antibodies on fibre optic probes. *Biosensors and Bioelectronics*, **9**, 585 - 592
- Williams, R.A. and Blanch, H.W. (1994)**
Covalent immobilisation of protein monolayers for biosensor applications
Biosensors and Bioelectronics, **9**, 159 – 167
- Willner, I Rubin S and Riklin A (1991)** Photoregulation of papain activity through anchoring photochromic azo groups to the enzyme backbone, *Journal of the American Chemical Society*, **113**, 3321 – 3325
- Willner, I and Willner, B (1997)**
Photoswitchable biomaterials as grounds for optobioelectronic devices
Bioelectrochemistry and Bioenergetics, **42**, 43 - 57
- Wilson, R and Turner, APF (1992)** Glucose oxidase – an ideal enzyme. *Biosensors and Bioelectronics*, **7** (3), 165 – 185
- Winter, G. and Frecht, A. (1984)** Engineering enzymes *Trends in Biotechnology*, **2** (5), 115 - 119

Wolfaardt, G, Lawrence, J, Robarts, R and Caldwell, D (1998) In situ characterisation of biofilm exopolymers involved in the accumulation of chlorinated organics. *Microbial Ecology*, **35** (3), 213 - 223

Wright D and Linck R (1999) Molecular imprinted polymers for the screening of antimalarial compounds. *Abstracts of the American chemical society*, **217** (1), 366-CHED

Zahavy, Rubin and Willner, (1994) conformation dynamics associated with photoswitchable binding of spiropyran modified concanavalin A. *Mol. Cryst. Liq. Cryst.*, **246**, 195 – 199

Appendix
A1 Published papers

Reprinted from

BIOCHIMICA ET BIOPHYSICA ACTA



Biochimica et Biophysica Acta 1428 (1999) 463–467

Rapid report

Photo-modulation of horseradish peroxidase activity via covalent attachment of carboxylated-spiropyran dyes

D.G. Weston, J. Kirkham, D.C. Cullen *

Cranfield Biotechnology Centre, Institute of BioScience and Technology, Cranfield University, Cranfield, Bedfordshire MK43 0AL, UK

Received 18 May 1999; received in revised form 31 May 1999; accepted 9 June 1999



Rapid report

Photo-modulation of horseradish peroxidase activity via covalent attachment of carboxylated-spiropyran dyes

D.G. Weston, J. Kirkham, D.C. Cullen *

Cranfield Biotechnology Centre, Institute of BioScience and Technology, Cranfield University, Cranfield, Bedfordshire MK43 0AL, UK

Received 18 May 1999; received in revised form 31 May 1999; accepted 9 June 1999

Abstract

The photo-modulation of the enzyme horseradish peroxidase modified with photochromic spiropyran dyes is reported. The degree of photo-modulation, greater than 90% reduction in enzyme activity under visible compared to UV illumination, matches the greatest degree of photo-modulation previously reported in the literature. The observation that only a small fraction of the conjugated photochromic molecules are photo-switched suggests that the dyes influence the enzyme activity via local interaction with the enzyme active site. © 1999 Elsevier Science B.V. All rights reserved.

Keywords: Spiropyran; Photochromic; Photo-modulation; Horseradish peroxidase; Optical switching

There is a rapidly growing interest in the photo-modulation of the biological activity of proteins, such as enzymes and affinity proteins. The interest arises from potential applications in areas including bio-electronics, biosensors, pharmaceuticals, affinity purification and as model systems for naturally occurring photo-activated biomolecules. Within the literature to date, there are a limited number of reports of the direct photo-modulation of protein activity achieved via the covalent attachment of photochromic dyes to protein molecules [1–4]. In these examples, reversible physico-chemical changes in the photochromic dye structure induced by exposure to different wavelengths of light, i.e. optical switching, affects directly or indirectly the structure of the protein active site resulting in photo-modulation of the protein function. Three issues of key concern for

useful applications of photo-modulated protein activity are: (1) photo-modulation of useful classes of proteins; (2) demonstration of large changes of activity between the two photo-modulated forms; and (3) elucidation of the underlying mechanisms of photo-modulation.

We report here a study that addresses the above issues via the modification of the enzyme horseradish peroxidase (HRP) with covalently attached spiropyran photochromic dyes and the subsequent photo-modulation of the enzyme activity. Firstly, HRP represents the important class of redox enzymes, the haem oxidases, and it and other class members have important roles in clinical diagnostics, drug metabolism and bio-transformations. Secondly, we will show a degree of photo-modulation that matches the largest modulation previously reported in the literature [3]. Thirdly, by observing the degree of photo-switching of enzyme conjugated photochromic dye, we have gained insight into the underlying mechanisms of photo-modulation.

* Corresponding author. Fax: +44-1234-754339;
E-mail: d.cullen@cranfield.ac.uk

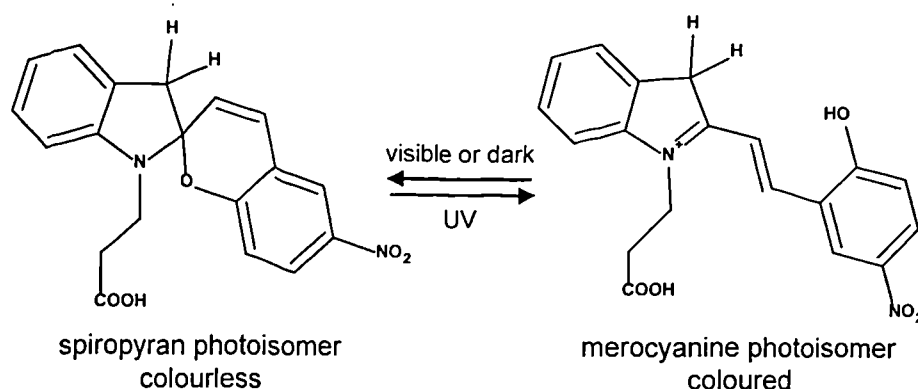


Fig. 1. Schematic of the photo-isomerisation of the spiropyran dye 1'-(2-carboxyethyl)3',3'-dimethyl-6-nitrospiro[2*H*-benzopyran-2',2-indoline]. Visible illumination converts the red spiropyran form into the yellow merocyanine form and the schematic represents the merocyanine form after a *cis-trans* isomerisation of the central double bond and protonation of the oxygen group. UV illumination reverses the conversion. In addition, a slow dark conversion of the spiropyran to merocyanine form can occur.

We chose a carboxylated spiropyran dye as these have been used previously to modulate the activity of proteins [5,6] and the carboxyl group enables the facile conjugation of dye to protein using standard coupling chemistries. The light induced structural changes of the spiropyran dye are shown in Fig. 1 and involve both a change in the geometry of the dye and the molecular dipole [7]. The carboxylated-spiropyran dye, 1'-(2-carboxyethyl)3',3'-dimethyl-6-nitrospiro[2*H*-benzopyran-2',2-indoline] (SP-COOH) suitable for covalent attachment to protein via the free carboxyl group was synthesised according to the method of Aizawa et al. [5]. Briefly, the SP-COOH precursor, 1-(2-carboxyethyl)-2,3,3-trimethyl-indolinium iodide (CE-TMI-I), was synthesised by the reflux of 2,3,3-trimethylindolenine with equimolar amounts of 3-iodopropionic acid in methyl ethyl ketone (MEK) resulting after crystallisation in a white crystalline product. The SP-COOH was produced by reflux of CE-TMI-I with 5-nitrosalicylaldehyde in MEK with the presence of piperidine followed by crystallisation resulting in a purple solid. All chemicals supplied by Sigma-Aldrich, Poole, UK.

Photochromic activity of the SP-COOH was confirmed by a change in absorption at 548 nm under alternating exposure to UV and visible light. For all experiments, optical illumination consisted of a 80-W tungsten filament lamp for visible illumination and for UV illumination, a UVG-54 UV lamp (UV Products, San Gabriel, CA, USA) with peak output at 245 nm. In both cases, the lamps were held approximately 5 cm above the sample solution contained in

a quartz 4-ml cuvette, normally mounted inside a spectrophotometer. For conjugation of the SP-COOH to HRP (EC 1.11.1.7 Type II, code: P8250, Sigma, UK), SP-COOH was dissolved in ethanol (2.5 mg in 2.5 ml) and added to HRP dissolved in 0.1 M MES buffer, pH 7.0 (10 mg in 7.5 ml) and the reaction initiated by the addition of 15 mg of 1-ethyl-3(3-dimethyl amino propyl) carbodiimide (EDC). Aliquots of the reaction mixture were taken at 20, 40, 60, 90 and 120 min and immediately purified to terminate the reaction. Purification consisted of centrifugation at 3000 rpm for 5 min (MSE Centaur 2)

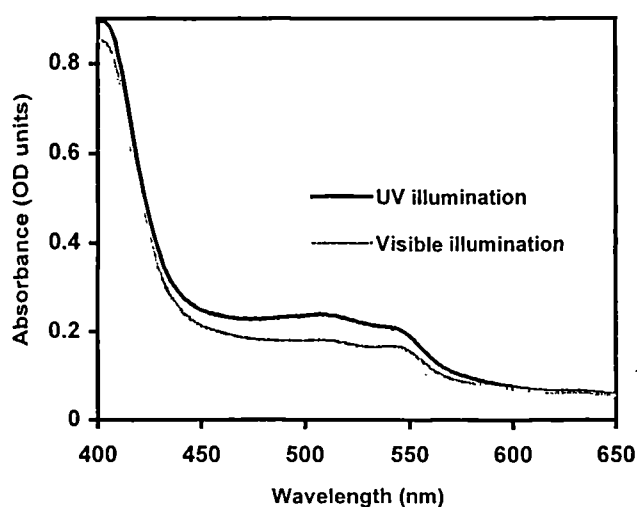


Fig. 2. Photochromic activity of SP-HRP under UV and visible light. Each sample was illuminated for 5 min with the appropriate light source prior to being scanned in a spectrophotometer. The sample consisted of HRP-SP (1:8.5 enzyme:dye ratio) at a concentration of 1 mg/ml in 100 mM MES buffer, pH 6.8.

to remove any insoluble urea products from the EDC reaction and gel filtration through a PD10 column (Pharmacia Biotech, Uppsala, Sweden) to remove any unconjugated SP-COOH and other low molecular weight species.

The resultant degree of modification of the HRP with SP-COOH with varying reaction times was determined by measuring the optical absorbance, under UV illumination, at 548 nm of the purified HRP/SP-COOH (HRP-SP) conjugates using a molar extinction coefficient for the SP-COOH of 422 l/mol/cm and by determining the protein content using a protein assay kit (Sigma protein assay kit, code: P5656, Sigma, UK). The results are shown in Table 1 and vary between a ratio of 6.5:1 and 9:1 dyes per HRP molecule for a reaction times of 20 and 120 min. It is known that HRP contains 12 lysine residues (entry 3ATJ in the Brookhaven Protein Database), the main sites for carbodiimide mediated covalent attachment, and this agrees with the observed ratios. The enzyme:dye ratio plateaus after a reaction time of 40 min, suggesting that all the accessible lysine residues have been conjugated to dye and further incubation does not significantly increase the enzyme:dye ratio.

Prior to assessing the photo-modulation of the enzyme activity of the HRP-SP samples, the photochromic switching of the HRP-SP conjugates was confirmed. Fig. 2 shows an example visible absorbance spectrum obtained immediately after either 5 min of UV or visible illumination. The absorption peak at 548 nm corresponds to the merocyanine photoisomer form of the spiropyran dye and under the illumination conditions available, is not fully converted to the spiropyran photoisomer form as can be seen by the remaining presence of a 548 nm ab-

Table 1

Effect of reaction time on the carbodiimide-mediated covalent coupling of a carboxylated spiropyran dye to the enzyme horseradish peroxidase expressed as the resultant ratio of enzyme to immobilised dye

Reaction time (min)	HRP:SP-COOH ratio
20	1:6.5
40	1:8.5
60	1:8.0
90	1:8.0
120	1:9.0

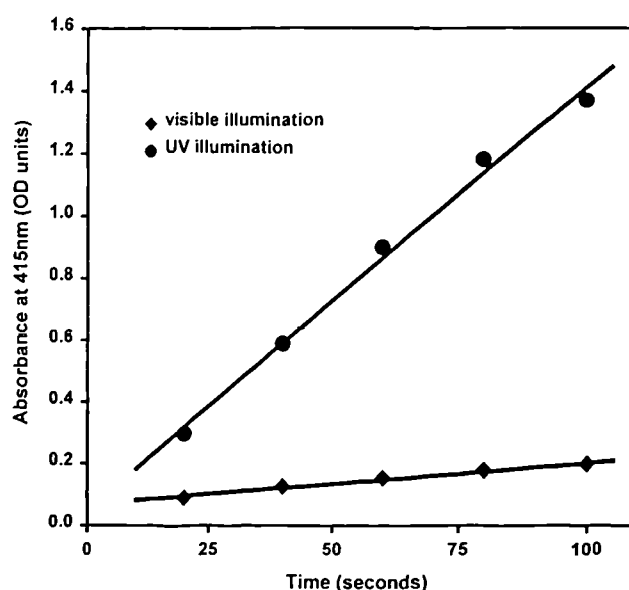


Fig. 3. Enzyme activity of a horseradish peroxidase-spiropyran dye conjugate (HRP-SP) under visible (♦) and UV (●) illumination. The example comprised a HRP-SP with an enzyme:dye ratio of 1:8.5 (40 min reaction conjugation time) at a concentration of 10 µg/ml in 100 mM MES buffer, pH 6.4. The data points are specific absorbance measurements and the lines represent linear regressions and used to calculate the specific enzyme activity of the HRP-SP under the different illumination.

sorption peak. A 23% reduction upon visible illumination is seen. Within the current study, it has not been determined if a sub-population of the conjugated dye has lost photochromic activity due to specific local protein environments.

The enzyme activity of the HRP-SP conjugates was determined under varying optical illumination and is summarised in Figs. 3 and 4. HRP enzyme activity was assayed using a coupled assay [8], comprising glucose and glucose oxidase (EC 1.1.3.4 from *Aspergillus niger*, code: G 7016, Sigma, UK) to produce hydrogen peroxide as a substrate for HRP to convert the indicator dye 2,2'-azino-bis-(3-ethyl)-benzthiazoline-6-sulfonic acid (ABTS) from a colourless to a coloured form with the reaction monitored by optical adsorption at 415 nm in a spectrophotometer (Camspec model M350). Optical absorption measurements to follow the enzyme assay were taken at approximately 20-s intervals by briefly removing the illumination source and measuring the absorbance. Illumination occurred in situ within the spectrophotometer. Fig. 3 displays an example of the rate of the reaction of a HRP-SP sample with an enzy-

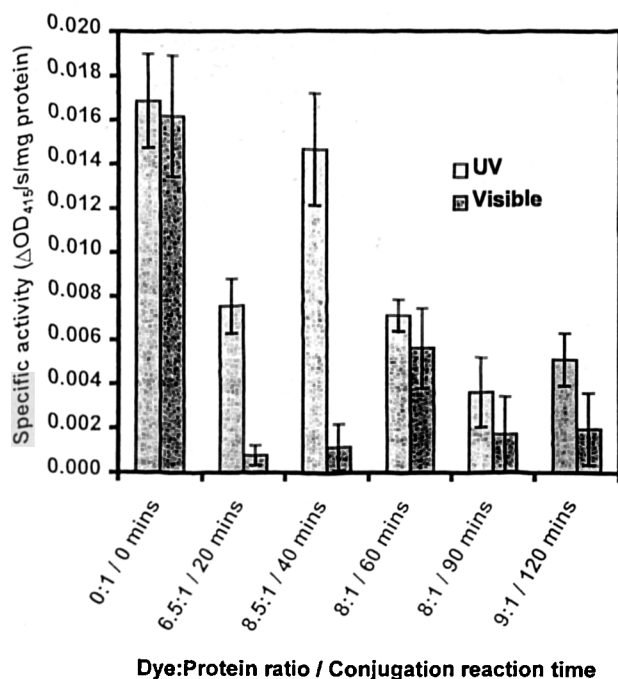


Fig. 4. Effect of conjugation reaction time on the photo-modulation of enzyme activity of horseradish peroxidase-spiropyran dye (HRP-SP) conjugates. Specific activities of the HRP-SP conjugates were determined via a spectrophotometric enzyme assay under either UV or visible illumination. The dye:enzyme ratios were determined spectrophotometrically. Error bars represent the standard deviation of three repeats.

me:dye ratio of 1:8.5. A reduction of 92% in the enzyme reaction rate can be seen when illumination was changed from UV to visible, i.e. from merocyanine photoisomer to spiropyran photoisomer. Each sample was pre-illuminated for 5 min at an appropriate wavelength to ensure the dye was maximally switched.

Fig. 4 summarises the specific enzyme activities for a range of HRP-SP conjugates obtained from various lengths of conjugation reactions. For the controls consisting of native HRP under visible and UV illumination, similar specific activities are seen, as expected. It is apparent that for HRP-SPs produced via long conjugation reaction times, greater than 40 min, specific activities under both UV and visible illumination are significantly reduced. Since the degree of conjugation does not increase, the formation of carbodiimide cross-linked enzyme aggregates may account for this observation. For reaction times of 20 and 40 min, a significant variation of enzyme specific activity is seen between UV and visi-

ble illumination. For the 40-min incubation, 1:8.5 enzyme:dye ratio, a reduction of 13% in enzyme-specific activity is seen under UV illumination compared to native enzyme and under visible illumination, a reduction of specific activity of 93% versus the native is observed. The reduction in specific activity for the HRP-SP under visible compared to UV illumination is 92%. At present, it is not understood why the HRP-SP produced via a 20-min reaction, 1:6.5 enzyme:dye ratio, demonstrates a reduced specific activity under UV illumination compared to both native HRP and HRP-SP produced via a 40-min reaction.

Proposed mechanisms for photo-modulation of protein function range from direct influence of the photochromic dye on the activity site [9] to distortion of the protein tertiary structure [10]. In the current study, it is interesting to note the observed amount of the conjugated photochromic dye that is switched from the merocyanine to the spiropyran form upon visible illumination (Fig. 2). This suggests, as determined from the remaining absorbance at 548 nm, that approximately 2–3 of the 8.5 attached dyes have switched. Thus the 92% reduction in specific activity observed is only due to the switching of 2–3 dye molecules. This indication that only a small number of the bound dyes are involved in the modulation of protein function suggest that modulation occurs due to close interaction of the dyes with the active site of HRP, either via direct steric effects or via local distortion of the protein around the active site.

A number of other issues remain to be addressed. A reduction in the conjugation reaction time to obtain dye:enzyme ratios between 0:1 and 6.5:1 would help to confirm the importance of the degree of dye modification. Also, within the current study, no attempt has been made to assess the reversibility of the enzyme activity upon alternating UV and visible illumination and any associated dye fatigue.

In conclusion, we have observed the first photo-modulation of the important redox enzyme horseradish peroxidase. The degree of photo-modulation reported here, 92% reduction in enzyme activity under visible illumination compared to UV illumination, matches the largest degree of photo-modulation previously reported in the literature. The observation that only a small fraction of the conjugated photo-

chromic molecules are photo-switched to cause the reduced activity suggests that for the studied system, the dyes influence the enzyme activity via local interaction with, or local to, the enzyme active site.

Acknowledgements

We gratefully acknowledge the Engineering and Physical Sciences Research Council for their support of J.K. via an Innovative Manufacturing M.Res Studentship and Professor Geoff Ashwell and Dr Andrew Green of the School of Industrial and Manufacturing Science, Cranfield University for their advice on spiropyran chemistry.

References

- [1] I. Karube, Y. Nakomoto, S. Suzuki, Photocontrol of urease activity in spiropyran collagen membrane, *Biochim. Biophys. Acta* 445 (1976) 774–779.
- [2] I. Wilner, S. Rubin, A. Riklin, Photoregulation of papain activity through anchoring photchromic azo groups to the enzyme backbone, *J. Am. Chem. Soc.* 113 (1991) 3321–3325.
- [3] P. Westmark, J. Kelly, B. Smith, Photoregulation of enzyme activity. Photochromic, transition state analogue inhibitors of cysteine and serine proteases, *J. Am. Chem. Soc.* 115 (1993) 3416–3419.
- [4] I. Willner, B. Willner, Photoswitchable biomaterials as grounds for optobioelectronic devices, *Bioelectrochem. Bioenerg.* 42 (1997) 43–57.
- [5] M. Aizawa, K. Namba, S. Suzuki, Photo control of enzyme activity of α -amylase, *Arch. Biochem. Biophys.* 180 (1977) 41–48.
- [6] E. Zahavy, S. Rubin, I. Willner, Conformation dynamics associated with photoswitchable binding of spiropyran-modified concanavalin A, *Mol. Cryst. Liq. Cryst.* 246 (1994) 195–199.
- [7] H. Gerner, Photochemical ring opening in nitrospiropyrans: triplet pathway and the role of singlet molecular oxygen, *Chem. Phys. Lett.* 282 (1998) 381–390.
- [8] A. Szutowicz, R.D. Kobes, P.J. Orsulak, Colorimetric assay for monoamine-oxidase in tissues using peroxidase and 2,2'-azinodi(3-ethylbenzthiazoline-6-sulfonic acid) as chromogen, *Anal. Biochem.* 138 (1984) 86–94.
- [9] M. Harada, M. Sisido, J. Hirose, M. Nakanishi, Photocontrolled uptake and release of photochromic haptens Mab's: evidence of photoisomerization inside the hapten binding site, *Bull. Chem. Soc. Jpn.* 67 (1994) 1380–1385.
- [10] O. Pieroni, A. Fissi, Synthetic photochromic polypeptides: possible models for photoregulation in biology, *J. Photochem. Photobiol.* 12 (1992) 125–140.

A2 Conference proceedings

D.G. Weston and D.C. Cullen (1998) Photomodulation of biomolecule function by spiropyran dyes. *Biosensors 98*, 3-5 June, Berlin

PHOTOMODULATION OF BIOMOLECULE FUNCTION BY SPIROPYRAN DYES

David Weston* and David C. Cullen

Cranfield Biotechnology Centre, Cranfield University, Cranfield,
Bedfordshire, MK43 0AL, UK

There are many situations within biotechnology where the ability to modulate the activity of biological molecules is needed. An example is the affinity modulation of biorecognition molecules for regeneration of affinity sensors. Most common approaches to modulation rely on the use of harsh extremes of temperature, pH or ionic strength to disrupt biomolecular function.

A limited number of reports, dating back to the 1970's, have demonstrated the photomodulation of biomolecule function via photochromic dyes. Examples include the photomodulation of the enzyme α -amylase, the binding protein concanavalin A and the antibody binding of a photochromic antigen. This general approach offers simple external modulation of biological function.

We report here the results of our initial investigations into the use of photochromic dyes to modulate the activity of biomolecules of relevance to the biosensor community. We report for the first time the direct photomodulation of the activity of the enzyme glucose oxidase.

A spiropyran photochromic dye has been synthesised with a carboxylate functionality (SP-COOH) suitable for covalent attachment to proteins. We have successfully immobilised SP-COOH to a number of different proteins and retained photochromic activity in aqueous and mixed aqueous-organic solvents. SP-COOH has been covalently linked to glucose oxidase (GOx), via carbodiimide chemistry, resulting in a ratio of approximately 13 SP-COOH molecules per GOx. When the illumination of the SP-GOx is changed from ambient visible light to UV, an increase in enzyme activity was observed as determined by a colourimetric assay. The increase in GOx activity corresponded to the spiropyran moiety switching from the merocyanine to spiropyran form. This effect was not apparent with unmodified GOx.

Other protein systems are currently being studied.

Keywords: photomodulation, photochromic dyes, spiropyran, glucose oxidase

A3 Conference Posters

D.G. Weston, D.C.Cullen, J.D. Newman and A.P.F. Turner (1997) Surface modification of optical biosensors for increased sensitivity and eases of manufacture. *Fifth European workshop on biosensors for environmental monitoring* 28 – 30 May 1997, Munich

D.G. Weston and D.C.Cullen (1998) The use of novel and mixed polymers as transducer modifying agents. *BIOSET workshop on biosensors for environmental monitoring: Technology evaluation* 12 – 15 May 1998, Kinsale, Ireland

D.G. Weston and D.C.Cullen (1999) Reverse Deposition: optimisation of bioactive interfaces for compatability with large scale manufacture. *4th International conference on seperations in Biotechnology*, 29 – 31 March 1999, University of Reading

Surface Modification of Optical Biosensors for Increased Sensitivity and Ease of Manufacture

D.G. Weston, D.C. Cullen, J.D. Newman and A.P.F. Turner

Cranfield Biotechnology Centre, Cranfield University, Cranfield, Bedfordshire, MK43 0AL, UK

Introduction

The purpose of the EC EnviroSense project is to develop a multi-analyte optical biosensor to detect EC defined levels of pesticides and their metabolites, and in particular atrazine, in drinking water. The project is specifically directed towards production of a multi-analyte optical chip based sensor centred upon Evanescent Wave Interferometry (EWI).

One aspect of the project which Cranfield Biotechnology Centre is undertaking concerns the development of biosensor interfaces suitable for manufacturable multi-analyte devices. This will involve the molecular engineering of immobilised polymer interfaces to control non-specific binding, optimise sensitivity and to be compatible with spatial patterning and high-throughput manufacture. In addition, optical transduction of biorecognition events, compatible with near-IR light sources, is considered.

This poster outlines the concepts we are adopting to achieve the above and presents preliminary experimental results.

Integration of Biorecognition Molecules into Sensors

There are a number of general approaches to the integration, i.e. immobilisation, of biorecognition molecules, such as proteins, with transducers in the construction of biosensors and immunosensors.

Those relevant to optical evanescent wave sensors consist of:

- Direct physical adsorption to the transducer surface
- Immobilisation via covalent attachment directly to the transducer surface
- Incorporation into various extended polymer interfaces

The varying thickness of sensing films produced by these approaches has a significant effect upon final performance of resulting optical sensors.

Optical Sensing Issues of Biosensor Interfaces

Due to the physical properties of evanescent waves, sensors based on EWI and other evanescent wave techniques such as Surface Plasmon Resonance (SPR) interrogate optical interactions which occur within a fraction of a wavelength of the sensor surface. Therefore, biorecognition molecules immobilised to the transducer surface by either physical adsorption or direct covalent coupling, typically utilises only the first 10 nanometres of the evanescent wave. Modification of the sensor interface with an extended polymer layer allows the biosensing region to be optimally matched to the depth of the evanescent wave and enables an increase in the concentration of biorecognition molecules within the sensing layer (fig. 1). This should lead to increased sensitivity and the possibility of direct detection of molecular interaction without the need for a labelled system.

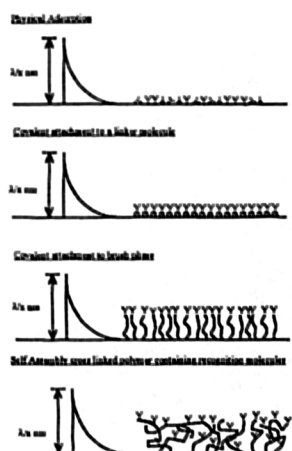


Figure 1. A schematic of the interaction of different deposited biorecognition layers with the optical evanescent wave summarising the main surface deposition approaches and the increasing levels of interaction with the evanescent wave which can be achieved.

Other Issues of Biosensor Interfaces

In addition to the optical issues of biosensor interfaces, the general desirable features to consider when coupling a recognition molecule to the transducer are:

- Integration process readily transferable to manufacture
- Minimal non-specific effects
- Non-reversible and mechanically robust coupling of the biorecognition molecule with the sensor
- Minimal loss of biorecognition function upon integration

An important additional feature is an integration system that is generic both towards biorecognition molecules and transducer surfaces.

Our Approach to Biosensor Interfaces

The compatibility of the deposition of the transducer interface with eventual large scale manufacture is the prime incentive of our approach. Self-assembled polymer layers represent a viable solution as the final integration of sensor components will involve only simple liquid handling steps. Complex chemistries are relegated to simple homogeneous bulk reactions.

Thus multifunctional polymer systems are envisaged with functionalities which:

- promote self-assembly on native or modified surfaces of EWI devices
- maintain an extended and open structure to optimise interaction with the evanescent wave, increase density of biorecognition molecules and to enable diffusion of analytes and labels
- facilitate stable, covalent integration of biorecognition molecules
- control non-specific interactions with sample components

Fabrication methods for use in biosensor manufacture

Likely methods to be utilised for the liquid handling steps envisaged for the final sensor manufacture include:

- Ink-Jet printing - involves the patterned deposition of nanolitre liquid droplets onto transducer surfaces. The technique is non-contact and is suitable for printing onto irregular and delicate surfaces.
- Cavity printing - involves an automated syringe pump for depositing reagents in the microlitre volume range.

Assay Development

To detect the interaction of pesticides with the biorecognition molecules attached to the transducer, a number of possibilities are being investigated:

- refractive index labelled ligands for displacement assays
- direct measurement

Refractive index labels amplify the refractive index signal from the low molecular weight analytes thus increasing the sensitivity of the sensor. Special consideration will be given to the near-IR wavelengths required by the EWI transducer. A label-free system is the ultimate goal and direct detection of the pesticide / biorecognition molecule interaction will be assessed.

Biosensor Interface Characterisation

Effective characterisation of the biosensor interface is central to a rational improvement of devices. A range of complementary techniques are to be applied within this project to the characterisation of biosensor interfaces including atomic force microscopy (AFM), SPR and contact angle measurement. Of special importance are techniques such as AFM that allow observation at molecular dimensions and which until recently have not been routinely available.

Preliminary Results

Initial work has focused on developing of simple extended polymer interfaces comprised of carboxymethyl cellulose (CMC) attached to amine silanised glass via carbodiimide chemistry. Characterisation of the CMC polymer films via AFM has highlighted the variability of the coatings at molecular dimensions (Figure 2) and thus the importance of characterisation methods. These interfaces will act as reference examples of "current" approaches to biorecognition molecule integration for comparison to the "self-assembled" approaches discussed previously. Current work is focus on optimising the CMC and related carboxymethyl dextran coatings and the integration of biorecognition molecules.



Figure 2. AFM image showing a carboxymethyl cellulose layer deposited on amine silanised glass. Attachment to the surface was achieved by spotting of 5 μ l of a 1% solution of CMC in 0.1 M MES (pH 7.0) with 30 mg/ml EDC and incubation for 10 minutes. The "gully" in the lower half of the image has allowed the CMC layer thickness to be determined as approximately 15 nm.

Conclusion

A general concept and framework for biosensor interface design has been established and preliminary results obtained showing (i) the creation of extended polymer interfaces and (ii) the importance of characterisation of interfaces at molecular dimensions.

The Use of Novel and Mixed Polymers as Transducer Modifying Agents

D.G.Weston and D.C. Cullen

Cranfield Biotechnology Centre, Cranfield University, Bedford, MK43 0AL UK

<http://www.cranfield.ac.uk/fbst>

Email: d.g.weston@cranfield.ac.uk

Introduction

Carboxylated polymers have been widely used to modify optical biosensors both in the research community and for commercially produced systems. Many of these systems have focused on carboxy-methyl dextran (CMD) as the principal polymer system.

Carboxy-methyl cellulose (CMC) can be used as a direct alternative to CMD. CMC has advantages over dextran as it is commercially available and is less readily degraded by micro-organisms. This is of central importance for continuous biosensor use in an environmental monitoring role. As an alternative to biologically-derived polymers, the synthetic polymer, carboxylated polynoxylin (CPN) has been synthesised and investigated and is expected to be resistant to biological degradation.

We are reporting initial studies into the effect of the various carboxylated polymers and polymer mixtures on (i) the morphology and (ii) the capacity to covalently bind protein to immobilised thin films of the polymers on model sensor surfaces.

Methods

Polymer Synthesis

The carboxylated polynoxylin was synthesised by the oxidation of polynoxylin (Borden Chemicals, Southampton, UK), by incubation with KMnO_4 in 0.2 M H₂SO₄ for 3 hours. CMD was synthesised from dextran (480,000 MW⁴, Sigma (Poole, UK), via the base catalysis method (Lofas, 1995). CMC (500,000 MW) was obtained from Sigma (Poole, UK).

Surface Modification

All surfaces, either cleaned microscope glass (for AFM) or silver (for SPR) were modified by vapour phase silanisation with aminopropyl trimethoxy silane (APTS) in an anhydrous atmosphere at room temperature for 8 hours. Polymer solutions were made containing 0.1% w/v total polymer (CMD/CMC 1:1 ratio, CMD/CMC/CPN 2:2:1 ratio) in 0.1 M MES buffer (pH 6.8). The polymer solutions were activated by addition of 30 mg/ml EDC (Sigma, Poole, UK) and 15 mg/ml NHS. The polymer solutions were immediately applied to APTS modified surfaces either via a static liquid cell to determine the rate of deposition via SPR or by pooling on the surface for AFM imaging. After 45 minutes incubation, the surfaces were washed with 0.1 M MES (pH 6.8). To determine the covalent binding capacity of the polymer films, glucose oxidase (GOx) was applied as a 1 mg/ml solution, in an identical manner to the polymer immobilisation, except for the omission of NHS, and observed via SPR.

Results and Discussion

When examined with AFM in lateral force mode, the surfaces of immobilised polymer films comprising of CMD, CMC and mixed CMD/CMC (Figure 1a) appeared uniform and homogenous with a regular crenulated texture. When the synthetic polymer CPN was introduced as an additive, the surface morphology becomes markedly different (Figure 1b) with an increase in the characteristic dimension of regular surface texture. The observed differences may be due to the difference in physical properties between the polysaccharide polymers and the aliphatic-backboned CPN.

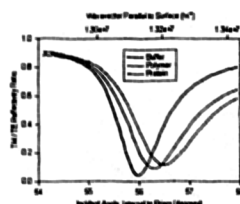


Figure 2: SPR responses obtained from a APTS-modified silver surface in 0.1M MES buffer, pH 6.8 (Buffer) and after immobilisation of a mixed polymer film of CMD, CMC and CPN (Polymer) and the subsequent covalent immobilisation of glucose oxidase to the polymer film (Protein).

Conclusions

We conclude from this work that:

- differing combinations of polysaccharide and synthetic polymers in immobilised thin films result in differing surface morphologies as determined by AFM
- the capacity of the various immobilised thin films to covalently bind protein, as determined by SPR, has been shown to vary as a function of the constituent polymers
- we believe that the flexibility and cross-sectional area of the various polymers results in the differing film mobility and porosity.

References

- Lofas, S. (1995) *Pure and Applied Chemistry*, 67, pp 829 - 834
 S. Tasker, G. Matthijs, M.C. Davis (1996) *Langmuir*, 12, pp 6436 - 6442
 S. Kosek, C. Padeste, L.X. Tiefenauer and H. Siegenthaler (1998) *Biosensors and Bioelectronics*, 13, pp 31 - 43
 B. Liedberg, I Lundstrom and E. Stenberg (1993) *Sensors and Actuators B*, 11, pp 63 - 72

The relative amount of immobilised polymer and the subsequent amount of incorporated protein in the immobilised polymer films were determined by SPR and the results are summarised in Table 1. From polymer solutions of identical concentration, a similar amount of polymer was immobilised for the CMD, CMC and CMD/CMC/CPN systems while the CMD/CMC system showed a relative increase of 67%. For the covalent incorporation of the protein glucose oxidase, the CMD and CMC systems displayed similar levels of incorporation while the mixed systems exhibited an approximately 60% decrease compared to the single polymer systems. The decrease in the protein binding capacity for the mixed polymer films may reflect a decrease of porosity thereby restricting diffusion of the protein into the films. It is important to note that at present we have not confirmed that for the mixed polymer systems, the stoichiometry of the immobilised polymer films is the same as the polymer solutions.

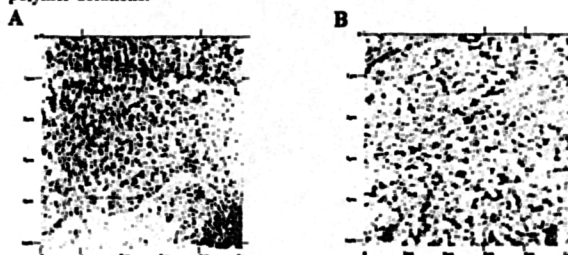


Figure 1: Examples of lateral force microscopy images of (A) a deposited CMD/CMC mixed polymer interface and (B) a deposited CMD/CMC/CPN mixed polymer interface showing differences between the morphology of the surfaces of the immobilised polymer films. For immobilised single polymers of CMD or CMC, similar morphologies to the mixed CMD/CMC polymer films were observed. Image processing has been used to level the images.

Table 1: The relative change in the angular position of the SPR minima for APTS-modified silver SPR surfaces during the stepwise covalent immobilisation of the relevant carboxylated polymers and the subsequent covalent incorporation of the protein glucose oxidase.

Condition	CMD	CMC	CMD/CMC	CMD/CMC/CPN
Relative change in position of SPR minimum (degrees \pm 1SD, n=2 or 3)				
Buffer	0.00	0.00	0.00	0.00
Polymer	0.22 \pm 0.12	0.24 \pm 0.00	0.39 \pm 0.13	0.24 \pm 0.10
Polymer & Protein	0.39 \pm 0.04	0.32 \pm 0.04	0.14 \pm 0.09	0.16 \pm 0.09
Total Change	0.61 \pm 0.15	0.56 \pm 0.04	0.53 \pm 0.21	0.39 \pm 0.19

In summary, the above observations suggest that the physical properties of individual polymers such as their cross-sectional area and "flexibility" (i.e. persistence length) controls the microscopic structure of the immobilised polymer films such as the porosity and mobility thereby influencing the ability of molecules to interact within the films.

Reverse Deposition: Optimisation of Bioactive Interfaces for Compatibility with Large-Scale Manufacture

David G. Weston and David C. Cullen

Cranfield Biotechnology Centre, Cranfield University, Bedfordshire MK43 0AL, UK
(<http://www.cranfield.ac.uk/biotech/>)

Introduction

Many areas of biotechnology require the immobilisation of biological elements to a solid support. Affinity chromatography and biosensors are two examples. Often relevant surfaces are modified by the attachment of hydrogel polymer layers prior to the immobilisation of biorecognition elements to the hydrogel. We call this approach "sequential deposition" and while appropriate for many applications, it can be time consuming due to the need for multiple handling steps involving the solid support. We here report an alternative approach, termed "reverse deposition", for the formation of surfaces modified with hydrogel layers that incorporate biorecognition elements and that address the handling problems mentioned.

Reverse deposition involves the covalent immobilisation of biorecognition elements to polymers in bulk solution before the covalent immobilisation of the biorecognition element-polymer conjugate to a solid support. In large-scale production this approach offers a simpler route because immobilisation to the solid support is only a single step reaction. The relatively complex, multi-step bulk synthesis of the required conjugate in free solution can be more efficient as large quantities or volumes of solid support do not have to be handled repeatedly.

The studies we report here compare reverse and sequential depositions using a model system, the enzyme horseradish peroxidase (HRP), via microtitre plate and surface plasmon resonance studies. We also highlight additional advantages of the reverse deposition approach.

Results

To compare the reverse and sequential deposition approaches, microtitre plate experiments have been performed. For sequential immobilisation, carboxymethyl dextran (CMD) is covalently attached to aminated microtitre plates (code: 2338, Corning Costar, Bucks, UK) using carbodiimide chemistry¹ and followed by covalent immobilisation of HRP to the immobilised CMD hydrogel layer. For reverse deposition, a CMD-HRP conjugate is synthesised in solution using carbodiimide chemistry² and purified prior to immobilisation of the conjugate to aminated microtitre plates again using carbodiimide chemistry. The resultant HRP activity incorporated was measured by using a colourimetric HRP assay using 2,2'-azino-bis(3-ethylbenz thiazoline)-6-sulfonic acid (ABTS). Table 1 summarises the results and shows that for similar reaction conditions, reverse deposition gives a 42% increase in immobilised HRP activity.

Table 1: HRP activity in a CMD surface layer produced by reverse and sequential immobilisation

	Absorbance at 495nm (\pm 1SD, n = 8)
Sequential Deposition	1.70 \pm 0.20
Reverse Deposition	2.41 \pm 0.23

To assess the total amount of immobilised material present for the reverse and sequential approaches, the immobilisations have been performed on aminated³ silver SPR devices using conditions identical to the microtitre plate experiments. SPR measurements enabled the relative angular shift in the SPR reflection curves caused by the increased refractive index/mass of the CMD/HRP layer(s) to be determined.

Table 2: Comparison of surface loading between reverse and sequential deposition as determined by SPR

	CMD (Δ 0.01°/degree)	CMD+HRP (Δ 0.01°/degree)
Sequential Deposition	0.51 \pm 0.2	0.50 \pm 0.22
Reverse Deposition	not applicable	0.53 \pm 0.2

Table 2 summarises the results and shows that for sequential deposition, a total shift of 1.01° is seen compared to 0.53° for the reverse deposition, i.e. approximately 50% more material is present for the sequential deposition. Only for the sequential deposition can the relative contribution of the CMD and HRP be seen as a 1:1 ratio.

¹ Polymer solutions are made to 0.1% w/v in 100 mM MES buffer, pH 6.7. Solutions are activated by the addition of 2.5 mg/ml EDC and 1 mg/ml NHS. Activated solutions are introduced to amino-modified surfaces and allowed to incubate for 40 minutes at 20°C. Following incubation, surfaces are washed with Tween 20 and water and blocked with 100 mM glycine.

² 20 mg of the carboxylated polymer dissolved in 10 ml of 0.1 M MES (pH 6.7) added to 10 mg of the protein dissolved in 10 ml 0.1 M MES (pH 7.1). 50 mg of EDC is added to the solution and stirred until dissolved. The solution is allowed to incubate for 2 hours at 20°C. The biopolymer conjugate is purified by centrifugation at 3000 RPM for five minutes and separation through a Sephadex G100 size exclusion column.

³ Silver surfaces aminated via vapour-phase deposition of aminopropyl-trimethoxy silane. SPR measurement performed on an in-house constructed SPR system.

Discussion

The results obtained suggest that an increased total interface activity of HRP can be obtained with reverse immobilisation. A model to account for the observation is shown in Figure 1.

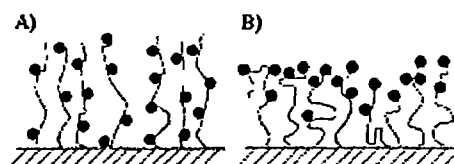


Figure 1: Schematic of possible difference of immobilisation for reverse (A) and sequential (B) immobilisation due to steric/diffusional constraints

In reverse deposition, the synthesis of the HRP-CMD conjugate in bulk solution results in a homogenous distribution of HRP molecules on CMD polymers. Subsequent immobilisation to a surface should retain the homogenous and random distribution.

For sequential deposition, the immobilised CMD hydrogel layer may act as a diffusional barrier restricting the homogeneous distribution of HRP throughout the CMD layer. HRP will thus be localised at the surface of the CMD hydrogel layer.

The presented data suggests that although more HRP is immobilised through sequential deposition, the activity of this is far less than that for reverse deposition. Steric issues, as suggested by the proposed model, may account for the observed difference.

Conclusions

We have compared reverse deposited and sequentially deposited approaches to immobilisation of biomolecules. For the specific conditions investigated we see that reverse compared to sequential deposition produces:

- An increase of ~40% in overall activity of the immobilised interface
- The increased activity obtained with ~50% less material present at the immobilised interface

For applications requiring large-scale immobilisation of biomolecules at polymer-modified interfaces in areas such as biosensors and affinity chromatography, the broad concept of reverse deposition offers:

- Reduction in processing steps involving the solid-phase material to a single step – synthesis of polymer/biomolecule conjugates easily achieved in separate bulk solution
- Alternative micro-distribution of biorecognition in immobilised hydrogel interfaces

References

- Liedberg, B. and Lundström, I. (1993)
Principles of biosensing with an extended coupling matrix and surface plasmon resonance
Sensors and Actuators B, vol 11, pp 63 – 72
- Marco, M. P. and Barcelo, D. (1996)
Environmental applications of analytical biosensors
Measurement in Science and Technology vol. 7, pp 1547 – 1562
- Huan, S.C., et al (1996)
Site Specific Immobilisation of MAb's using spacer-mediated antibody attachment
Langmuir, vol. 12 pp 4292 – 4298